Seismic Risk Assessment of Unreinforced Masonry Buildings at a Territorial Scale

Dissertation

submitted to and approved by the

Department of Architecture, Civil Engineering and Environmental Sciences
University of Braunschweig – Institute of Technology

and the

Faculty of Engineering
University of Florence

in candidacy for the degree of a
Doktor-Ingenieur (Dr.-Ing.) /
Dottore di Ricerca in "Riduzione del Rischio da Catastrofi Naturali su Strutture ed Infrastrutture" *)

by

Jorge Muñoz Barrantes
Born 10.09.1980
from Curridabat, Costa Rica

Submitted on	21 March 2012
Oral examination on	8 May 2012
Professorial advisors	Prof. U. Peil
	Prof. A. Vignoli

2012

*) Either the German or the Italian form of the title may be used.

Earthquakes don't kill people, buildings do

ABSTRACT

Masonry constructions represent a significant portion of building stocks in many seismic regions around the world. The seismic response depends on the singularities of construction techniques and materials. The building vulnerability categorization by the European macroseismic scale (EMS-98) state that the unreinforced masonry (URM) typologies present the greatest seismic vulnerability. This statement agrees well with recently extensive damage observed in URM building stock after Kashmir (2005), Peru (2007), L'Aquila (2009) and Christchurch (2011) earthquakes.

The seismic assessment of unreinforced masonry structures is a complex task. The complexity arises due to the material particularities, construction techniques and loading variability characteristics. Modeling these uncertainties has a significant influence on the estimation of the global behavior of a masonry building. In order to evaluate the uncertainties in seismic analyses of URM constructions, the SAUMAC methodology is proposed. SAUMAC stands for Seismic Assessment of Unreinforced Masonry according to local Architectural and Code conditions. In SAUMAC, results (structural risk and fragility curves) are obtained from a synthetically generated building population associated to a specific building typology. In other words, it is creating results to a particular condition (theoretical building archetype) from the behavior observed in a building population of similar structural conditions.

In the methodology, in-plane and out-of-plane failure mechanisms of walls were considered separately. In case of the in-plane failure mode, three aspects are considered for developing the fragility curves: a normalized storey resistance, a seismic coefficient and a dimensionless variable related to the building architectural characteristics per storey. Monte Carlo simulations, computed by means of a MATLAB code, are used for obtaining the storey resistance and the architectural parameters. Once the parameters are founded, fragilities are constructed by solving the limit state equation (*resistance* > *seismic demand*) for incremental seismic intensities.

Fragility curves obtained by means of SAUMAC, describe many possible building configurations of common low rise URM in a fast and economical manner for two performance levels: life safety and serviceability. This was implemented by assuming that the seismic loading condition is equal to the elastic response spectra and elastic storey resistance for the serviceability limit state, and is equal to the code design response spectra and ultimate floor resistance in case of life safety limit state.

The structural risk is calculated by the convolution of the seismic hazard curve and the structure fragility function. The acquired structural risk is then evaluated, based on the likelihood of a situation and the analysis of target reliability values presented in bibliography.

Results could be used in a qualitative and quantitative manner for typological building evaluation (building sets), but, they are limited to a qualitative use in case of single structures. Despite this restriction, single structures are found to be safe when presenting low seismic risk and unsafe for high risk structural values.

The SAUMAC methodology results are compared with the damage statistics gathered at Castelnuovo town after the L'Aquila earthquake (2009). At Castelnuovo, rubble stone URM buildings are more than 90% of the whole population. Damage statistics found in Castelnuovo fit well with the results of the proposed methodology. High structural vulnerabilities were founded for the simulated typologies, in particular for buildings with dominant out-of-plane failure modes.

ACKNOWLEDGEMENTS

During the periods of my studies in the interesting field of masonry structures, many people have contributed in various ways to this final manuscript. Firstly, I would like to express my gratitude to my tutors, Prof. Udo Peil and Prof. Andrea Vignoli for their guidance and teaching during my period of research. Without their support and advice, this work would not be possible.

A special thanks to Prof. Claudio Borri for his helpful guidance during my stay in Italy and the support, together with Prof. Vignoli, to join some of the first field surveys performed by the University of Florence to the earthquake damage area in L'Aquila city and surroundings in 2009 and 2011.

I would like to express my sincere gratitude to my colleagues and staff at the Institute for Steel Structures, TU Braunschweig, for their practical recommendations, discussion, reviews of my work and personal help during my stay in Germany. In special, I would like mention Dr. Mathias Clobes and Ing. Hodei Aizpurua, for their advices in reviewing essential aspects of this work. I would also like to thank Dr. Matthias Reininghaus, Dipl. Ing. Andreas Willecke, Dr. Tobias Wagner, Dipl. Ing. Thomas Höbbel and Ivonne Wissmann.

My gratitude goes as well to Ing. Alberto Ciavattone, Dr. Andrea Borghini, Arq. Palma Patore and Ms Serena Cartei, for their help during the field surveys at Castelnuovo town in 2009 and 2011, and my stay at Florence.

Finally I would like to thank my friends for their constant support and to my family, though separate by distance, were permanently close to me.

CONTENTS

1 INTRODUCTION ……..…... **1**

Motivation and Objectives 1
Thesis Overview 3

2 RISK MANAGEMENT IN CIVIL ENGINEERING ……...…….…….. **5**

2.1 Assessing Acceptable Risks 5
2.2 Natural Hazards 7
2.3 Managing Risk 10

3 SEISMIC HAZARD ……...…….….... **15**

3.1 Description of Earthquakes 16
3.1.1 Magnitude 16
3.1.1 Intensity and intensity scales 17
3.1.3 Occurrence of earthquakes 20
3.2 Approaches for Computing the Seismic Action 21
3.2.1 Deterministic seismic hazard approach DSHA 22
3.2.2 Probabilistic seismic hazard approach PSHA 22
3.3 Response Spectra and Seismic Coefficient 25
3.3.1 Seismic action 26
3.3.2 Design base shear 28
3.3.3 Structural irregularities 30
3.3.4 Seismic actions for non structural elements 32
3.4 Performance Requirements 34

4 UNREINFORCED MASONRY BUILDINGS URM ……...…….……. **35**

4.1 Typologies and Seismic Performance 35
4.2 Building Stock 37
4.3 Material Properties 39
4.3.1 Masonry walls 40
4.4 Building Components 42
4.4.1 Floor diaphragm systems 43
4.4.2 Spandrels 44
4.5 Capacity of URM Walls 46
4.5.1 Orthogonal capacity (out-of-plane) 46
4.5.2 Lateral capacity (in-plane) 49
4.5.2.1 Rocking failure 50
4.5.2.2 Shear cracking 51
4.5.2.3 Sliding 52
4.5.2.4 Stiffness and bilinear model for piers 52
4.5.3 Wall capacity and structural behavior factor 54
4.6 Uncertainties in URM 56

5 ASSESSING EXISTING STRUCTURES …….. **59**

5.1 Assessment Sophistication Levels 59
5.2 Basic and Modeling Variables 61
5.3 Reliability Assessment Methods 62
5.3.1 Reliability of systems 65
5.4 Reliability Verification Methods 66
5.5 Quantification and Evaluation of Structural Seismic Risk 67
5.5.1 Fragility curves 68
5.5.1.1 Defining building typologies 69
5.5.2 Risk and target reliability 70

6 SEISMIC ASSESSMENT OF URM ACCORDING TO LOCAL BUILDING CONDITIONS, SAUMAC ..…..… **73**

6.1 Methodology Description and Assumptions 73
6.2 The Stochastic House Model 76
6.2.1 Architectural considerations 77
6.3 Obtaining I_S, I_R and A_M for the in-plane 81
6.4 Obtaining I_S, I_R for the out-of-plane 87
6.5 Simplify Steps to Obtain I_S, I_R, A_M 89
6.5.1 The seismic structural index I_R 89
6.5.2 The seismic demand I_S 93
6.5.3 The architectural mass index A_M 94
6.6 Structural Vulnerability and Computing the Risk 95

7 CASE STUDY: SEISMIC DAMAGE ASSESSMENT AT CASTELNOUVO TOWN; ABRUZZO, ITALY ……..…..... **99**

7.1 L'Aquila Earthquake 2009 100
7.2 Building Characterization and Seismic Damage in Castelnuovo 103
7.3 SAUMAC Application 112
7.3.1 Defined building typologies 115
7.3.2 Structural vulnerability and computing the risk 123
7.4 Reviewing Results 126
7.4.1 Comparison with survey damage 127
7.4.2 Comparison with other methodologies 128
7.4.3 Evaluation of rubble stone low-rise URM 130

8 SYNOPSIS …….. **133**

Concluding Remarks 133
Future Developments and Possibilities 134

APPENDIX A: Castelnuovo Damage Photographic Description for L'Aquila Earthquake 137

APPENDIX B: Standard Normal Distribution 147

APPENDIX C: MATLAB Functions for SAUMAC and Fragility/Risk Calculation 149

APPENDIX D: Seismic Design Base Forces According to Various Seismic Codes 161

LIST OF ABBREVATIONS ANS SYMBOLS 165

REFERENCES 171

1 INTRODUCTION

Masonry is one of the most important construction materials in the history of mankind. It had been used in wide variations as the base of our constructions. Masonry structures had been appreciated due to durability, resistance and isolation properties. As an example of the successful behavior and extensive use masonry structures, a great number of well preserved old masonry edifications still exist nowadays worldwide. Many of these structures are considered of historical and cultural heritage importance. Many old, and even new, masonry constructions are unreinforced masonry buildings (URM). URM consist of structures with no steel reinforcing within the walls or any sort of confinement to masonry panels such as reinforce concrete frames.

Masonry constructions had been founded particularly susceptible to damage after seismic actions. From the masonry building categories, URM is the one presenting the greatest vulnerability [Gr 98]. Earthquakes had been proved to be one of the most destructive natural hazards. Total earthquake devastation narrative is founded since biblical times and up to today news. For example, two major catastrophic events had occurred recently in Haiti 2010 and Japan 2011.

Great amount of resources and research efforts are focused on seismic analysis and restoration of historical URM structures. On the other hand, small research efforts are focused on the majority of small common masonry buildings constructed in the last century; many of them before the introduction and enforcement of actual seismic design codes.

Research on URM field presents challenges even to simple structural configurations due to the variability of local construction techniques and low confidence in the material properties. Because of these, evaluation and correlation among results is difficult. The dilemma of seismic assessment of unreinforced masonry can be solved in the context of the risk management framework. This study present a methodology to obtain, in a fast economically manner, the structural risk of URM structures.

1.1 Motivation and Objectives

Extensive damage was observed following earthquakes in unreinforced masonry structures. Experience shows that after the collapse of URM, there is great amount of people that are killed or seriously injured. The sum of all the people that become homeless generates not only an economical but a big social problem difficult to deal with. Bam (2003), Kashmir (2005), Peru (2007) and L'Aquila (2009) are recent examples of earthquakes causing major damage to URM building stock.

L'Aquila earthquake took the lives of over 294 people and more than 25,000 were displaced [AKTB 09]. A total of 10,000 buildings suffered significant damage, and economical losses exceed US$ 16 billion including financial and reconstruction cost [MY 09]. Figure 1.1 shows damage on URM constructions at Castelnuovo, 25 kilometers distant from L'Aquila city (Italy). For Castelnuovo, extensive or complete damage was founded in approximately 80% of the whole building population which was composed in more than 90% of URM structures [CF 10]. In L'Aquila region, the masonry construction typology represents up to 68% of all the building stock, and buildings below or with 3 stories are the 95% of the whole population [RdLV 10]. These facts suggest on focusing research efforts to develop tools that emphasizes in these particular conditions, commonly observed in many middle and small size cities in seismic prone countries.

Beside the intrinsic vulnerability of URM to earthquakes, actual assessment procedures of masonry are mostly based on deterministic data inputs. The results are then used to categorize the structure into a vulnerability ranking or its safety evaluated by means of partial safety factors.

Figure 1.1: Building damage in L'Aquila 2009

Meanwhile, uncertainties of significant influence have been found on the estimation of the global behavior of a masonry structures. In particular, a low confidence in the mechanical properties of masonry is a fundamental role in the assessment of seismic vulnerability of the structure [AP 09]. Few studies, such as those presented by Rota [RPM 08] and Augenti [AP 09], took into account the uncertainties of material properties, in terms of probability density functions (PDFs), for deriving seismic vulnerability of URM. Seismic vulnerability of an individual building or a typical building archetype may be presented in terms of fragility curves. Structural fragility curves described a wide spectrum of the seismic behavior of a structure related to a specific damage level. Methodologies such as HAZUS [HAZUS 99] could develop fragilities or obtain fragilities from a typological building database. Besides the material properties, doubts in URM arise from many different sources, including the human variable; an important structural failure source [Sc 97]. In URM, variation of elements geometry and structural changes (e.g. new openings, change of use) are common.

These facts, advise that probabilistic methods are more suitable to assess the structural behavior of this kind of structures. Despite the variability of the structural resistance of the system, there are also the uncertainties regarding the seismic actions (section 3.2.2).

The main objective of this study is to take into account uncertainties related to the seismic assessment of URM. The complementary practical objective is to organize results into the context of the risk management framework by means of a new evaluation methodology proposal. In order to fulfill these objectives, a number of minor goals were investigated:

- *Overview of uncertainties related to the seismic actions (seismic hazard)*
- *Review target reliabilities (safety level) for evaluating URM, and risk levels*
- *Overview of the structural behavior factor and proposed value to use in SAUMAC*
- *Investigation of the seismic action for different seismic codes*
- *Investigation on seismic behavior of in-plane and out-of-plane failure mechanisms*
- *Investigation of different assessment complexity levels and reliability methods*
- *Review of the exposed URM buildings (building stock worldwide)*
- *Investigation of uncertainties in URM*
- *Description of factors and basic variables related to seismic assessment of structures*
- *Structural fragility curve generation (structural vulnerability)*
- *Quantification and qualification of structural seismic risk*

The SAUMAC methodology was developed to fulfill the goals of this study. SAUMAC stands for Seismic Assessment of Unreinforced Masonry according to local Architectural and Code conditions. Local conditions refer as an example to common local materials, construction techniques and regional seismic provision.

In SAUMAC, the variability criteria is extrapolated to the level of proposing an assessment based on a possible structure configurations (stochastic house generation) rather than typical judgment performed directly on a determinate well known structure.

1.2 Thesis Overview

Along this study, several topics are discussed. Large amount of variables and issues related to both, seismic and unreinforced masonry were considered. In addition to this, concepts related to reliability analysis and risk management are constantly integrated into the discussion.

The work presents an initial introductive chapter dealing with basic engineering concepts and how they are treated along the study. This is of importance since some concepts such as risk, probability of failure or safety can be defined in several ways and their application related to many fields. In the chapter, an overview of natural hazards effects on the civilization is presented as an important justification of this study based on the observed consequences of these events. The chapter is finished with a review of the risk management framework developed by the Graduate College group GKR-802 [Pl 07], which is also the risk framework of this study.

Section 3 describes the seismic hazard. It is focused on two points: a complete explanation of seismic hazard curves generation and the provision's descriptions of the seismic base shear force. The hazard curve generation is of importance to overview uncertainties related to the seismic input parameters. The curve is used later on to compute the structural risk. The seismic base shear is of importance in the traditional code assessment procedures of normal structures. This concept is used as the main aspect for deriving seismic fragilities in the SAUMAC methodology. This section explains as well assumptions presented in the proposed methodology, such as; a simplified distribution of forces along the storeys and structural layout irregularity factors.

For section 4, a panorama related to the experienced behavior of URM in earthquakes is presented. Details concerning the two possible failure mechanisms of walls: in-plane and out-of-plane are discussed in depth. The section provides in addition a description of how a typical masonry structure could be analyzed separately for different structural components; each of the components presents different functions into the structural system in SAUMAC. For the in-plane failure failing mode, masonry wall piers are the basic resistant components. Their behavior has been evaluated in three basic failure criteria: rocking, diagonal tension shear and Mohr-Coulomb shear. Structural behavior factors are suggested for the seismic assessment according to the most probable failure mechanism for the life safety limit state. Limit states are previously reviewed in section 3.4.

The goal of section 5 is the solution of the typical engineering reliability problem $R \geq S$, where R stands for resistance and S for solicitation or demand. The result of this formulation for a specific performance limit state is used for obtaining the structural fragility of the building system. After the study of sections 3 and 4, the most relevant factors describing the seismic solicitation and URM building capacity are commented. To each of these factors, models and basic variables are associated. These basic variables are expressed in terms of probability density functions (PDFs) to estimate their variability. The reliability problem is solved by means of the limit state equation ($G(X)$), methodologies of how to solve $G(X)$ and to create fragility curves are also included in the section.

Finally, section 5 establishes how the structural risk (R_S) is computed as the convolution of the structural fragility function with the hazard curve.

Section 6 presents the details of the SAUMAC methodology. The methodology is based on finding three basic parameters to solve the limit state equation. One parameter is related with the seismic loading. This is strongly influenced by the so called seismic coefficient in earthquake norms. Another is related with a normalized storey resistance, obtained from the normalization of resistant shear forces to the average normal load in the storey. The third aspect is a dimensionless variable related to dispersion of the building architectural characteristics. This third variable is obtained from the so called stochastic house model (SHM) explained in section 6.2. A simplified procedure to find all this basic variables and obtain the structural fragilities is exposed in section 6.5.

A case study is presented in section 7. After the L'Aquila earthquake of 2009 a town called Castelnuovo, distant approximately 25 km from the seismic epicenter, was heavily damaged. Characterization of damage to buildings in the town was developed by the research group coordinated by Professor Andrea Vignoli of the University of Florence and corroborated independently by two field surveys by the author of this study on May 2009 and October 2011. Seismic fragilities for 12 town building typologies are founded by means of the SAUMAC procedure and compared to local edifications evaluated as vulnerability A and B according to the European Macroseismic Scale (EMS-98)[Gr 98]. The section includes the risk quantification and evaluation for the structures, and a comparison of the methodology results with other studies and the observed damage statistics in Castelnuovo.

2 RISK MANAGEMENT IN CIVIL ENGINEERING

2.1 Assessing Acceptable Risk

How to assess the acceptable conditions on engineering design practice? The answer to this question is the aim of this chapter and section 5. The responsibility of the engineer is to find an economical and safe solution viable for a specific project. In every day engineering practice, individual judgment can lead to the two extremes illustrated in figure 2.1. For the temporal support in a cave excavation, there is a safety perception related to each solution [HKB 98]. On to the left, even though it's safe, is economically unacceptable; meanwhile, the one to the right possibly violates most safety standards.

To homogenize criteria about acceptable safety/economic conditions, engineering judgment is guided by practical and theoretical studies summarized on building codes and other local regulations; however, there are no simple universal rules for acceptability parameters since every project is unique and the individual perception of safety is different. Public, in general, admit fail as an extremely rare situation and consciously rely on professional care of experts involved in planning, design, construction and maintenance of structures [Sc 97]. The definition of safety taking into account the elements described before is as follows [Sc 97]:

"*Adequate safety with respect to a hazard is ensured provided that the hazard is kept under control by appropriate measures or the risk is limited to an acceptable value. Absolute safety is not achievable*"

In this definition, the term risk is introduced as an opposite aspect to safety in a qualitative way. The term adequate safety refers to the desirable safety according to the structure´s importance and the expected life span service of the structure. Commonly, the characterization of an appropriate safety level in civil engineering is based on possible direct human/economical failure cost. Other parameters include the indirect consequences that could lead to social, cultural, historical and ecological losses [Pl 07].

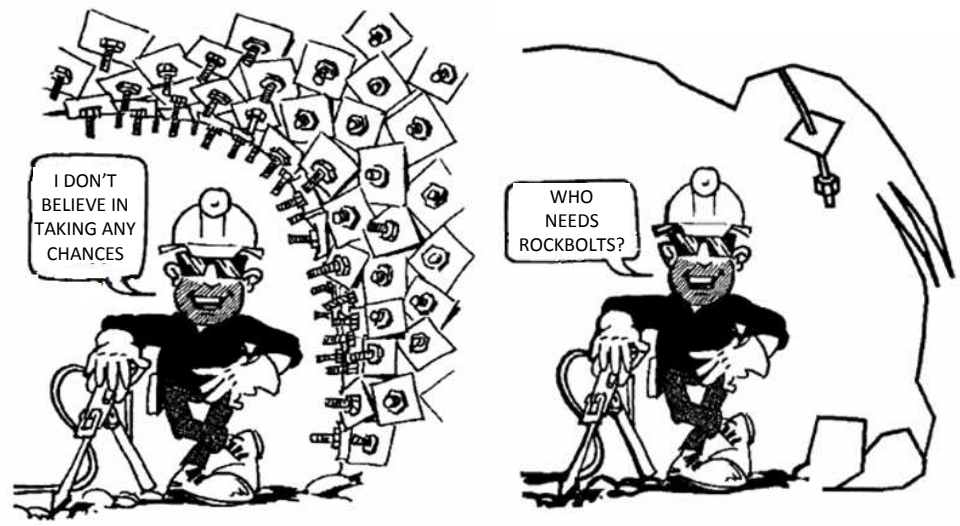

Figure 2.1: Rockbolting alternatives according to individual judgment [HKB 98]

The failure of structures is typically expressed in terms of probabilities or frequencies. Events (e.g.: missing the airplane), occur with a certain probability, which, can be defined by three traditional approaches [Sc 97]:

"Classical (Laplace): Probability is the number of cases in which an event occurs, divided by the total number of cases"
"Frequency (Von Mises): Probability is the limiting case of the relative frequency with which an event occurs, considering many independent recurrences under the same condition"
"Subjective (Bayes): Probability is the degree of belief or confidence of an individual in the statement that a possible event occurs"

The classical approach from Laplace is apparently the one most fitting in engineering practice. Probabilities are expressed by a dimensionless value between zero and one. They are found for events concerning to some period of time or frequency, usually for structural engineering practice, in terms of annual probability.

Reliability is defined as the probability that an object will perform in a desirable way, for the expected period of use and conditions. The reliability r could be seen as the opposite of the probability of failure p_f as:

$$r = 1 - p_f \qquad \text{Eq 2.1}$$

Different from safety, reliability is a quantitative variable, useful in engineering field to reflect safety. As mentioned before, risk is opposite to safety and in general it refers to the possibility of damage to occur and as well could be define in terms of a p_f. There are many definitions of risk as it is a concept widely applied in many science disciplines, as exposed by Sperbeck [Sp 08]. Perhaps the most used definition is the one proposed by the United Nations Development program [UN 04] and it refers to it as:

*"The probability of harmful consequences, or expected loss of lives, people injured, property, livelihoods, economy activity disrupted (or environment damage) resulting from interactions between human and natural induced hazards and vulnerable conditions. Risk is conventionally expressed by the formulation Risk=Hazard*Vulnerability"*

This definition is not fitting well in engineering practice since risk is just explained in a qualitative manner as function of vulnerability and hazard. Einstein [Ei 88], proposed a simple and easy applicable to engineering definition of risk:

*"Risk is the probability of an event multiplied by the consequences if the event occurs. Risk=Probability*Consequences"*

This is risk definition in the context of this study. Consequences, are related to loss or damage; hence, the Einstein [Ei 88] definition is proposed in terms of these parameters. The following expressions are used here for the definition of risk [Pl 07]:

*Total Risk = Prob.*Loss [Loss unit / year]* $R_T = p_f L_O$ Eq 2.2

*Structural Risk = Prob.*Damage [Damage measure / year]* $R_S = p_f D_{LS}$ Eq 2.3

Equations 2.2 and 2.3, were used by Pliefke [Pl 07] for summarizing the general risk management framework (figure 2.6). For the total risk, all consequences are taken into account and are transformed, if possible, into a common unit, usually a monetary one. This transformation is difficult because of the intangible value of some objects (i.e. a historical building) or the monetary quantification of human life. The values of loss estimations results are very variable depending on the applied methodology and the data treatment. Good loss estimations are of importance for governments and international organizations stakeholders.

In a second instance, the relation between the hazard intensity and the resulting damage is called structural risk. It is evident that this is of special interest in structural design and assessment of structures for performance evaluation of a structure, or structural typologies, to an applied load. When risk is mention in this work, it is commonly related directly to structural risk. This risk, is associated with the damage level times the probability of occurrence of a hazard. Different structural damage levels are defined in section 3.1.2; meanwhile for the hazard, earthquake annual probabilities of occurrence are described on section 3.1.3. This work is focused on the risk assessment of existing not reinforced masonry structures. Details about theoretical background of assessment procedures are discussed on section 5.

Finally, regarding the question, how safe is safe enough?, Schneider [Sc 97] presents an interesting discussion on the topic by formulating new questions: "*What could happen, in what way and how often?*" or "*What may be allowed to happen, how often, and where?*"; the answer to these questions provide the sufficiently safe situation. Afterwards, as will be observed in section 5, the required safety conditions take the form of safety factors, partial safety factors and reliability values.

2.2 Natural Hazards

In general, there is a hazard when a situation posses a certain level of threat to an appreciate value (life, health, property, etc); they are typically categorized into natural and the civilization/anthropogenic groups. The separation is mainly related to the source of the risk, but in reality, it's difficult to separate one from the other since many are man triggered hazards, just like technological failures, are many times related to lack of preparedness and response to natural hazards. The combination of different risk scenarios is evaluated in a risk management framework discussed in section 2.3. Other human related risks, such as terrorism or economical crisis, are normally less correlated to a natural event, and respond merely to random social dynamics.

A natural hazard is a threat of a natural occurring event with negative impact on people or the environment; events such as droughts, floods, landslides, volcano eruption and hurricanes belong to this category. This project deals with the earthquake hazard. Seismic hazards belong to the so called geophysical threat group, which accounts for a significant percent of great catastrophes as observed in figure 2.2. According to Munich Re [MRe web], a great catastrophe is defined as leading to any of this conditions: thousands of fatalities, the economy being severely affected, considerable insured losses, interregional or international assistance is necessary, and hundreds of thousands are made homeless (UN definition).

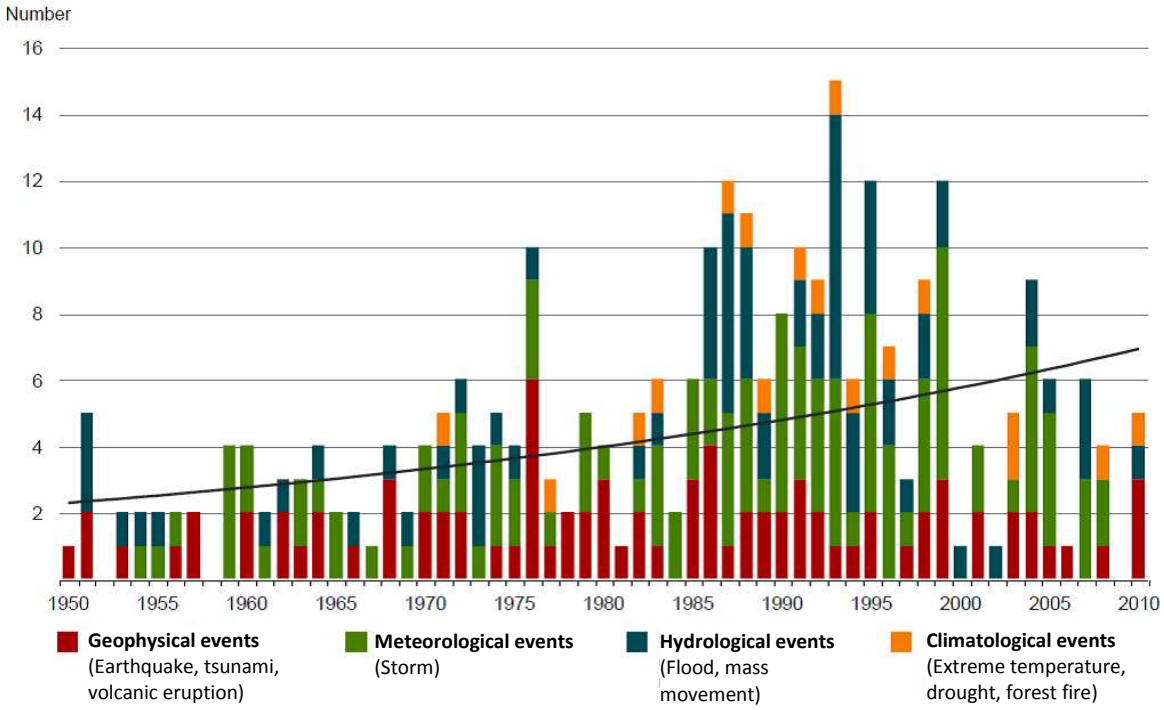

Figure 2.2: Great natural catastrophes 1950 - 2010 [MRe web]

In figure 2.2, it is observed that the amount of great natural catastrophes had been increasing since 1950. As the number of events increases, particularly those related with climate, expect loss had been increased as reported by Munich-Re [MRe web]. On the other hand, it is important to note that the amount of events has also increased worldwide over time due to economic development and population incremental; this makes the definition of great catastrophe adjustable to more and more events each year. The amount of loss in terms of fatalities, economic losses and insured losses is summarized in figure 2.3.

The presented data in figure 2.3, shows that earthquakes are of major concern regarding natural hazards, since, they have a high killing potential (figures 2.3, table 2.1) and produce big economical losses of non-insured values (figures 2.4).

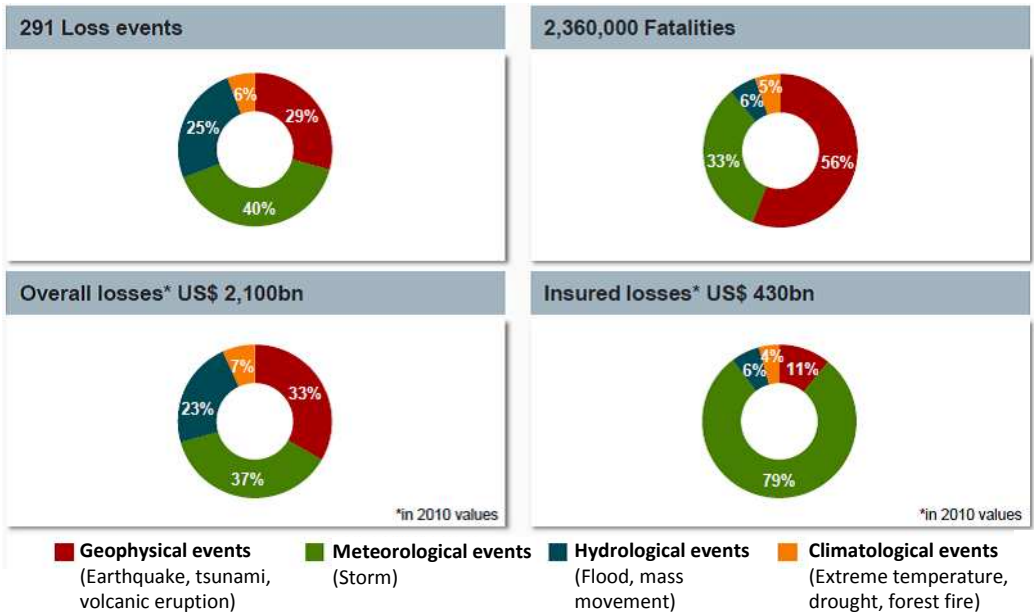

Figure 2.3: Loss description, natural catastrophes 2050 - 2010 [MRe web]

Table 2.1: 10 Deadliest events worldwide 2050 - 2010 [MRe web]

Period	Event	Affected Area	Overall losses	Insured Losses	Fatalities
			US$ m, original values		
12/1/2010	Earthquake	Haiti	8,000	200	222,570
26/12/2004	Earthquake, tsunamis	Sri Lanka, Indonesia, Thailandia, India, Malaysia	10,000	1,000	220,000
2-5/5/2008	Cyclone, storm surge	Myanmar	4,000		140,000
29-30/4/91	Cyclone, storm surge	Bangladesh	3,000	100	139,000
8/10/2005	Earthquake	Pakistan, India, Afganistan	5,200	5	88,000
12/5/2008	Earthquake	China: Sichuan, Mianyang, Beichuan, Wenchuan	85,000	300	84,000
July-August 2003	Heat wave, drought	France, Germany, Italy, Portugal, Romania, Spain, UK	13,800	20	70,000
July-Sept. 2010	Heat wave	Russian Federation: Moscow region, Kolomna, Mokhovoje	400		56,000
20/6/1990	Earthquake	Iran	7,100	100	40,000
8-19/12/99	Landslide, flash flood	Venezuela, Colombia	3,200	220	30,000

Some possible reasons for high seismic killing ratio were the lack of event prediction or real time monitoring (limited forecast), as it is currently possible and viable for volcano eruptions or hurricanes, plus the long return period of events. This last aspect makes people gradually less aware of danger. Earthquakes can trigger tsunamis, landslides, fires and technological hazards. Landslides are similar to earthquakes in a way that their prediction is difficult even though monitoring is possible in some cases. As an example, landslides were the cause for death of 24 from 25 victims of the Chinchona (M_S=6.2) earthquake in Costa Rica 2009 [LIS web]. Also, a series of at least 180 landslides caused ecological damage and a series of debris avalanches, one of which heavily damaged one important hydroelectric power plant that stood without damage after the initial seismic event.

Tsunamis cause also a big number of the fatalities as those observed in the 2004 Indian Ocean and 2011 Tohoku events. For the Tohoku earthquake in Japan, a technological risk was triggered after explosions in Fukushima Dai-Ichi nuclear power plant and oil tanks around Tokyo.

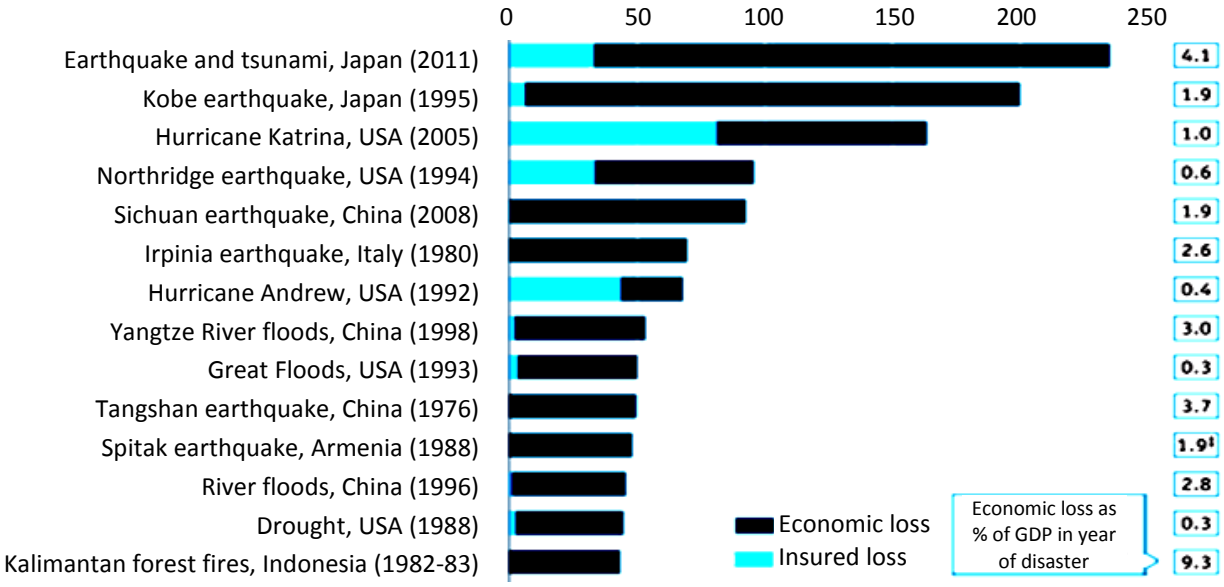

Figure 2.4: Top event for economical loss from 1965 in $bn (adapted from [TheEc web])

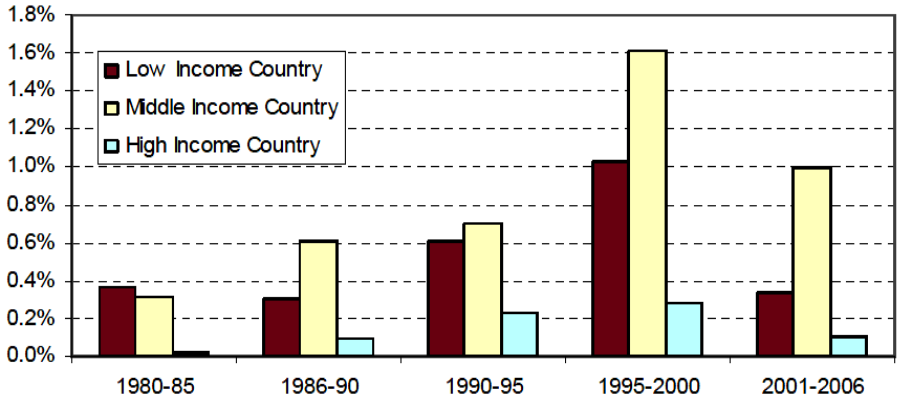

Figure 2.5: Average annual direct losses from disaster compared with GDP [CM 09]

The main Japanese 2011 seismic event became the new top for economic loss, as it is observed in figure 2.4. In this figure important data is also detailed on the amount of insured losses in relation with the total loss, and the total loss in relation with the national gross domestic product GDP. This last parameter is of relevance, especially for developing countries since it reflects better the real impact in the country's economy, which, are not be so productive as the ones of the develop ones. Some cases of poor economical recovery after a major event are observable for countries like Guatemala and Nicaragua after the 1976 and 1972 earthquakes [BB 83]. In figure 2.5 the impact of disasters in terms of the GDP for different income countries is shown.

Small countries economies are more fragile to natural hazards, since a single event could affect the whole country at the same time, greatly reducing its own response capacity. For example, the losses due to hurricane Gilbert 1988 in Santa Lucia were up to the 1 $bn representing 345% of the country's GDP. On the other hand Katrina 2005 losses of more than 150 $bn represents just 1% of the total GDP of USA [CM 09].

2.3 Managing Risk

Nowadays, risk management is an extensively used tool. It is defined as the systematic application of management policies, procedures and practices to task the identification, assessment, treatment, communication, review and monitoring of risk [Pl 07].

Its modern application origins are probably found in early economic theories around the 1920's [Sp 08], and is currently applied to several disciplines such as finance, insurance, production, disaster management and so on; basically, the process could be applied to any risk situation. The work presented here deals specifically with the seismic risk related to unreinforced masonry structures, URM.

So far, there are many different methodologies used for the risk management formulation; these, are usually adapted to the particular discipline. The methodology used here is the one proposed by the International Graduate College GRK-802 and published by Pliefke [Pl 07]. The methodology was projected as standardization of involved elements in risk management in such a way to facilitate the communication among different stakeholders.

The risk management methodology process is composed of three main aspects: risk identification, risk assessment and risk treatment; with all the steps subjected to risk monitoring. The general framework is shown in figure 2.6.

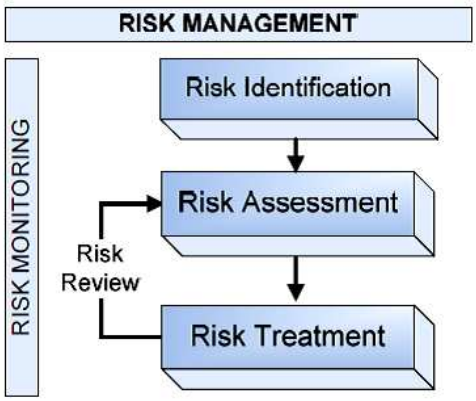

Figure 2.6: The general risk management framework [Pl 07]

The three elements in figure 2.6 are interacting over time. For example, a new risk could be identified at the risk assessment or risk treatment phase. A risk review is always needed to evaluate the effectiveness of a treatment solution. The whole is an iterative process. Risk monitoring is necessary to guarantee a good collaboration and communication between interdisciplinary groups involved in the risk management framework.

After a dangerous condition is detected in the risk identification phase, risk is quantified and compared to other hazards in the risk assessment phase. The assessment of seismic risk for existing URM structures to the seismic risk is the main goal of this study. This is done through the proposed SAUMAC methodology to obtain the structural risk of a system. The SAUMAC methodology is intended to be applied on existent buildings. Another possible use for the method is for new URM structures where no/poor engineering conception, deficient construction quality or structural use changes and modifications are expected.

The Risk assessment phase in a more detailed form is presented by Pliefke [Pl 07] and shown in figure 2.7. It is composed of analysis and evaluation sub-phases. The risk analysis represents the major effort of the assessment phase; the goal of it is to quantify the risk in terms of damage or a loss by the use of equations 2.2 and 2.3.

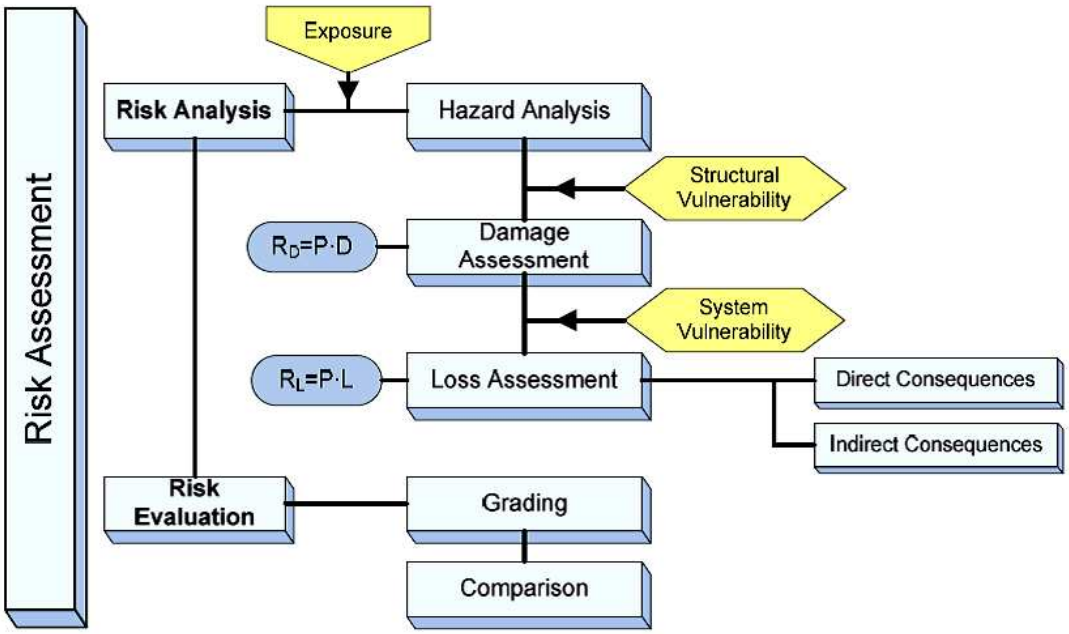

Figure 2.7: The risk assessment phase [Pl 07]

The hazards exposure is a parameter sometimes taken separate or enclosed with the vulnerability or the hazard aspects according to the United Nations Development program [UN 04] definition of risk. Directly regarding the structural vulnerability, it is important to separate both aspects, as the exposition to a hazard is a facet not related with the structure itself but to other circumstances, usually to the location of the object. For example in an area of a heavy winds, a high vulnerable house located inside a forest may still present a relatively low risk because of a low level of exposition of the analyzed element. In case of earthquake hazard, small physical variations of location (1 to 5 km), does not represent usually a significant reduction for the risk analysis regarding the exposition of the building to the shake, but, the exposure could become of very important relevance in relation with other hazards triggered by earthquakes at the same moment such as landslides, liquefaction, tsunami, debris flow and any technological risks such as the failure of a nuclear power plant or fire.

Since a hazard is identified and data collected for a determinate zone, hazard analysis is perform in order to evaluate vulnerable exposed elements. For our interest earthquake hazard analysis there are different procedures grouped into those that follow deterministic or probabilistic approaches. In section 3.2 the advantages of each of the approaches is discussed. For everyday design, hazard maps are develop for countries based on the probabilistic estimations of the seismic forces. Seismic Hazard maps for different countries are presented in appendix D.

Once the hazard potential is established, the structural vulnerability is input into the methodology flow to obtain the structural risk according to equation 2.3. The description of structural vulnerability is the main objective of this work. Here a procedure is established to determine fragility functions corresponding to different building typologies and for the evaluation of individual structures according to the target reliabilities review in section 5.

Adjacent to the risk analysis, there is the risk evaluation. The purpose of this evaluation is to categorize the risk in a way to make it comparable to other risks, and as an instrument for decision making in the next step of risk treatment. Many grading risk methodologies give a qualitative risk description in terms of a matrix where the severity of losses and the frequency of the event are the variables [FEMA 97][T&T 06]; later on, the consequences are established according to a risk group.

Regarding the quantitative measurement of risk, methodologies such as HAZUS, proposed by FEMA [HAZUS 99], or the Exceedance Probability Methodology used by the World Bank [ADB 09], expressed risk in terms of economical and social losses. These tools are useful for direct objective comparison in between risk scenarios. Total risk losses are presented in terms of some unit, as explained in Equation 2.3; the selection of the unit may be of great relevance. In the example proposed by Sperbeck [Sp 08] for the mortality rate related to transport system, airplanes are the safest mean of transport per kilometer travelled, but, the deathliest per travel. In this mode, risk is usually presented in the most advantageous way according to the sector. Risk acceptance judgment, is not free from the human psychological perception factor; for instance in table 2.2 different hazard events are compared. It is observed that frequent/familiar events such as smoking, present high tolerable level while they represent high consequences for human life.

Finally, in the risk treatment phase (figure 2.7), a decision is made of how to handle a determinate hazard. Decisions whether to accept, to transfer (insurance), to reject and finally to mitigate a given risk are derived. If the risk is considered unacceptably high and not transferable, it must be reduced. A risk mitigation plan could include possibilities ranging from technical prevention, social preparedness, response, and recovery actions [Pl 07].

Table 2.2: Comparison of individual risk of death from hazards in New Zealand.
Annual average between 1840 and 1990 [GAC 06]

Hazard	Deaths per year	Probability of death per person per year
Smoking	4,000	1.1×10^{-3}
Road accident	600	1.7×10^{-4}
Suicide	380	1.1×10^{-4}
Falls	300	8.6×10^{-5}
Drowning	120	3.5×10^{-5}
Homicide	50	1.4×10^{-5}
Fire	32	9.0×10^{-6}
Natural hazards	6	1.6×10^{-6}

The focus of this work is to increase the prevention to seismic hazard by means of a fast structural assessment tool for URM, in a way that retrofitting possibilities (technical prevention) could be easily re-evaluated and risk quickly recalculated. In section 5 assessment procedures for existing structures are overviewed.

3 SEISMIC HAZARD

From seismic intensities, equivalent demand forces are obtained to be input into the structure analysis methods and structural safety could be evaluated. The goal of this section is to address how these equivalent forces are obtained as a function of the seismic hazard parameters.

Seismic related hazards are of relevance since their consequences in terms of causalities and economic losses could be devastating as explained on section 2. Seismic hazards are not only those related directly with the ground shaking on structures, but, in second order there are those natural events triggered by a seismic event such as soil liquefaction, landslides and tsunamis, and those in relation to structural failure hazard that can turn out into fire, nuclear crisis, etc. Major magnitude seismic events, are a consequence of the tectonic plate dynamics. On boundaries of major tectonic plates and at local fault systems, the sudden rupture in the Earth's crust release energy in terms of seismic waves. The rupture is due to high stresses developed from the relative displacement of plates.

The point where the rupture begins is called hypocenter or seismic source, and its projection to the earth surface is called epicenter. The waves generated at the source propagate through different layers of rock and soil. In the propagation path, waves are filtered and amplified (or attenuated) according to the terrain characteristic. Records at the surface represent not only the characteristics of the source and fault mechanism, but also the bedrock and overlaying layer properties [To 99].

The seismic waves are characterized in terms of their propagation; the main categories are body (figure 3.1) and surface waves [Kr 96]. The body waves are those that travel through the interior of the earth. They are subdivided into compression or primary *p-waves* and secondary or shear *s-waves*; the names are due to the first ones having a faster propagation velocity. The *p-waves* travel by compressing and rarefacting the material; meanwhile *s-waves* cause shearing deformation. Surface waves results from interaction in between body waves and the earth surface. *s-waves* and *p*-waves propagation velocities parameters are used commonly to characterize building foundation materials (figure 3.2). Seismic provision, like the EC-8.1, commonly define a soil coefficient to be applied on the seismic force computation according to the soil type described by the shear wave velocity; in case for the EC-8.1, the velocity in the first 30 meters V_{s30} [EC-8.1].

Events with origin directly between the boundaries of tectonic plates are called interplate; meanwhile, intraplate is the denominations for those events located in the interior of the tectonic plate and are the ones related to local faulting systems. From a practical engineering point of view, structures are designed typically for 475 year return periods; the faults that have exhibited no deformation (and hence no capacity to generate stress in the rock up to rupture) within the last 11,000 years are considered as "not active"; nevertheless, criteria is stronger for special structures like nuclear power plants where the period could be up to 500,000 years [To 99].

Intraplate earthquakes are expected not to develop the very strong earthquakes such as the interplate ones; but, the proximity of a local active fault to populated areas, the shadow depth of the hypocenter, plus the long period of recurrence of the events makes then particularly dangerous. L'Aquila earthquake 2009 is example of a destructive intraplate earthquake.

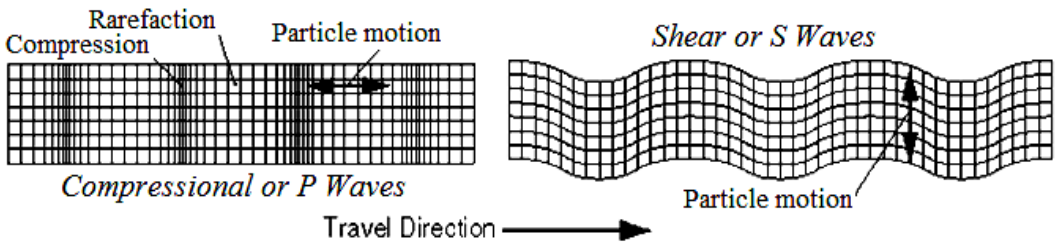

Figure 3.1: Body waves motion description

Material	p-waves (m/s)	s-waves (m/s)
Sand	300-900	100-500
Clay	400-2000	100-600
Sandstone	2400-4300	900-2100
Limestone	3500-6500	1800-3800
Granite	4600-7000	2500-4000
Basalt	5400-6400	2900-3200

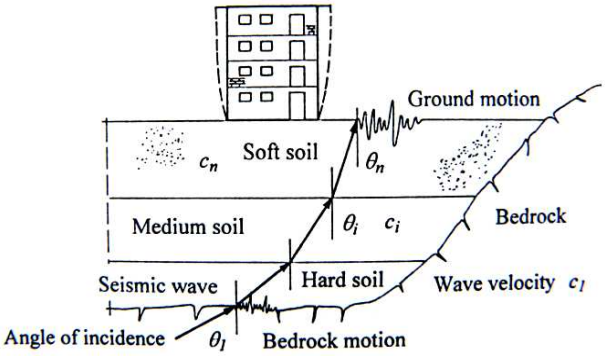

Figure 3.2: Body waves travel velocities and wave propagation to surface [To 99]

3.1 Description of Earthquakes

In earthquake engineering, seismic characteristics are distinguished into parameters in relation with the seismic source and the result ground motion at a specific site. The earthquake magnitude is a quantification of activity at the source; in contrast, the intensity is a qualification of vibration at a specific site. A review of these aspects is develop in these section based on Kramer textbook [Kr 96].

3.1.1 Magnitude

The measure of the energy released at the source is called magnitude *M*. There are different types of magnitudes. The first was proposed by Richter and therefore is called "Richter magnitude", also refered as local magnitude *M*. It's given by the logarithm of maximum amplitude *A* (in μm) of displacement recorded by a Wood-Anderson seismometer located at 100 km from the epicenter.

$$M = \log_{10} A \qquad \text{Eq [3-1]}$$

Since the instrument is never located exactly at the mentioned distance, the magnitude is computed from modifications according to epicentral distance and the wave propagation characteristics. In earthquake records, arrival times from different waves types can be distinguish. Based on this, the body wave magnitude m_b and the surface wave magnitude M_S are defined. Moreover, the energy magnitude M_E (related to the wave energy) and the moment magnitude M_O (related to the seismic moment) are other magnitudes used to describe earthquakes. A comparison between magnitudes is presented by Kramer [Kr 96]. The *M* is linked with released energy by Eq(3.2); there, energy is enlarged ≈32 times by each increased magnitude unit [GR 54].

$$\log_{10} E = 4.8 + 1.5M \qquad \text{Eq [3.2]}$$

The parameter that is more closely related to the physical seismic strength of earthquakes is the moment magnitude M_O, and it's usually used to describe seismic potential of faults and strong quakes magnitude description. In equation 3.3, G_m is the material shear modulus near the rupture area A_f, and D_{sf} the average amount of slip over the fault plane.

$$M_O = G_m L_f D_{Sf} \qquad \text{Eq [3.3]}$$

3.1.2 Intensity and intensity scales

The observed level of damage concerning to people, property and nature due to earthquakes at a specific site, describes the seismic intensity. Seismic intensity is measured by means of various intensity scales. A 12-grade Mercalli-Cancani-Sieberg MCS scale has been used in Europe since the beginning of the 20th century [To 99], a 12-grade modified Mercalli MM scale is use in USA, a 7-grade scale proposed by the Japanese Meteorological Agency JMA is use in Japan and finally the 12-grade Medvedev-Sponheuer-Karnik MSK scale is used and referenced in many actual seismic codes in Europe. The advantage of the MSK scale is that it presents well defined building typologies; this brings into a better estimation of the intensity due to the fact the different building types present different vulnerabilities (figure 3.3). The new 12 grade European macroseismic scale EMS-98 [Gr 98] is a modification of the MSK scale.

Classification of damage to masonry building				
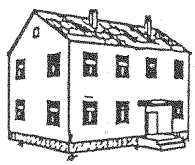		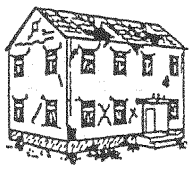	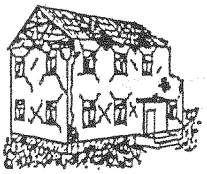	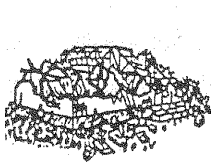
Grade1: Negligible to slight damage. No structural damage.	Grade 2: Moderate damage. Slight structural damage, moderate non- structural damage.	Grade 3: Substantial to heavy damage. Moderate structural damage, heavy non-structural damage	Grade 4: Very heavy damage. Heavy structural damage, very heavy non-structural damage	Grade 5: Destruction. Very heavy structural damage.

Type of masonry	Vulnerability Class					
	A	B	C	D	E	F
Rubble stone, field stone						
Adobe (earth-brick/terracotta)						
Simple stone						
Massive stone						
Unreinforced brick/concrete block						
Reinforced brick with RC floors						
Reinforced brick (confined masonry)						

Figure 3.3: EMS-98 Seismic damage levels and vulnerability classes for masonry buildings (Adapted from [Gr 98])

For the EMS-98 the definitions are based on: a) effects on humans, b) effects on objects and nature (excluding damage to buildings, and effects on ground and ground failure), and c) damage to buildings. For the EMS-98, the damage for reinforced concrete and the masonry structures are detailed (e.g. figure 3.3 for masonry buildings). The risk concerning each different masonry building's typology vulnerability is detailed also in figure 3.3. Its observable, that URM presented vulnerabilities from A to D. Table 3.1 described in detail the EMS-98 scale levels as this is going to be the seismic scale used in this study.

There are many parameters that are used to capture intensity of the seismic activity on a specific site, since damage, itself, cannot be used as a design parameter unless it is correlated with variables used in design (accelerations, forces, displacements).

Parameters had been commonly computed from a time history ground motion records. Ground motion parameters are acceleration, velocity and displacement. The maximum amplitude values for this time histories records are called peak ground acceleration PGA or a_g (figure 3.4), peak ground velocity PGV and peak ground displacement PGD.

Table 3.1: EMS-98 seismic intensity scale description [Gr 98]

EMS-98 Intensity	Definition	Description of typical observed effects
I	Not felt	Not felt
II	Scarcely felt	Felt only by very few individual people at rest in houses
III	Weak	Felt indoors by a few people. People at rest feel a swaying or light trembling
IV	Largely observed	Felt indoors by many people, outdoors by very few. A few people are awakened. Windows, doors and dishes rattle
V	Strong	Felt indoors by most, outdoors by few. Many sleeping people awake. A few are frightened. Buildings tremble throughout. Hanging objects swing considerably. Small objects are shifted. Doors and windows swing open or shut
VI	Slight damaging	Many people are frightened and run outdoors. Some objects fall. Many houses suffer slight non-structural damage like hair-line cracks and fall of small pieces of plaster
VII	Damaging	Most people are frightened and run outdoors. Furniture is shifted and objects fall from shelves in large number. Many well build ordinary buildings suffer moderate damage: small cracks in wall, fall of plaster, parts of chimneys fall down; older buildings may show large cracks in walls and failure of fill-in walls
VIII	Heavily damaging	Many people find difficult to stand. Many houses have large cracks in walls. A few well build ordinary buildings show serious failure of walls, while weak older structures may collapse
IX	Destructive	General panic. Many weak constructions collapse. Even well built ordinary buildings show very heavy damage: serious failure of walls and partial structure failure
X	Very Destructive	Many ordinary well built buildings collapse
XI	Devastating	Most ordinary well built buildings collapse, even some with good earthquake design are destroyed
XII	Complete devastation	Almost all buildings are destroyed

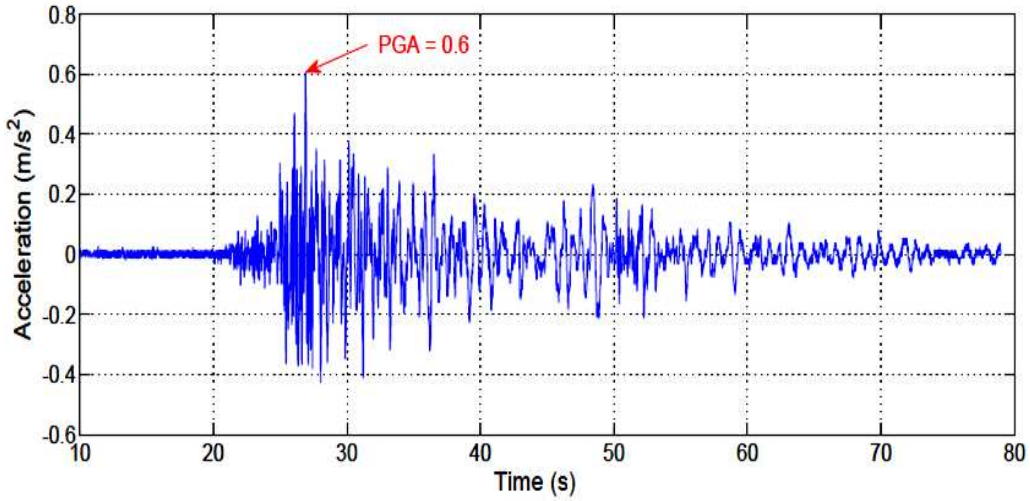

Figure 3.4: Acceleration time history record of the Cinchona earthquake of 2009 (Costa Rica) [LIS web]

The PGA is often considered the parameter to determine the earthquakes intensity because it presents good correlation with the forces acting on the building. The PGA value had been therefore related with the intensity levels described by intensity scales as shown in figure 3.5.

From the time history (figure 3.4), another important aspect to the seismic intensity is the ground motion duration. Many physical processes related to the number of cycles, such as degradation of stiffness drift into higher damage levels. The significant duration D_{s95}, is defined as the time between the 5% and 95% of the Arias intensity I_A. The I_A is a measure of the strength of ground motion; it is computed directly from the time history as the time-integral of the square of the ground motion acceleration:

$$I_A = \frac{\pi}{2g}\int_0^{T_d} a(t)^2\,dt \qquad \text{Eq [3.4]}$$

where g is the gravity acceleration (9,8 m/s) and T_d is the duration of the record. The Arias intensity is used to compare and scale ground motions.

It is also useful to present ground motion measurements in terms of their frequency content. The discrete Fourier transform of the data presented in figure 3.4 is shown on figure 3.6. From the figure, it is evident the predominance in the signal of a frequency around one hertz. Buildings with a natural frequency close to the ground motion frequency peaks are expected to suffer a higher structural response because of a resonance effect. The first fundamental period of vibration T_1 for lateral motion in case of a masonry structures, of total height H_T, is computed according to EC-8.1 [EC-8.1] as:

$$T_1 = 0.05H_T^{3/4} \qquad \text{Eq [3.5]}$$

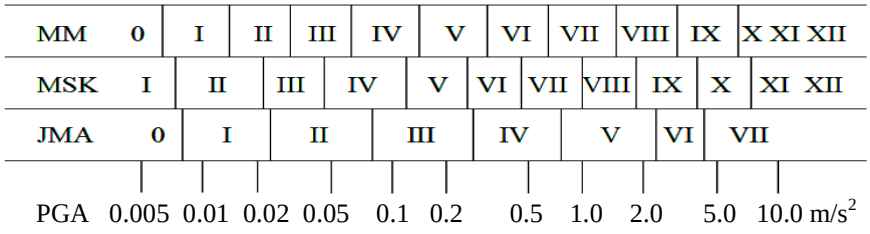

Figure 3.5: Relationship in between seismic scales and PGA [P-C 08]

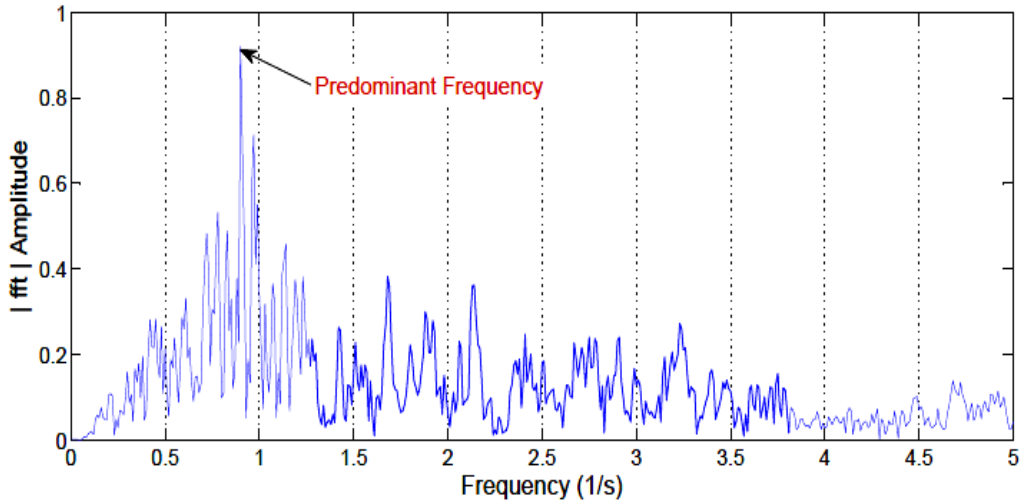

Figure 3.6: Frequency content of the Cinchona earthquake of 2009 (Costa Rica)

3.1.3 Occurrence of earthquakes

Earthquakes prediction of a seismic event occurrence at a given location needs further studies and observations [To 99]. Generally, for current earthquake engineering practice, the seismic hazard for a site is determined according to observation of historical events for a time interval. The return period R_P, is the estimate time in between two events of a determinate (or greater) magnitude. The term is widely used for seismic hazard analysis. The probability of occurrence of an earthquake with a return period R_P in one year is:

$$P_1 = \frac{1}{R_P} \qquad \text{Eq [3.6]}$$

The probability of not occurrence in the same year is consequently 1-P_1. This relation could be used to calculate probabilities of occurrence for longer period of time. The probability that an earthquake of given or greater magnitude will occur in a time interval T_V is given by:

$$P_{T_V} = 1 - (1 - P_1)^{T_V} \qquad \text{Eq [3.7]}$$

The value of T_V is usually the life span of the designed structure. According to Equation 3.7, any probability of occurrence for a determinate life span could be represented in terms of the return period of the earthquake magnitude. Recommended R_P values according to different structural performance limit states (section 3.4) are presented in table 3.2 according to actual Italian normative [NTC-09]. Common structures (residence, office, type II for the Italian normative) are usually designed to a life safety limit state and for a reference PGA with a probability of exceedance of 10% within a period of 50 years; it could be found from equation 3.7 or by inspection of table 3.2 that the R_P value is of 475 years.

Table 3.2: Return period R_P of seismic actions at different limit states and reference design periods T_V [NTC-09]

Expected life interval T_V = 10 years									
Importance/ Use class		I	II	III	IV	I	II	III	IV
LS**	P_{Ref} *	R_P in years				P_{50} %			
OLS	0.81	21	21	21	21	91	91	91	91
DLLS	0.63	35	35	35	35	76	76	76	76
LSLS	0.1	332	332	332	332	14	14	14	14
CPLS	0.05	682	682	682	682	7.1	7.1	7.1	7.1

Expected life interval T_V = 50 years									
Importance/ Use class		I	II	III	IV	I	II	III	IV
LS**	P_{Ref} *	R_P in years				P_{50} %			
OLS	0.81	21	30	45	60	91	81	67	56
DLLS	0.63	35	50	75	100	76	63	48	39
LSLS	0.1	332	475	712	949	14	10	7.0	5.0
CPLS	0.05	682	975	1462	1950	7.1	5.0	3.4	2.5

Expected life interval T_V = 100 years									
Importance/ Use class		I	II	III	IV	I	II	III	IV
LS**	P_{Ref} *	R_P in years				P_{50} %			
OLS	0.81	42	60	90	120	69	56	43	34
DLLS	0.63	70	100	150	200	51	39	28	22
LSLS	0.1	664	949	1424	1898	7.3	5.1	3.5	2.6
CPLS	0.05	1365	1950	2475	2475	3.6	2.5	1.7	1.3

**Common referenced probability values are in the shaded boxes. **For LS refer to section 3.4.*

3.2 Approaches for Computing the Seismic Action

Regarding earthquake demand safety assessment, two principles are used: The deterministic safety concept, also referred in this work as deterministic seismic hazard analysis (DSHA), uses the already known seismic sources near a specific site, and historical earthquake and geological data to create a discrete, single-valued events or models of the ground motion at the site [Fl 07]. On the other hand, the probabilistic seismic hazard analysis (PSHA), aims to deal with uncertainties such as the location, size and the resulting shaking intensity to produce a description of future events that may occur at a site. The results of a PSHA are more suitable to assess seismic risk since the risk is time-dependent conveniently expressed in terms of annual probability of exceeding some level of earthquake shaking for a range of intensities and for the difficulties in DSHA to characterize the critical event possible at the site.

Uncertainties regarding the seismic hazards are those related directly with the source, such as: faulting type, rupture area, location, magnitude, constitutive materials; those related to the wave path like distance from hypocenter, regional soil type, and attenuation/amplification; and finally those related to local soil site conditions and topography.

3.2.1 Deterministic seismic hazard analysis (DSHA)

The DSHA is proposed on the condition of choosing the worst-case earthquake scenario. In practice, this can be difficult and is not exempt for a subjective character due to variability in magnitude and intensities [Ba 08].

A typical DSHA approach consist of four steps according to Flesch [Fl 07]: identification and characterization of all sources, selection of a source-site distance parameter, selection of controlling earthquake and finally definition of hazard using the control earthquake.

The use of DSHA is of some significance still for the design of special structures such as nuclear power plants, large dams or bridges and hazardous waste disposal facilities. Typically one or more earthquake simulated time histories are presented for a site; the motion is estimated deterministically by a given magnitude, source distance and site conditions. Also existing scaled normative historic time series and artificial time history (generated to match the elastic response spectra [EC-8.1]) are used as input for dynamic analysis. Seismic codes establish a minimum of ground motions to be used, usually in between 3 and 5 as summarized by Nguyen [Ng 06]. In practice, big dispersion in the structural response is still observed up to 7 records; this is dependent on the analyzed structure characteristics [Ok 01].

3.2.2 Probabilistic seismic hazard analysis (PSHA)

The PSHA aims to deal with uncertainties about location, size and frequency in earthquakes to produce an explicit description distribution of future shaking that may occur at the site. As mentioned before, this procedure is more suitable to seismic risk assessment criteria as results are presented in terms of probabilities of occurrence or exceedance of a determinate seismic action.

Figure 3.7 reveals that observations scatter significantly about the predicted values presented by the attenuation curve. Attenuation curves describe how the ground motion action reduces due to distance D_S from the source. Attenuation curves shown in figure 3.7 where computed by Boore attenuation relationship for strike slip earthquakes on firm soil site [BJF 97]. The points are data observed in southern California for events within 0.2 of each magnitude (e.g. 6.0 ±0.2 on figure 3.7). Probability density functions (PDFs), could be computed at a determinate distance and magnitude for taking into account uncertainties. Log-normal PDFs are accurately at assessing the problem.

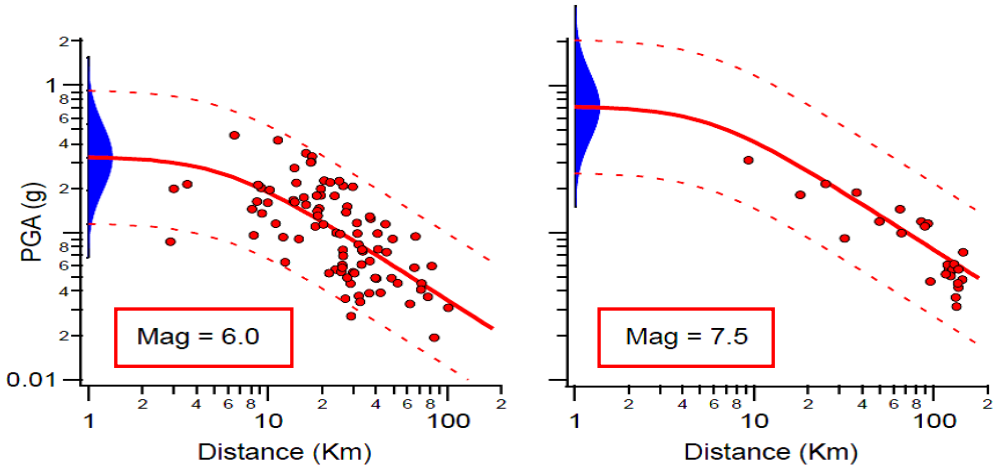

Figure 3.7: Attenuation curves for events observed for south California and PGA PDFs [Fi 10]

In PSHA procedure, all possible earthquake events and resulting ground motions are considerated, along with their probabilities of occurrence. A basic PSHA consist of 5 steps according to Baker [Ba 08]:

1- *Identify all earthquake sources capable of producing damaging ground motions*
2- *Characterize the distribution of earthquake magnitudes (rates at which earthquakes of various magnitudes are expected to occur)*
3- *Characterize the distribution of source-to-site distances.*
4- *Predict the resulting ground motion intensity as a function of earthquake magnitude, distance, etc*
5- *Combine uncertainties in earthquake size, location and ground motion intensity, using the calculation known as the total probability theorem.*

The source-to-site curves are obtained according to the source area and the closest distance to the fault. This parameter takes into account the occurrence of the rupture among any point in the fault longitude, plus, the area source deals with the uncertainty that arise when faults near a site are not clear, so that, earthquake are possible to occur at any location of the area source. The five steps of the PSHA are summarized in figure 3.8. The seismic hazard curve generated by Rota [RPM 08] for L'Aquila city is shown in figure 3.8(e). This curve is used later on for the computation of risk for Castelnuovo town due to its proximity to L'Aquila city.

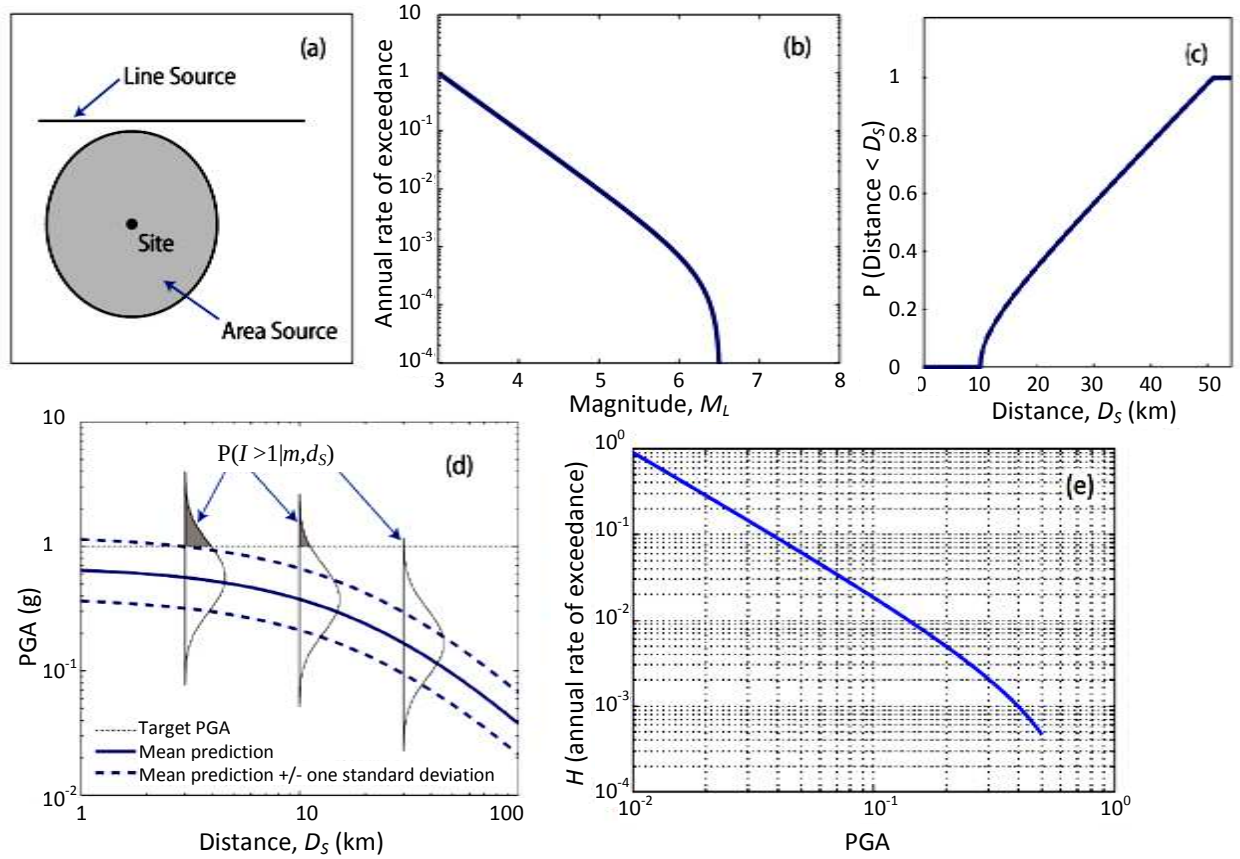

Figure 3.8: The five steps of PSHA: a) identify earthquake sources, b) characterize magnitudes from each source, c) characterize source-to-site distances for each source, d) resulting distribution of ground motion intensity [Ba 08], e) final obtained annual rate or probability of occurrence of earthquakes H, here the curve for L'Aquila city [RPM 08]

A detail explanation for obtaining each step parameters is presented by Baker [Ba 08] and Kramer [Kr 97]. To combine all the information from steps 1 to 4 in other fulfill step 5, the total probability theorem can be used [PGF 04][Ba 08], so that the $P\{I > i\}$ or the probability of intensity (*i)* exceeding a determinate intensity *I* is:

$$P\{I > i\} = \int_{m_{\min}}^{m_{\max}} \int_{0}^{d_{S\max}} P(I > i | m, d_S) f_M(m) f_{D_S}(d_S) dd_S dm \qquad \text{Eq [3.8]}$$

where equation 3.8 is a particular formulation for Pinto general expression [PGF 04]. *I* represents the value of measurable intensity factor (usually PGA), $P(I>i|m,d_S)$ comes from the ground model prediction (figure 3.8d), $f_M(m)$ and $f_{Ds}(d_S)$ are PDFs for magnitude recurrence (for an activity rate per year) and distance (steps b and c, figure 3.8). $P(I>i|m,d_S)$ is the probability of having intensities bigger than *i* (e.g. *i*=1 in figure 3.8d), could be easily computed for each magnitude and distance with the use of its cumulative density function CDF, described with the operator $\phi(\cdot)$.

$$P\{PGA > x | m, d_S\} = \int_{x}^{\infty} \frac{1}{\sigma_{\ln PGA}\sqrt{2\pi}} \exp\left(-\frac{1}{2}\left(\frac{\ln x - \ln \overline{PGA}}{\sigma_{\ln PGA}} \right)^2 \right) dx$$

or

$$P\{PGA > x | m, d_S\} = 1 - \Phi\left(\frac{\ln x - \ln \overline{PGA}}{\sigma_{\ln PGA}} \right) \qquad \text{Eq [3.9]}$$

Where $\ln\overline{PGA}$ is the mean calculate PGA value for the respective *M* and D_S conditions obtained from proposed attenuation curve and $\sigma_{\ln PGA}$ is the standard deviation in the log space ($\sigma_{\ln PGA} \approx$ 0.5 [Fi 10]) that is considered constant for all magnitudes and distances; values of 0.37 are reported by Campbell [Kr 97]. It is of special interest to obtain $P\{I > i\}$ in terms of a mean annual rate of exceedance; this is obtained by multiplying equation 3.8 by the mean annual rate of events per year λ_O (earthquakes per year of any magnitude) so that:

$$\lambda(i) = \lambda_O P\{I > i\} \qquad \text{Eq [3.10]}$$

According to Pinto [PGF 04], under the assumption that a Poisson process describes the temporal sequence of events and considering that, in the seismic case, one has to deal with small rates of $\lambda(i)$ (λ_O = 1). A good approximation of the annual probability of exceedance is:

$$\lambda(i) \approx P\{I > i | 1 year\} = H(i) \qquad \text{Eq [3.11]}$$

The approximate annual probability of exceedance *H(i)* is well described by a negative exponential so that:

$$H(i) = k_O i^{-k} \qquad \text{Eq [3.12]}$$

Where k_O and *k* are constants obtained from the attenuation curves [PGF 04]. For L'Aquila *H* is presented in figure 3.8e, the values are k_O = 0.0005 and *k* = 1.63. These are the values used in this study for the computation of the seismic risk in chapter 7.

3.3 Response Spectra and Seismic Coefficient

Most of the data needed for earthquake resistance verifications and design is obtained by means of the response spectra [Ne 82]. The response spectrum is defined as the relationship between the maximum responses of a single degree of freedom (SDOF) system to a given ground motion and the system's natural period of vibration ($2\pi/\omega$), and a damping ratio [CP 93]. A parameter derived from the response spectra is called the seismic coefficient C_S. The C_S is used in the simple linear-elastic lateral force method for computing equivalent seismic forces.

An example of an elastic response spectra (ERS) computed from the time history of figure 3.4 is given in figure 3.9. The spectral acceleration is approximately equal to the so called pseudo-acceleration Sp_a [Ch 01], which is usually the one presented in seismic codes.

Elastic response spectrum curves are standardized on seismic codes according to statistical analysis of data obtained from many response spectra for different soil profiles as observed in figure 3.10. The top spectral value observed ($2.5a_{gR}S_S\eta\gamma_I$) is linked with the reference peak ground acceleration a_{gR}, the design acceleration a_g (equal to $a_{gR}\gamma_I$), the damping coefficient η (=5%), a soil parameter S_S, and the importance factor γ_I as defined by EC-8.1. The inflection points of the spectrum at T_B, T_C and T_D are variable according the soil typologies.

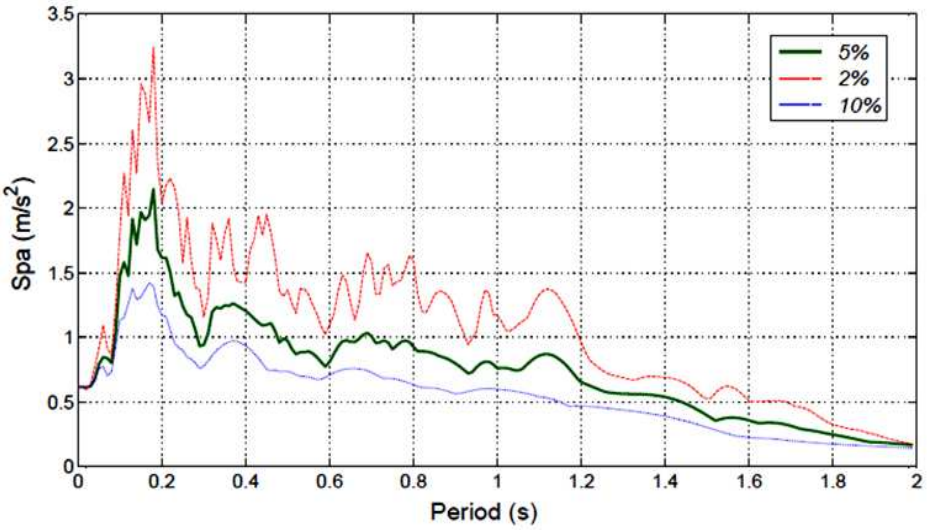

Figure 3.9: Elastic response spectrum for different values of damping ratio for Cinchona earthquake 2009 (Costa Rica)

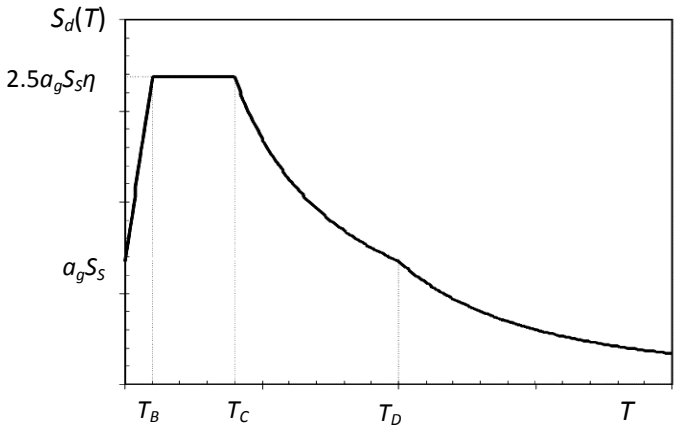

Figure 3.10: Shape of design elastic response spectrum [EC-8.1]

The reference PGA, as presented on Seismic Hazard maps in codes, is lower than the real PGA from figure 3.4 since: a) damage may not be related to one peak of acceleration but to several repeated cycles of high amplitude to be developed [MK 11], b) the peaks may be of high frequency to which most structures are not sensible, and c) statistical derivation of ERS from many seismic records. Due to this, Newmark [Ne 82] described the concept of effective acceleration as "that acceleration which is closely related to structural response and to damage potential of an earthquake".

To take into account structural non-linear behavior, the elastic response spectrum is reduced according to the structure's ductility and energy dissipation observed behavior. Concerning masonry buildings, it is important to underline that they present short natural periods of vibration, typical for rigid structures; so, most building cases of low-rise and mid-rise buildings fall into the response spectra plateau of figure 3.10, with a the natural period computed using equation 3.5.

3.3.1 Seismic action

The seismic action on the structure could be represented in various forms. They may come directly from time histories (like the ones produced by DSHA), response spectrum, and power spectra (obtained from Fourier spectra (figure 3.6)). To decide which form of seismic action is going to be used, the importance of the structure analyzed plus its structural complexity must be assessed. Taking into account the structural regularity of masonry buildings, the response spectra representation is adequate for most cases [To 99]. Since the structural response is already computed by ERS, only the effect of the load must be calculated.

As explained before, most structures presents some grade of resistance to seismic load in the non-linear range, therefore it will be too conservative to design for the elastic range. The ERS is therefore changed to take into account the non-linear capacity where, after the initial damage, the stiffness degraded with greater energy dissipation capacities (damping increased). Non-linear dynamic analyses, take into account the non-linear characteristics of masonry to precisely judge the effect of seismic loading. However, the non-linear behavior and energy dissipation capacities are usually simplified and taken into account as a reduction in response spectrum and called the seismic design spectrum (SDS). The SDS is obtained by the introduction of the so called structural factor or behavior factor q and according to equations 3.13 [EC-8.1]. Behavior factors for URM are further commented on section 4.6.3.

$0 \le T \le T_B$ $\quad S_d(T) = a_g S_S \left(\frac{2}{3} + \frac{T}{T_B} \left(\frac{2.5}{q} - \frac{2}{3} \right) \right)$ Eq [3.13a]

$T_B < T \le T_C$ $\quad S_d(T) = a_g S_S \left(\frac{2.5}{q} \right)$ Eq [3.13b]

$T_C < T \le T_D$ $\quad S_d(T) \begin{cases} = a_g S_S \frac{2.5}{q} \left(\frac{T_C}{T} \right) \\ \geq \beta a_g \end{cases}$ Eq [3.13c]

$T_D < T$ $\quad S_d(T) \begin{cases} = a_g S_S \frac{2.5}{q} \left(\frac{T_D T_C}{T^2} \right) \\ \geq \beta a_g \end{cases}$ Eq [3.13d]

where β is a bound factor for recommend by EC-8.1 of β=0.2, and S_d is the design spectrum value; a_{gR} is normally presented as a normalized value with relation to the gravitational acceleration $\alpha = a_{gR}\gamma_I$ /9.8 m/s^2.

Table 3.3: Seismic structural analysis according to structural regularity [EC-8.1]

Regularity		Allowed Simplification		Behavior factor
Plan	Elevation	Model	Linear-elastic Analysis	(for linear analysis)
Yes	Yes	Planar	Lateral force*	Reference value
Yes	No	Planar	Modal	Decreased value
No	Yes	Spatial**	Lateral force*	Reference value
No	No	Spatial	Modal	Decreased value

**Lateral force method analysis described by EC-8 section 4.3.3.2.*

***Under special conditions a separate planar model may be used in each horizontal direction.*

According to EC-8, q is also modified in relation to the allowed structural analysis methodology. Table 3.3 presents the allowed structural analysis methods according to the building's structural regularity; in the case of modal analysis q is decreased to $0.8q$. Non-linear structural static analyses, such as the pushover analysis, are widely used to describe the performance of URM. Non-linear dynamic analyses are rarely performed for structural assessment of low-rise URM because it's not justifiable for this kind of structures (excluding monumental URM). Since common static linear lateral force method is widely used for typical URM, it's the one follwed in this work for assessing the structural seismic resistance of buildings.

q is represented in different forms to modify the EDS; other norm terminologies refer to it as global assigned ductility or response reduction factors, for reductions to be applied on seismic actions. The value of S_d, in terms of α, is referred in many normative as the seismic coefficient C_S and will be explained in detail in the next sections. The variation of the C_S in URM is of importance for different seismic codes as it can be observed in figure 3.11. The value is computed according to the variation on the approximated PGA values; the approximation of a_{gR} is realized where PGA is not mentioned as a variable on C_S formulation (appendix D). C_S values for URM are high if compared with those obtained usually for steel or concrete structures thanks to the adoption of smaller q values due to URM brittle behavior. A difference for countries with low seismicity areas can be observed in seismic codes C_S values. The International Building Code (IBC) formulation, for USA, is not the reference code for high seismic risk USA areas such as California, where the SEAOC (blue book) recommendations are used, presenting much bigger C_S minimum values [SEAOC-95]. Low seismicity areas are defined by EC-8.1 as those where a_{gR} values are not bigger than $0.1g$ (the gravitational acceleration g = 9.81 m/s^2) [EC-8.1]. The equations to compute the seismic coefficients of figure 3.11 are shown in figure 3.12.

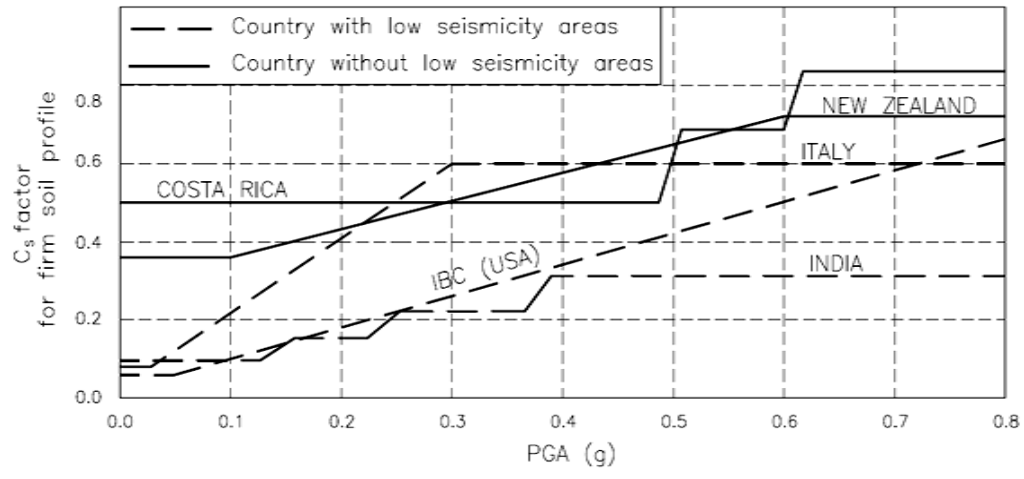

Figure 3.11: Variation of seismic coefficients according to local code formulations for URM

3.3.2 Design base shear and seismic coefficient

Once the seismic coefficient has been calculated, the total forces acting laterally along the height of the structure are expressed in terms of the design base shear force V_b. As it is observed from figure 3.12, many seismic codes described the seismic actions in terms of a seismic coefficient (C_S, C, A_h,$S_d(T_1)$) and a seismic action (S_S,a_{ef},a_{gR},Z), where the action is related to reference PGA or a seismic zone Z. Z correlates well to a PGA range. Details of each V_b calculation for the presented codes are included in appendix D.

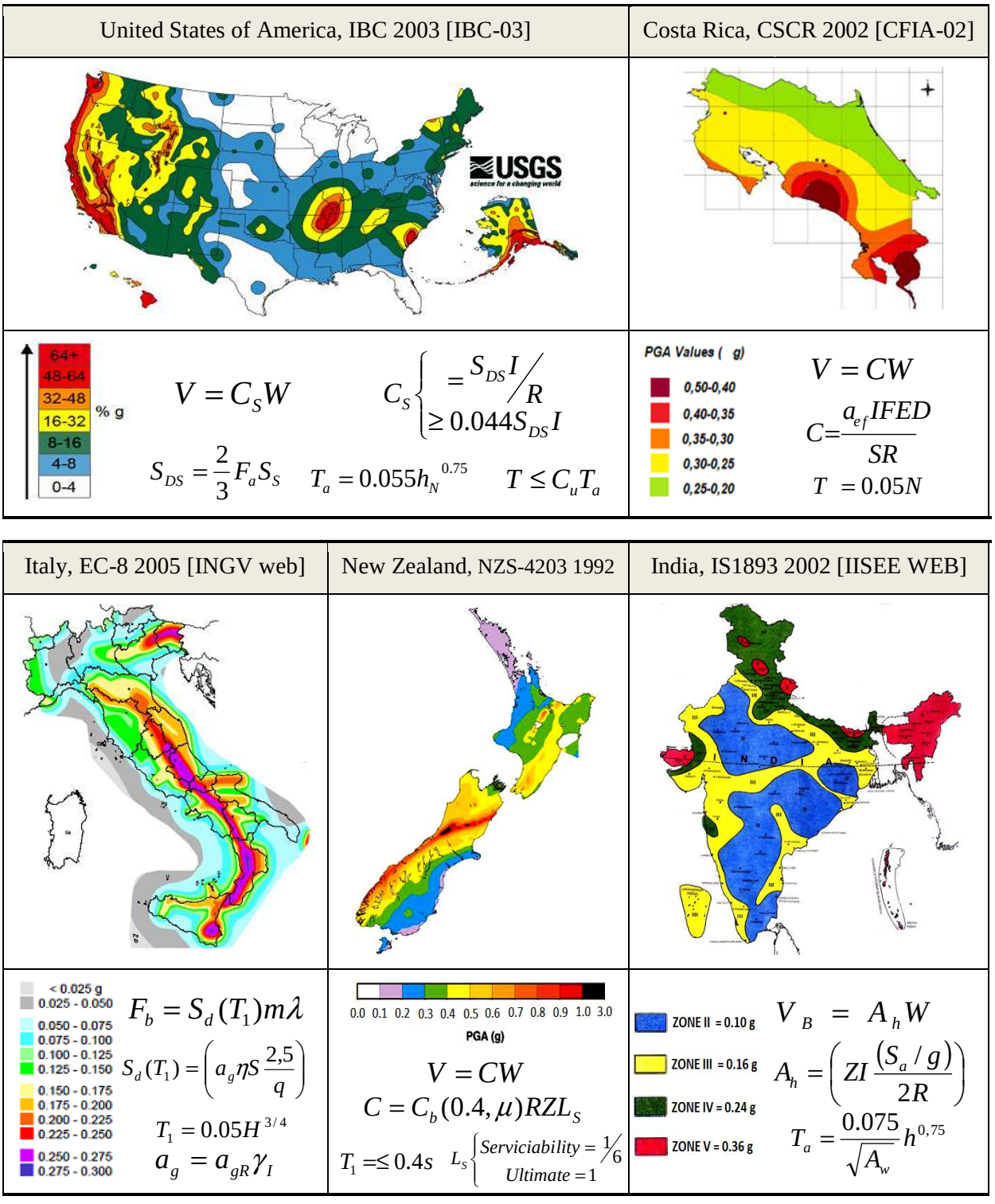

Figure 3.12: Seismic base shear for URM according to different normative

It is of importance for this study to underscore the similitude of most concepts in between existent codes worldwide for seismic design. It is one of the objectives of this work to propose a generalized methodology in terms of PGA values in order to quantify the structural vulnerability and risk (section 5.5). As observed in figure 3.12, the reference PGA is probably the parameter most used to define the seismic action worldwide by leading codes. In the case of EC-8, the V_b forces are computed as [EC-8.1]:

$$V_b = S_d(T_1)m\lambda \qquad \text{Eq [3.14]}$$

where m is the total mass of the building above the foundation or a rigid basement, and λ is a correction factor with value of 0.85 if $T_1<2T_C$ and more than 2 storeys, or 1.0 otherwise. The total weight W of the building is obtained simply multiplying m by the gravitation acceleration g so that $W=mg$. The value of W is obtained from a load combination according to local codes for self structural weight (permanent action) and a quasi-permanent action (normally called live load). For EC-8, in case of residential and office building $W=\Sigma G_k+0.3Q_{kt}+(n-1)0.15Q_{kav}$ where ΣG_k is the sum of all permanent actions of the build and Q_{kt}, is live load for the top storey, n is the total number of stories, and Q_{kav} is the live load average per storey. Sometimes it is convenient to present a normalized design base shear coefficient BSC_b:

$$BSC_b = \frac{V_b}{W} = C_S \qquad \text{Eq [3.15]}$$

The normalization concept of the base shear will be used later on for assessing out-of-plane failure of masonry walls, meanwhile other similar normalizations are prepared for solving the reliability problem $G(X)=R-S$ as observed in sections 5 and 6.

For design of different elements in structures, V_b is distributed, for the simple linear lateral force procedure, along the buildings height in terms of the first mode of vibration. This can be further simplified to a triangular distribution calculated from W_i concentrated at each storey i and its location from the foundation z_i. This is expressed by equation 3.16. The results for equation 3.16 in the case of $2.5\text{x}10^4$ different URM building created by the SHM (section 6) are shown in figure 3.13.

$$F_i = V_b \frac{z_i W_i}{\sum_{j=1}^{n} z_j W_j} \qquad \text{Eq [3.16]}$$

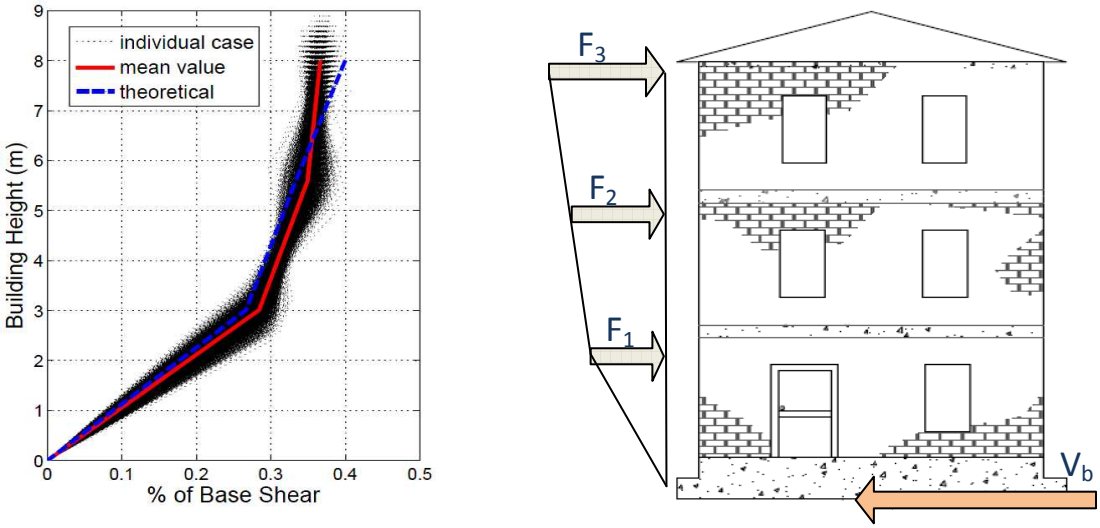

Figure 3.13: Distribution of base shear along the structure

The results from equation 3.16 are further simplified in this study according to the proposal of the Japan Building Disaster Prevention Association JBDPA, for the seismic evaluation of RC buildings [JBDPA-01]. The JBDPA and FEMA-310 [FEMA-310] proposed a story-shear modification factor $(n+1)/(n+i)$ to reduce the resistance of elements due to different force magnitudes per storey as observed in figure. The modification factor is represented $(n+i)/(n+1)$ regarding the force incremental to each story. For the three floors building in figure 3.13, the factors are 1, 1.25 and 1.5; the sum of all is 3.75; the acting force on each storey is $0.27V_b$, $0.33V_b$, and $0.4V_b$. This is represented by the theoretical curve on the graph in figure 3.13. The relation is conservative and shows a relative good agreement with the mean of individual value results on the figure.

3.3.3 Structural Irregularities

Experiences have been learned from past earthquakes regarding the influence of architectural layout on seismic behavior of masonry constructions. Buildings with regular layout, good connections and amount of resisting walls have performed well, even without earthquake resistance design [To 99]. Buildings in regulations are grouped into those who respect structural simplicity, regularity and symmetry, for which a good performance is expected, and those that present irregularities along their height and structural layout.

Structures present irregularities in elevation when there is no continuous shape of the building along its height, there is an important change in between inter-story stiffness, or when there is the presence of a mixture of structural systems and/or construction materials. This last situation is common in presence of a vertical building aggregate. Edifications are considered regular, according to EC-8.1, if irregularities in height, according their shape, are in the range delimited by figure 3.14. For structures not satisfying criteria of figure 3.14, regular linear lateral force procedure is not recommended so that a modal analysis must be perform. This kind of structures is out of the scope of this work; also buildings presenting an inverted pendulum shape are not allowed to be analyzed by simple formulations. In URM inverted pendulum structures are rare. An irregularity, regarding mixture of construction materials, in the structure is possible to assess, with the proposed methodology, meanwhile the structure stills posse's typical URM construction characteristics.

Concerning irregularities in plane (architectural layout), they are analyzed in common structures with respect the two main orthogonal axis, from now called *X* and *Y*. According to EC-8.1 [EC-8.1] the ratio *X/Y* should not be bigger than 4, were *X* is the larger longitudinal dimension of the building. This value is restricted even more in the proposed methodology (a value of 3), in order to avoid important eccentricities.

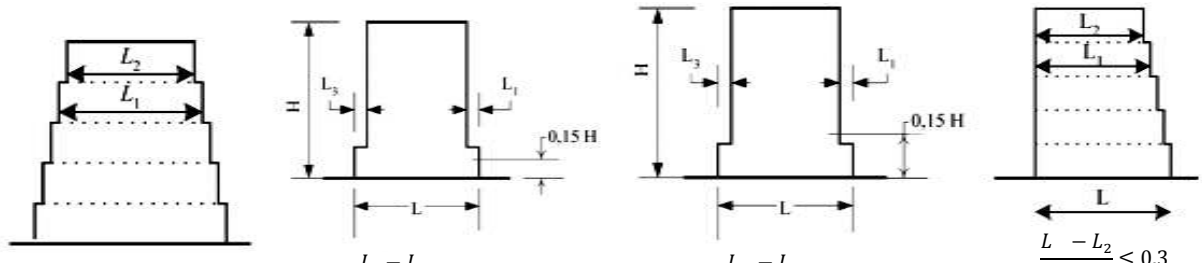

Figure 3.14: Tolerance for irregularities in building with setbacks according to EC-8.1

Structural eccentricities e_o refers to the distance in between the center mass and stiffness in a presence of a stiff/rigid floor diaphragm capable of distributing lateral forces uniformly along the structure. Thanks to eccentricity, additional forces due to torsion are added to resisting elements. For flexible building diaphragms, lateral forces are distribute to each element according to local loading, e_o is not considered any more as an acting variable, but the structure in general loses strength capacity due to the lack of joint wall action.

Regularity in plain is evaluated in terms of the structure having a limited structural eccentricity according to each normative. For simple well distributed buildings not exceeding 10 m of height and with rigid diaphragms, simple linear lateral force procedure is allowed even for irregular layout structures [EC-8.1]. For this particular case analysis, seismic actions should be increased in 1.25; in terms of the resistance, this means a reduction factor of 0.8. The reduction of elements resistance due to structural irregularity is called in the context of this study the irregularity index F_{EC}. In presence of a rigid floor slabs, the minimum value of F_{EC} should not be less than 0.8.

To accomplish the goal of presenting a fast evaluation procedure for structures, individual URM buildings are receiving a F_{EC} value up to the methodology proposed by the JBDPA. Here the F_{EC} is calculated according to the usual building characteristics as presented in figure 3.15 and equation 3.17. Description of the parameters q_i used to compute the irregularity index, are explained by the JBDPA; they take into account aspects like soft storey, building shape, expansion joints, voids in the slabs, etc. Buildings are separated into regular/irregular, and in isolated or forming part of a group. A deeper classification into inner or corner constructions is performed for buildings in a group. The values of F_{EC} presented in figure 3.15 are the ones used in this study to characterize typical layouts in URM.

$$F_{EC} = q_{1a} q_{1b} q_{1c} q_{1d} q_{1e} q_{1i} q_{1j} \qquad \text{Eq [3.17]}$$

	Building Group				Individual	
.	Regular B_{RI} and B_{RC}		Irregular B_{II} and B_{IC}		Regular B_{RS}	Irregular B_{IS}
Schematic	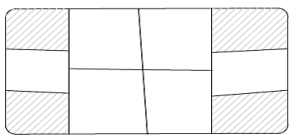		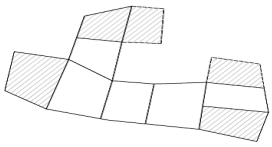		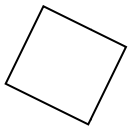	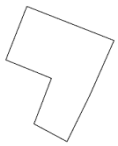
Found at Castelnuovo						
q_{1a}	1	1	1	0.9	1	0.9
q_{1b}	1	1	1	0.9	1	0.9
q_{1c}	1	1	0.9	0.9	1	0.95
q_{1d}	0.95	0.95	0.95	0.95	1	1
q_{1e}	0.95	0.95	0.95	0.95	0.95	0.95
q_{1i}	1	1	1	1	1	1
q_{1j}	1	0.9	1	1	1	1
F_{EC}	0,9	0.81	0.81	0.66	0.95	0.73

Figure 3.15: F_{EC} values for URM obtain according to JBDPA procedure [JBDPA-01]

3.3.4 Seismic action for non-structural elements

The action of the seismic forces on not resistant building components (non-structural) should be reviewed when their failure represents a hazard to people or relevant damage to important building facilities. The EC-8.1 [EC-8.1] recommends appropriate seismic analysis to be carried out using realistic models of the system and floor response spectrum derived from the primary structure, in case of important or hazardous non-structural elements. For common situations, such as walls loaded in the orthogonal direction in URM houses, the design seismic action is simplified to a horizontal force F_a acting in the center of mass of the component. The F_a formulation for a building importance factor of 1 for the non-structural member is [EC-8.1]:

$$F_a = \frac{S_a W_a}{q_a} \qquad \text{Eq [3.18]}$$

where W_a is the weight of the non-structural element, q_a is the behavior factor for non-structural elements and finally S_a is the seismic coefficient. The value of q_a is equal to 1.0 for parapets, chimneys, mast and tanks on legs acting as un-braced cantilevers along more than one half of their height. For exterior and interior walls, partitions and facades, and other non-structural elements acting as unbraced cantilevers in less than half of their height, or braced/guyed to the structure at or above their center of mass the q_a is at maximum 2.0. The S_a of non-structural elements is [EC-8.1]:

$$S_a = \alpha S_S \left[\frac{3\left(1 + {z_a}/{H_T}\right)}{\left(1 + \left(1 - {T_a}/{T_1}\right)\right)} - 0.5 \right] \geq \alpha S_S \qquad \text{Eq [3.19]}$$

where α is, as commented before, the reference PGA divided by g, z_a is the distance from the ground to the mass center of the analyzed component, H is the total height of the building and T_a is the fundamental period of vibration of the non-structural element. The first natural period for walls is obtained from equations 3.20 to 3.22 [BP 09].

$$T_a = \frac{2\pi}{\omega_1} \qquad \text{Eq [3.20]}$$

$$\omega_1 = \frac{\pi^2}{H_i^2} \sqrt{\left(\frac{EI}{m} \left(1 - \frac{N}{N_{crit}} \right) \right)} \qquad \text{Eq [3.21]}$$

$$N_{crit} = \pi^2 \frac{EI}{H_i^2} \qquad \text{Eq [3.22]}$$

where E is the elastic modulus of the material, I is the moment of inertia of the wall and is equal for an unitary length to: $t^3/12$, t is the thickness of the wall, m is the mass per length unity $t\gamma/g$, γ is the material density, H_i is the height of the storey analyzed, N is the normal force acting on the wall, N_{crit} is the critical Euler normal force (second moment maximum load) and finally ω_1 is the natural angular frequency. A summary of seismic action proposals according to different code regulations, apart from EC-8.1 reviewed here, are found in the work of Menon [MM 08].

3.4 Performance Requirements

After the occurrence of important earthquakes in the 90's such as Kobe 1995 and Northridge 1994, scientist and engineers improve their knowledge about seismic design safety criteria and upgrading of existing buildings aspects. As a result, the need for a new generation of seismic design led to the development of performance-based engineering [MOIT 03]; with life-safety, reparability and functionality as the framework issues of design.

This concept came into the definition of the so called structural limit states (LS) to evaluate the structure performance over different demand magnitude events. Limit states are usually separate into two different groups: the ultimate limit state (ULS) and the damage limitation (serviceability) (SLS) as mentioned in the EC-8.1. Furthermore, ULS and SLS are subdivided according to the performance criteria. At EC-8 part 3 [EC-8.3] the LS are defined as near collapse, significant damage and damage limitation LS; the definition of no-collapse LS described on EC-8 part 1 is similar to the one of significant damage proposed on EC-8 part 3 generating confusion about the limit state formulation; in addition, in near collapse LS there a 2475 return period event (2% fail probability in 50 years) is proposed so the verification asked for this seismic level does not represent a realistic situation for design of normal structures and is incoherent with the not collapse request on part 1 of EC-8 when the common R_P of 475 is described.

Due to these reasons, the limit states are described in this work as they are formulated in the Italian normative [NTC-09] which present four clear LS. For SLS the LS are: fully operational limit state (OLS) (facility continues in immediate operation with negligible damage) and the damage limitation/functional (DLLS) (facility operate with minor damage and disruption of non-essential services). For USL, the LS are defined as: life safety limit state (LSLS) (life is substantially protected and damage is moderate) and near collapse or collapse prevention limit state (CPLS) (life is at risk, damage is severe but structural collapse is prevented). R_P of seismic actions for the different explained LS were presented in table 3.2. These LS definitions are essentially the same discrete states proposed by the Vision 2000 committee [SEAOC-95]. Performance criteria present correlation to damage levels (figure 3.3). Damage is typically quantified in terms of story drift values Δ (figure 3.16).

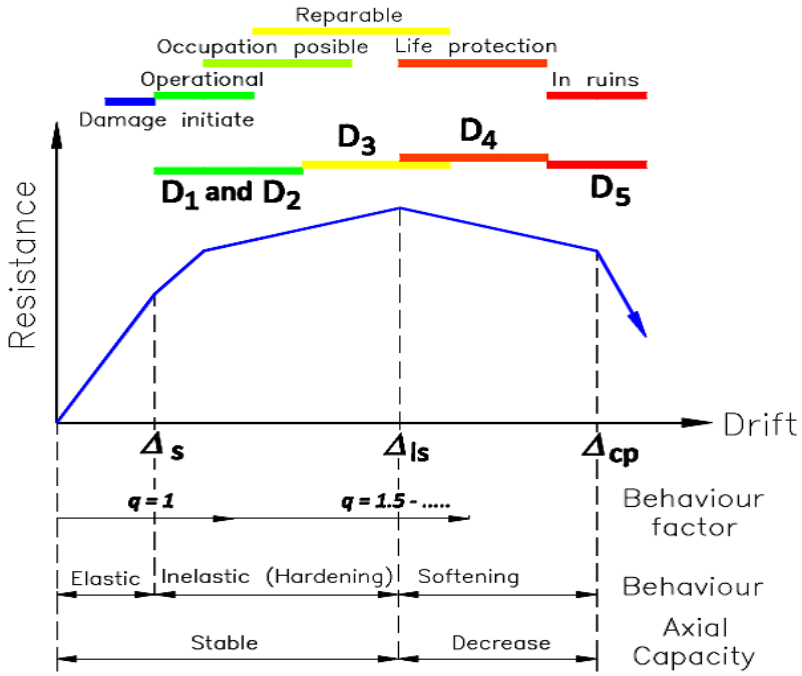

Figure 3.16: Performance and damage states for URM (modify from [BBŽ 08] and [AFPS 10])

Table 3.4: Drift values limitations for URM [NTC-09] and values obtain for different normal forces *N* for cement-lime URM [BBŽ 08]

Limit State		Δ (%) [NTC-09]	Δ (%) Moderate *N* [BBŽ 08]	Δ (%) Low *N* [BBŽ 08]
Damage limitation limit state SLS	OLS	0.2	0.1	-
	DLLS Δ_S	0.3	0.1 – 0.5	-
Ultimate limit state ULS	LSLS Δ_{LS}	0.4 rocking and 0.6 shear	0.6 - 0.7	0.9
	CPLS Δ_{CP}	-	0.8 – 0.9	1.8

Description of a structure in terms of its performance is very useful so that potential damages are more accurately quantified in terms of possible losses related to each damage level.

Drift is a basic concept used in earthquake engineering to describe maximum lateral displacement of the story δ related to a limit state (damage) and the total height at storey *i*, so that the drift is computed as $\Delta(\%)=\delta/h_i$. Typical drift value limitations according to Italian normative [NTC-09] are presented on table 3.4 and compared with values obtained for URM with cement-lime mortar for different normal loading [BBŽ 08]. Normal loading magnitude is highly related to the failure mode of masonry from ductile rocking/flexural to brittle one as it is explained in section 4.5.2.

The typical drift values according to different limit states, Δ_S, Δ_{LS}, and Δ_{CP} as observed on figure 3.16, and refereed for new structures. In existing URM this value could present big dispersion, other similar values of drift for URM are presented by Costley for flexible slab URM [CA 95] and Calvi for a displacement-based seismic assessment of building [Ca 99].

q, as used in common linear force methodologies, can be associated to a drift limit value (figure 3.16). Different values of *q* can be assigned according to failure modes described on section 4.5.2. A value of $q = 1$ is used to quantify in this study the SLS which corresponds directly to $S_d(T_1)$ values obtained in the elastic response spectrum; values up to 2,5 may be used in URM for to describe the non linear behavior of the structure for the LSLS. The increment of *q* values is consequent to increments of damping and ductility [Ca 99]. Performance is intended to be correlated with damage. To compare LS results from studies worldwide, uniform damage equivalences is needed. Till proposed the equivalences shown in table 3.5 [TR 08]. A correlation with figure 3.16 is not found entirely for the relevant life safety and near collapse damage states, or they are not clear (non continuous line). In this study D3 is considered equal to life safety from HAZUS.

Table 3.5: Damage state equivalence description for URM (adapted from [TR 08])*

HAZUS [HAZUS 99]			Slight		Moderate		Extensive		Complete			
FEMA-356 [FEMA-356]		Operational		Immediate occupancy	Life safety		Collapse prevention					
Vision 2000 [SEAOC-95]	Fully operational		Operational		Life safety		Near collapse		Collapse			
EMS-98t [Gr 98]		Grade 1			Grade 2		Grade 3		Grade 4		Grade 5	
GNDT [GNDT-07]		Light			Moderate-significant				Very significant			
RISK-UE [MT 03]	D0: None	D1: Minor			D2: Moderate		D3: Substantial to heavy		D4: Very heavy		D5: Destruction	
Equivalence figure 3.16		$\approx \Delta_S$				$\approx \Delta_{LS}$			$\approx \Delta_{CP}$			

* *Non continuous line were equivalences can vary in a small range.* [t] *Refer to figure 3.3 for a complete description.*

4 UNREINFORCED MASONRY BUILDINGS URM

Unreinforced masonry buildings URM consist of structures in which there is no steel reinforcing within the walls or any sort of confinement to masonry such as reinforced concrete frames. URM is found in many regions around the world since masons had been used from ancient times in constructions. Their variety types and material components are very wide, even for the same region, making this particular structure one of the most complicated to analysis. Due to this, simple analysis methodologies are not recommended for URM with flexible diaphragms as mentioned by FEMA-310 [FEMA-310]. In many occasions URM were constructed, and are even still constructed, without technical provisions (especially in developing countries). In most occasions, masonry structures represents a majority of common house stock that have been constructed before the introduction of the seismic codes; this, due to the fact that masonry constructions have greater periods of removal when compared with other much temporal structures such as those made of timber.

4.1 Typologies and Seismic Performance

According to material disposition, climate, functional requirements, technical knowledge and traditional practices specific to a region, different masonry typologies can be found [To 99]. Their response to natural event actions, such as earthquakes, depends on the type of the singularities of constructions and materials. URM was usually found to be highly vulnerable to seismic actions after past earthquake damage experiences as shown in table 4.1. Vulnerable behavior is expected due to the brittle performance, out-of-plane failure mode, and the URM non-engineered building condition. This last aspect is not always certainly true. For some old URM build on basis of tradition and experience, a good seismic behavior had been observed, even when other recent constructed buildings had collapsed [To 99]. In figure 4.1 a traditional stone URM with rubble walls, heavy stone roof and other stone components is compared with a new single layer clay brick, light roof and rigid diaphragm house. The response to lateral actions is evident to be quite different for each one. On this study, special interest is paid to rubble stone buildings. About 90% of the building stock at the analyzed case study, in section 7, is composed of this building typology, representative of large portion of the building stock in central and south Italian regions.

a) *b)*

Figure 4.1: a) Traditional URM at Grad Stanjel (Slovenia), and b) new URM at Sarajevo (Bosnia-Herzegovina)

Table 4.1: Important events with losses powerfully linked to URM collapse after 2001

Earthquake	Killed	Injured	Homeless
Gujarat, India (2001) Mw 7,9	20,000	167,000	600,000
Bam, Iran (2003) Mw 6,6	26,271	30,000	1 M
Kashmir, Pakistan (2005) Mw 7,6	86,000	69,000	3 - 4 M
Ica, Peru (2007) Mw 8,0	514	1,366	58,000 bd*
L'Aquila, Italy (2009) Mw 6,3	308	1,500	60,000
Christchurch, New Zealand (2011) Mw 6,3	181	1,500-2,000	10,000 bd*

**Building heavily damaged, probable to be demolish*

Even though some URM buildings may perform well during seismic actions, there is a lot of seismic survey reports describing the poor performance of URM after earthquakes. Particularly for buildings located in low-moderate seismically active areas were the seismic risk conscience is difficult to build-up. The earthquake of Haiti in year 2011 is an example of the catastrophic result of a occurrence of a long return period of event.

Recent earthquakes like those of Gujarat 2001, Bam 2003, Kashmir 2005, Peru 2007, L'Aquila 2009 and Christchurch in year 2011 are examples of heavy damage on URM buildings in the last decade (table 4.1).

Despite the economic market cost of URM buildings not high (if it is not considered a monumental structure), the collapse of heavy URM is a big threat to human life, severe injures (particularly fractures as observed for Bam 2003 [Ga 08]), and turn out into thousands of homeless and economical losses. All these facts develop into a big social problem that is difficult to deal with, particularly for a developing country's economy and governments.

The seismic response of some URM typologies, such as of adobe and stone-masonry buildings, is generally poor and suffer severe damage [To 99]. For stone masonry, the poor quality of mortar results into disaggregation of masons and consequently the lost the floor's support. Regarding the observed damage, for old or historical URM structures, cracks are common at wall corners and intersections consequence of inefficient wall connections and flexible floor diaphragms. If the action is strong enough, a separation of the wall occurs and it fails in the so called out-of-plane wall direction (weak resistant direction of the wall). Typical damage pattern for out-of-plane bending of walls, in the orthogonal direction for the seismic forces, is presented in figure 4.2 by green colors. Sections of walls and individual units in the other direction (in-plane) usually came together along with the failing wall due to friction and, if any, cohesion in between stone/brick elements.

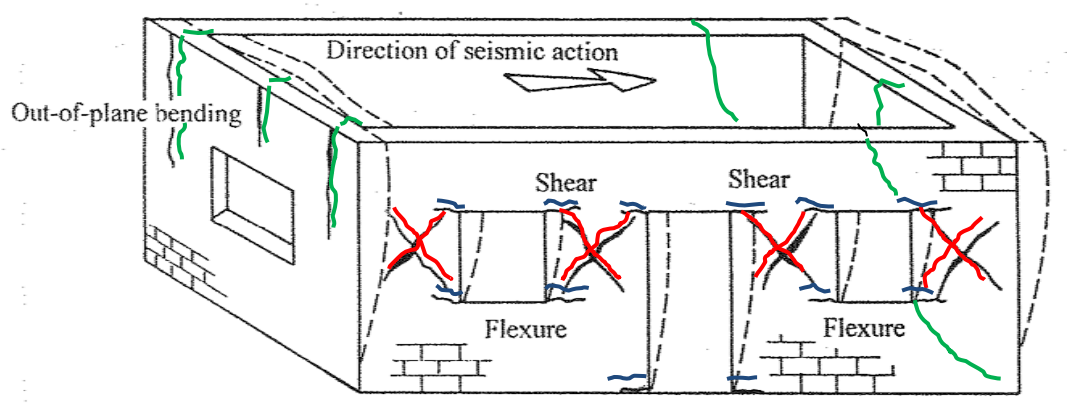

Figure 4.2: Damage pattern according to the failing mode [To 99]. Green color is related to out-of-plane cracks. For in-plane mechanism, red color refers to diagonal shear and blue to flexure cracks

a) *b)*

Figure 4.3: Damage at Castelnuovo town Italy. a) out-of-plane and b) in-plane (shear sliding)

Out-of-plane damage was commonly observed at Castelnuovo town for L'Aquila 2009 earthquake (figure 4.3a). Out-of-plane failure modes produce severe damage on the structure but, not necessarily, a total collapse of it; this condition was usual at Castelnuovo Town. For urban areas, collapsing walls in the out-of-plane represents also a high risk for pedestrians and adjacent building, particularly for many narrow streets in Europe's old city centers. On the other hand, total lack of resistance at piers (e.g.: after in-plane failure mode of diagonal shear) could drive easily into a full collapse of URM. Full collapse of URM is considered to leave small chances of survivor possibilities since empty voids after collapse is rare; this because to disaggregation of wall's elements burying people [Sp 09].

For newly constructed URM buildings with rigid diaphragms, inappropriate structural layout, large openings, and poor quality of materials are the reasons for most of the damage [To 99]. Buildings with big layout eccentricities (section 3.3.3) and insufficient amount of shear walls, present characteristic diagonal cracks damage at the pier elements of the wall, this is typical for insufficient shear capacity (figure 4.2). When damage is observed in the same direction of the seismic action, it is referred as in-plane failure. Shear sliding and rocking of pier elements are other possibilities on in-plane failing mode for low normal loading (section 4.5).

4.2 Building Stock

In order to quantify the relevance and importance to assess URM building typologies, it is necessary to overview how frequently these structures are found worldwide together with seismic hazard zones.

URM are practically disseminated worldwide. Materials accessibility, durability, resistance and good isolation properties make masonry structures popular. Most of the important the Cultural-Social-Historical (CSH) patrimonies are URM structures concentrated in old city centers worldwide. After this simple observation, it could be expected that in most of the cases old structures are masonry, usually URM constructed before the existence and enforcement of seismic codes. In other cases, even structures constructed following old regulations are found to be unsatisfactory to actual regulations and must be retrofitted. In figure 4.4, building description is shown, by age of construction, for 25 countries in Europe.

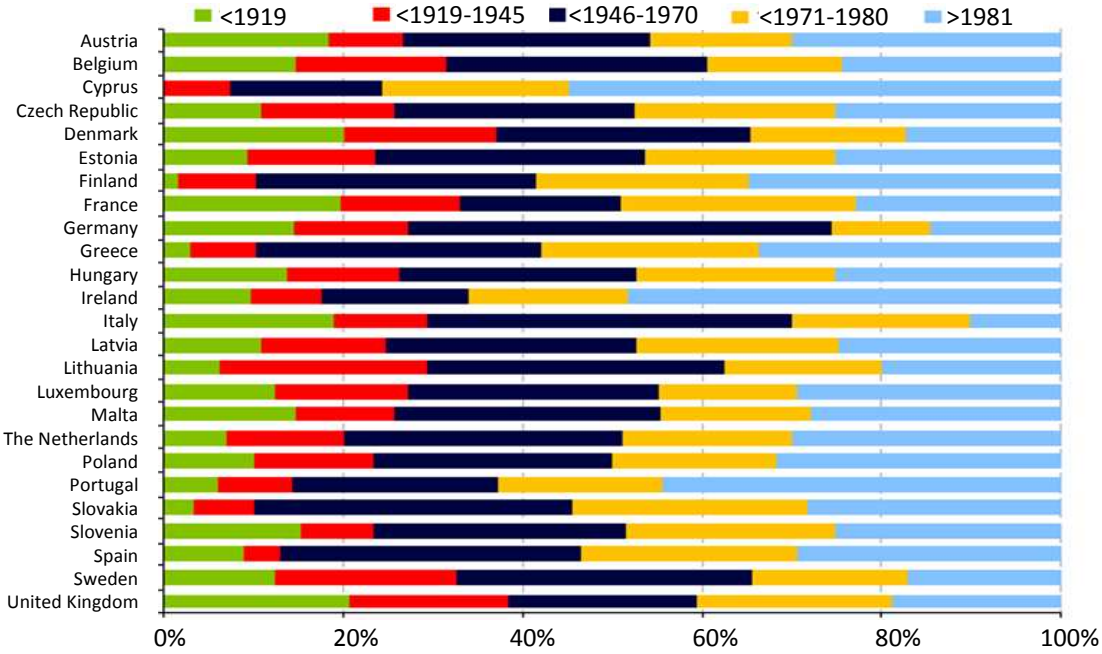

Figure 4.4: Age distribution of housing stock for 25 countries in Europe (Nemry 2008)

From figure 4.4, it is evident that Italy possesses one of the oldest housing stock. Nemry detailed that for figure 4.4, 53% of the total buildings are single-family (1-2 levels), 37% multi-family (3-5 levels commonly) and 10% were high rise buildings [NU 08]. Concerning directly to URM, Russell [RI 10] found that 86% of all URM in New Zealand are 1-2 storeys buildings. These facts justify efforts toward the developing of assessment methodologies focused on low-rise buildings. A summary regarding URM building stock for some selected countries with high to moderate seismic areas was presented by Frankie [Fr 10] based on Jaiswal global building inventory proposal [JW 08]. According to different sources, table 4.2 gives a good idea of the exposed URM values worldwide.

Table 4.2: URM building stock for 17 countries [Fr 10]

Country	Vintage	Data Source	URM % *
Algeria	1983	Petrovski [Pe 83]	15
Australia	2000	Census of Population and Housing [JW 08]	53
El Salvador	1990	Census of Population and Housing [JW 08]	48
Indonesia	2001	Census of Population and Housing [JW 08]	60
Iran	2005	Ghafory-Ashtiany and Mousavi [JW 08]	57
Iraq	1983	Petrovski [Pe 83]	80
Italy	2006	Dolce et al. [Do 06]	62
Jordan	1983	Petrovski [Pe 83]	70
Mexico	2000	Housing Study Report [JW 08]	76
New Zealand	1998	Dowrick [Do 98]	7
Pakistan	1998	Pakistan Population Census Organization [JW 08]	93
Peru	2007	UN-HABITAT [JW 08]	73
Philippines	2000	Housing Census [JW 08]	31
Sudan	1983	Petrovski [Pe 83]	80
Syria	1983	Petrovski [Pe 83]	60
Turkey	2002	Bommer, Spence et al. [Bo 02]	47
USA (CEUS)	2002	HAZUS inventory 2006 [FEMA web]	15

**URM as % of total building stock. URM denotes: Adobe, stone block masonry, and brick block masonry houses*

4.3 Mechanical Properties

To estimate the mechanical performance of a masonry walls, basic parameters related to mason units, mortar and the entire wall are needed. The goal of this section is to illustrate briefly about simple procedures to characterize masonry, and to present and explain some of the material parameters used in this study.

URM must be considered as a composite, heterogeneous, nonlinear structural material with properties that depend on the properties of their two main constituent components: brick and mortar. The failure results from fail in one or both of its components of the composite. Furthermore, mechanical properties of masonry are strongly anisotropic, which means that they also depend on the orientation of the bed joints to the principal stresses (type of brick/stone arrangement and shape) even when individual properties of bricks and mortar are considered isotropic.

All the aforementioned should be carefully considered in the process of evaluation of the displacement capacity of the structure. The displacement capacity of buildings is the most relevant characteristic to find structural behavior factors (section 3.3.1 and section 4.5.3).

Units in masonry structures can be separated in two groups: natural and artificial. Artificial elements can be divided according to percentage of voids ϕ_v in the element as: full elements (ϕ_v <15%), semi-full (15%<ϕ_v <45%) and hollow (45%<ϕ_v <55%) [NTC-09]. Masons are the basic constituent of masonry walls. Their mechanical properties are considered to dominate the behavior of walls. In particular, damage on masonry units turns into more dangerous brittle failure, meanwhile failure on mortar in presence of regular shape units shows generally good energy dissipation behavior. The dry masonry, without presence of mortar, usually presents good seismic behavior. Nowadays this technique is seldom used, and a layer of mortar is commonly deployed for new constructions.

A number of properties are determined separately for mortar and units: tensile strength, compressive strength, elastic and shear modulus, Poisson ratio, density, ductility, fractural energies and softening. In figure 4.5 the fracture energy is outlined as G_f and G_c, of a quasi-brittle material, where it is evident that compression behavior of masons is, in general, more ductile than the tension one. That is the reason why some failure modes, such as diagonal shear where the fail is due to tensions on the units, present low ductile behavior.

The resistance of artificial masons depends on the material of origin, the shape of the unit and the manufacturer. If units are prefabricated under a quality controlled environment, compression resistance is usually obtained from at least 3 samples failed by simple compression test and by using equation 4.1, following the NTC criteria, where f_{bc} is the characteristic unit compression strength and f_{b1} is the minimum resistance obtained from the 3 samples [NTC-09]. Under no manufacture quality certainty, the f_{bc} is obtained from the mean value of 30 samples f_{bm}, and after equation 4.2 [NTC-09].

$$\frac{(f_{b1}+f_{b2}+f_{b3})}{3} \geq 1.2\, f_{bc} \qquad \text{or} \qquad f_{b1} \geq 0.9\, f_{bc} \qquad \text{Eq [4.1]}$$

$$f_{bc} = f_{bm}(1-1.64\, v_{bc}) \qquad \text{Eq [4.2]}$$

where v_{bc} is the coefficient of variation of the 30 samples. The direct tensile strength f_{bt} of units is another important characteristic used widely to assess masonry because it is related to brittle behavior. According to the NZSEE in absence of direct tensile test, this could be approximated as 85% of the strength of masons from splitting test, or 50% of the unit modulus of rupture from bending strength test [NZSEE 06].

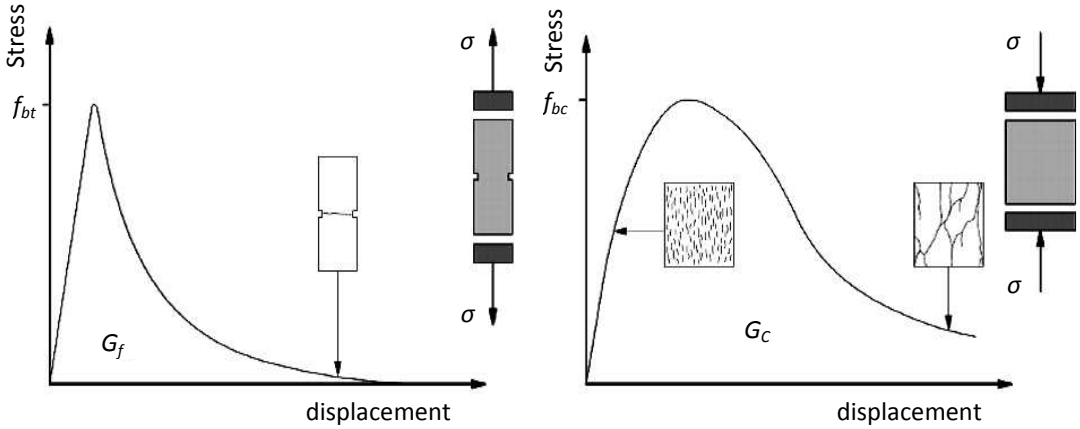

Figure 4.5: Behavior of quasi-brittle materials under uniaxial loading, f_t denotes the traction load and f_c the here compression load of units [Lo96]

4.3.1 Masonry walls

When the capacity of URM walls panels is assessed, the following intrinsic mechanical properties of masonry should be obtained: compressive strength f_m, shear strength f_v, flexural (bending) strength f_x, and finally the stress-strain relationships [EC-6]. The f_x wall capacity is usually neglected and must not be confused with f_{bt},or f_{tu} (tension).

Other wall parameters to be obtained in order to describe the performance of the structural system are the modulus of elasticity E_m and the shear modulus G_m. The elastic modulus is usually approximated as $1000f_m$ [NTC-09], but authors like Tomaževič suggested a range of $200f_m < E_m < 2000f_m$ [To 99]. In the same way, G_m could be approximated as $0.4E_m$ [NTC-09].

The compression of masonry is usually obtained from laboratory testing of wall masonry wallets, with 1.5 units of length and 3 units of height for low loading rates. The value of the masonry f_m can be also obtained according to the mortar and mason characteristics detailed in table 4.3.

The mortar resistant values in table 4.3 are in terms of their resistance to compression for the different typologies of lime/cement/sand ratios. This is common for Italian practice [BP 09]. The masonry shear strength f_v, is defined as the combination of an initial shear strength under cero compressive stress and the increment of f_v strength due to compressive normal stress. The initial shear strength at zero compressive stress f_{vo} could be determined by triplet specimens according to EN 1052-3 as shown in figure 4.6a [EN 1052-3].

Table 4.3: Masonry compression strength f_m for natural stone squared units [BP 09]

Characteristic unit compression resistance f_{bc} (MPa)	Mortar M_1 (12 MPa)	Mortar M_2 (8.0 MPa)	Mortar M_3 (5.0 MPa)	Mortar M_4 (2.5 MPa)
2.0	1.0	1.0	1.0	1.0
3.0	2.2	2.2	2.2	2.0
5.0	3.5	3.4	3.3	3.0
7.5	5.0	4.5	4.1	3.5
10.0	6.2	5.3	4.7	4.1
15.0	8.2	6.7	6.0	5.1
20.0	9.7	8.0	7.0	6.1
30.0	12.0	10.0	8.6	7.2
40.0	14.3	12.0	10.4	-

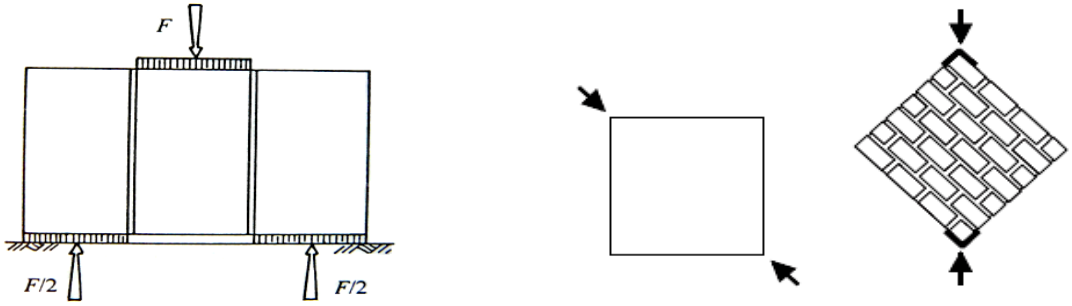

a) *b)*

Figure 4.6: Tests for obtaining shear strength parameters; a) test layout to obtain f_{Vo} [EN 1052-3], b) diagonal compression test layout to obtain f_{tu} [Ma 92]

A minimum of 5 triplets must be tested with a maximum acceptable normal stress of 0.03 MPa. For zero stress condition admissibility, the characteristic shear strength f_V is then [NTC-09]:

$$f_V = f_{Vo} + 0.4\sigma_N \qquad \text{Eq [4.3]}$$

where σ_N is the normal compressive stress perpendicular to shear. Equation 4.3 correspond to the well known expression for the Mohr-Coulomb criteria ($\tau = c+\mu\sigma_N$). The value of shear resistance of equation 4.3 is valid when the units are strong resistance and poor mortar; there, the cracks are oriented to pass through the mortar joints. A different approach is also used in URM, where shear is assessed in terms of the maximum the principal tensile strength developed in a wall of specific geometry, and idealized as elastic- isotropic panel. The principal tensile stress, originated in the wall under those assumptions of shear failure, could be represented by the tensile strength of bricks f_{bt} [NZSEE 06]. The NZSEE also proposes material properties according to visual inspection (table 4.4).

In the same way, the tensile strength value of a wall panel f_{tu} is directly obtained from diagonal compression test such as the one shown on figure 4.6b. According to the NTC norm [NTC-09], the value of f_{tu}, obtained from test layout like that of figure 4.6b, is equal to rupture load divided by two times the middle panel section. For the NTC, the f_{tu} could be equal to $1.5\tau_0$, where τ_0 is called as the reference shear value (table 4.5). τ_0 represents the strength obtained from diagonal shear testing without normal forces action. Finally for FEMA-306 the f_v value could be taken equal to an in-plane shear test [FEMA-306], based on the mean bed-joint shear strength [FEMA-273].

Table 4.4: Material properties according of mortar and clay bricks types, in MPa [NZSEE 06]

		Visual Characteristic and Hand Test	c	μ (-)	f_m	f_{bc}	f_{bt}	E	v
Mortar	Stiff	High cement content (cement : lime : sand = 1:0.25:3). Punch test < 10mm	0.4	0.8	8.0			12000	0.11
	Firm	Lime based (lime/sand=1/3), but in interior is not weathered. Punch test < 20mm	0.2	0.6	4.0			9000	0.07
	Soft	Lime bind, possibly mildly leached, can be raked out of joint, but stays bount. Punch test < 30mm	0.1	0.4	1.0			7000	0.05
	c = 0	Lime-based mortar is heavely weathered. Sand-like, easily raked out by hand, aggregate is unbound. Not suitable for earthquake resistance	0	0	0				
Brick	Hard	Dense, hard surface, well fired, dark red.				20-30	2-3	18000	0.2
	Stiff	Common brick, can be scored with a knife.				10-20	1-2	13000	0.2
	Soft	Weathered, pitted, distint colour variation with depth, bright orange, probably under-fired				1-5	0.1-0.5	4000	0.35

It is of importance to state that this section has focused on European material qualification practice, particularly Italian ones since the analyzed case study is placed in Italy. Data regarding the material properties of different Italian masonry typologies is presented in table 4.5.

Table 4.5: Material properties according to different URM typologies [NTC-09]

Wall Type	f_m (MPa)	τ_o (kPa)	E_m (MPa)	G_m (MPa)	γ (kN/m^3)
Erratically arranged stone wall (rounded or irregular stones)	1,0-1,8	20-32	690-1050	230-350	19
Wall with roughed blocks with limited thickness and inner core	2,0-3,0	35-51	1020-1440	340-480	20
Wythe wall with good texture	2,6-3,8	56-74	1500-1980	500-660	21
Soft blocks wall (tuff, limestone, etc)	1,4-2,4	28-42	900-1260	3005-420	16
Wall with square blocks	6,0-8,0	90-12	2400-3200	780-940	22
Wall of clay bricks and poor mortar	2,4-4,0	60-92	1200-1800	400-600	18
Wall with hollow bricks and cementicius mortar (hole area < 40%)	5,0-8,0	240-320	3500-5600	875-1400	15
Wall with hollow bricks (hole area > 45%)	3,0-4,0	300-400	3600-5400	1080-1620	12
Concrete mason or expansive clay mason (void area from 45% to 65%)	1,5-2,0	95-125	1200-1600	300-400	12
Concrete block (perfored area < 45%)	3,0-4,4	180-240	2400-3520	600-880	14

4.4 Building Components

A building structural system could be described in terms of lateral/orthogonal resistant subsystems according to floors, walls and wall elements. The building elements or components are represented schematically in figure 4.7 in order to make clear the terminology used for this study. The description of the elements is as follows:

- *Floors/storeys:* structural unit composed of vertical structural walls and diaphragms/slabs at different buildings heights. For this study, the number of floors in the building is limited to 3-4 storeys, corresponding to a maximum 10 meters of total building height.
- *Floor diaphragms:* Connecting elements between two storeys, the building foundation and the roof. They are horizontal elements, and define the different horizontal typologies. Concerning the structural design, they could be considered rigid or flexible.
- *Walls:* a structural element of the building with a length L_T (e.g. of the front-wall/ façade) and the height of the storey H_S. It is composed by piers and partially by nodes and spandrels in the same axis. They define the vertical typologies.
- *Piers:* is a wall lateral resistant element of length l_P and of a height h_P.
- *Spandrel:* is a part of the building laying in between two openings in the vertical direction, thus joining the wall's piers in one plane. Geometry: length l_S and of a height h_S.
- *Openings:* open space in structural walls were door, windows, etc, are placed.

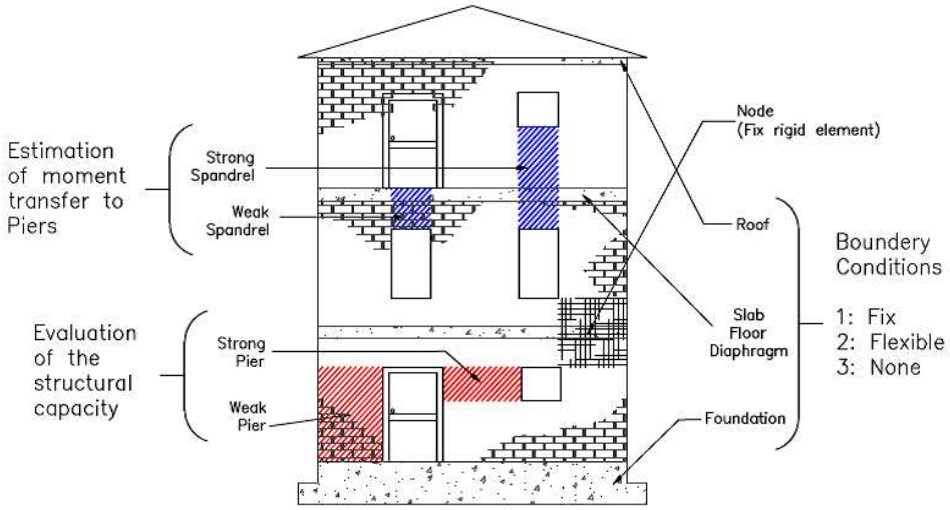

Figure 4.7: Building structural components

The in-plane seismic resistance is dominated by the lateral performance of wall piers since they are the direct lateral restrains of movement. Wall piers are joined by the joint action of spandrels and slabs so that a coupling effect is produced. Depending on the extent of the spandrels and the horizontal typology, this coupling effect will be bigger or smaller. For this reason, elements like spandrels or floor diaphragms (foundation/roof) are structural components presented in this approach as important elements to define the boundary condition of piers. Fix or flexible boundary condition values are assigned a priori according to wall's in-situ properties.

Nodes in figure 4.7 are considered as rigid elements by most assessment methodologies since damage of this component is seldom founded in earthquakes [FEMA-306]. In case of differential subsidence, damage is presented on building nodes, particularly at the corners and could contribute to damage after seismic actions, especially for out-of-plane mode. Foundations are also considered rigid, as this may be a conservative assumption for non-excessive rocking condition. Moderate rocking of foundation, could be recognized as favorable source of damping rather than damage [FEMA-306].

4.4.1 Floor Diaphragm Systems

For buildings, the floor diaphragm system plays a very important role in the overall seismic behavior of the structure [EC-8.1]. The distribution of earthquake-induced inertial forces on the vertical pier elements depend on the geometry and the rigidity of the floor diaphragm system. For the design, the connections between floor diaphragms and vertical resisting elements must have sufficient strength to transfer the maximum calculated diaphragm shear forces. For the real building stock condition, these connections are not always so efficient for transferring shear forces due to a low stiffness state of many floor diaphragms, such as those made of wood. Floor diaphragms can be classified as flexible, stiff and rigid [FEMA-368].

The prediction of the behavior of a structure with rigid diaphragm is relatively easy compared to that of structures with non-rigid ones. That occurs because rigid diaphragm does not deform appreciably. It could be assumed that its behavior remains elastic and the earthquake-induced internal forces are well distributed to vertical elements in proportion to the relative rigidities of the elements. On the other hand, for non-rigid diaphragm structures, the horizontal force within the vertical elements due to the lateral excitation depends on the rigidity and strength of the diaphragms [SW 03]. Non-rigid floor diaphragms and poor connections between slabs and walls are the reasons for walls failing in the out-of-plane as it is observed in figure 4.8a, 4.8b.

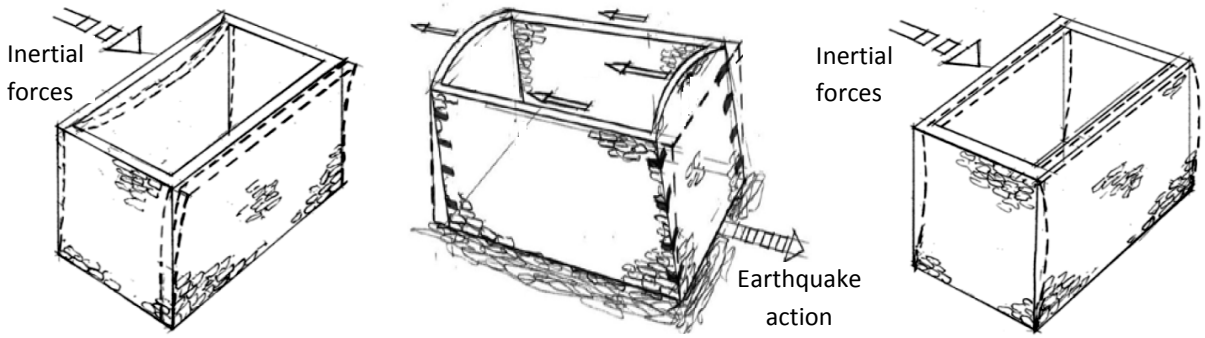

Figure 4.8: Structure behavior according to floor diaphragm: a) poor connection of walls with slab (cantilever condition), b) good connection flexible slab, c) rigid floor diaphragm [BB 11]

According to the NEHRP normative [FEMA-368], diaphragms shall be considered flexible when the maximum lateral deformation of the diaphragm along its length is more than twice the average inter-story admissible story drift of the floor immediately below the diaphragm. Conversely, diaphragms are considered rigid when the maximum lateral deformation of the diaphragm is less than half the average inter-story drift of the associated story. Stiff diaphragms are those situated in between the rigid and flexible condition. In this work, a slab is only referred as rigid or else flexible; the cases of stiff diaphragms are conservatively considered as flexible ones.

For buildings with flexible diaphragms at each floor level, each resistant element may be designed independently, with seismic masses assigned on the basis of tributary area [FEMA-368]. According to FEMA-306 and UFC [UFC-07], reinforced concrete slabs with not important horizontal openings and span-to-depth ratio of 3 or less are considered rigid. Hollow concrete planks and brick arch on steel beams are stiff intermediate systems (considered flexible in this work). Finally, diaphragms constructed of wood panels or un-topped steel decking are idealized as flexible. Wood floors are considered flexible when the reinforced concrete topping is not more than 4 cm of thickness.

4.4.2 Spandrels

A Spandrel is the part of the building wall laying in between two openings in the vertical direction, thus joining the wall's piers in one plane. Their possible damage disrupts the join function of different piers. If spandrels are weak in the in-plane action or previously damage, the building walls could behave like a multi-storey continuous element (figure 4.9a). That changes the failing mode of the wall. For weak spandrels with continuous non-damaged iron/steel ties (figure 4.9b 4.9c) or rigid slabs, the spandrel adequately transfer actions to piers at each storey. Failing settings for damaged spandrels are presented by Boscotrecase [BP 09] and FEMA 306 [FEMA-306].

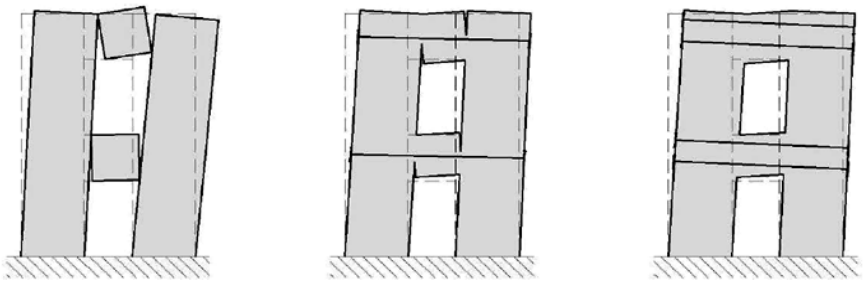

Figure 4.9: Possible on weak spandrel action: a) not coupling walls, b) coupling piers with tie rods c) coupling piers with rigid slab and/or a series of tie rods [CF 10]

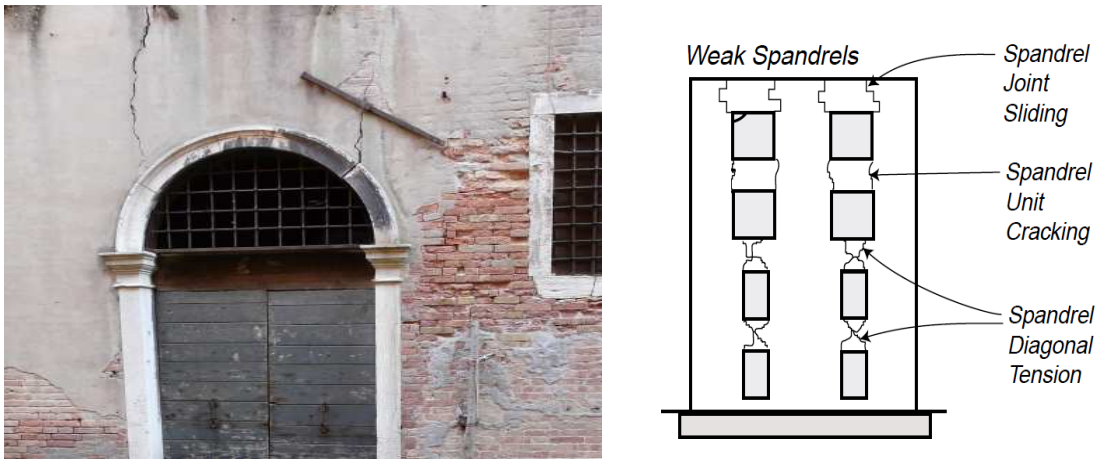

a) *b)*

Figure 4.10: Damage patter on spandrels; a) damage due to differential settlements in Venice (Italy), b) damage possibilities of weak spandrels [FEMA-306]

Studies on spandrels are relatively new. The importance of spandrels, in this study, is according to its initial damage condition and its geometric h_S/l_S ratio. It was concluded by Parisi that cyclic test on the pre-damaged wall show a significant drop in the lateral resistance due to damage in the spandrel panel [PAP 11]. Therefore, spandrels should be included in the capacity models of perforated walls as structural elements with limited strength and flexibility under bending and shear conditions. After the spandrel is damaged, rocking of piers govern lateral stiffness and hysteretic response of specimens. Foraboschi also study the couple effectiveness of spandrels in URM [Fo 09].

Pre-damage on spandrels is frequently found on URM, probably mainly due to differential subsidence which can induce rigid displacements and tilting of buildings [Cr 01]. Burd [BHAL 98] studied the damage patterns caused by tunnel construction induced subsidence; here damages on spandrels such as shown in figure 4.10a are caused. On piers, subsidence cracks are either vertical thanks to building tilting or horizontal caused by tension. Damages caused by lateral actions, such as those founded after earthquakes, are presented in figure 4.10b.

The geometric ratio h_S/l_S, defining the weak or strong characteristics of spandrels in absence of especial bonding elements, must be greater than 0.75 for all spandrels in a wall to be considered as a strong spandrel in this study; otherwise it is considered as weak. According to FEMA 306 once spandrel damage occurs, higher energy dissipation properties are developed on piers but lateral resistance is reduced. For this study, damage on spandrel is related with structural damage up to D3 of EMS-98 ([Gr 98], Section 3.1.2), so that, the performance related with LSLS or CPLS is evaluated by the effects occurring on piers failing mode due to spandrel's damage. Special elements like wood, steel ties or chains also modify the boundary condition (figure 4.9b). Figure 4.11 shows different types of anchor used to improve URM structures and that are visible from the outside of the building.

a) *b)* *c)*

Figure 4.11: a) external anchors in Arta (Greece), b) tie rod with plate and c) traditional tie in Castelnuovo (Italy)

4.5 Capacity of URM Walls

During an earthquake, the ground surface moves in all directions. The most damaging effects on buildings are caused by lateral movements which disturb the stability of the structure, causing it to topple or collapse sideways. Since normal structures are limited just to be stable to gravitational forces, many traditional systems of edification are not inherently resistant to horizontal forces. Thus, design for earthquakes consists largely of solving the problem of bracing structures against lateral actions.

Analyzing the seismic damages on masonry structures, it is possible to underline particular global behaviors for different structural characteristic and different types of layout variation. Typical damages of the masonry walls can be separated in two fundamental modes of collapse. The first type mechanism is for ways of collapse related with the out-of-plane behavior of the walls; this consists of a flexural behavior mainly (section 4.5.1). The other mechanism is the one called in-plane (strong resistance plane). Archetypal in-plane mechanism failures are pier rocking, toe crushing, shear diagonal shear and sliding (section 4.5.2).

The behavior of URM is dominated initially by the out-of-plane collapse. The presence of a good connection among the parts of the building produces, instead, the collaboration among the components in the seismic response. In this case, the probability to have the first type mechanisms of collapse is very low and eventually the resistance of walls to in-plane loading (which is higher) became the important aspect to evaluate. Therefore, for in-plane condition, the structural conception of buildings must be similar to a closed box (figure 4.8c). There walls are positioned along two orthogonal directions and they present good connections between each other and among the floors.

Once the seismic demand parameters are established according to the hazard assessment explained on section 3, the structural capacity of the URM can be mostly assesed from the building structural piers (section 4.4). In this study, piers are considered the most important lateral resistant component of a wall for in-plane failure modes for damage levels over D3 of EMS-98 [Gr 98]. Spandrels and floor diaphragms are considered as important input proposed to assign local boundaries condition and structural behavior wall characteristics (section 4.5.4).

Capacity, or resistance R of piers, is also naturally related to the wall's material properties (section 4.3) and to the failure criteria function according to initial loading normal conditions (section 4.5.2). For out-of-plane mechanism descriptions, there are many different proposed methodologies [DS 03] [MMMM 09] [SA 02]. In this study, capacity for the out-of-place is assessed according to the tri-linear model methodology proposed by Doherty [DGL 02].

4.5.1 Orthogonal capacity (out-of-plane)

The out-of-plane mode of collapse is largely observed when URM structures present poor connection conditions between the walls. Assessment for out-of-plane seismic resistance on existent masonry is of big concern. There is strong damage observed in recent earthquakes such as those mentioned in table 4.1, particularly for old structures.

In design of structures, URM walls shall be considered to resist the out-of-plane action as isolated components spanning between floor levels [FEMA-273]. Hence, the seismic action on them is the one detailed for non-structural elements on seismic codes. For new structures, conservative rules for URM design in the elastic domain are usually applied and the flexural cracking resistance should not be exceeded. For URM with good connections, the EC-8 [EC-8.1] and FEMA-273 [FEMA-273] present simple permissible tables, in order to avoid complex dynamic analyses because static procedures are not recommended by norms to assess performance for this fail mechanism.

Table 4.6: Permissible H_S/t ratios and thickness t for URM in the out-of-plane

FEMA-273 [FEMA-273]				EC-8 Part 1 [EC-8.1]		
Wall types	H_S/t < 0.24g	0.24g < H_S/t < 0.37g	0.37g < H_S/t < 0.5g	Masonry type	t minimum (mm)	Maximum H_S/t
Walls of one-storey buildings	20	16	13	URM, with natural stone	350	9
First-storey wall of multistory building	20	18	15	URM, with artificial units	240	12
Wall in top storey of multistory building	14	14	9	URM, with artificial units for low seismicity	170	15
All other walls	20	16	13			

For existent buildings, the application of conservative code requirements (elastic domain) for a new building may turn into expensive retrofitting solutions. This fact is not the best situation in terms of economical viability for common cheap URM housing.

Doherty [DGL 02] proposed the so called "reserve capacity" of rocking brick to model URM walls in the out-of-plane. The seismic resistance of out-of-plane bending is assessed by a simplified linear displacement-based method using a tri-liner relationship (figure 4.12) to approximate the real non-linear behavior of URM. This methodology is convenient to be used in this study due to its simplicity and compatibility with the performance base criteria (section 3.4).

The seismic resistance is based on stability mechanisms rather than static strength, where a cracked URM wall is modeled as rocking rigid blocks (figure 4.13b). The force-displacement profile of rocking walls is used for a simple degree of freedom idealization SDOF of the wall. The response of the cracked wall is similar to that of a lumped mass in a SDOF model [MM 08]. The assumption of cracked wall is based and justified on observations of common damage on URM with low mortar strength. Initial damage is due to reasons such as footing settlements, temperature cycles, any dynamic previous action (quake, wind, machinery vibrations), etc. The cracked section assumption is also on the conservative side of design.

For a simply rocking wall, the triangular-shaped displacement profile on figure 4.12 had been found accurate enough after verification by shaking table testing [Do 00]. After the assumption of moment equilibrium at the point of incipient rocking of the upper half of the wall (about mid-way of the cracked section), the rigid threshold resistance F_O can be easily obtained from figure 4.13b. In the same way, for a cantilever wall, F_O is obtained for the pivot point at the base of the wall. After F_O is exceeded, the gravitational restoring moments are affected by a degrading P-Δ phenomenon, evident by the negative stiffness behavior up to the final stable displacement Δ_u.

A more realistic force-displacement condition than the one obtained by the rigid block assumption, is obtain by a semi-rigid formulation of the wall. With this approach, F_O is degraded by the material properties condition and state of degradation of idealized mortar joints (figure 4.12).

State of degradation at cracked joint	Δ_1/Δ_u %	Δ_2/Δ_u %
New	6	28
Moderate	13	40
Severe	20	50

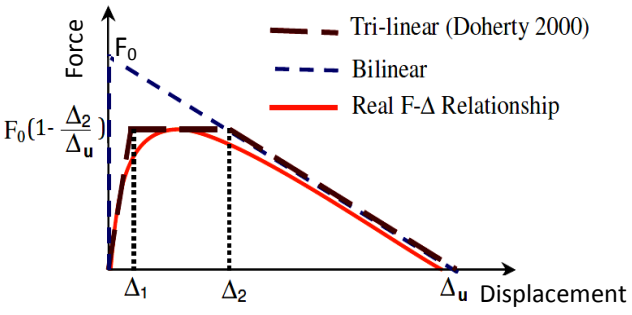

Figure 4.12: Tri-linear F-Δ formulation for URM out-of-plane behavior [DGL 02]

With the Δ_1 and Δ_2 displacement parameters, the tri-linear formulation is finally obtained. It can be deduced that, the new material conditions present a greater capacity. For all cases, plateau ductility values are over 2.5. Melis [Me 02], observed a variation of Δ_1/Δ_u in between 5-20% and Δ_2/Δ_u of 25-50% from dynamic time history analyses, falling into the parameters proposed by Doherty in figure 4.12. The resistance plateau of the tri-linear formulation is detailed by equation 4.4.

$$f_{Ro} = F_O\left(1 - \frac{\Delta_2}{\Delta_U}\right) \qquad \text{Eq [4.4]}$$

where f_{Ro} is the resistance for the out-of-plane failure. Further URM wall conditions are detailed on figure 4.13. The effect of normal loading is considered according to rigid and flexible diaphragm formulations (figure 4.13c, 4.13d). The normal loading factor ψ is obtained from the ratio of total normal force divided by half of the analyzed wall weight W.

$$\psi = \frac{N}{W/2} \qquad \text{Eq [4.5]}$$

Multi-storeys wall failing mechanisms, like those presented by Milano [MMMM 09], are similarly evaluated in this study as equivalent cantilever or simple supported walls with an average inter-storey wall thickness; this is a conservative assumption, proper to the analysis detail of the SAUMAC methodology uncertainty of input data and the assessment level formulations. Multilayer "wythe walls" are a special condition; here t_{eq} value varies according to the effectiveness of connectors in between wall layers.

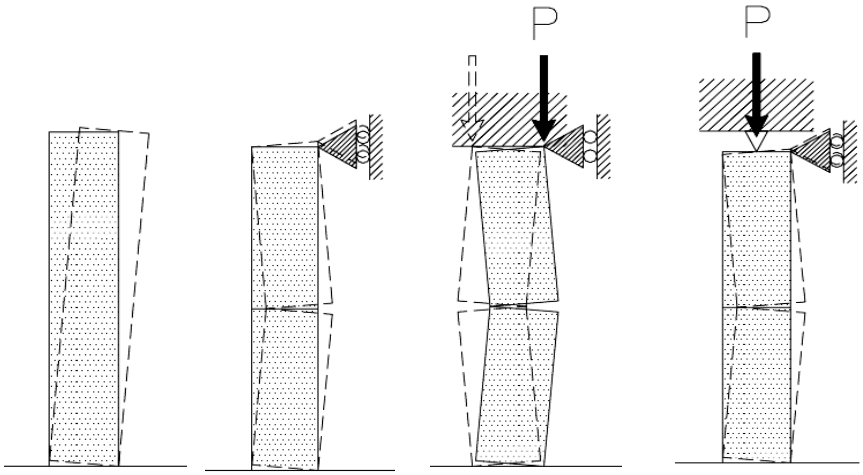

Wall Description	a) Cantilever Wall (rigid parapet)	b) Simple supported Wall (rigid non-loadbearing)	c) Simple supported loadbearing Wall-A (with rigid slab)	d) Simple supported loadbearing Wall-B (Timber bearer / flexible diaphragm)
Equivalent thickness value t_{eq}	$1t$	$1t$	$1t$	$\approx 0.8t$
F_O Eq (4.6a, 4.6b, 4.6c, 4.6d)	$F_O = \frac{4}{3} W \frac{t_{eq}}{H_S}$	$F_O = 3W \frac{t_{eq}}{H_S}$	$F_O = 3W \frac{t_{eq}}{H_S}(1+\psi)$	$F_O = 3W \frac{t_{eq}}{H_S}(1+\psi)$

Figure 4.13: Wall stability mechanisms modeled as rocking rigid blocks [Do 00]

4.5.2 Lateral capacity (in-plane)

Once the out-of-plane collapse mechanism is discarded or not likely anymore a source of damage to the structure (rigid slabs or table 4.6 criteria), the building presents a global response enclosing the collaboration of the different components. This is referred as the in-plane building capacity or resistance. The in-plane capacity is extensively dependent on the characteristics of the pier elements as these are the only lateral load resistant components. Their joint interaction in the storey describes both: lateral force capacity and, approximately, the lateral drift values of the storey. Generally speaking, in-plane walls provide the stability necessary in URM to prevent collapse.

Due to anisotropic characteristics, the masonry behavior under a biaxial state of stress cannot be solely defined by the uniaxial loading conditions, as it could be suitably approximated for materials like concrete or steel. A biaxial strength envelope can be generalized in terms of [BBŽ 08]:

- *Stresses in a fixed set of material axes*
- *Principal stresses and the angle between the principal stresses and material axes*
- *The properties of its constituents (brick, mortar and the joint/bond)*
- *A combined form of all or some of the above*

The orientation of the principal stresses to the bed joints has a significant influence on URM masonry failure modes. Also important is the ratio in between principal stresses, obtained for diverse normal-lateral loading configurations. The most common way is to illustrate the range of possible failing modes is in terms of normal σ_N and shear f_V stresses acting on a horizontal bed joint configuration (figure 4.14). Here, σ_N is normalized in terms of the maximum possible normal capacity of the wall f_m. It is evident that the value at the e point in the figure is equal to 1 and present not shear capacity, failing purely to normal loading action.

Figure 4.14 could be reformulated in terms of the most likely failure mechanisms. For low-rise and middle-rise buildings, this could be done according to the physical location of the pier components as it is observed on figure 4.15a proposed by FEMA-306. Nevertheless, due to the non-homogenous composite nature of masonry, component behavior is difficult to predict and hence to duplicate in laboratory testing [MC 97]. In the figure 4.15b-c, equivalent damage patterns to those proposed by FEMA-306 were observed in Castelnuovo town (Italy) damage recognition campaign.

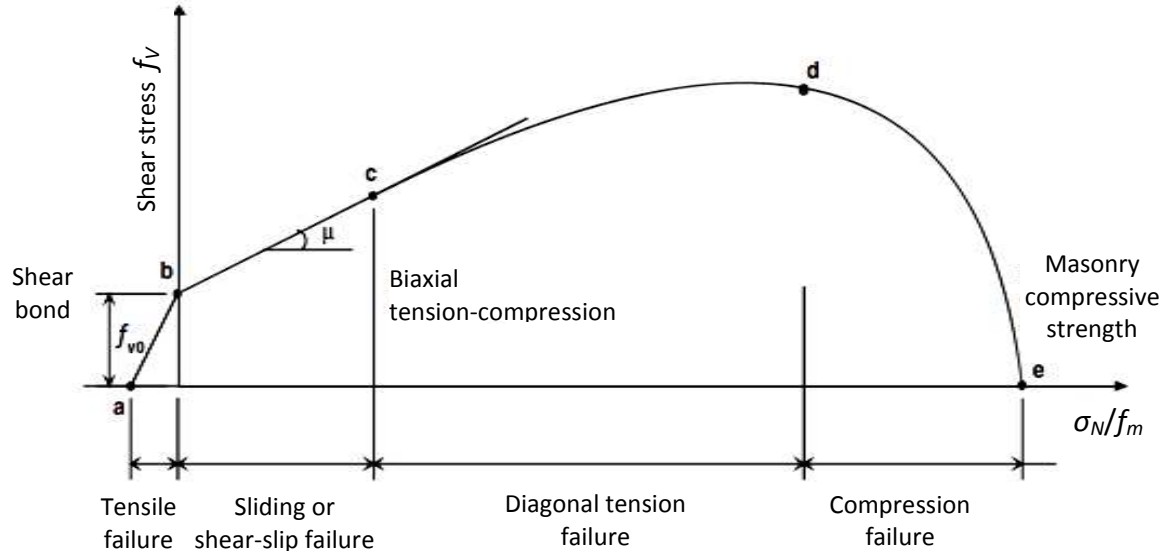

Figure 4.14: Behavior of URM piers under de effect of combined shear and normal stresses [DHB 94]

a) *b)* *c)*

Figure 4.15: Weak pier: a) damage possibilities of weak piers [FEMA-306], b) Toe crushing in middle storey at Castelnuovo (Italy), and c) bed joint sliding at Castelnuovo (Italy)

The mechanisms for lateral force resistance on figure 4.14 depend on four primary aspects: pier geometry, wall boundary conditions, normal loading, and finally the material characteristics of bricks, mortar and the brick/mortar interface [MC 97].

Bibliography is wide over possible models to describe URM under a combination of lateral and normal action [TČ 71][EC-8.1][MM 80][FEMA-306][Ga 85][GL 97][Lo96]. An appropriate model should be chosen according to sophistication of assessment level and/or modeling strategies used (discrete/homogenous models [Lo96]). For this study, modeling of building components (figure 4.7) is done in terms of homogeneous elements (smeared, continuum, macro elements). Detailed discrete models are believed to be not reliable in the presence of many diverse URM uncertainties. The principal failure mechanisms of piers to seismic actions could be summarized as follows [MC 97]:

- *Rocking failure:* for incremental lateral loading, bedjoint cracks in tension and shear are carried out by compressed masonry. Failure is obtained by overturning of the wall and compressed corner crushing.
- *Shear cracking:* peak lateral resistance is governed by the development of inclined diagonal cracks, which follow the path of joints or go through the bricks, depending on material properties (mortar, brick and brick-mortar interface).
- *Sliding;* due to formation of horizontal tensile horizontal crack in the bedjoints; subjected to reverse action, potential sliding planes form along the crack, failure typical for low levels of vertical normal loading.

These main failure modes are discussed briefly by the simple descriptions proposed by Magenes [MC 97], which corresponds to what is described in NZSEE and the NTC, two of the most recently edited seismic standards.

4.5.2.1 Rocking failure

In the rocking mode of failure, horizontal cracks occurs in masonry walls when the tensile stresses developed in the wall under a combination of vertical and horizontal loads exceeds the tensile strength of the masonry material resulting in the building tipping over. At the same time, the toe in the lower corner of the masonry panel is crushed due to stress concentration (figure 4.16).

The acting moment on the pier is expressed by the next equilibrium equation [BP 09]:

$$M_f = \frac{l_P{}^2 t \sigma_N}{2}\left(1 - \frac{\sigma_N}{0{,}85\, f_m}\right) \qquad \text{Eq [4.7]}$$

where M_f is the rocking moment (also called of flexural-compression,), l_P is the length of the pier element and t is the thickness of the wall. The moment could be expressed in terms of a shear force V_f by the shear ratio α_V, taking into account the effective pier height H_O (distance from zero moment)

$$V_f = \frac{l_P t}{\alpha_V}\frac{\sigma_N}{2}\left(1 - \frac{\sigma_N}{0{,}85 f_m}\right) \qquad \text{Eq [4.9]}$$

$$\alpha_V = \frac{M_f}{V_f l_P} = \frac{H_O}{l_P} = \frac{\psi' h_P}{l_P} \qquad \text{Eq [4.10]}$$

Considering typical layouts for piers, ψ' parameter is equal to 1 when the pier is fixed to rotate on one end and free to rotate in the other and 0.5 when it could be considered fixed in both ends. For low normal loading, f_m effect is almost irrelevant, meanwhile the shape of the pier and the ψ' condition is of great importance.

4.5.2.2 Shear cracking

The shear failure of URM associated with diagonal cracking is difficult to describe since it is the result of several interacting factors due to masonry heterogeneity properties. Two main types of simplified procedures are used for the prediction of shear strength in case of diagonal cracking: diagonal tension shear and sliding shear (M-C shear).

The sliding shear or Mohr-Coulomb shear is derived from equilibrium of forces acting over the compression zone of the cross section. The strength is assumed in terms of cohesion c and a friction coefficient μ, as it is shown on equation 4.4. Taking into account a mean value of vertical stress on the wall and the length of the effective un-cracked according to the procedure described by Magenes [MC 97], equation 4.11 is obtained. A correction factor of (1+ α_V) is proposed by Magenes to obtain the shear resistance for the whole section (Equation 4.12). The minimum value of V_{SSc} and V_{SSw} should be taken as the resistant shear force.

$$V_{SSc} = l_P t\left(\frac{1{,}5c + \mu\sigma_N}{1 + \frac{3c\alpha_V}{\sigma_N}}\right) \qquad \text{Eq [4.11]}$$

$$V_{SSw} = l_P t\left(\frac{c + \mu\sigma_N}{1 + \alpha_V}\right) \qquad \text{Eq [4.12]}$$

The Mohr-Coulomb failure criterion had been found satisfactory when the α_V ratio is small and diagonal cracks are associated with the poor bond mortar/brick or poor mortar. For the diagonal tension shear V_{DS}, equation 4.13 had been proposed by Turnšek [TČ 71]. In V_{DS} failure is considered

possible throughout the bricks. The tensile strength of masonry parameter f_{tu} (not the tensile strength of bed joints or the bricks) is a parameter well correlated with V_{DS}. f_{tu} is obtained from figure 4.6b test layout. This formulation is widely adopted in norms, including the NTC [NTC-09].

$$V_{DS} = \frac{f_{tu} l_P t}{b} \sqrt{1 + \frac{\sigma_N}{f_{bt}}} \qquad \text{Eq [4.13]}$$

where b is dependent on the pier aspect ratio h_p/l_p, varying in between 1and 1.5. For greater or smaller ratios the values are fixed to these upper and lower limits. Magenes [MC 97], proposed a formulation more suitable than equations 4.12 and 4.11. In the case of high normal loading or strong mortar conditions, the failure may be initiated by the shear-tensile cracking of bricks. The acting diagonal shear strength on the pier is expressed by [MC 97]:

$$V_{DSb} = \frac{f_{bt} l_P t}{2.3(1+\alpha_V)} \sqrt{1 + \frac{\sigma_N}{f_{bt}}} \qquad \text{Eq [4.14]}$$

Equation 4.14 is adjusted to the correction factor of $(1+\alpha_V)$ attain from Mann [MM 80].

Equivalences for values with respect to the material properties f_{tu}, f_{bt}, can be roughly approximated by equation 4.15, by making $V_{DSb}=V_{DS}$ and $f_{tu} = 1.5\tau_0$. This may be of use since both parameters f_{tu}, f_{bt} are difficult to obtain in bibliography. Normative tables, such as table 4.5, present the shear values for zero normal loading σ_N.

$$\tau_0 = -\frac{\sigma_N}{3} + \frac{1}{3}\sqrt{\sigma_N^2 + 4b^2\left(\frac{f_{bt}^2}{5.3(1+\alpha_V)^2}\right)\left(1 + \frac{\sigma_N}{f_{bt}}\right)} \qquad \text{Eq [4.15]}$$

4.5.2.3 Sliding

Sliding failure mode along horizontal joints is typical in case of low vertical loading (no brick damage) and poor mortar conditions. The strength of a pier undergoing sliding, under lateral seismic excitation, is expressed as:

$$V_S = \mu\sigma_N \qquad \text{Eq [4.16]}$$

In equation 4.16 any sort of cohesion is neglected after the joint is assumed as already cracked. The μ value is actually a residual friction value (kinetic friction). Equation 4.16 tends to underestimate significantly the onset loading for sliding, but it could be taken as a lower limit for high α_V ratios. Sperbeck (Sperbeck 2008) used values of μ in between 0.21 and 0.4 for concrete hollow block masonry. μ values for stone masonry are suggested by the TDAES [TDAES-00]. Sliding is not possible for rubble masonry walls since evident disaggregation of elements will occur instead.

4.5.2.4 Stiffness and bilinear model for piers

To evaluate the performance of masonry structures, the elastic stiffness of piers and their deformation conduct are important to be assessed. According to Tomaževič [To 99], the pier ductility factor for masonry μ_P (equation 4.17) could be found from a bilinear model formulation (elastic-

perfectly plastic) in between $0.9V_{max}$ and $0.8V_{max}$. δ_E at $0.9V_{max}$ describes the deformation at which the elastic stiffness K_E is found. δ_u is found from the pier hysteretic behavior when the resistance is decreased up to $0.8V_{max}$. V_{max} is the maximum value of shear resistance, corresponding to the minimum value found from equations 9,11,12,14. Following the theory of elasticity, for laterally loaded masonry pier presenting both bending and shear deformation, the elastic stiffness K_E could be computed as:

$$\mu_P = \frac{\delta_u}{\delta_E} \qquad \text{Eq [4.17]}$$

$$K_E = \frac{1}{\delta_E} = \frac{G_m l_P t}{1.2 h_P \left[1 + k' \frac{G_m}{E_m}\left(\frac{h_P}{l_P}\right)^2\right]} \qquad \text{Eq [4.18]}$$

where δ_E is function of the flexural and shear lateral deformation; k' is 0,83 for both fixed boundary conditions and 3.33 for cantilever walls. Tomaževič [To 99] suggest for URM μ_P values from 2 to 3. Bilinear model formulations and μ_P are assigned in this work according to figure 4.16.

Damage to cyclic loading		Hysteresis Loops / Bilinear model	Comments
Shear sliding and simple Sliding (μ_P=3)	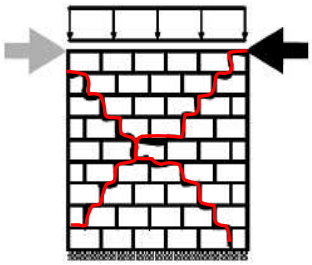	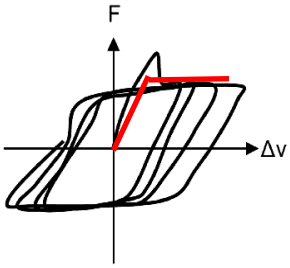	Cracking occurs at the mortar or mortar-brick interface, initial higher strength and then residual value; Mohr-Coulomb criteria describe well the behavior. High ductility and very energy dissipation (good performance). Wall approximated by bilinear model
Diagonal tension Shear (μ_P = 2)	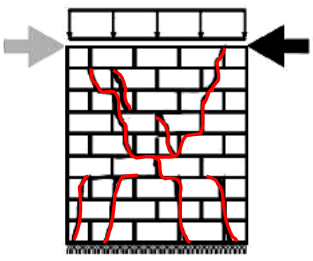	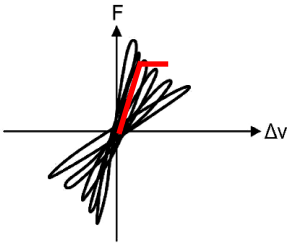	Cracks developed on bricks, mortar and mortar-brick interface. High loading capacity but brittle behavior with presence of negative stiffness. Poor ductile behavior; considerably less energy dissipation compared with sliding. Approximated with a conservative bilinear model formulation
Rocking and corner toe crushing (μ_P = 3)	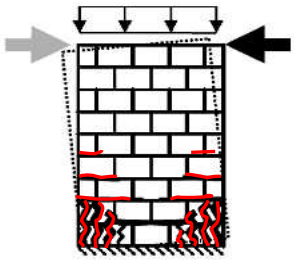	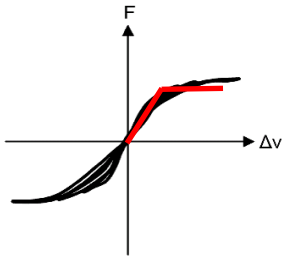	Common mechanism for slender piers; stiffness degraded for incremental loading due to horizontal tension cracks in bedjoints. Units crushing in corners due to stress concentration; brittle fail because of low energy dissipation. High ductility, especially when toe crush is avoided. Fit to bilinear model

Figure 4.16: Behavior of URM piers under combined shear and normal stresses (adapted from [Mi 06])

4.5.3 Wall capacity and structural behavior factor

A structural wall is an element of the building with a length L_T (e.g. of the front-wall/ façade) and height of the storey H_S. It is composed of piers and partially by nodes and spandrels acting in the same coordinate axis. A storey is composed of at least 2 walls on each main analysis directions (*X*,*Y*). It is assumed commonly that walls are able only to carry loads in their strong axis (in plane) and not in the orthogonal direction.

Assuming that wall's piers had good boundary conditions, the capacity curve for the wall in one direction can be obtained by superimposing the capacity curves of all the piers acting in the analyzed direction as [To 99][LB 04]:

$$V_W(\delta) = \sum_n V_i(\delta) \qquad \text{Eq [4.19]}$$

where $V_W(\delta)$ is the total shear resistance of the wall as a function of lateral displacement δ, n is the total number of piers and $V_i(\delta)$ the individual capacity of piers. The result of equation 4.19 is better understood by means of figure 4.17. An example is presented there for the case of 3 pier elements. Each pier element is described in terms of their deformation capacity to lateral actions computed from the bilinear model as it is proposed in figure 4.16 and equations 9,11,12,14,18. In figure 4.17, a wall could be described by the wall factor f_W, used in this study to characterize a determinate wall's total lateral capacity in function of the element with greater resistance $V_{max}(\delta)$.

According to equations 9,11,12,14, the resistance is significantly affected by the geometry of the pier; the same happens for the elastic stiffness calculation. Taking into account these two aspects, and no material change, the behavior of the wall is dominated by the resistance-deformation characteristics of the pier with greater resistance. The F_W of a wall is computed from equation 4.20. The F_W value for the serviceability limit F_{WE} is obtained from equation 4.21 after estimating the elastic limit at 0.7 $V_{max}(\delta)$ [To 99]. The F_W and F_{WE} are of importance to characterize the walls in plane performance according to the proposed SAUMAC procedure.

$$F_W = \frac{V_W(\delta)}{nV_{\max}(\delta)} \qquad \text{Eq [4.20]}$$

$$F_{WE} = \frac{V_{EW}(\delta)}{0.7nV_{\max}(\delta)} \qquad \text{Eq [4.21]}$$

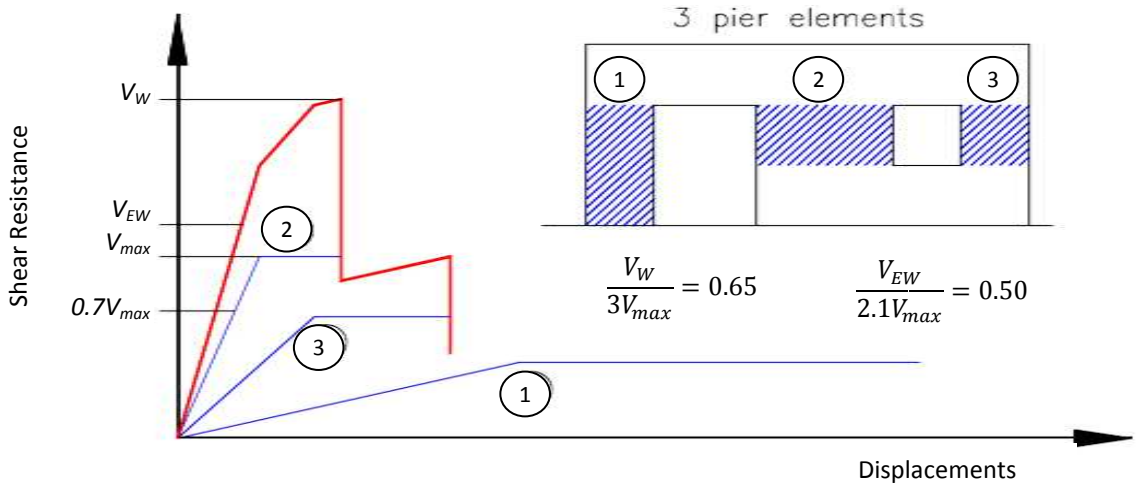

Figure 4.17: Individual wall capacity description

As explained before, the structure behavior factor q is of relevance for the estimation of seismic action, which is a function of the structural response (equations 3.13). From this point of view, q could be used as a performance description of a determinate structure. This is clearly observed in figure 3.16 where the elastic behavior of the structure is found for q=1 (serviceability performance level). Other performance characteristics could be associated to a behavior factor value in relation to the specific LS.

Structural factor values, had been presented by several authors (table 4.7 for European practice) and norms (Appendix D). There, it is referred also as structure's equivalent ductility, response reduction factor, or any other equivalent expressions resulting in the reduction of estimated lateral forces. The behavior factor takes into account the deformation capacity of the story, energy dissipation and the redundancy. Conservative assumption of q values is suggested by Tomaževič as the reason for buildings survival after important earthquake events, yet when they were designed originally for low seismic actions [To 99]. In simple words, low values of q represent big over-strength ratios (ratio of actual to design strength resultant from safety factor methods).

In the context of this study, q factors are suggested for the LSLS according to the maximum-minimum ranges proposed by the EC-8 [EC-8.1] despite these two aspects: evidenced performance to floor diaphragms [SW 03][SA 02], and assigned ductility referred to predominant failure modes of each storey. Equivalent q values are given at each storey for the SAUMAC methodology, taking into account that: immediate under story must have an equal or lower value of q so that $q_B \leq q_1 \leq \ldots \leq q_n$ where q_n is the q for upper floor (n up to 3-4) and q_B is respectively for the base floor. The proposed shear force incremental $(n+i)/(n+1)$ (section 3.3.2) is a conservative formulation for lateral forces distribution. Behavior factors for out-of-plane were detailed in section 3.3.4.

Table 4.7: Structural behavior factors q for URM buildings (in SAUMAC values per storey)

	Behavior factor q			Comments
EC-8 [EC-8.1]	$\underline{1.5} < q < 2.5$			Recommended factor to use is underline. Enlarger q values could be used based on ductility tests and National Annex
EC-6 [EC-6]	1.5			Recommended only for low seismicity cases
Tomaževič [To 99]	$1.0 < q < 1.5$			Proposed for assessment of URM, were 1.5 is recommended for buildings with rigid floors or good tie connections; 1.0 suggested for flexible floors and poor link
NTC [NTC-09]	$2.1 < q < 3.6$			Values suggested according the regularity in height and number of storeys criteria
SAUMAC (used for the proposed methodology)	2.5	Shear sliding and rocking	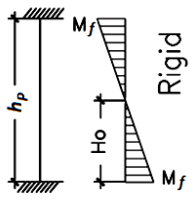	Value proposed in the case of rigid slabs and dominant shear sliding or rocking of pier elements (usually at the upper storey)
	2.0	Diagonal tension Shear		Value proposed in case of rigid slabs and dominant shear in diagonal tension of pier elements (usually at the base storey)
	1.75	Shear sliding and rocking	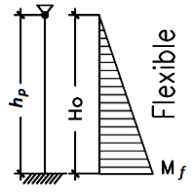	Value proposed in case of flexible slabs and dominant shear sliding or rocking of pier elements (usually at the upper storey)
	1.5	Diagonal tension Shear		Value proposed in case of flexible slabs and dominant shear in diagonal tension of pier elements (usually at the base storey)

4.6 Uncertainties in URM

There are many typical sources of variability related with URM. Some are related to human factors during the building lifetime such as aggregates, opening in walls and change of use. Others are related to the intrinsic material variability and non-standardized construction techniques. The wide dispersion of uncertainties associated to URM makes difficult the selection of appropriate parameter values to be used in traditional deterministic assessments procedures. This suggests that the use of probabilistic methods is more suitable to assess the structural behavior of this kind of structures.

The main result of a probabilistic assessment procedure is to calculate a probability of failure or exceedance p_f of a structure according to a defined seismic action and damage level. The probability of exceedance depends directly on the uncertainties in the load and resistance parameters. Uncertainty is possible to be quantified by means of the probability theory. One of the most common techniques to describe variability is by the use of the best fitting probability density distributions (PDFs) to each basic variable. In a seismic assessment context, the loading conditions and resistance of an individual wall are subjected to basic initial conditions or basic variables (section 5.2) such as: the magnitude of normal forces (self weight and live loads), the seismic ground motion characteristics, and other important building parameters like the geometry of pier elements, building shape, the distribution of walls, materials types, etc.

In addition to those uncertainties corresponding to basic variables, there are the ones introduced by the analysis model, related to the accuracy of both structural resistance estimations from building's parameters and loading simplifications (section 5.1). In common practice, conservative models are used. The obtained mean model value is under the mean experimental value and is also related to greater data dispersion. According to Schneider [Sc 97], poor accurate resistance models, like those for shear and punching resistance, present coefficients of variation from 10% to 20%. Figure 4.18 explains graphically the used value for estimating resistance in usual code formulations. It's expected that for URM models tend to be conservative because of data dispersion.

The variety of types and sources of uncertainty, along with the lack of agreed terminology, can generate considerable misunderstanding. In order to avoid confusion about the source of uncertainties in this study, three types are defined according to ISO 2394 [ISO-2394]:

- *inherent random variability or uncertainty:* subdivided into uncertainties which can, or cannot, be affected by human activities.
- *uncertainty due to inadequate knowledge:* subdivided into uncertainties which can, or cannot, be decreased by research activities
- *statistical uncertainties:* precision of the statistical tool used

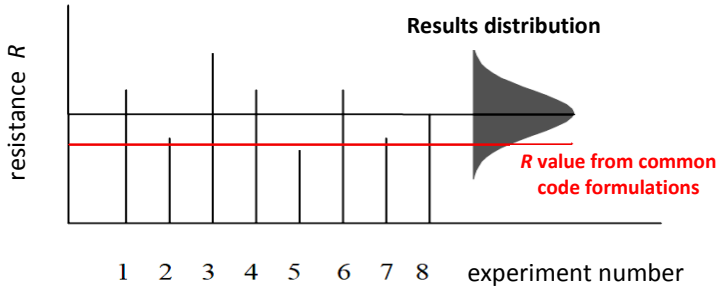

Figure 4.18: Estimation of model uncertainties from test results (adapted from [JCSS-00])

There are many typical sources of inherent variability related with URM. Some examples are those related with the change of use of the building during lifetime, vertical and/or horizontal aggregates in the structure and changes in the internal/external wall configuration. All these aspects are related to the initial structural design, which may vary significantly during the lifetime of the structure due to human modifications. In many cases changes are done without an engineer or any other authority approval. For example, a building could easily be modified from housing use to storage use, a new story could be added because the need of additional space, an internal wall could be eliminated to make a larger room or a new window could be added. Particular examples of this situation are presented on Figure 4.19.

In the group of those uncertainties that could be reduced due to greater investigation, there is the description of the mechanical material properties (mortar, brick,wall), shape, size, overlapping and configuration of wall units, stiffness and thickness of mortar joints, thickness of the walls (or layered walls), the strength of the unit-mortar interface and degradation of the materials. For assessing URM, it is important to remember that due to the highly variable nature of URM, testing must be conducted not only on individual materials, but on their interactions between elements, particularly the interaction among mortar and bricks [RMI 07]. Non destructive testing such as radar test, infra-red thermography or ultrasonic pulse give a good approximation of consistency for URM walls and properties if used together with some destructive in-field testing (e.g. flat jack).

The reduction of scatter in URM usually comes together with considerable amount of economic and time resources to be invested. The economic factor is of importance, the cost of appropriate assessing of the building is significantly high if compare with the usual low market value associated with many URM houses. This economic barrier is a reason that justifies the application of less detailed assessment methodologies. Because of the particularities of URM, some codes actually included a proposed conservative “range of values” for estimating some basic variables of masonry wall mechanical material properties (min/max values) to be used in structural assessment.

Guidelines such as the EC 8-3 [EC-8.3], SAMCO [SAMCO-06], JBDPA [JBDPA-01] and FEMA-310 [FEMA-310] include different assessment levels or degrees to be in accordance to the available data and the uncertainties presented as explained on section 5; in other words, an assessment according to the level of structural knowledge. The methodology proposed in this study will fall on the so called limited knowledge assess according to EC-8.3 and EC-0 [EC-0].

a) *b)* *c)*

Figure 4.19: URM uncertainties: a) Change of use from roman amphitheater to housing in Lucca (Italy), b) irregular house aggregates in Katmandu (Nepal), and c) material variation for a single wall at Castelnuovo (Italy)

5 ASSESSING EXISTING STRUCTURES

The need to assess a structure may arise from different causes regarding safety hesitation for a particular structure. The two main objectives of assessment of existing structures are to insure structural safety and serviceability, in a context of minimization of costs and time. Costs include inspection, evaluation, maintenance, and repair works.

For typical individual building assessment, possible solutions are in fact binary: yes or no; meanwhile for an edifice population answers can be expressed in terms of risk qualifications (low/moderate/high risk). For individual building safety description, a flowchart like the one proposed by Schneider in figure 5.1 can be used [Sc 97].

If a building is found unsafe, different options are possible according to figure 5.1. Usually, for common building housing, it is not a possible to intensify monitoring. Load reduction, from a seismic engineering point of view, can be accomplish by changing the use of the structure (e.g. form storage to office) or by changing heavy elements in the structure such as heavy roofs. The decision neither to demolish nor strengthen of a structure is mainly taken on an economical or CSH basis.

Regarding building groups, risk quantification is useful in a macro-scale in order to give stake holders relevant information about mitigation treatment such as: future investment on building infrastructure rehabilitation or demolish (prevention), location of hazardous areas (response, preparedness) and recovering strategies.

In this section we will develop a step by step assessing process, starting from commenting appropriate sophistication levels criteria applicable to our URM structures according to available resources. A discussion about the importance of accurate models and description of initial basic parameters, overview of reliability verification possibilities, assessment tools, the determination of seismic structural risk and an evaluation proposal of results according to target reliabilities is also included in this section.

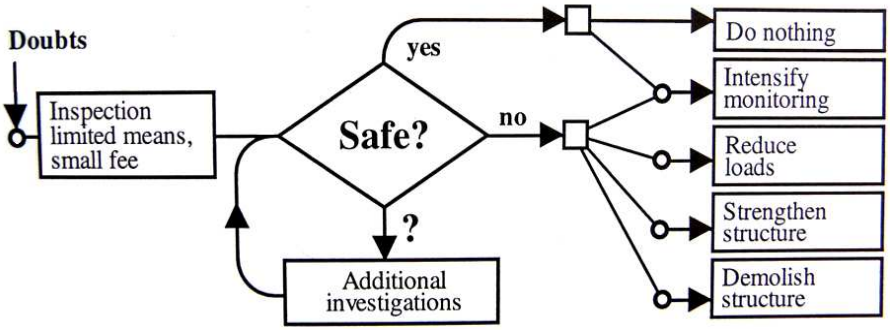

Figure 5.1: The risk assessment phase for an individual edification [Sc 97]

5.1 Assessment Sophistication Levels

Assessment procedures vary in sophistication. It is of common practice to start, if possible for a building category, with basic evaluation procedures such as the FEMA-154 rapid qualitative screening based on only general info such as building typology, number of storeys, year of construction, soil type, and structural irregularity [FEMA-154]. Structural assessment norms present different grades of sophistication possibilities; usually related with the initial information available (according to cost-time possibilities) and the importance of the structure to be inspected.

The sophistication of the chosen assessment procedures must be proportional to the accuracy of analysis models and input parameters. For instance, the use of advanced material/structural models and verification procedures with poor materials and structural characterization, drives into a description not much different than the one obtained from simplified methodologies. The principle of junk-in = junk-out is valid even with the most powerful available analyses tools. On the other hand, an excellent description of material properties with field and laboratory data is not consequently admissible to be analyzed later with simple model and verification procedures; although, this second situation is more desirable than the first one.

Due to high intrinsic uncertainly related to most URM (especially with flexible diaphragms), assessment descriptions such as FEMA-310 recommend extensive evaluation procedures such as the one of tier 2 (in the same norm), but this condition is not always in agreement with available resources for assessment. For URM typologies in FEMA-154, structures require always a more detailed professional evaluation since the suggested cut-off value of 2 is never achievable for low rise URM. Due to this aspect, the proposed methodology (SAUMAC) is planned into a framework of a typical basic (limited knowledge) assessment for individual buildings.

On table 5.1, equivalent procedures to the one proposed in SAUMAC for an individual building were overviewed. The table is composed of data acquisition details, recommended analyses and verifications. For the SAUMAC methodology, it is of much importance to comment that results are obtained from some sophisticated probabilistic verification tools (section 5.3). This might seem like a contradiction with the discussion of some paragraphs before. In particular for individual buildings, SAUMAC results are likely to be used in a qualitative form, since, neither a detailed analysis nor a specific deterministic building was introduced for the assessment procedure.

Table 5.1: Basic level assessment procedures

Norm	Assessment Level	Data Acquisition (Structure/Materials)	Analysis or Model	Verification
EC-8.3 [EC-8.1]	KL 1: Limited knowledge	From common practice and limited in situ inspection, material up to standards and limited in situ testing	Linear static and linear dynamic	Increased code partial safety factors values
SAMCO [SAMCO-06]	LEVEL 2- and some aspects of LEVEL 3	Document review, inspections and monitoring of existent damage (e.g. cracks, deformations)	Basic structural models	Partial safety factors
JBDPA [JBDPA-01]	FIRST SCREEN	Material strength and cross sections, cracks and structural layout	Lateral force	Comparison with trigger seismic demand index
FEMA 310 [FEMA-310]	TIER 1 for Moderate seismicity	Material properties from normative, basic structural and non-structural checklist	Pseudo lateral force	Triggered by evaluation of Checklist (locate deficiencies)
SAUMAC		Layout from common practice and limited in situ inspection: visual outdoors description. Material characteristics from norms	Lateral force (with non-linear considerations at each storey)	Probability reliability based quantification for building groups, risk qualification for individual buildings

5.2 Basic and Modeling Variables

It is usual to formulate a problem in civil engineering as the comparison of two aspects: the demand or solicitation *S*, and the capacity or resistance *R*. In the context of seismic hazard assessment of structures, *S* is expressed as an inter-story drift due to seismic actions, meanwhile *R* represent a permissible drift value linked to a performance level. *R* must be equal or bigger than *S*, so that no failure occurs in the context of the desirable performance condition.

Checking for structural safety $R \geq S$ follows a deterministic pattern. Repeating the deterministic safety formulation $R \geq S$ allows engineers to test the variation of results to the basic input, so that, safety criteria according to this sensibility can be proposed.

In a probabilistic approach, different from using deterministic input values, basic variables are randomly generated from probability distribution functions (PDFs) for load and resistance factors. Their function, however, is also dependent on the so-called model precision [Sc 97]. The accuracy of a model, at the same time, is assessed simply by introducing in the probabilistic solution formulation another basic variable M_i (equation 5.1 for resistance *R* case), where *M* stands here for model and *i* to the analyzed phenomenon.

$$M_R = \frac{resistance\ results\ from\ experiments}{resistance\ results\ from\ model} \qquad \text{Eq [5.1]}$$

A good model presents a mean value $\mu_{MR} \approx 1$ with a low standard deviation σ_{MR}. However, as commented in section 4.6, conservative models are often used for determining engineering resistance so $\mu_{MR} > 1$. Most of the relevant basic variables for seismic design are shown in figure 5.2.

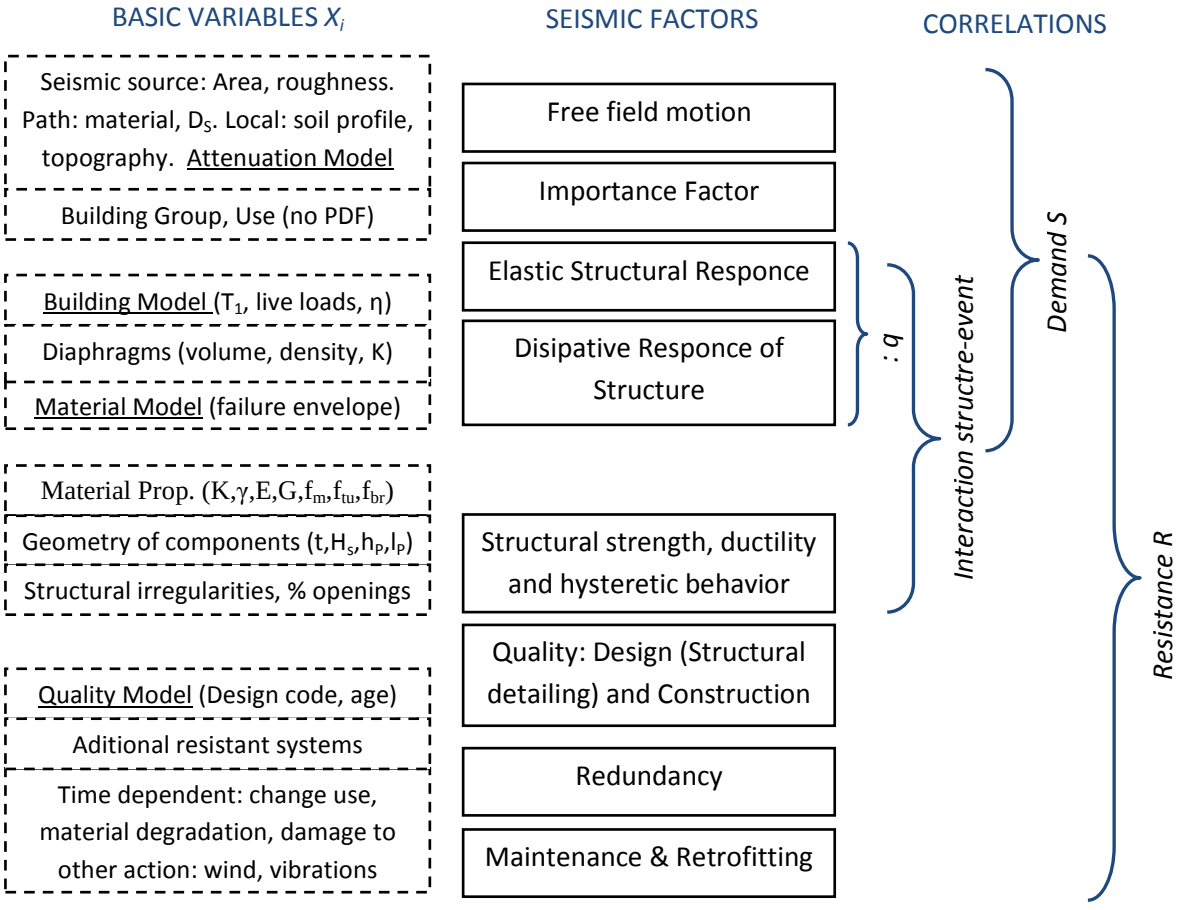

Figure 5.2: Basic variables and factors ruling the seismic structural response (based partially on [Fl 07])

Seismic action models, based on attenuation curves, present much more variability than resistance, so, it is of great importance to introduce also this variability on assessment for *S*.

Basic variables are linked to a series of factors or phenomena used to describe the response of structures to earthquakes (figure 5.2). A single basic variable may contributed to explain many of the factors presented in the figure. Most of these factors had been previously explained in sections 3 and 4. Additional to the factors commented in the sections 3 and 4, there are quality aspects (in design and construction) and maintenance/retrofitting related to changes in resistance behavior on the structural response indirectly. An initial quality parameter can be established as a function of local constructions practices and existent normative at the time of construction. On the other hand, aspects like maintenance or additional retrofitting works on the structure can be taken into account in case of life cycle analysis of the structure. Finally, redundancy (or robustness), consists of a series of independent measures, not linked to the main resistant system, conceived to increase safety in the structure. Failure occurs just after all independent resistance systems fail.

For seismic assessment, it is observed in figure 5.2 that there are many factors involved in both, resistance and solicitation aspects. Hence, there are no independent variables and a correlation exists between *S* and *R* since the action modifies the resistance and, at the same time, S is subjected to changes in *R* behavior in an iterative process. As a result of this interaction, the seismic design response spectrum is proposed to decide the seismic action (section 3.3.1). After the SDS parameters are obtained, *R* and *S* are considered (for static design approaches) as independent in between parameters; hence, equation 5.2 can be solved by formulating PDFs according to basic variables for both *R* and *S*. Figure 5.2 will be retaken in section 6 since a new factor is introduced by the SAUMAC procedure, this factor is a stochastic architectural factor proposed to assess URM buildings from a probabilistic point of view considering many possible building configurations according to some basic parameters. This is different from traditional procedures were the factors in figure 5.2 are taken into account just to solve equation 3.2 for a particular "deterministic" building configuration.

5.3 Reliability Assessment Methods (safety factor β)

In the sections before, it has been overviewed that limit states (LS or performance levels) are described according to well known damage or malfunction definitions. Damage in seismic structural engineering is proposed in terms of stress on elements or excessive drift values (figure 3.16 and table 3.5). The expression "limit state" is thought to represent a separation between desirable and unaccepted behavior. In the reliability context (probabilistic approach), the measure of safety is provided by the probability of any given LS to be exceeded at least once during the structure's lifespan.

For the defined LS, the so called limit state equation $G(X)$ represents, in terms of a PDF, the reliability characteristics of a system. X here represented all design parameter (basic variables). Equation 5.3 is a particular formulation of $G(X)$ to PDFs of *R* and *S* taking into account that usual engineering formulation separates factors regarding to loading or resistance aspects.

$$G(X) = \begin{cases} > 0 \; if \; LS \; is \; not \; exceeded \\ = 0 \; if \; LS \; is \; attain \\ < 0 \; if \; LS \; is \; exceeded \end{cases} \qquad \text{Eq [5.2]}$$

$$G(X) = R - S \qquad \text{Eq [5.3]}$$

The formulation of X inputs to solve $G(X)$ determine the possible assessment tool (level of sophistication) to be used. According to Schneider [Sc 97] they are:

1) Variables X are single valued (normally mean values). This is the usual situation of actual codes: p_f´s cannot be computed but are supposed to be small enough according to applied safety factors on actions and resistance factors.
2) Variables X are introduced in terms of the two probabilistic moments μ and σ: p_f´s can be obtained but, the possible uses are very limited (e.g. comparison & sensibility analysis).
3) Variables X are introduced using suitable PDFs: p_f results, from adequate input variables, can be used in an extended concept. Results are very dependent on the "tail" of the distribution (particularly sensible when very low p_f´s are required)

The proposed SAUMAC methodology follows the conditions mentioned in point number 2; distribution types are chosen to describe the probabilistic moments over few available information and after decisions over which type of distribution to be used. Because of this, results are limited to be used in a qualification basis for individual structures. In case of a building population, results are proper to meet the criteria to be fully used as a tool in risk assessment methodologies.

The formulation $G(X)$ can be solved analytically, numerically or by simulations (figure 5.5). For the analytical formulation, the probability of failure is found when $G(X)$ becomes a random variable itself so that:

$$p_f = P(G \le 0) = F_G(0) \qquad \text{Eq [5.4]}$$

where $F_G(\cdot)$ is the cumulative distribution function (CDF) of G. Equation 5.4 is very difficult to compute, close form solutions are only possible for elementary cases [PGF 04]. Considering the simple common case of equation 5.3 and assuming both R and S as independent variables, the probability of failure is obtained by either of the next formulations:

$$p_f = \int_{-\infty}^{\infty} F_R(x)\, f_S(x)\, dx \qquad \text{Eq [5.5a] or}$$

$$p_f = 1 - \int_{-\infty}^{\infty} F_S(x)\, f_R(x)\, dx \qquad \text{Eq [5.5b]}$$

Here f_S refers to the PDF of S. Both equations 5.5a-b can be easily solved numerically. A close form solution for equation 5.5 is obtained for independent normal distributes R and S via a transformation of the variables into a Gaussian space ($\mu = 0$ and $\sigma = 1$). In the particular case $G=R-S$, G in this case is also referred as the safety margin Z, with $\mu_Z = \mu_R - \mu_S$ and $\sigma_Z = \sqrt{\sigma_R^2 + \sigma_S^2}$ so that the probability of failure is found to be:

$$p_f = \Phi\left(\frac{-(\mu_R - \mu_S)}{\sqrt{\sigma_R^2 + \sigma_S^2}}\right) = \Phi\left(\frac{-\mu_Z}{\sigma_Z}\right) = \Phi(-\beta) \qquad \text{Eq [5.6]}$$

where $\Phi(\cdot)$ is the standard Gaussian CDF; and β is the so-called "safety index". Equation 5.6 can be solved without computing the Gaussian CDF by means of Appendix B. Target reliabilities are usually expressed in terms of β. For lognormal distributions describing the resistance and actions we have that when $\ln R$ and $\ln S$ are Gaussian with a mean and standard deviation of $\lambda_R = \ln\mu_R - 0.5\zeta_R^2$ and

$\zeta_R = \sqrt{\ln(1+v_R^2)}$ for R, and $\lambda_S = \ln\mu_S - 0.5\zeta_S^2$ with $\zeta_S = \sqrt{\ln(1+v_S^2)}$ for S (where v is the coefficient of variation $v=\sigma/\mu$) equation 5.6 is equal to:

$$p_f = \Phi\left(\frac{-(\lambda_R - \lambda_S)}{\sqrt{\zeta_R^2 + \zeta_S^2}}\right) \qquad \text{Eq [5.7]}$$

Equation 5.7 is of extensive use since many variables tend to be described by lognormal PDFs. It is also of special interest to obtain the sensibility factors (α_R and α_S) as a way to measure the participation of a variable in the final safety index. This is used later on for the explanation of how partial safety factors are obtained from reliability analyses. The graphical 3D representation of the problem ($G=R-S=0$, linear state equation) is shown for normally distributed S and R in figure 5.3. The volume under the red area represents p_f, the total volume is equal to 1.

Close form formulation like in equations 5.6 and 5.7 is not usually possible since PDFs for variables are frequently non Gaussian, they can be more than two basic variables, and finally limit states could be non-linear. Results of p_f for these conditions are approximately obtained after following an iterating procedure in the so-called first order reliability method (FORM). The FORM procedure is based on the Hasefor-Lind idea of bringing random variables X_i of a given $G=G(X_1,X_2,...X_n)$ into a standard space ($G = a_0 + \sum_{i=1}^{n} a_i X_i$) and then developing G as a Taylor series [HL 74]. If only the first terms (linear terms) of the Taylor series are taken into account, the procedure is called FORM method. When the second order term is used, then it is called the SORM method. Detailed explanations of FORM method are found in Melchers [Me 99], Schneider [Sc 97], and Pinto [PGF 04]. In order to solve equation 5.4, the Monte Carlo simulation technique is frequently used in this work.

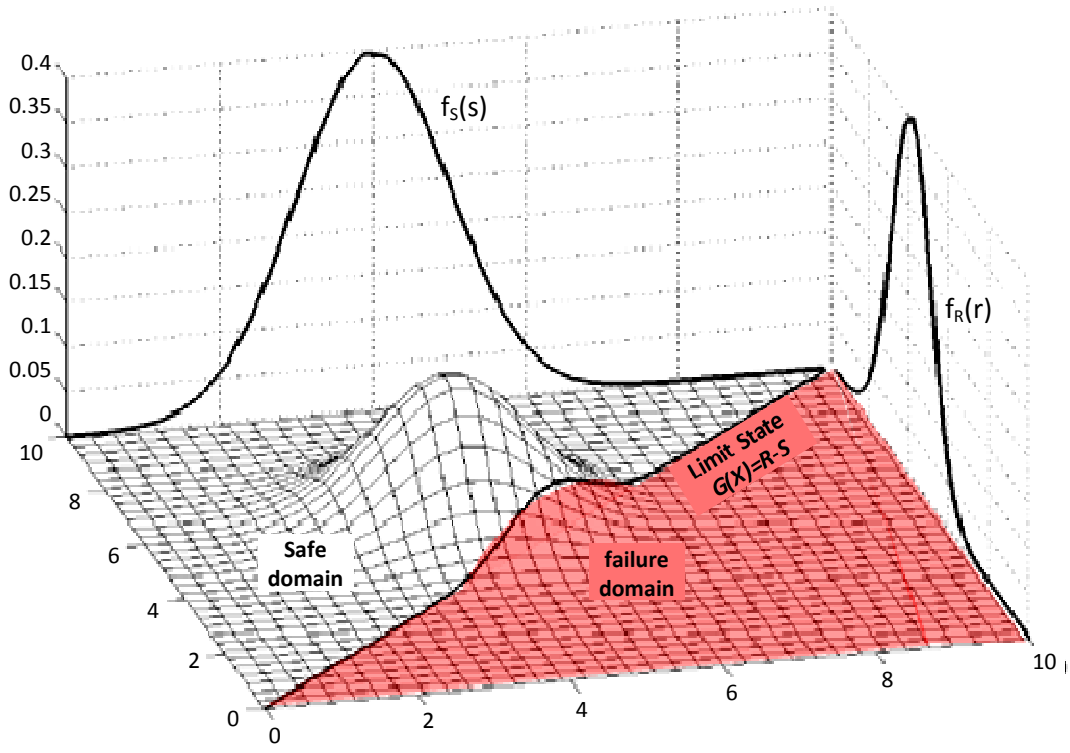

Figure 5.3: Graphical description of failure domain (Adapted from [SAMCO-06])

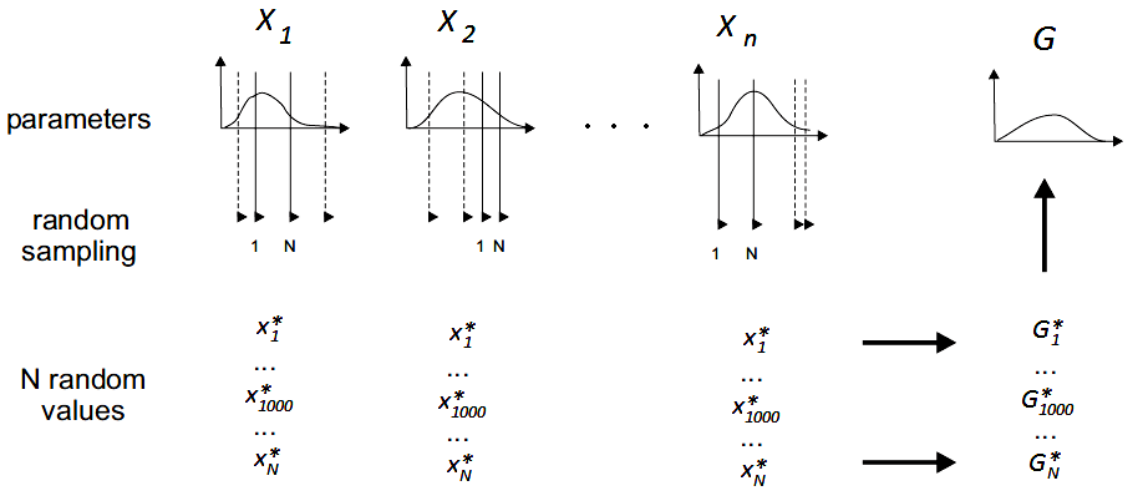

Figure 5.4: Monte Carlo process (Modify from [St 04])

The Monte Carlo approach (MC), is a powerful simulation technique largely in use nowadays after the recent development of computers, increasing its application. In a MC simulation, the exact or approximate calculation of a probability density to an arbitrary limit state $G=G(X1,X2,\ldots Xn)$ is replaced by statistically analyzing a large number of individual evaluations. The process is observed in figure 5.4 for n number of basic variables and N random sampled values, taking into account each basic variable PDFs. In MC approach, each uncertain input basic parameter is modeled as a random variable characterized by the most likely PDF.

The resulting N values are investigated according to the number of fails ($G<0$) represented by N_0, so that the probability of failure is:

$$p_f \approx \frac{N_0}{N} \qquad \text{Eq [5.8]}$$

The results are dependent of the number N of simulations. A big number of N are needed to investigate the usual required low values of p_f in a crude Monte Carlo approach. An initial estimation of N can be approximated, for a usual 95% value of confidence level, as [Me 99]:

$$N \approx \frac{-\ln(1-0.95)}{p_f} \qquad \text{Eq [5.9]}$$

If G is assumed as a normally distributed PDF, the safety index can be as well found as $\beta = \frac{\mu_G}{\sigma_G}$. Similarly, as it is observed in equation 5.6, p_f can be computed from β.

5.3.1 Assessing reliability of systems

The p_f is established to characterize individual elements that form part of a reliability system. In the SAUMAC methodology, each storey is considered as an individual element into the whole system of a house. In a structural system, an individual or combined failure of elements may lead to collapse, or exceedance of defined LS. For statically indeterminate systems, usually only combinations of failing elements lead to the failure of the system [Sc 97].

Reliability systems are formulated in terms of parallel and series systems. In a series system the failure of a single element compromises the whole structure. Hence, in a parallel system failure occurs only when all the elements had failed; parallel formulations are related with the redundant properties of a structure.

If elements are perfectly correlated, the probability of failure in series systems P_f is found as the maximum p_f value of the system P_f=max[p_{fi}], for independent variables $P_f = 1 - \prod_{i=1}^{n}(1 - p_{fi})$. In the same way for a parallel system with perfectly correlated elements P_f=min[p_{fi}], if variables are independent then $P_f = \prod_{i=1}^{n} p_{fi}$ [Sc 97].

In the context of SAUMAC methodology, elements are considered perfectly correlated, this is a common practical assumption (also normal in normative). In reality elements do not present a perfect correlation between themselves along the building. Because of this, the building formulation is summarized to the expression P_f=max[p_{fi}], specified for a good correlated series system. Regarding the different failures types according to the formulation of the building in two main axes of analysis (*x*,*y*), results are evaluated in SAUMAC as:

$$P_{fx,y} = 1 - \left(1 - p_{fin}\right)\left(1 - p_{fout}\right) \qquad \text{Eq [5.10]}$$

where p_{fin} is the probability of failing in the in-plane failure mode and p_{fout} represents consequently the failure for the out-of-plane mode. When computing equation 5.10, the full seismic action must be applied for both in-plane and out-of-plane modes. The maximum of p_{fx} and p_{fy} is the p_{fin} to be used in the equation 5.10.

5.4 Reliability Verification Methods

Safety and serviceability margins can be physically described just as the distance in between the actual real state of the structure and a limiting state, expressed in terms of equation 5.2. The verification process is carried out to ensure that a target reliability level for a defined structural performance is reached. The way safety is evaluated varies according to the reliability verification procedure. A verification technique must be chosen according to the available data and structural analysis tools used to describe seismic actions and structural capacities as it is observed in table 5.1.

Diverse methodologies are applicable according to the deterministic global safety factor approach (traditional experience based) and the probabilistic limit states one as observed in figure 5.5. Probabilistic assessment verifications are nowadays extensively used for seismic hazard analysis due to the fact that the seismic force is conceived from PSHA procedures due to some limitations linked with DSHA as commented previously in section 3.2.1.

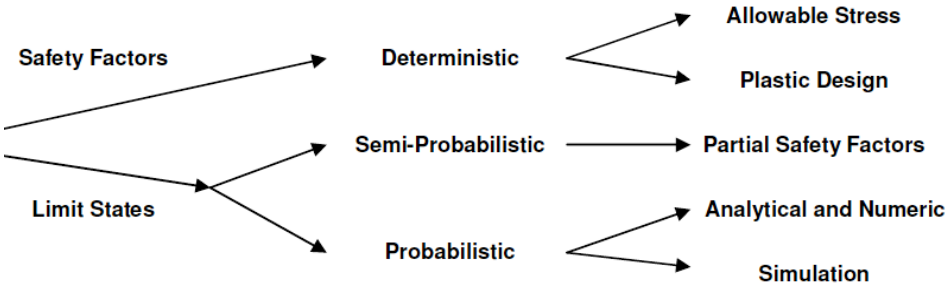

Figure 5.5: Reliability verification approaches and related design philosophy [SAMCO-06]

In normative, safety verification is frequently proposed by increasing the load effect and decreasing the resistance capacity in terms of partial safety factors (applied to important variables) derived from target reliability index β_O for a determinate period of time (time dependent problem). The factor β_O as observed in equation 5.11 is also called safety target index. Values of β_O are usually proposed for simple loss-cost analyses and will be discussed in section 5.5.2. From β_O, partial safety factors for R and S (basic reliability problem from equation 5.3), γ_R and γ_S, are formulated as [SAMCO-06]:

$$\gamma_S = \frac{S_{di}}{S_{ki}} = \frac{1+\beta_O \alpha_S v_S}{1+k_S v_S} \qquad \text{Eq [5.11a]}$$

$$\gamma_R = \frac{R_{di}}{R_{ki}} = \frac{1-k_R v_R}{1-\beta_O \alpha_R v_R} \qquad \text{Eq [5.11b]}$$

where S_{di} is the solicitation design, S_{ki} is the characteristic solicitation value ($S_{ki}=\mu_S-k_S\sigma_S$), v_S is the coefficient of variation and finally k_S and k_R are parameters related to the characteristic values; values of k_R and k_S are usually taken as 1.64 (corresponding to 0.05 fractile of a normally distributed PDF). k_R values are presented by Kücker [SAMCO-06]. In SAUMAC methodology full probabilistic verification tools are used to obtain β values (MC simulation).

5.5 Quantification and Evaluation of Structural Seismic Risk

Now that aspects related with the seismic hazard, the performance LS of structures, and some of the most common tools used to quantify safety have been overviewed and commented regarding our URM structures of interest, the risk assessment of the structural damage, as explained in equation 2.3, can be quantified/qualified and evaluated.

Traditionally, the seismic risk has been qualified in terms of ranges, areas, etc; describing a potential impact of a hazard. Methodologies such as the risk matrix approach (figure 5.6) are useful to anticipate losses, to evaluate potential impacts and to, in general, provide important information on the nature and level of risk in a given region but do not yield in loss estimates. It is clear from the figure 5.6 that class A events are of the highest priority (losses: death, fatal injury, high property damage), conversely class D presented a low risk (losses: first aid injury, low economical loss).

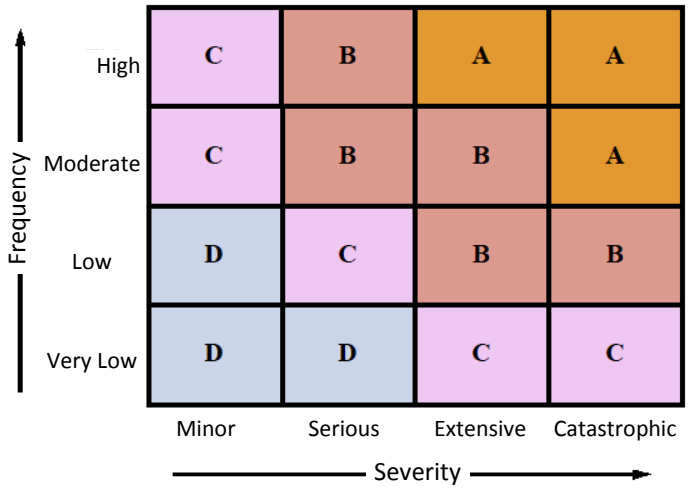

Figure 5.6: Risk matrix approach formulation [FEMA 97]

Nowadays, there are some available methodologies capable to quantify risk in terms of probabilities. Perhaps the most used risk assessment tool is HAZUS, proposed by FEMA [HAZUS 99]. Other similar tools are RADIUS and the proposal of the RISK-UE group for the European context [Ok 00][Mo 04].

A common aspect in between the methodologies just mentioned is the formulation of building structural vulnerability in terms of fragility functions. The computation of structural fragilities to actions has been subjected to intense research efforts to validate these methodologies. For HAZUS, fragilities are proposed for generic buildings after intense studies. In SAUMAC, the purpose is to propose fragilities damage functions adapted to local buildings obtained after a simple procedure.

5.5.1 Fragility curves

Structural vulnerability is evaluated in the context formulated and explained in figure 2.7 as it is an important aspect in the risk management procedure. Qualitative descriptions by classes, like the one presented by the EMS-98 in figure 3.3[Gr 98], or after computing some index reference value like IQM [BdD 09], Regione Toscana [FDPS 04] or Tomaževič [To 99], are useful for developing risk criteria in terms of the risk matrix approach (figure 5.6). In the context of quantitative formulation of risk, assessment procedures such as HAZUS describe vulnerability in terms of structural fragility functions. Fragility curves are also widely used to capture the effect of improvement measures for incremental seismic actions [PD 08].

A fragility function stands for the probability of exceeding a given limit state according to the specific performance requirement P_f, as a function of (conditional to) one parameter describing the intensity of the ground motion, typically the PGA or S_{pa} [PGF 04]. Most of the LS of interest (e.g. life safety or collapse prevention) are in the non-linear range of structural behavior. Evaluating the fragilities requires non-linear simulations to obtain the maximum response of the structure. In the context of this work, the structural response is inferred from the q values as proposed in figure 4.18 and the influence of PGA according to lognormal PDFs assumption. After obtaining the statistics for the response (modeled here as lognormal) and knowing the cumulative density function (CDF) corresponding to the URM capacity, the fragility in a time-invariant problem for an intensity parameter PGA is:

$$p_f(PGA) = \int_0^{\infty} F_R(x|PGA)\, f_S(x)dx \qquad \text{Eq [5.12]}$$

In equation 5.12, *(PGA)* stands for dependence on the intensity measure. The curve is obtained for different values of PGA. Figure 5.6 present fragilities computed by HAZUS procedure.

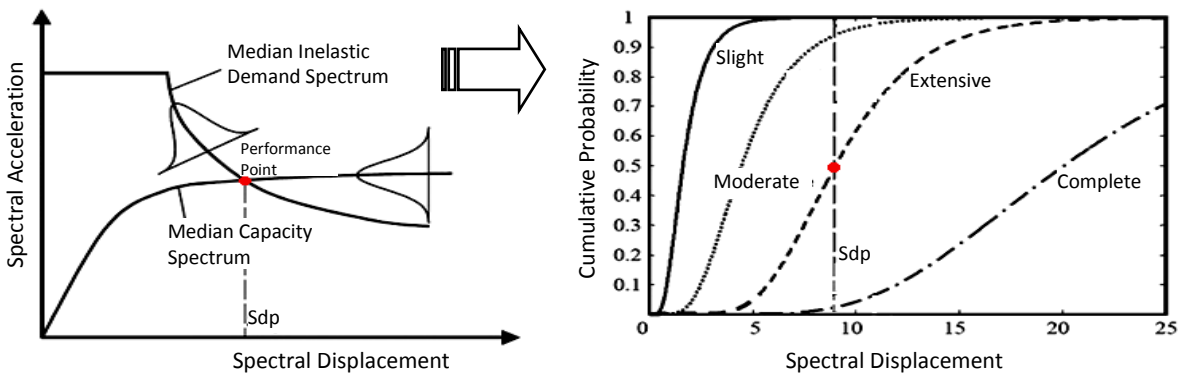

Figure 5.6: Fragility curves formulation according to a performance point [HAZUS 99]

In HAZUS fragility curves, equation 5.12 is computed once, just for the performance point (interception dot between demand and capacity in figure 5.6) that corresponds to the median points of the lognormal PDFs (2-quintile). HAZUS proposed performance points according to each building typology and performance level; the dispersion of the resultant $G(X)$ function (equation 5.2) in terms of a ζ_G value. ζ_G is given subjectively according to some parameters to shape the damage curve. The value of ζ_G is of importance since the tail values of a lognormal distribution may vary greatly the results of the probabilities of exceedance.

Equation 5.12 is used not in SAUMAC for computing P_f(PGA) directly. Fragility curves are computed by solving $G(X)$ for incremental seismic action PDFs as it is observed left in figure 5.7 for a specific capacity PDF and three varying action PDFs. It must be comment here that the demand parameters correspond to the "plateau" of the seismic response spectrum since it is simplified for the SAUMAC methodology for the life safety limit state. The possible results according to 3 different seismic levels are marked right in figure 5.7 as 1, 2 and 3. For the in plane formulation, the solution is obtained after a FORM or a MC simulation procedure since more than the two basic R and S variables are used. The MC method is the one preferred in this study. After the points describing the fragility are found and lognormal PDFs is observed to describe properly P_f(PGA).

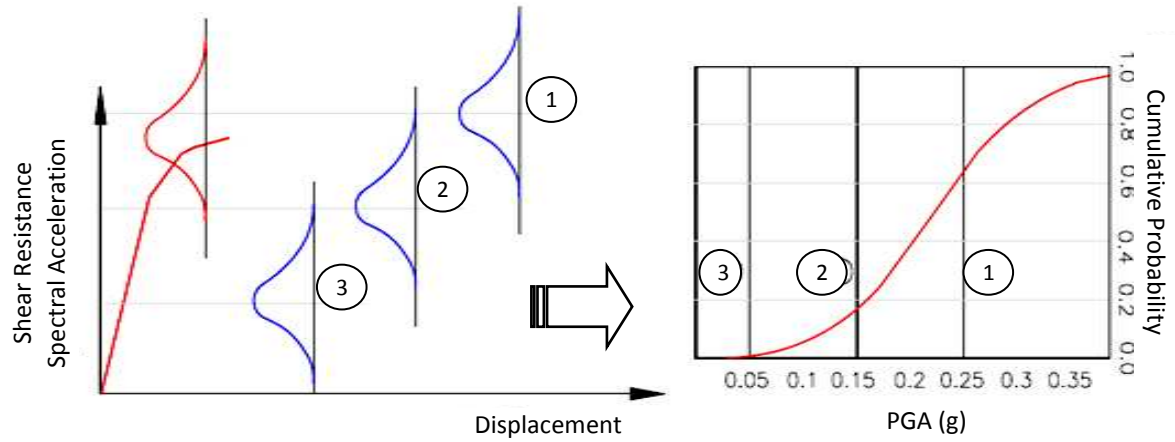

Figure 5.7: Fragility curves formulation according to SAUMAC

5.5.1.1 Defining building typologies

To avoid the need of unnecessary individual assessment of houses, in the context of regional risk management, grouping building by typologies is useful. Many so-called Rapid Visual Screening methods were developed in countries such as Japan, USA, Canada, New Zealand, Turkey, Greece and India based on typological characterizations [Sr 10]. These methodologies allow to difference between building structural types (RC, steel, etc). The URM, itself, is sort as a common structural typology by seismic codes and assessment methodologies. URM building categorization criteria can be related to aspects such as:

- *Special structural configuration*
- *Location of the building (ex: corner, isolate, in between two other building)*
- *Number of storeys*
- *Material types (Vertical typology)*
- *Floor diaphragm (Horizontal typology)*
- *Material mixing (e.g.: different material for inner and outer walls and aggregates)*
- *Building period (normative, age)*

Because it`s intrinsic characteristics, URM structures are very seldom behaving in the same way, even into the same URM material typology; here, the importance of formulating all the relevant possible different types according to combination of the parameters mention before.

The number of the categories is up to the study resolution and to the local structural variability. It is usual in towns to distinguish common construction particularities after the use of dominant materials and/or a construction technique. Once a particular standard type of building is defined, the procedure to obtain a β is the goal of the SAUMAC methodology. If a particular construction is common in an area, fragility curves are easily developed for a straightforward calculation of the seismic risk in a regional scale.

5.5.2 Risk and target reliability

The structural seismic risk is obtained from the convolution of hazard H and vulnerability functions (fragility). The typological risk is defined according to Pinto as the unconditional probability of exceeding a given limit state [PGF 04]. With a defined H function and well known typology fragility curve, the structural risk R_S is directly expressed as:

$$R_S = \int_0^{\infty} \left| \frac{dH}{dPGA} \right| P_f\left(PGA\right) d\,PGA \qquad \text{Eq [5.13]}$$

where the parameter proposed in this study to quantify the seismic risk is directly the peak ground acceleration (PGA). Other parameters can be used as well according to the formulation of the $H(i)$ and $P_f(i)$, were i refers to a seismic intensity variable. As the hazard curve is formulated in terms of annual rates of exceedance, the value of R_S is also corresponding to an annual probability one. By inspection of equation 5.13, the structural risk is obtained at each point of interest for different hazard magnitudes. The hazard magnitude to be inspected in H is up to the specified requirements of norms such as: the seismic action return period, and performance limit states (e.g. those in table 3.2).

It is clear that only to find a risk value is nonsense without limits to judge if the risk is acceptable or not. Table 5.2 gives a qualitative description of event likelihood.

Limits, like the ones described by the Australian Geomechanics Society in table 5.2 [AGS 00], are a reference criteria to illustrate the likelihood of an event and not the consequences. Figure 5.8 offers a better panorama as a consequence parameter is presented in terms of exposed values, for this case: human life loss. So it is evident from the figure that as more human lives are in danger, the acceptable risk is lower.

Table 5.2: Qualitative measures of likelihood (Australian Geomechanics Society [AGS 00])

Level	Descriptor	Description	Annual R_S
A	Almost certain	The event is expected to occur	$>= 10^{-1}$
B	Likely	The event will probably occur under adverse conditions	$= 10^{-2}$
C	Possible	The event could occur under adverse conditions	$= 10^{-3}$
D	Unlike	The event might occur under very adverse circumstances	$= 10^{-4}$
E	Rare	The event is conceivable but only under very exceptional circumstances	$= 10^{-5}$
F	Not credible	The event is inconceivable or fanciful	$<= 10^{-6}$

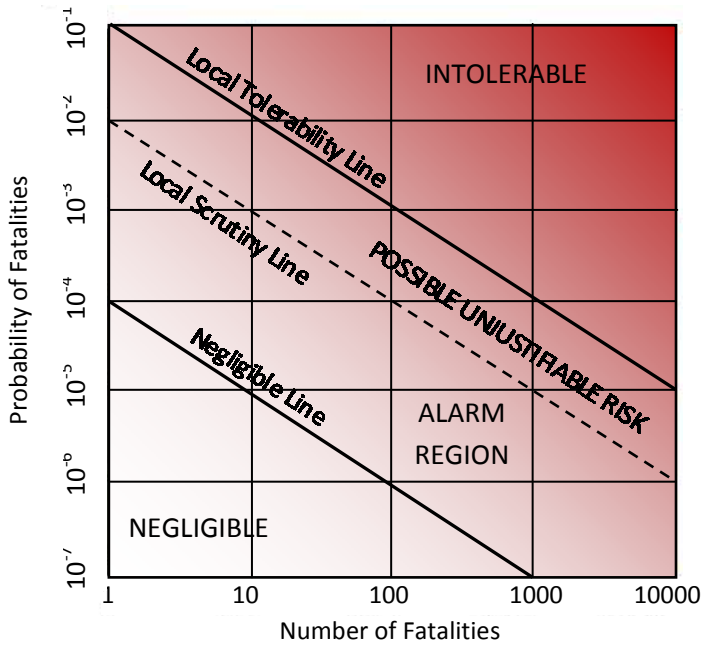

Figure 5.8: Tolerable risk as a function fatalities [Tephra-96]

Figure 5.8 can be taken into account to assess the life safety limit state (LSLS) for low-rise and middle size URM (up to 4 storeys which are the focus of this study). The LSLS is assumed in this work approximately equal to that described by D3 damage level in table 3.5 and figure 3.16; hence, a fatality estimation for LSLS in figure 5.8 will correspond to those related up to D3 damage of structures (accepted fatalities corresponding to D3). According to results obtained by Spence, human loss in URM structures after resent earthquakes in Pakistan, Indonesia and Peru is not likely to be more than 6% of the URM building inhabitants for D3 damage [Sp 09]. According the population dynamics of a region, a total population per building unit can be estimated. Taking into account that the structures under analysis are of small size URM and damage equal to D3, fatalities bigger than 5 are not likely, with a common assumed value of around 1, this corresponds to the value most to the left in figure 5.8.

It is important to mention that the figure is not minded to describe fatalities when failure occurs, but the initial accepted causalities linked to a p_f. It is evident that for bigger structures like a 20 storey RC building more will be exposed values (economical, life, etc). In this case, the tolerable P_f should be reduced when the fatality ratio of D3 is hypothetically maintained similar to the one of URM buildings. Figure 5.8 can be used for different LS since for each performance level a mortality ratio can be found. Special attention must be paid for the collapse consequences related to damage degree D5, where different description possibilities for D5 damage can be distinguished [CSP 92]. A similar graph to the one of figure 5.8 is presented by Bhattacharya for different construction importance groups (military facilities, ports, industry, housing, etc) [BBM 01].

Rather than presenting figures such as the ones overviewed before, many codes (not usually the seismic ones) offer acceptability criteria according to a target safety index β_0. They define different reliability indices β_0 as function of failure consequences, costs of a safety measure (improvement measure) or structural behavior of an analyzed structure. For example in case of existing structures, there are larger costs related to the safety improvement compared to those at the design step and this fact is taken into account to lower β_0

The target reliability values are commonly only proposed for two conditions: Ultimate state and serviceability state, as observed for various authors in figure 5.9. This statement may turn into

ambiguous values of β_0 since it is not evident, especially to the ultimate states, to which performance level damage is it equivalent.

There are very few works relating seismic behavior and reliability, one is presented by Aoki [Ao 00]. Aoki obtained β for typical steel and concrete buildings in Osaka and Tokyo areas. In case of concrete structures a value of β = 2.2 for initial concrete cracking (Δ=1/200), β = 2.7 for cracking in secondary elements (Δ=1/100), β = 3.3 for failure in structural elements (Δ=1/50), and finally β = 4.0 for building collapse (Δ=1/30) were found. This study is a good reference regarding the correlation of β to damage values and can be used to better understand the used ultimate state β_0 and serviceability β_0 in norms, since explicit reference to specific performance levels is not clear for them. Values of optimal reliability can be obtained for design and upgrading of structures directly from cost-loss analyses as proposed by Wen and Ang in figure 5.9 [WCHE 96][AdL 97]. The β values in normative has been obtained in most cases for reinforced concrete structures.

From figure 5.9, it can be concluded that β_0 obtained from EC-0 [EC-0] and ISO 2394 [ISO-2394] are probably related to a near collapse LS, meanwhile the other authors may related it to a life safety LS. Also some confusion is found from the formulation of β in terms of annual value or for the whole expected life of the building. In the context of this work, the annual values, as proposed by the joint committee of structural safety (JCSS) [JCSS-00], are the ones of reference to which structures are evaluated later on.

Important to mention is that for the particular formulation of structural seismic risk in this study, risk is directly related only to the action of ground motion on the structure (in terms of PGA). Other structural aspects related to exposition of the structure to other phenomena, such as the effect of ground motions to cause soil liquefaction or any other soil movements that evidently will damage the structure, are out of the scope of this study and must be assessed into a multi-hazard scenario according to figure 2.7.

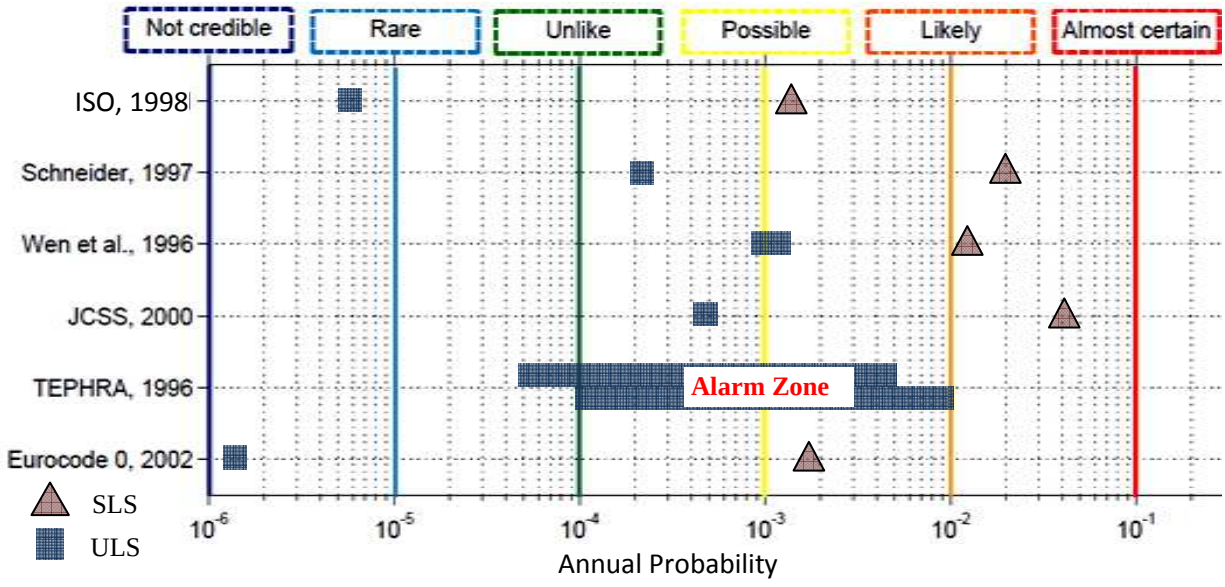

Figure 5.9: P_f annual values according to different authors and likelihood of event (equivalent β_0 values: [ISO-2394]: ULS = 4.4, SLS = 3.0; [Sc 97]: ULS = 3.5, SLS = 2.0; [WCHE 96]: ULS = 3 to 3.15, SLS = 2.2 to 2.4; [JCSS-00]: ULS = 3.3, SLS = 1.7; [EC-0]: ULS = 4.7, SLS = 2.9)

6 SEISMIC ASSESSMENT OF URM ACCORDING TO LOCAL BUILDING CONDITIONS SAUMAC

6.1 Methodology Description and Assumptions

Throughout this section, the SAUMAC methodology will be explained in depth. The mail goal of the proposed methodology is to estimate the structural risk R_S regarding unreinforced masonry buildings (URM) to a specific limit state (LS) as explained in section 3.4. The most relevant LS in case of common housing importance category for URM is the life safety limit state (LSLS); much of literature is focused on acquiring information to this LS and standards requested an adequate safe design for it (e.g. Eurocode 8.3 [EC-8.3]). To obtain a R_S value of local URM buildings, the SAUMAC methodology develops fragility functions P_f (PGA) (section 5.5.1) to estimate the URM performance to different seismic loading. After finding the P_f (PGA) for an individual house or a building group, the risk is computed from the convolution of the seismic hazard curve H (section 3.2.2) and the P_f (PGA) by means of equation 5.13 [PGF 04]. Results are evaluated qualitatively for individual buildings and quantitatively for building groups according to the required target reliability value β_O as discussed in section 5.5.2.

$$R_S = \int_0^{\infty} \left| \frac{dH}{dPGA} \right| P_f(PGA)\, dPGA \qquad \text{Eq [5.13]}$$

To obtain P_f(PGA), the limit state equation $G(X)$ is solved for each building storey and failure mechanism (in-plane and out-of-plane). The limit state formulation has already been explained with detail in section 5 and aspects from failure modes discussed in section 4.5. For solving $G(X)$, the storey resistance I_R is formulated based on a dimensionless shear resistance value of the storey`s wall piers, a dimensionless seismic action I_S in terms of a percentage of the reference peak ground acceleration (PGA), and finally another dimensionless variable A_M related to dispersion of the building architectural characteristics. A_M is obtained from the so called stochastic house model (SHM) explained in section 6.2. So finally in SAUMAC we have:

$$G(X) = G(I_R, I_S, A_M) \qquad \text{Eq [6.1]}$$

The parameters I_R, I_S and A_M can be all expressed in terms of the mean value and a standard deviation and assumed as lognormal probability density functions. Finding I_R, I_S and A_M is the aim of sections 6.3 and 6.4. In depth, to obtain the I_R at each storey, a Monte Carlo simulation MC is performed according to a series of basic storey variables (pier geometry, material properties, etc) and the masonry resistance model equations proposed by Magenes to attain probability density functions (PDFs) for different pier geometries [MC 97]. For I_S, the seismic solicitation PDFs are found after the factors affecting the seismic response spectra and PGA. Finally, the A_M PDFs are obtained from basic variables regarding architectural possibilities of the building (size, shape, number of internal wall, number of windows, doors, etc) and calibrated to an amount of resistant wall ratio ρ at each storey as it will be explained in section 6.2.

For the limit state condition $G(X)$=0, a division is made for values that fall on the acceptable safe region $G(X)$>0 and the ones in the unsafe region or failure condition. It is of interest here that the

probability of exceedance is computed as the possibility of *G(X)* to yield into values lower than 0. The probability of failure p_f is express as:

$$p_f = P\{G(X) \leq 0\} \qquad \text{Eq [5.4]}$$

The methodologies to solve equation 5.4 are presented in section 5.4. The solution of this equation for incremental seismic actions allows the development the characteristic fragility curve to each storey (section 5.5.2). Assuming a good correlation in between structural components of each storey, the total building fragility for the in-plane failure mode is dominated by the one of the most fragile storey found in both main axis analyses (*x*,*y*).

For recent code-designed constructions, the out-of-plane failure mechanism is of no relevance. In case of existing URM structures with poor connections, the out-of-plain failure mode is many times activated before the in-plane one. Out-of-plane and in-plane failure modes are considered as mutually independent, because of this, total probabilities should be formulate as expressed by equation 5.10.

$$p_{fx,y} = 1 - (1 - p_{fin})(1 - p_{fout}) = P_f(PGA) \qquad \text{Eq [5.10]}$$

where p_{fin} correspond to the maximum p_f in the in-plane of the building for all storeys and main analyzed directions (*x*,*y*) , p_{fout} correspond to the out-of-plain failing probability. The methodology assessment is resumed in figure 6.1 starting from the formulation of structural risk of equation 2.3 down to acquiring the PDFs for variables I_R, I_S and A_M. If a evaluation process is introduced into the formulation, a cyclic procedure can be conceived, ending only when the structure is finally considered safe or to be demolish.

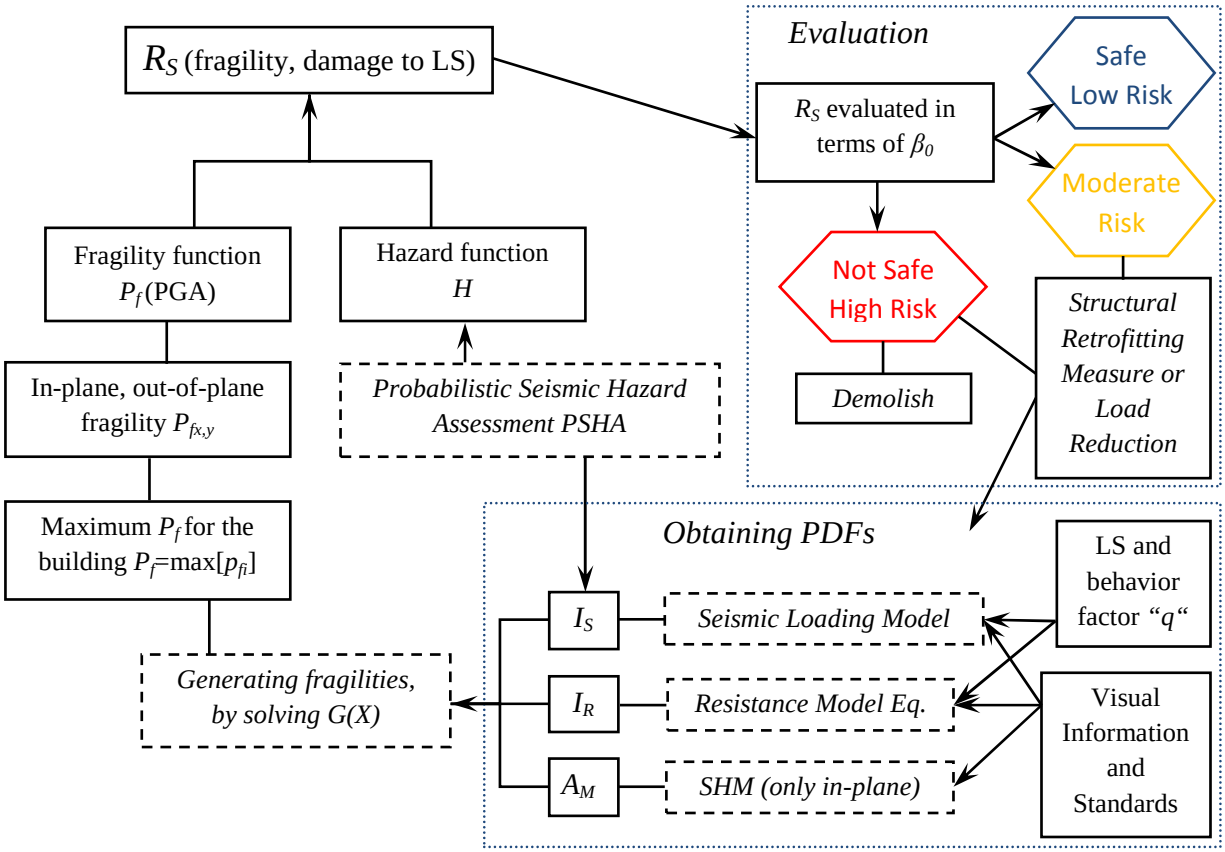

Figure 6.1: Assessment cycle to obtain and evaluate R_S

Different from just giving some structural vulnerability assessment procedure, the developed methodology is minded to measure in an easy way the effect of some possible rehabilitation solutions, this can be done by following the box chart in figure 6.1 for an individual building (safe?) or building groups (risk?). It can be assessed how changes in some building components affect the global expected behavior of the structure, do noting in case of safe structures and demolish in case of non important high risk ones.

Throughout the SAUMAC methodology, a series of assumptions had been made. According to this, the methodology is not fitting entirely into a specific standard. The EC-8.1 [EC-8.1], EC-8.3 [EC-8.3] and the NTC [NTC 09] are the standards that fit better to the methodology, basically because the analyzed case study is in Italy. The most important assumptions in the SAUMAC method concerning the principal aspects to find the fragility functions P_f(PGA) are:

- *1) The building is only composed of URM:* in the formulation of the methodology, other common techniques such as confined masonry or reinforced masonry are not included into the assessment for any storey. From the practical point of view, combination of systems is common for house aggregates.
- *2) Normal loading is applied uniformly in all storey piers:* according to the SHM statements all normal loads from floors (and life load) are distributed equally on piers, independently of the position or shape of the element.
- *3) Simplified seismic lateral force distribution:* the distribution of lateral forces is done according the proposal of FEMA-310 (tier 1 [FEMA-310]) and JBDPA [JBDPA-01], and after result corroboration like it was observed in figure 3.13.
- *4) Good resistance correlation in between floors and failure modes:* pier elements and building floors are considered to be well correlated (correlation factor close to one) in case of no change in materials. The assumption is related to the fundamental Eigen vector of the structure for the linear lateral force method.
- *5) Simple non-linear formulation for storeys:* a non-linear analysis was performed on each storey based on *q* factors linked to a failure mode in figure 4.18 for the life safety LS.
- *6) Variation of q values per storey:* to take into account different failure modes and floor diaphragm conditions according to rules presented in section 4.5.3.
- *7) Predefined architectural limitations:* related with SHM formulations limit the size of target buildings in terms of area and number of storeys (up to 4-3 storeys or 10 m height).
- *8) Eccentricity factor only applied in case of rigid diaphragms:* the F_{EC} value is applied only in case of rigid slab condition. Flexible diaphragms are not considered to distribute effectively lateral loads in between the elements.
- *9) Applied eccentricity factor:* the F_{EC} are only approximations according to a usual found condition in relation with the building position and the correspondent q_i values to be used in the JBDPA methodology.
- *10) No additional normal loads computed from lateral action:* for the simple lateral force structural formulation, not increments/reductions of normal loads were taken into account on elements. This can be of significance for piers in case of slender buildings.
- *11) The p_f related to failure in compression is not evaluated:* the p_f related with the simple compression failure is not included initially since building are low rise (section 6.2).
- *12) The in-plane and out-of-plain are mutually independent:* from a practical point of view the in-plane deformation of walls is not consider to affect the out-of-plane mode. Full actions are taken conservatively for both mechanisms. Out-of-plain can be neglected when the wall conditions, such as the ones observed in table 4.6, is archived.

6.2 The Stochastic House Model (SHM)

The SAUMAC methodology is based in obtaining the PDFs of the variables I_R, I_S and A_M to solve $G(X)$. For I_R and A_M this could be done by a random building generation process called Stochastic House Model (SHM). The proposed SHM process is based on Monte Carlo simulations MC for obtaining characteristic PDFs. For the MC simulation, a MATLAB code was developed for a house generation process following local building architectural rules as established according to each individual or local house typology. The MATLAB code is observed in Appendix C.

The idea is simple, from many synthetic produced buildings, a database of relevant different structural characteristics is developed according to possible local building conditions inputs. This information can be used to with analyze a particular house. In case of I_R, it is of interest the average normal load N acting on the piers. A_M is a parameter used to describe mass distribution on resistant elements at each storey according to architectural considerations.

The normal forces N acting on a wall is an important aspect for the calculation of the lateral resistance of piers. Studies, like the one perform by Sperbeck [Sp 08], made clear the large effects of the headmass m_N and PGA parameters on wall resistance assessment in terms of drift and local unit damage. This justifies most of the statements presented throughout this study were N and PGA are considered and discussed continuously. Other assessment procedures, such as VULNUS [Be 99], FAMINE [DS 03] and FEMA 154, characterized also single buildings (or building sets) in terms of PGA values [Gi 05].

The mass acting on resistant elements defines the lateral seismic force (inertial forces) to be applied on each storey. Variable A_M in deep, describes a ratio of how the building total acting mass m_T is participating on the resistant walls for each main analysis direction (x,y) in terms of the m_N acting on the same resistant element. According to assumption #2, m_N is constant for all the resistant elements in a storey. The m_T of a building includes the floor/roof systems, walls and a percentage of the live loads. Meanwhile, m_N is composed by overlaying walls and partly by floor diaphragms according to rigid or flexible floor formulations as presented graphically in figure 6.12.

As mention before, simulation results most be calibrate to a particular needed conditions of the analyzed storey. Data is presented, in case of A_M, to be used into a specific house or house typology in terms of the number of resistant walls elements, in other words, the wall cross section area. When the wall cross section area is attained for the direction analysis (x,y), it divided by the total floor area, and the wall ratio ρ is obtained as observed in equation 6.2 for a rectangular house.

$$\rho_x = \frac{\text{total resistant wall cross section area } (A_x \text{ in } x \text{ direction})}{\text{total floor area } (XY)} \qquad \text{Eq 6.2}$$

ρ is a useful variable to describe building behavior. For instance, some existing simple design procedures, such as EC-8.1 or Boscotrecase already used the value of ρ as an important parameter to check the earthquake stability of small and regular URM [BP 09]. The EC-8.1 simplified design proposal is based on the idea that relates greater amount of resisting wall area to greater lateral force resistance, but, it don't took into account the individual shape of piers. Additionally, it is only applicable for a rigid slab, good material conditions and limited PGA range. A graphical explanation for ρ is observed in figure 6.2. There, the total wall area in x direction A_x is shadowed and the external dimensions of the house X and Y are observed.

The value of ρ for existing structures can be approximated, pre-known from a building stock catalog or finally measured at field. This parameter is used in this study for two aspects: estimate the

value of A_M as it is presented in section 6.3, and also it is associated to an incremental or reduction of lateral shear resistance capacity of walls.

After the basic objectives of the simulation has been overviewed and the parameters of interest defined, the step now is to explain the initial architectural formulation of the house utilized in the SHM, after this to review the SHM results, and finally to determine the number MC simulations to be performed as explained in section 6.2.1.

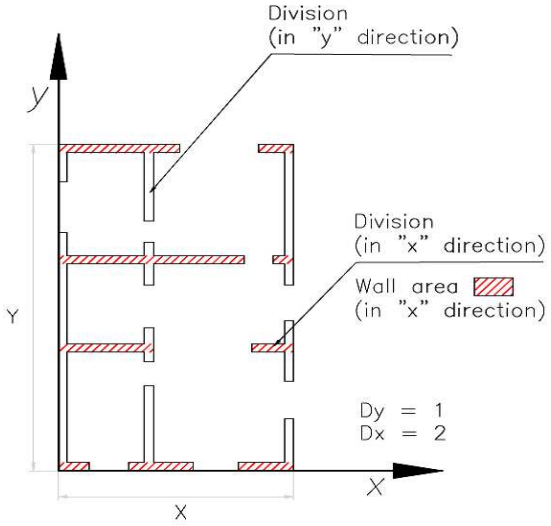

Figure 6.2: Example building resistant wall layout used for computing ρ

6.2.1 Architectural considerations

Hundreds of different building configurations are simulated by a Monte Carlo approach (MC) to estimate the acting axial loads N and acting mass A_M on wall pier elements. Both N and A_M are expressed in terms of probability density functions PDFs. In the first step of the simulation, there is needed to characterize rules related with architectural conditions of the particular structure in study. This will define at the same time the architectural building limitations of the methodology applicability as it was already state in assumption #7.

For the house modeling parameters, they are presented in table 6.1. Triangular PDFs are assumed in case of geometric parameters for the calculation of random variables; hence a minimum P_{min}, a common P_{mid} and a maximum P_{max} values are requested for geometric variables. Shape or geometric variables are: the house façade length X, deep of the building Y, the shape of voids in the walls (v_o) for generating doors and windows in external and internal walls, the weight of slabs and roofs (P_{PB}, P_{P1}, P_{P2}), the height of the floors (H_{PB}, H_{P1}, H_{P2}), the density of URM materials γ and finally thickness of the walls t at the façade for the first storey.

Other aspects are described by rectangular PDF such as: the amount of internal walls which is limited for all housing types to a clear span ranging from C_{Smin} = 2 up to a maximum of C_{Smax} = 9 meters, the percentage of resistant area for internal and external walls (f_{ex}, f_{ix}, f_{ey}, f_{iy},), and life loads.

The parameters conditions are chosen in accordance to a local inspection. The minimum, mean and maximum values recommended to be used in the MC simulation are those presented in table 6.1. These limitations are corresponding to what it is believed in this study to be the common architectural limitations of normal houses. The methodology results are restricted to this range of values that had been investigated, but can be even narrower by the user for very standardized housing units. Variable values out of these ranges generate conditions that may be no realistic (e.g. a 1x1 dimension room) or out of the scope of this study (e.g. complex layout, big irregularity in height).

Table 6.1: Recommended simulation limit values for generation of houses

Triangular PDFs	3 stories building	2 stories building	1 story building
	min / mid / max	min / mid / max	min / mid / max
Height of first story H_{PB} (m)	2 2.8 4.0	2 2.8 4.0	2 3.0 4.0
Height of second story H_{P1} (m)	2 2.6 3.6	1.6 2.6 3.6	
Height of third story H_{P2} (m)	1.6 2.6 3.2		
Facade length X (m)	3 7 14	3 8 14	3 8 14
Deep length Y (m)	4 12 22	4 12 26	4 12 26
Thickness of the facade wall t (m)	0.15 to 0.9	0.12 to 0.9	0.1 to 0.8
Thickness of the internal wall e_i (m)	0.15 to 0.5	0.12 to 0.5	0.1 to 0.5
Floor weight 1st Story P_{PB} (kPa)*	3.0 5.0 no limit	3.0 5.0 no limit	1.0 3.5 5.0
Floor weight 2nd Story P_{P2} (kPa)*	2.0 5.0 6.5	1.0 3.5 5.0	
Floor weight 3rd Story P_{P3} (kPa)*	1.0 3.5 5.0		
Density range γ (kN/m^3)	12.0 -- 28.0	12.0 -- 28.0	12.0 -- 28.0
Void dimension v_O (m)^{t,v}	0.4 1.2 2.0	0.4 1.2 2.0	0.4 1.2 2.0
Rectangular PDFs	**3 stories building**	**2 stories building**	**1 story building**
Clear span C_S	2 -- 8	2 -- 8	2 -- 8
Inside void factor f_{ix}	1.2 -- 2	1 -- 2	1 -- 2
External void factor f_{ex}	1.1 -- 2.5	1.1 -- 2.5	1.1 -- 2.5
Inside void factor f_{iy}	1.2 -- 2	1 -- 2	1 -- 2
External void factor f_{ey}	1.1 -- 2.5	1.1 -- 2.5	1.1 -- 2.5
Live load in (kPa)**		code	

slab or roof load, [t] window or door (length dimension), [v] height in between 30 and 75% of total floor height,computed for floors and roof*

Aspects related to the use of these basic variables into the generation of houses are explained in detail throughout the MATLAB code (Appendix C). The most important statements are:

- *The ratios X/Y and Y/X:* are limited in the code to a range between 3 and 1/3.
- *Clear wall spans C_S:* are correlated so that very big rooms are not possible. After a span of 5 meters, there should be a wall in the other direction with less 4 meters. If 9 is the maximum possible span, 9x4 is the maximum room area.
- *Minimum value of effective resistant distance per wall (L_{eff}):* it is of 40% of the total wall length. It is computed according to f_{ex}, f_{ix}, f_{ey}, f_{iy},. The maximum value of any of this variables is 2.5 (1/2.5=0.4)
- *Amount of doors and windows:* Computed from f_{ex}, f_{ix}, f_{ey}, f_{iy}, for estimating the total wall length and v_O for the length of the windows and doors. These two factors define the number of windows, doors and its dimensions.
- *Variation of wall thickness:* wall thickness in the opposite direction of the façade differ a maximum of 25% to the one estimate in the façade. The thickness of walls in storeys different from the 1st storey can be reduced up to 70% of the total in the top storey of a 3 storeys building (default values, with a minimum thickness of 12 mm).
- *Minimum pier geometry, length and height:* the minimum pier length l_P is of 0.4 m, for h_P the minimum is of 0.4 m, and the minimum ratio h_P/l_P is of 0.25.
- *Height of windows and doors:* the maximum possible height of doors is $0.75H_S$, the minimum height of windows is of 0.3 H_S (default values).
- *Continuity of walls:* structural walls are assumed to be continued from the base storey except for the top storey. Light division walls are not considered as structural elements.

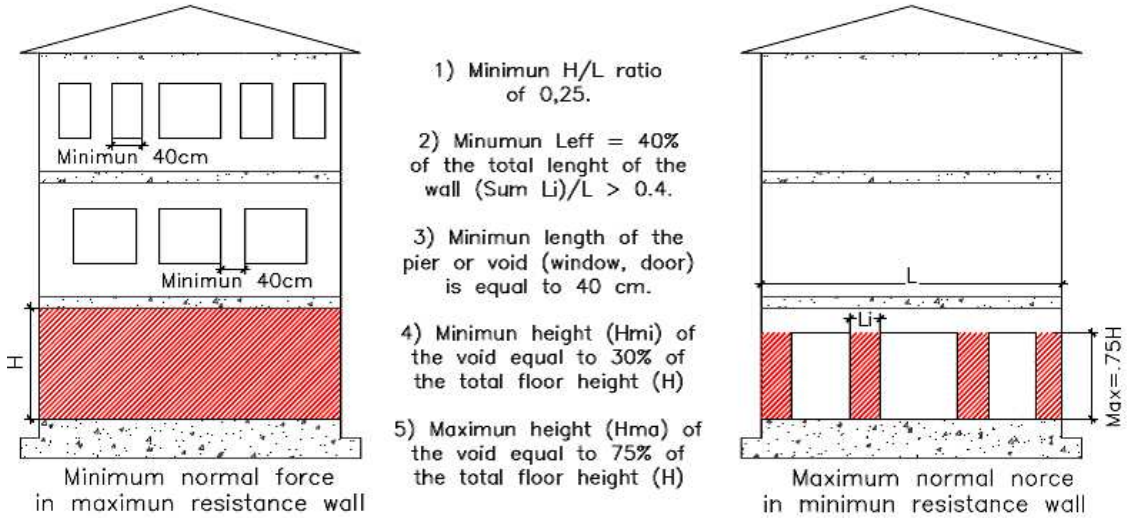

a) b)

Figure 6.3: a) Maximum wall lateral resistance at the 1st storey, b) minimum possible capacity at the 1st story in case of diagonal shear failure mode and poor material properties in a 3 storey building

As it can be inferred from the last table, the assumed shape of the building is rectangular. For other buildings shapes like L, T, +, etc; the structure can be assume as approximate rectangular and walls will suffer a reduction of the resistance in terms of the eccentricity factor F_{EC}. In other cases the structure may be analyzed as two or more different structures, especially when there is a horizontal aggregate area of other material type in the house so that a bad connection can be expected.

Other limitation that had been discussed in the study is the building maximum number of storeys to 3-4 (maximum 10 meters height). This is due to the applicability of this method is focused initially on low-rise house conditions of URM and limitations for the code recommended applicability of simple linear lateral force analyses.

The significance of f_{ex}, f_{ix}, f_{ey}, f_{iy}, and void shape v_O factors is described graphically in figure 6.3. It consists mainly on parameters to define the shape and the amount of the voids in the wall. The figure 6.3 also shows the possible maximum and minimum possibility of normal loading for the 1st story walls.

In the simulation, the relevant parameters are found from very simple equations to compute the normal forces N on the wall, the mass parameters acting over the wall (m_N, m_T), and the amount of cross section wall area ρ (MATLAB code Appendix C). The significance of the void amount and the shape in walls is described by ρ. ρ is the wall cross section area divided by the total floor area in the direction of interest (x direction in figure 6.2). In terms of the basic variables presented in table 6.1, this factor is described by the equations 6.3 to 6.5 as:

$$D_x = D_{\min x} \cdots D_{\max x} \qquad \text{Eq 6.3}$$

$$D_{\min x} = \frac{(Y - e_x)}{(C_{S\min} + e_x)} \quad \text{and} \quad D_{\max x} = \frac{(Y - e_x)}{(C_{S\max} + e_x)} \qquad \text{Eq 6.4}$$

$$\rho_x = \frac{(\frac{2}{f_{ex}} - \frac{D_X}{f_{ix}})e_x}{Y} \qquad \text{Eq 6.5}$$

where D_x corresponded to a random generated number of internal divisions in the x direction in figure 6.2. It is obtained from any value in between D_{minx} and D_{maxx}.

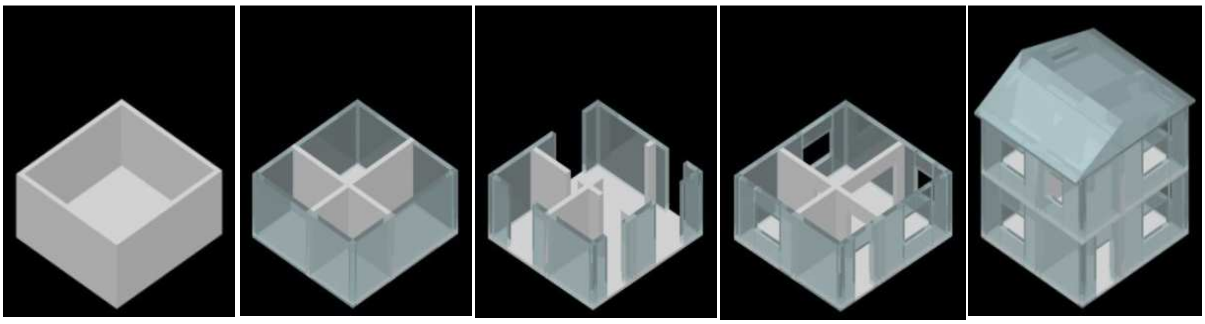

a) b) c) d) e)

Figure 6.4: House generation process: a) external dimensions, b) internal wall, c) location and amount of voids, d) shape of voids, e) repeating a to d for each storey and add storeys and floors

The MATLAB code follows a random procedure to generate houses; it is presented graphically in figure 6.4. The sequence shows initially the geometrical definition of the building shape (X,Y in figure 6.4a), then the definition of initial number D_x and D_y according to equation 6.3 and a random location inside the house (figure 6.4b). After computing the ρ, the voids are distributed on the walls according to v_O for each direction (figure 6.4c), and then the shape of wall void is developed according to if it is assumed to be a door or a window and following the rules shown in figure 6.3 (figure 6.4d). A similar process is perform for each story and finally slabs and stories are added one to the other to finish the house generation process (figure 6.4e).

In figure 6.5, graphics are showing the normal forces values change according to ρ values for two different materials (brick: γ=14 kN/m^3 , t=0.2 m, heavy stone: γ=22 kN/m^3 , t=0.4 m). The figure was generated following the rules of SHM and basic parameters values presented in table 6.1 and for small variation of γ and t values. It is observed here the great influence of the two possible diaphragm types. Variability of the forces values increased largely for small values of ρ, this aspect will affect both I_R and A_M obtained PDFs.

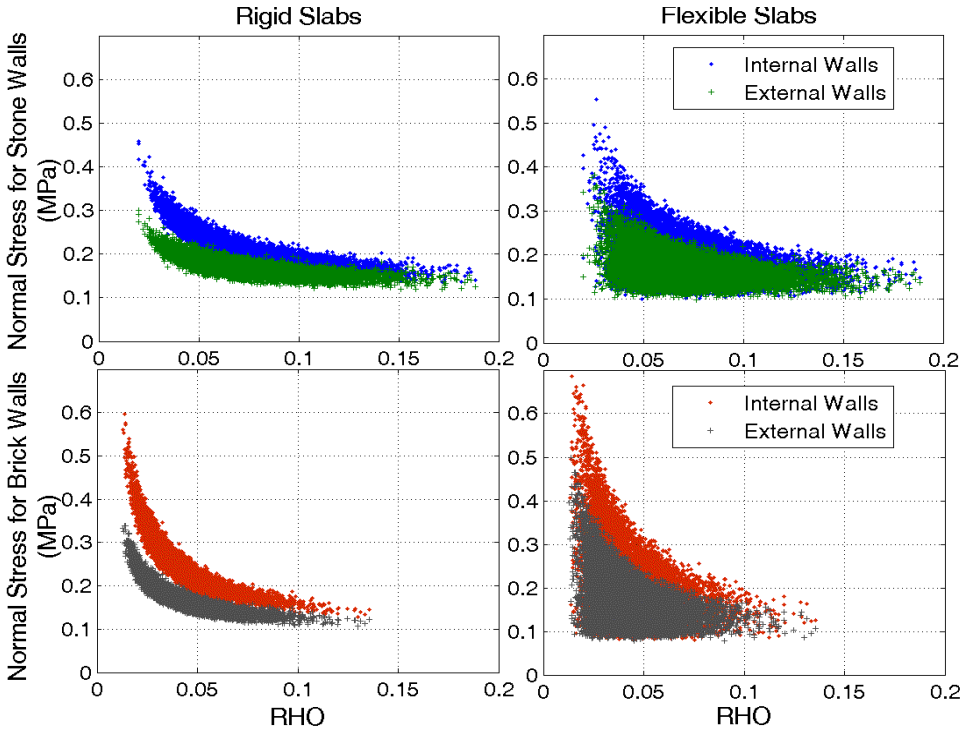

Figure 6.5: Variation of average normal forces, per storey acting on piers. 1.5x10^4 modeled houses.

It is observed from figure 6.5 that the normal load is increasing with the reduction of the amount of resistant walls. This is important because it shows the convenience of using ρ to describe normal forces, especially for values smaller than ρ = 0.05 where the effect of axial loads due to floor slabs increased significantly. It is also observed a considerable dispersion difference according to the type of diaphragm (rigid, flexible). The reason is that the distribution of the normal loading in flexible slabs or roofs is dependent on the direction of the slab beams and roof structure, meanwhile for rigid slabs it is well distributed among walls in both structural directions.

Walls under approximately ρ = 0,01 are not possible to be obtain this because the initial establish architectural conditions in table 6.1. For poor material walls, this ratio will be hardly stable even for just gravitational axial forces in buildings higher to two stories.

Regarding the number of simulations to be performed, the number is based on the behavior of the mean values and the coefficient of variation. A number of $1x10^4$ houses have been found to be sufficient for the all basic variables generation. In figure 6.6 the behavior of the mean and coefficient of variation for normal stress in flexible and rigid diaphragms (for $\rho = 0.08 \pm 0.005$) is showed.

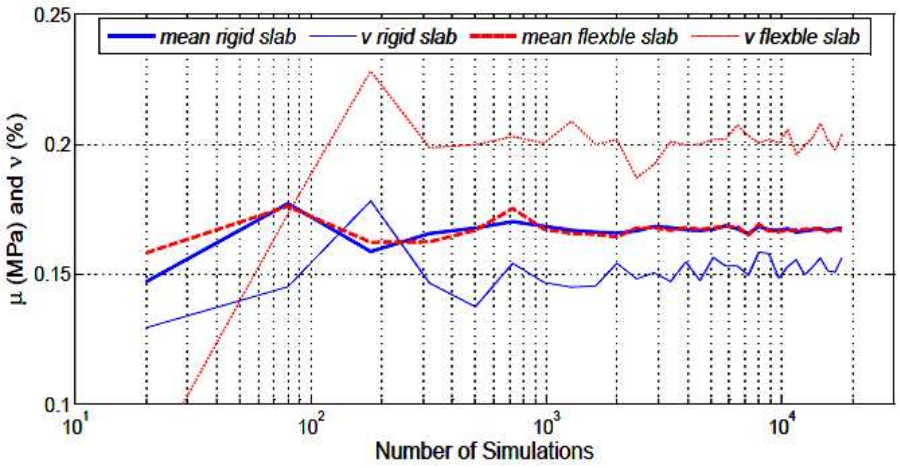

Figure 6.6: Variation of average mean and *v* values normal forces according to the number of simulations

6.3 Obtaining I_S, I_R *and* A_M for the in-plane

For solving *G(X)*, the seismic action I_S, the storey resistance I_R and the so called architectural mass ratio A_M must be obtained. The aim of this section is to explain the source of each of these parameters and how they are interacting for the formulation of structural fragility curves for the in-plane failure mechanism.

The A_M is obtained directly by the ratio m_T /m_N computed at each floor from the building architectural characteristics by means of the SHM. The I_S is obtained in terms of a normalized reference PGA according to the value obtained from the elastic design spectrum (section 3.3). I_S is equivalent to the non-dimensional seismic coefficient C_s formulation.

In case of I_R, the resistance is expressed in terms of a normalized value *V/N*, where *V* means any sort of shear resistance and *N* an applied normal force. The average normal forces action on the elements is obtained from the SHM. *V* values can be presented for different h_p/l_p ratios and boundary conditions (figure 6.7a). For analyzing the values of shear resistance obtained from the different equations 4.9, 4.11, 4.12, 4.14, an appropriate direct judge of *V* cannot be made due to factors such as: not evident failing mode, poor correlation in between modes and finally a great dispersion of data as it is evident in figure 6.7b (MC simulation for $2.0x10^3$ points).

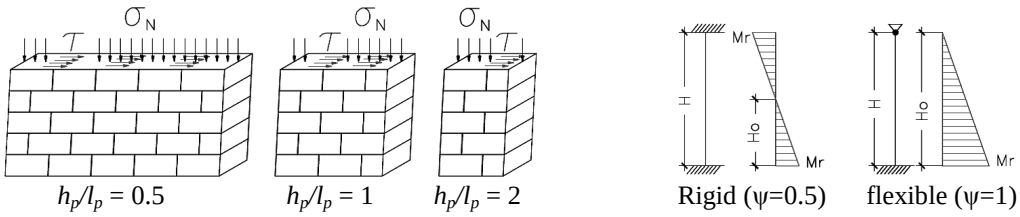

Figure 6.7a: Pier shape ratios and possible boundary conditions ($N=\sigma_N A_P$, $V=\tau A_P$, where A_P= pier cross area)

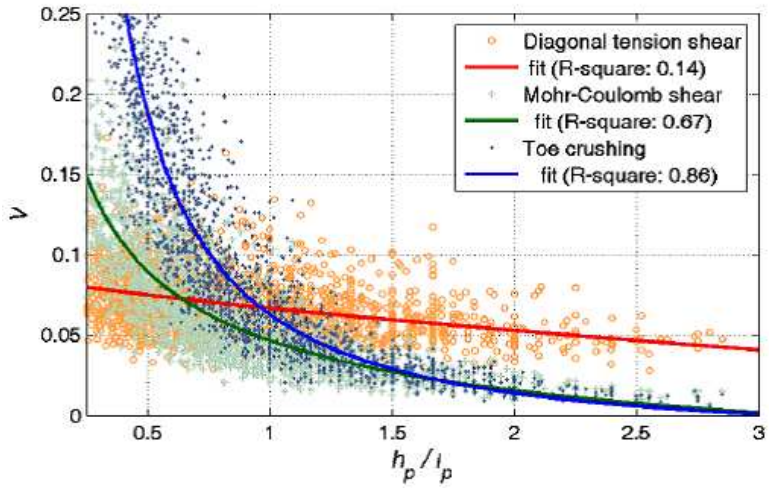

Figure 6.7b: Variation of the pier shear value (V in MN). Value corresponds to the base storey of three storey building with very poor material properties (f_{bt} = 0.15, c =0.1, f_m = 1 MPa, and μ = 0.4) and rigid slab

When the normalization is made in terms of an average acting N, figure 6.7b changes into figure 6.8. Now, failing modes results showed a better correlation and less data dispersion. Taking into account normal loading makes evident the difference in between failure modes in the h_p/l_p spectrum and that is another reason for making the normalization of the data. Now, in figure 6.8, it is also evident that the diagonal tension shear failure mode is dominant when the normalization is performed. This failing mode is what actually would be expected in field damage for a building with good wall connections, a rigid diaphragm and very poor material properties.

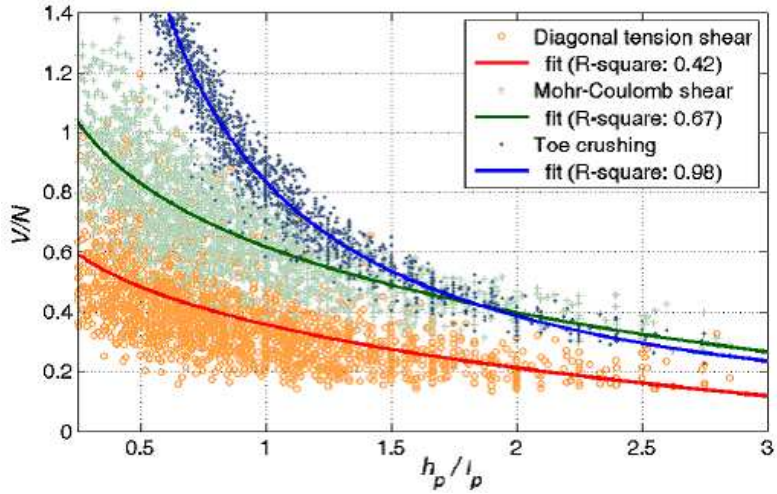

Figure 6.8: Variation of the pier shear ratio V/N. Value corresponds to the base storey of three storey building with very poor material properties (f_{bt} = 0.15, c =0.1, f_m = 1 MPa, and μ = 0.4) and rigid slab

The results obtained from figure 6.8 don't correspond yet to the value of I_R, just to a shear ratio value of a single pier in a masonry wall R_E. For the MC simulation of individual piers, the simulation takes into account different wall parameters like density, thickness, geometrical shape, material resistance, and boundary conditions. A characteristic R_E is established for particular material and different failure modes. The result of this simulation, for many pier cases, is used to a particular pier or an entire wall giving the statistical mean and standard deviation parameters needed for obtaining the needed value of I_R. The material properties are input into the simulation as normal PDFs. When a material property is used from bibliographical references such as the one proposed in table 4.4 or table 4.5, the mean value is assumed to have a coefficient of variation of 20% in this study. In case of minimum and maximum ranges (X_{max},X_{min}), they correspond to two times the standard deviation with $\mu = \frac{X_{max}+X_{min}}{2}$.

The pier boundary conditions are taken into account for the resistance equations by the shear ratio factor α_V showed in the equations 4.9, 4.11, 4.12, 4.14 [MC 97]. For flexible slab and weak spandrel assumption, local values of ψ' must be equal to ψ'=1 and for rigid slab condition ψ'=0.5 (figure 6.6 and equation 4.10). The ψ' is just changing in between 1 and 0.5 integer values for the shear related failures and sliding on each floor. For the case of the flexural failure or rocking, a modified ψ' is proposed in this study to modify equation 4.9 in order to take into account the moment transfer down from upper to the lower levels. The modified ψ' is calculated in function of the assumed boundaries conditions in the whole building as shown in figure 6.9. The factors are computed from an assumed force distribution according to equation 3.16 for equal storey height, equal mass concentrated at the floor for every storey except the top one where is assumed as half of the mass is used. The ψ' modification case for flexural condition is resumed in equation 6.6.

$\psi = 0.85\psi_1(1.33\psi_3 + 0.79\psi_2 + 0.30\psi_1)$	1st storey in a 3 stories building	Eq 6.6a
$\psi = 0.85\psi_2(1.30\psi_3 + 0.53\psi_2)$	2nd story in a 3 stories building	Eq 6.6b
$\psi = 0.85\psi_1(1.30\psi_2 + 0.53\psi_1)$	1st storey in a 2 stories building	Eq 6.6c

Here the ψ_1, ψ_2 and ψ_3 are the local value of ψ' at each story according the flexible or rigid condition. These equations are proposed for a maximum of three storey flexible diaphragm building.

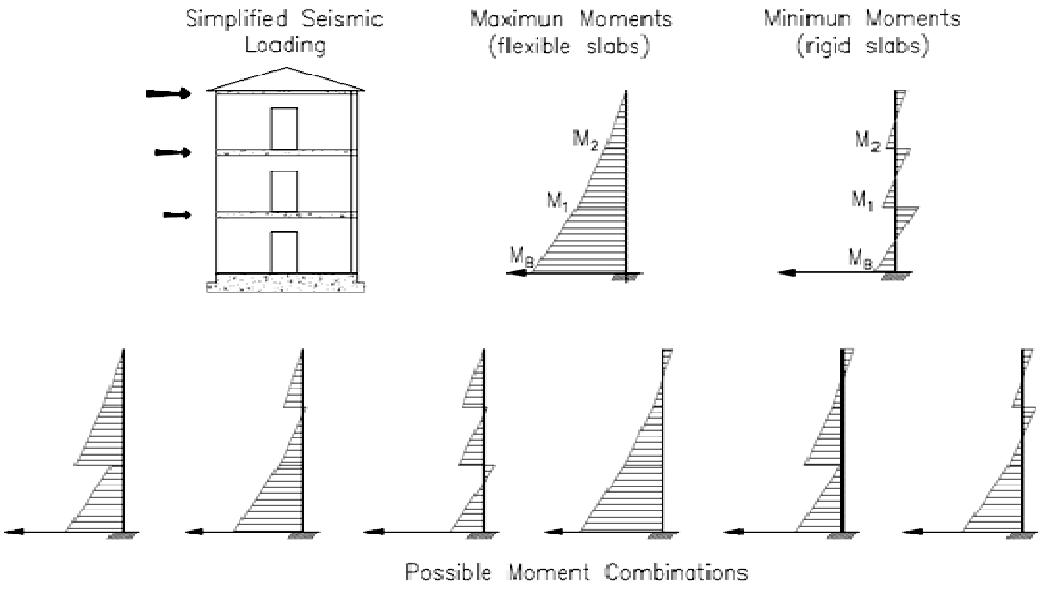

Figure 6.9: Moment combinations on pier elements according to slab/spandrel conditions

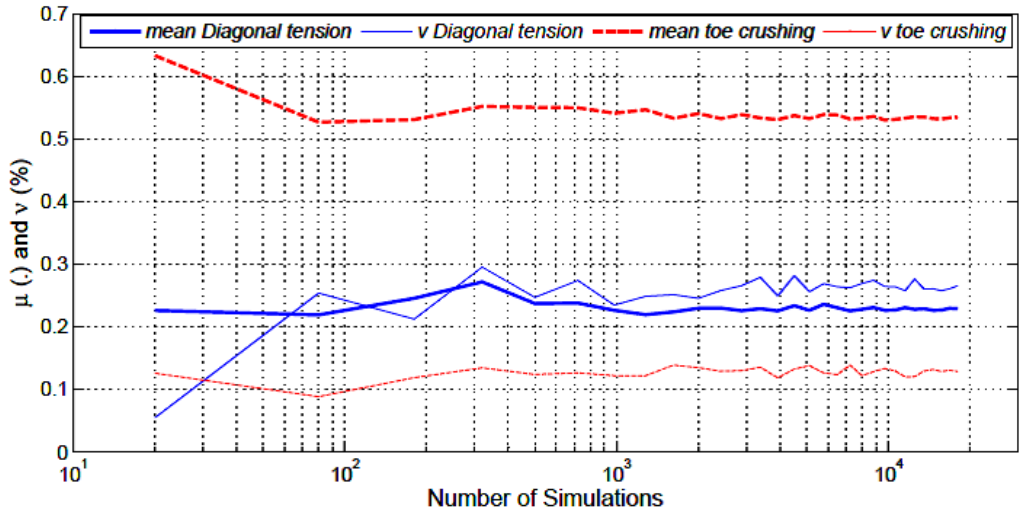

Figure 6.10: Behavior of average mean and *v* for *V/N* according to the number of simulations

The R_E can be found for any pier in any storey. The characteristic R_E value of the pier most be the dominant one obtained from figure 6.8 to an analyzed shape ratio h_p/l_p. The convergence value for determining the number of simulations needed in the MC process can be observed in figure 6.10 for two different pier failing modes (rocking - diagonal tension shear) and for a h_p/l_p equal to 1.5. A total of $1x10^4$ simulations are considered to be enough to describe the variable.

The value of R_E, obtained so far from equations 4.9, 4.11, 4.12, 4.14, correspond to maximum shear values useful for the life safety LS.

The total storey resistance index I_R is still not found. It is estimated in this work that I_R is computed in agreement with the boundary conditions of the pier observed from the condition of the spandrels and floor diaphragms. According to this there are three possible situations for the LSLS:

- *Poor spandrel and flexible diagrams:* I_R is computed from the minimum observed value of R_E for the external walls or for h_p/l_p equal to 1 for an assumed internal walls. The minimum value of *V/N* from these two is used (critical pier).
- *Good spandrels and flexible diaphragms:* I_R is computed from the maximum value of R_E found in the wall and a modification factor F_W to take into account the participation of the other elements of the wall according to figure 4.17 and equations 4.20 and 4.21. The wall resistance is called then R_W. R_W for internal walls is set up to a h_p/l_p equal to 0.75 and F_W to 0.75. The minimum value of R_W found in the storey is used (critical wall).
- *Rigid diaphragms:* I_R is computed from the maximum R_W value found in the storey and the F_{EC} as it has been defined in section 3.3.3. This condition is assumed also for the SLS.

For the last statements, some aspects are important to underscore. First, it has been assumed that there is good correlation in between pier elements in the storey (assumption #4). The minimum criteria to describe elements as well correlated is of be constituted of the same material type. Equivalent series reliability systems have been formulated for the two first statements. For the last statement, the storey system is assumed as a parallel reliability system with walls well correlated. After the maximum resistant wall is found, the normalized shear resistance value is multiply by the structural layout irregularity factor F_{EC} (minimum value of F_{EC} = 0.8). F_{EC} values are illustrated in figure 3.15, where the value is estimated according to the building location and shape.

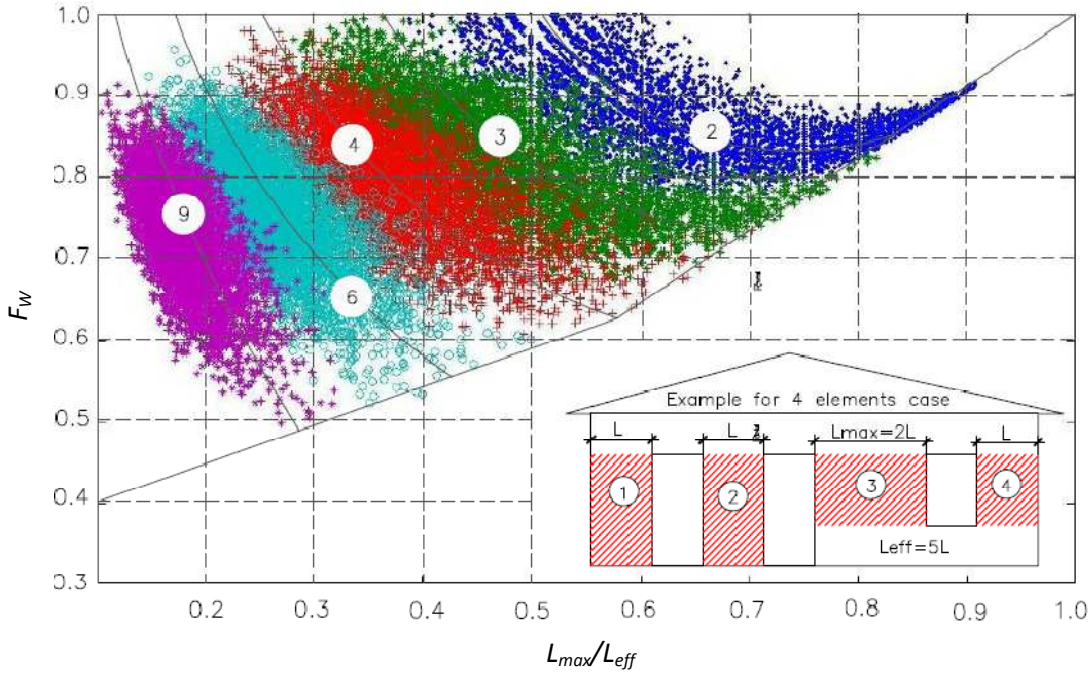

Figure 6.11: Simulation data and calculation for F_W, with an example of computation of L_{max}/L_{eff} for 4 pier elements wall.

In agreement to figure 4.17, all pier elements participated to achieve the final shear resistance of a wall in accordance to their deformation capacity and location. To take this fact into account, a bilinear capacity element curve (elastic-perfectly plastic) was adopted for the wall behavior (section 4.6.2.4). By displacement estimations of wall elements, the capacity can be assessed by the strongest element, the number of elements and its percentage in comparison with the strongest one. This aspect is represented by the application of a capacity reduction wall factor F_W in figure 6.11.

Each resistance reduction point in figure 6.11 is computed from the calculation procedure described in the figure 4.17. Different ductility values are assigned according to the failure mode (figure 4.16). Ductility values of 3, 3 and 2 are assigned to the rocking, M-C shear and diagonal tension shear failure modes. The values of F_{WE} are found from simulations similar to the one in figure 6.11. To practical reasons it can be just approximated as $0.75F_W$.

After aspects related to the computation of I_R have been cleared out, the I_S is obtain in terms of the reference PGA value according to the elastic design spectrum (section 3.3). I_S is equivalent to the non-dimensional seismic coefficient C_s formulation. For obtaining the seismic base shear, the recommendations EC 8-3 are followed in this study according to section 3.3. SAUMAC procedure is opened to any other code formulation just by finding a non-dimensional factor C_S. The total base shear force V_b due to earthquake in any horizontal direction is calculated as follows:

$$V_b = S_d(T_1) m_T \lambda \qquad \text{Eq [3.14]}$$

For an elastic analysis and small structures like the ones analyzed here, the value of $S_d(T_1)$ can be formulated just in terms of the so called "plateau" of the design spectrum (independent of the natural period T_1) and simplified to:

$$S_d = a_{gR}\gamma_I S_S \frac{2{,}5}{q} = \alpha S_S \frac{2{,}5}{q} g \qquad \text{Eq [3.13b]}$$

In equation 3.13b g is the gravity acceleration 9.8 m/s^2 and α a normalized reference acceleration. With these, finally the base shear can be expressed as:

$$V_b = \alpha S_S \frac{2{,}5}{q} gm\lambda = F_S S_S \alpha m_T g \qquad \text{Eq [6.7]}$$

where F_S is a constant relative to code equations constant variables. The seismic base shear must be distributed among all the stories in the building according to equation 3.16. This formulation is simplified in agreement to the JBDPA and FEMA 310 by a shear modification factor [JBDPA-01] [FEMA-310]. The results of this estimate are observed in figure 3.13. The formulations states that:

$$V_{bi} = \left(\frac{n+i}{n+1}\right)\left(\frac{W_i}{W_T}\right)V_b \qquad \text{Eq [6.8]}$$

where V_{bi} is the shear force at storey i, Wi is the total mass of all the storeys above the analyzed storey i, W_T is the total weight of the building and finally n is the total number of storeys. Equation 6.8 can be reformulated as:

$$V_{bi} = \left(\frac{n+i}{n+1}\right)\left(\frac{m_i g}{m_T g}\right)F_S S_S \alpha m_T g = \left(\frac{n+i}{n+1}\right)F_S S_S \alpha m_i g \qquad \text{Eq [6.9]}$$

Now, for the limit state formulation $G(X)$, we have that the resistant shear per storey Vi must be greater than the applied load of equation 6.9 so that:

$$V_i \geq V_{bi} \qquad \text{Eq [6.10]}$$

Since V_i can be normalized in terms of the total normal forces acting on pier elements as explained before we have:

$$\frac{V_i}{m_{Ni} g} \geq \frac{V_{bi}}{m_{Ni} g} \qquad \text{Eq [6.11]}$$

where m_{Ni} is the mass contributing to the normal loading on the pier for all the storeys above the analyzed level i. Now bringing the expression of equation 6.9 to equation 6.11 we have:

$$\frac{V_i}{m_{Ni} g} \geq \left(\frac{n+i}{n+1}\right)\frac{F_S S_S \alpha m_i g}{m_{Ni} g} = \left(\frac{n+i}{n+1}\right)\left(\frac{m_i}{m_{Ni}}\right)\left(F_S S_S \alpha\right)$$

or

$$I_{Ri} \geq \left(\frac{n+i}{n+1}\right)A_{Mi} I_S \qquad \text{Eq [6.12]}$$

and finally:

$$G(X) = \left(\frac{n+1}{n+i}\right)I_{Ri} - A_{Mi} I_S \qquad \text{Eq [6.13]}$$

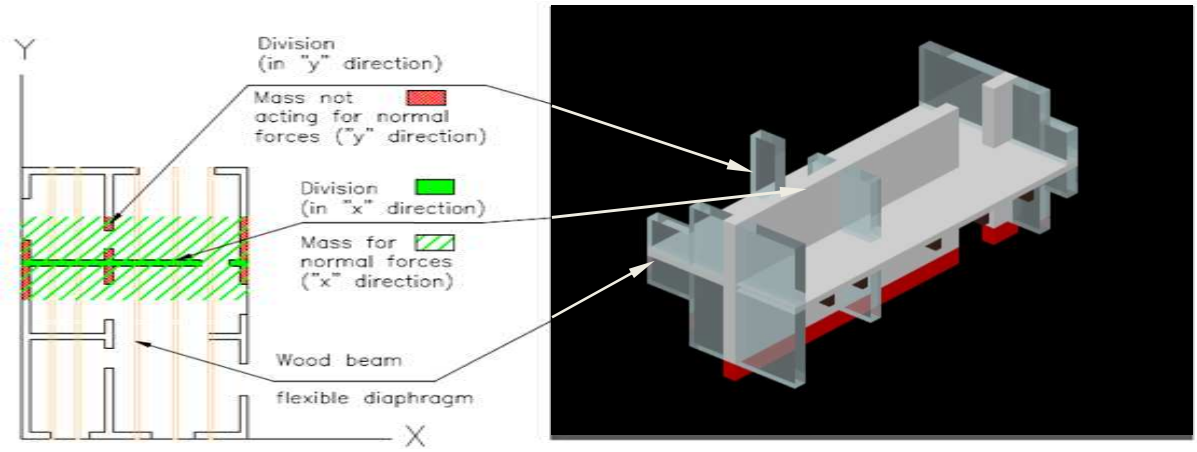

Figure 6.12: Physical conceptual description of A_M

It is observed in the equation 6.13 that the values of I_R and A_M must be calculated for each storey meanwhile I_S is a constant (for uniform q). This aspect make possible to assess each storey as an individual element in the building. The physical meaning of A_M is better explained by the figure 6.12. There, a 3D model of a cut section of a building is presented in case of a flexible slab.

The amount of simulations required for computing A_M is shown in figure 6.13 for the base storey in a 3 storey building with rigid diaphragms and for a value of ρ = 0.08 ± 0.005. From the figure, it is observed that the recommended number of simulation in order to get a stable value must be no less than 2.0x10^4 simulations. It is concluded from figure 6.13 that flexible slabs presented bigger values of A_M with greater dispersion; this is expected for more variable flexible diaphragm systems.

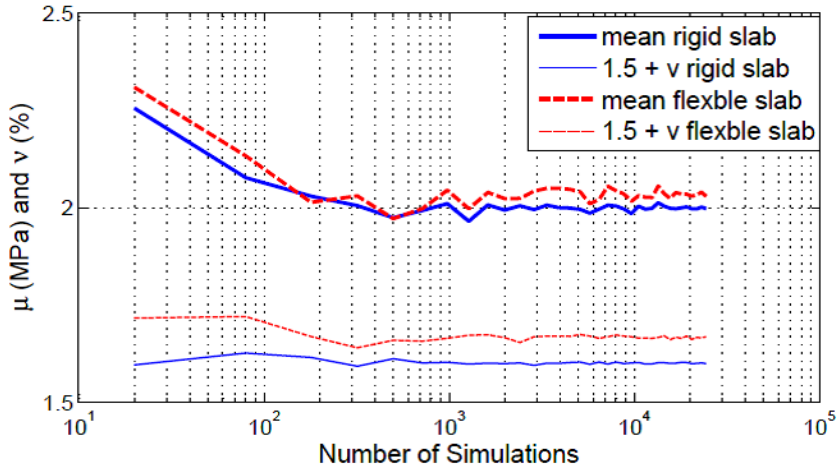

Figure 6.13: Behavior of average mean and v for A_M according to the number of simulations

6.4 Obtaining I_{So} and I_{Ro} for the out-of-plane

The values for I_{So} and I_{Ro} are obtained for the out-of-plain failure modes in a similar way to those obtained for the in-plane, but formulated in a much easier procedure since the critical element is assumed always located in the top storey if a good correlation exist among storeys. The wall normalized resistance I_{Ro} is evaluated graphically directly for all four possible wall configuration (figure 4.15) used to estimate the initial resistant force F_O (equations 4.6a, 4.6b, 4.6c, and 4.6d). The possibility of multistory out-of-plane fail is assessed in-situ from floors condition.

When the limit reliability condition $f_{Ro} \geq F_a$ according to equations 4.4 and 3.18 is formulated we have:

$$F_O\left(1-\frac{\Delta_2}{\Delta_U}\right)\psi \geq \alpha S_S\left[\frac{3\left(1+{}^{z_a}/_{H}\right)}{\left(1+\left(1-{}^{T_a}/_{T_1}\right)\right)}-0.5\right]\frac{W_a}{q_a} \qquad \text{Eq [6.12]}$$

The equation can be reformulated as:

$$\frac{1}{\left[\frac{3\left(1+{}^{z_a}/_{H}\right)}{\left(1+\left(1-{}^{T_a}/_{T_1}\right)\right)}-0.5\right]}\frac{F_O}{W_a}\left(1-\frac{\Delta_2}{\Delta_U}\right)\psi \geq \frac{\alpha S_S}{q_a}$$

or

$$I_{Ro} \geq I_{So} \qquad \text{Eq [6.13]}$$

where I_{So} is defined in function of a soil parameter, the normalized reference PGA and the behavior factor for the out-of-plane (equal to 1 or 2 (section 3.3.4)). In figure 6.14 the values of I_{Ro} are presented in case of mean thickness wall of 30 cm and for $1.5\text{x}10^4$ points of simulation. The values are useful for any kind of severe degraded URM because it is only based on geometrical stability. Results are presented in terms of the H_S/t where, H_S is the total storey high and t is the thickness of the wall.

It can be inferred from the figure 6.14a that the cantilever failure mode is weak to seismic actions compared with the supported conditions. In cantilever, the resistance index I_{RO} is low for any kind of H_S/t ratios. Architectural parapets present usually a cantilever condition which explains the usual damage on these elements. Some URM structures walls can be considered as well as in cantilever for bad connections with the floor system.

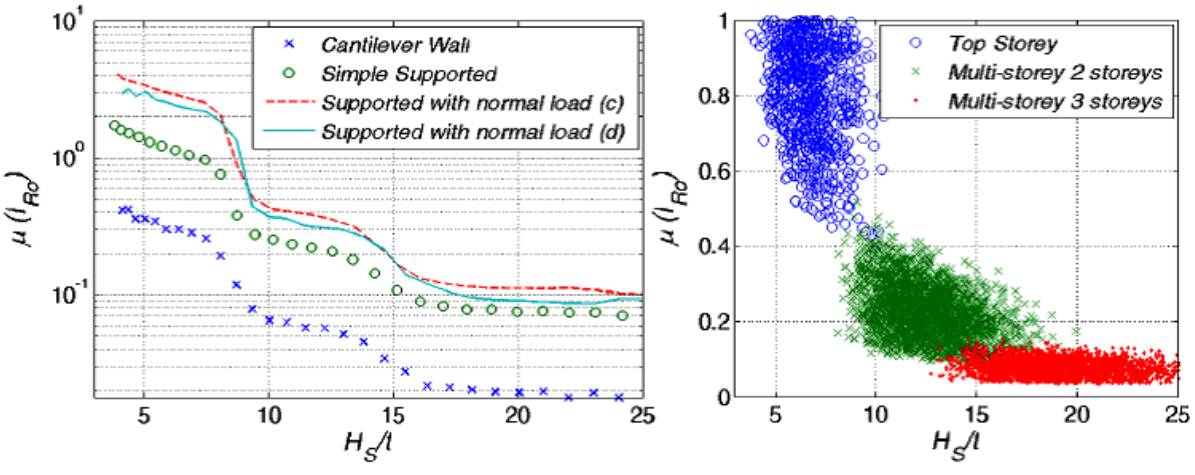

a) b)

Figure 6.14: a) I_{RO} according to support conditions and severe degraded URM (figure 4.15), b) data for simple wall support. Single storey failure mode for (blue), and two storeys (green) - three storeys (red) multistory fail

6.5 Simplify Steps to Obtain I_S, I_R, A_M

A number of steps are formulated for the fast and simple use of the SAUMAC methodology once the concepts from the sections 6.1 to 6.4 had been understood. The steps are resumed as follow:

6.5.1 The seismic structural index I_R

The seismic structural indexes I_R and I_{Ro}, are values that described the in-plane and the out-of-plane resistance or capacity R at each storey of the building in terms of its mean value and standard deviation for a particular predefined serviceability or life safety damage limit state (SLS, LSLS). It should be calculated at each floor and in each principal horizontal direction of the house. The index is formulated in a way to envelop the aspects related intrinsically with the building shape, configuration of walls, materials and floor diaphragms.

The index is computed after two components for the in-plane failure case: the irregularity index F_{EC} and the story resistance index R_{SW}. The R_{EO} is the story resistance for the out-of-plane case.

$$I_R = R_{SW} F_{EC} \qquad \text{Eq [6.14]}$$

$$I_{RO} = R_{EO} \qquad \text{Eq [6.15]}$$

where: R_{SW} = Story in-plane resistance index
F_{EC} = Irregularity index (F_{EC} = 1 for flexible diaphragms)
R_{EO} = Story out-of-plane resistance index as computed in figure 6.14.

The story resistance index R_{SW}, is a non-dimensional value conceive to evaluate the seismic performance of the structure and should be calculated at each floor and for each main horizontal directions. It is based on the mean normalized ultimate strength of three basic wall failure modes (rocking toe crushing, diagonal tension shear and M-C shear), the shape and location of resistant pier elements and walls, the material properties and finally the type of slab/roof systems.

The R_{SW} of the *i*-th storey in an *n*-storey building is given by the product of the wall strength values R_W and the slab/roof types (boundary conditions). In addition, a story-shear modification factor, which is expressed as $(n+1)/(n+i)$, is applied to take into account for the lateral earthquake force distribution along the building height. The value of R_{SW} is calculated finally according to the next equations:

$$R_{SW} = \left(\frac{n+1}{n+i}\right) R_{W\max} \qquad \text{for rigid slab/roof condition (section 4.4.1)} \qquad \text{Eq [6.16]}$$

$$R_{SW} = \left(\frac{n+1}{n+i}\right) R_{W\min} \qquad \text{for flexible slab/roof condition (section 4.4.1)} \qquad \text{Eq [6.17]}$$

where: $R_{W\min}$ = Minimum wall strength value of the floor in the analyzed direction
$R_{W\max}$ = Maximum wall strength value of the floor in the analyzed direction
n = Number of stories of a building
i = Number of the storey, where 1 is for the first level and n the top one

The R_W is the resistance value associated to a specific wall. R_W values should be also estimated for internal walls as approximately $R_W = R_E$ with a R_E value computed from a $h_p/l_p = 0.75$. R_E is the normalized pier resistance value. The wall resistance R_W depends on the strength of wall

vertical elements (piers) R_E. The shape of the wall and the boundary conditions (spandrels, diaphragm types) are important for the force distribution in between the different pier elements. The value of R_W is calculated according to the next formulations:

$$R_W = F_W R_{E\max} \quad \text{for good spandrel condition (section 4.4.2)} \quad \text{Eq [6.18]}$$

$$R_W = R_{E\min} \quad \text{for poor spandrel condition (section 4.4.2)} \quad \text{Eq [6.19]}$$

where: R_{Emin} = Minimum pier resistance element
R_{Emax} = Maximum pier resistance element
F_W = Correction factor to wall shape and the maximum pier resistant element

R_E value should be also estimate also for the unknown internal walls as approximate to the value for R_E computed from a $h_p/l_p = 1.0$.

The F_W is a factor idealized to describe the interaction of piers for a wall in presence of good spandrels. In this case, the resistance of the wall is greatly described by the strength of the strongest pier element which is usually, not necessarily, the one with the greatest l_P value, where L_{max} is the horizontal length of the wall with greater resistance. The sum of all piers l_P is called L_{eff}.

In Figure 6.15, an example of a four piers in a one story house is presented. F_W shows small variation in between floors; the graphic in figure 6.15 can be therefore applied for all floors. For different amount of wall elements to the ones presented in the figure, a linear interpolation can be performed. F_W for serviceability LS can be assumed as F_{WE}.= $0.75F_W$.

The normalized pier resistance R_E is one of the fundaments of the assessment procedure. Its value is computed from the PDFs derived from the SHM. It is dependent on the failure mode, the material properties, the diaphragm conditions, the specified limit state, and finally the story where the pier is located. The resistance curves are expressed in terms of the equivalent normalized shear resistance ratio V/N and the pier shape h_p/l_p (figure 6.7a).

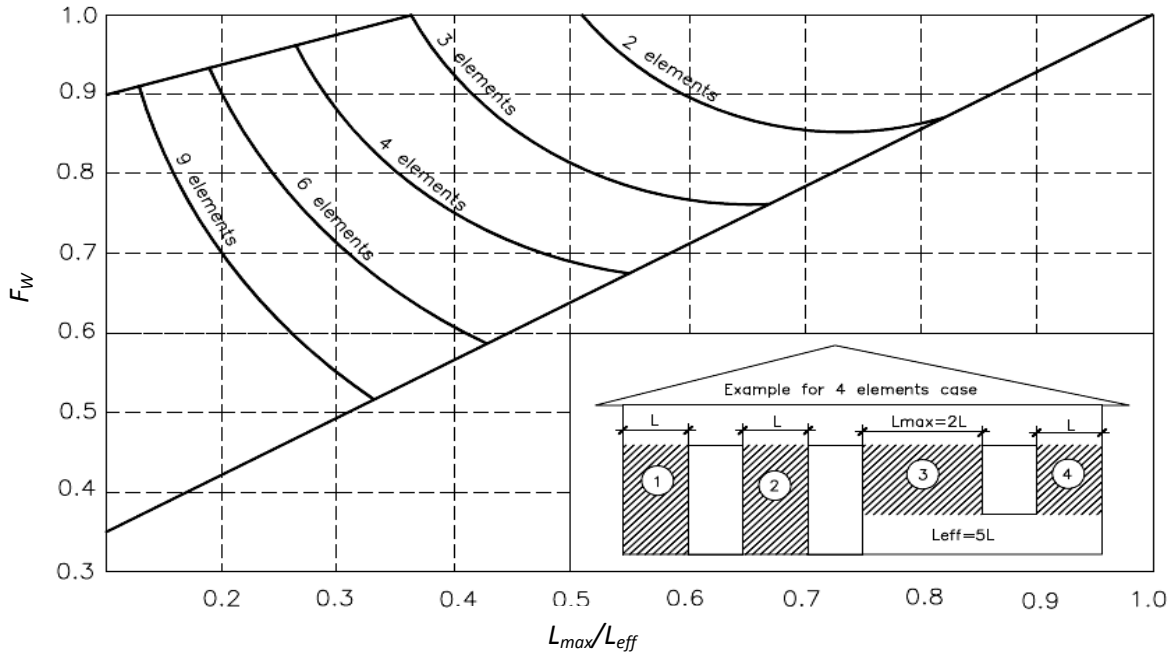

Figure 6.15: Definition of the wall shape correction factor F_W

Results of R_E shear values for poor resistance materials are obtained from equations 4.9, 4.11, 4.12, 4.14 and after performing a MC simulation. Results are presented in figures 6.16a, 6.16b, 6.16c for the rocking shear, the M-C shear and the diagonal tension shear obtained from a MC simulation with $2.5x10^4$ points for each curve. In the figures the equations used to obtain the curves are presented again to the right with some explanation to provide a full understanding of how the curves where obtained and which curve should be chosen to the analyzed case. With figures like figure 6.16 for a material database, the MC simulation can be avoided and simplified just to obtain parameters from normalized graphics. Rocking shear failure mode at low level of normal loading is almost not sensible to material properties so that it can be considered independent of them.

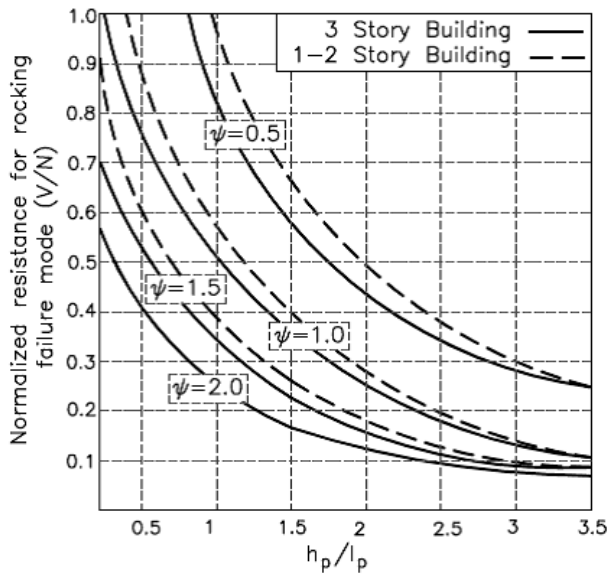

Rocking shear

The resistant moment on the pier is expressed by the next equation:

$$M_f = \frac{L^2 t \sigma_N}{2}\left(1 - \frac{\sigma_N}{0{,}85\, f_m}\right)$$

The moment is showed in terms of a shear force by the shear ratio α_V, to take into account the effective height H_O.

$$V_f = \frac{Lt}{\alpha_V}\frac{\sigma_N}{2}\left(1 - \frac{\sigma_N}{0{,}85 f_m}\right) \qquad \alpha_V = \frac{M_r}{V_r L} = \frac{H_O}{L} = \frac{\psi H}{L}$$

ψ' is equal to 0.5 for rigid slab and 1 for a flexible one. The value of ψ' is also corrected due to the location of the pier:

$\psi' = 0.85\psi_B(1.33\psi_2 + 0.79\psi_1 + 0.30\psi_B)$ Base level (3 story h.)

$\psi' = 0.85\psi_1(1.30\psi_3 + 0.53\psi_2)$ Middle level (3 story house.)

$\psi' = 0.85\psi_B(1.30\psi_1 + 0.53\psi_B)$ Base level (2 story house)

Figure 6.16a: R_E for rocking failure mode, and life safety LS

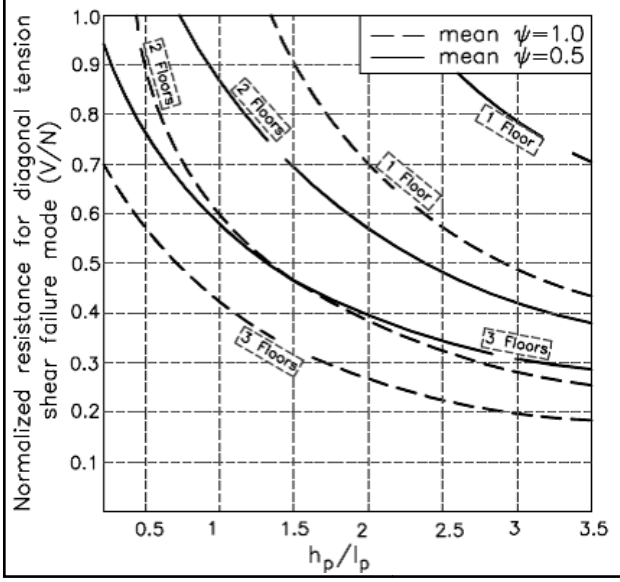

Diagonal tension shear

The resistant diagonal shear strength on the pier is expressed by the next equation:

$$V_{DSb} = Lt\frac{f_{bt}}{2{,}3(1+\alpha_V)}\sqrt{1+\frac{\sigma_N}{f_{bt}}}$$

ψ' is equal to 0.5 for rigid slab and 1 for a flexible one on each floor. No ψ' correction must be done. A f_{bt} value can be approximated from τ_0 by equation 4.15 for σ_N equal to 0. τ_0 values are obtained from table 4.5.

Figure 6.16b: R_E for diagonal tension shear mode, poor material conditions (f_{bt} = 0.15 MPa) and life safety LS

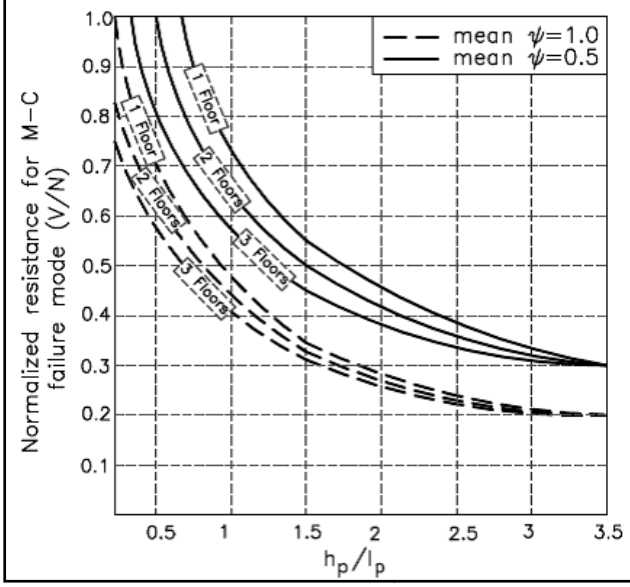

Mohr-Coulomb Shear

The resistant M-C shear strength on the pier is expressed by the minimum of next equations:

$$V_{SSc} = Lt\left(\frac{c + \mu\sigma_N}{1 + \alpha_V}\right)$$

or

$$V_{SSw} = Lt\left(\frac{1{,}5c + \mu\sigma_N}{1 + \frac{3c\alpha_V}{\sigma_N}}\right)$$

ψ' is equal to 0.5 for rigid slab and 1 for a flexible one on each floor. μ in the equations is equal to the fiction coefficient. Material parameters can be approximated from table 4.4.

Figure 6.16: R_E Mohr-Coulomb shear mode, poor material conditions (c = 0.1 MPa, μ = 0,4) and life safety LS

From the graphics and equations in figure 6.16, the mean values of normalized pier resistance for the considered failure modes are presented for small ranges of h_p/l_p ratios. For this small range of h_p/l_p a lognormal PDF is found, the equivalent mean value μ of a normal distribution are presented in the figure according to the transformation detailed in section 5.3 (figure 6.17). The values of the standard deviation σ are derived to each failure mode.

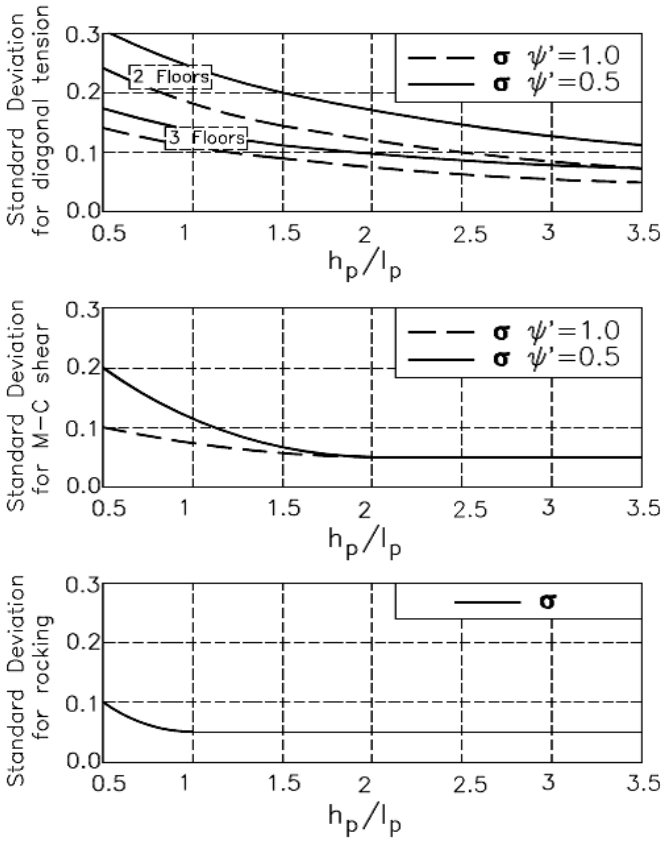

Figure 6.17: Lateral resistance normalized standard deviation σ values according to the failure mode, for poor material conditions and LSLS

The value of R_E is expressed finally as:

$$R_E = \mu\left(\frac{V}{N}\right) \pm \sigma\left(\frac{V}{N}\right) \qquad \text{Eq [6.20]}$$

$$\mu\left(\frac{V}{N}\right) = \min\left\{\frac{V_f}{N}, \frac{V_{SS}}{N} \cdot \frac{V_{DS}}{N}\right\} \qquad \text{Eq [6.21]}$$

Both the mean value and standard deviation of R_E are multiplied later on by F_{EC}, F_W, and certainly multiplied by the storey-shear factor $(n+1) / (n+i)$. The most complex parameter to be computed in SAUMAC is I_R. All the information needed for any useful possibilities of R_E are shown in table 6.2. At last, only one of all possibilities found, per storey and analyzed direction (x,y), values of R_E in the table is used to compute I_R according to the boundary conditions.

Table 6.2: Useful summary table for R_E possibilities (for y or x analyzed directions)

Base floor type	Top floor	External walls**				Internal wall^T	
		1		*2*			
Flexible / rigid (ψ = ___)		Spandrel good/poor	R_E / F_W	Spandrel good/poor	R_E / F_W	----	R_E
	$h_p/l_{p\,min}$	visual	cal*	visual	cal	0.75	cal
	$h_p/l_{p\,max}$	visual	cal	visual	cal	1	cal
	$L_{max}/L_{eff.}$	visual	cal	visual	cal	-------	
…intermediate floors…							
Top floor type	Base floor	External walls**				Internal wall^T	
		1		*2*			
Flexible / rigid (ψ = ___)		Spandrel good/poor	R_E / F_W	Spandrel good/poor	R_E / F_W	----	R_E
	$h_p/l_{p\,min}$	visual	cal*	visual	cal	0.75	cal
	$h_p/l_{p\,max}$	visual	cal	visual	cal	1	cal
	$L_{max}/L_{eff.}$	visual	cal	visual	cal	-------	

**cal refers to calculation of R_E or F_W according to the pier geometry in the wall. ** At least 2 external walls. ^{T}Assumed for internal wall*

6.5.2 The seismic demand I_S

The seismic demand index I_S describes the seismic solicitation S in terms of its mean value and standard deviation. The index is attained from the seismic coefficient C_S as computed by the normative to be used for the in-plain mechanism, and by equation 6.13 for the out-of-plane one.

$I_S = C_S$ in-plane failure mode Eq [6.22]

$I_{SO} = \frac{\alpha S_S}{q_a}$ out-of-plane failure mode (equation 6.13) Eq [6.23]

At the same time de value of C_S is subdivided into three different parameters as:

$$C_S = F_S S_S \alpha \qquad \text{Eq [6.24]}$$

F_S = Constant related to the seismic code formulations. This takes into account aspects like spectral response amplification, behavior factor (table 4.7), etc (assumptions #4 and #5 applied)

α = reference normalized ground acceleration (expressed in %g of PGA),

S_S = Terrain or soil factor as defined by the local code

The F_C and S_S values may vary according to different codes formulations. Almost for all the cases of low rise URM, the first natural period is lower than 0.4 seconds. The variation of α is depends then directly on the reference PGA value. Lognormal PDFs describe well the behavior of PGA as observed attenuation curves in section 3.2.2. The standard deviation for PGA is assumed constant and of value equal to 0.5 in the normalized lognormal space.

6.5.3 The architectural mass index A_M

The architectural mass distribution index A_M calculates the ratio in between the total accumulate weight of all storeys over the analyzed storey and the total mass acting as normal forces on the resistant wall elements. It is expressed in terms of the wall cross section area ratio ρ. This parameter is a ratio in between the total resisting wall area in one structural direction and the total floor area (equations 6.2 and 6.5)

A ρ value can be obtained from a simple scheme of the house per floor from local knowledge information or after in-situ inspection (more accurate way). If this information is not available, some approximation due to a geometrical factor can be done. This factor is defined as:

$$G_{eo} = 0{,}75\left(1+\frac{10e_x(2+D_x)}{Y}\right) \qquad \text{Eq [6.24]}$$

The G_{eo} factor in equation 6.24 is used for obtaining ρ in the x direction. The values of D_y and D_x are approximated by figure 6.18. In the figure, the PDF related to each number of walls in function of the building depth are plotted. Here, the values are proposed for the x direction but they are equally found with the same graph for the y direction.

The value of G_{eo} is just a parameter without any physical meaning. In figure 6.19 an estimate value of A_M for two different material types is computed. In the procedure, graphics like the ones presented below can describe most of the URM housing conditions. The important parameters for the computation of this factor are the material density, wall thickness and the slabs weight.

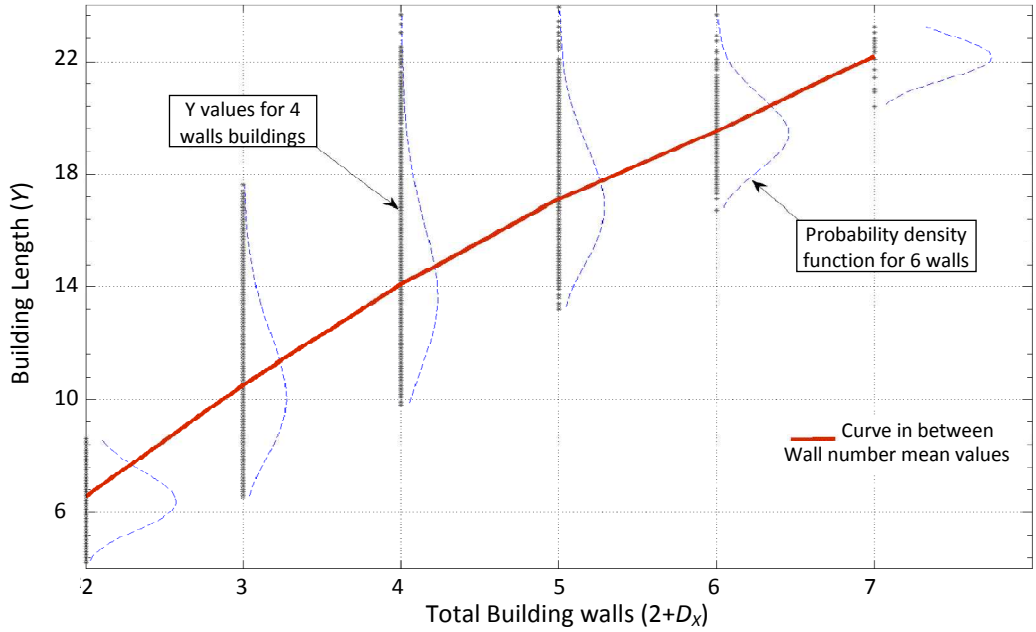

Figure 6.18: Approximation of internal walls D_x in x direction

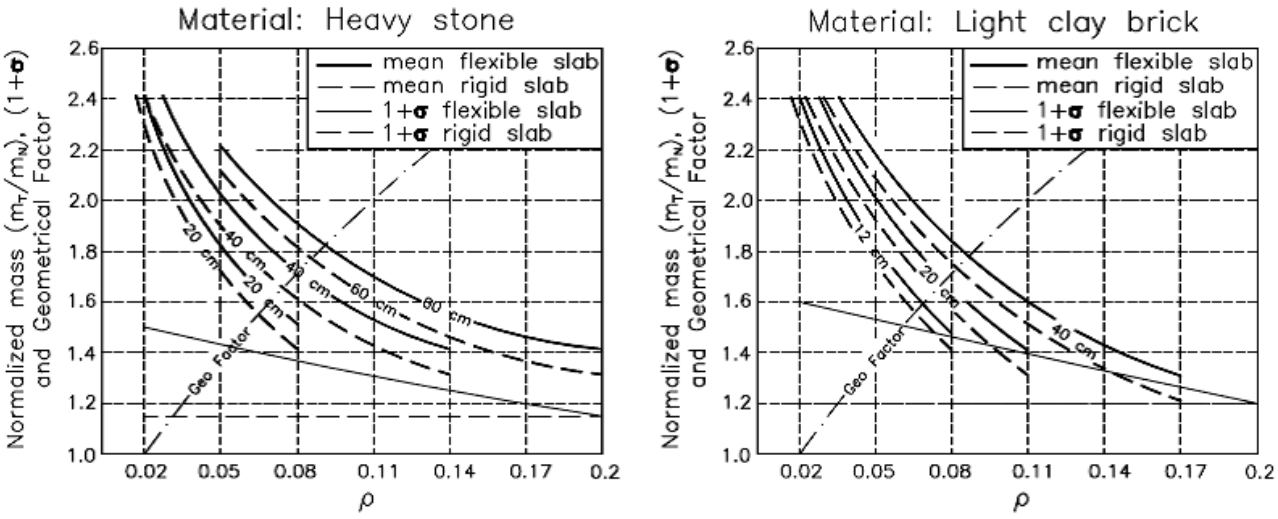

Figure 6.19: A_M (m_T/m_N) according to the resistant wall ratio for two different materials (sandstone 22 kN/m^3 and clay brick 14 kN/m^3) for different mean wall thickness and the G_{eo} factor

6.6 Structural Fragility and Computing the Risk

Once the parameters I_R, I_S and A_M had been obtained the limit state equation $G(I_R, I_S, A_M)$ for the in plane and $G(I_{Ro}, I_{So})$ for the out of plane can be finally solved. In section 5, possible procedures to solve $G(X)$ are overviewed. Their possible applications to this study are:

- *The FORM procedure:* can be used to approximate solve both $G(I_{Ro}, I_{So})$ and $G(I_R, I_S, A_M)$. All variables should be in the lognormal space.
- *Close form:* the analytical solution from equations 5.6 or more likely equation 5.7 is used for getting $G(I_{Ro}, I_{So})$.
- *Monte Carlo simulation:* is used to approximately solve both $G(I_{Ro}, I_{So})$ and $G(I_R, I_S, A_M)$. The number of simulations can be estimated by equation 5.8 and a probability of failure of 0.001. The simulation is performed many times for small PGA steps for defining the fragility curve as represented in figure 5.7. The result points obtained from the MC simulation are observed in figure 6.20 together with the lognormal approximation obtained from the result of the Monte Carlo simulation.

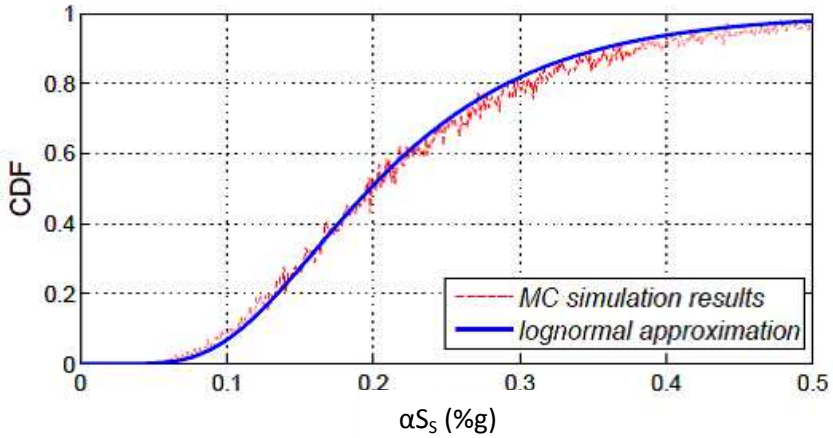

Figure 6.20: MC solution for the fragility and the resultant lognormal approximation

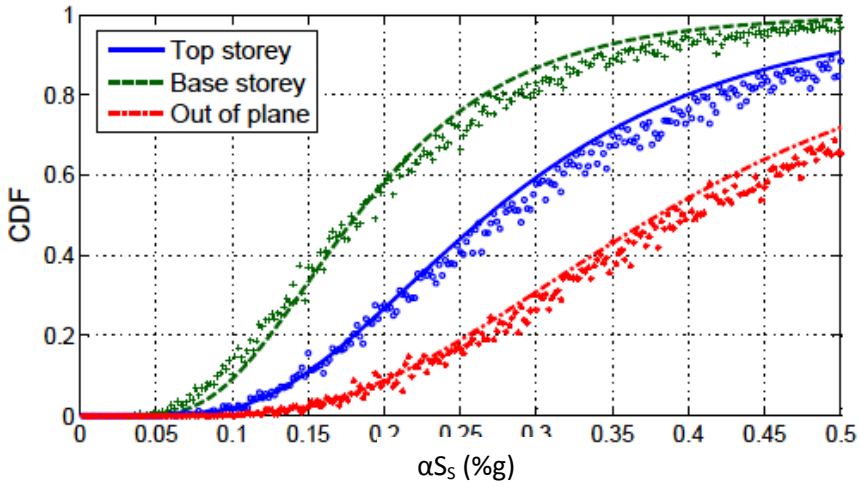

Figure 6.21: Fragilities for a 3 storey building with rigid diaphragms and good spandrels

The MC process must be performed $2n+1$ times to obtain the representative fragilities functions P_f(PGA) for in-plane and out-of-plane (n = number of storeys). Normally the most critical situations in the in-plane failure mechanism are created at the top and the base storey when the building stands alone or together with buildings of the same height. Critical fragilities can be also found in middle storeys when surrounding building are of lower height.

In case of material combination at any storey, the total fragility must be computed similarly to equation 5.10. Storeys cannot be considered any more correlated for different materials and so total fragility must be incremented.

Results for fragilities for building with poor property material, good connections and rigid diaphragms are plotted for the top, base floors (in-plane), and out-of-plane (figure 6.21). For each point of the graph, a number of 3.0×10^3 simulations were run; this number of simulations is obtained by default from equation 5.8.

Once the fragilities characteristic for the in-plane and out-of-plane have been chosen (e.g. Base storey and out-of-plane curves in figure 6.21), the final fragility is computed from equation 5.10. The joint fragility or final total fragility curve is obtained finally. Results for the joint fragility are showed, after following the example in figure 6.21, in figure 6.22.

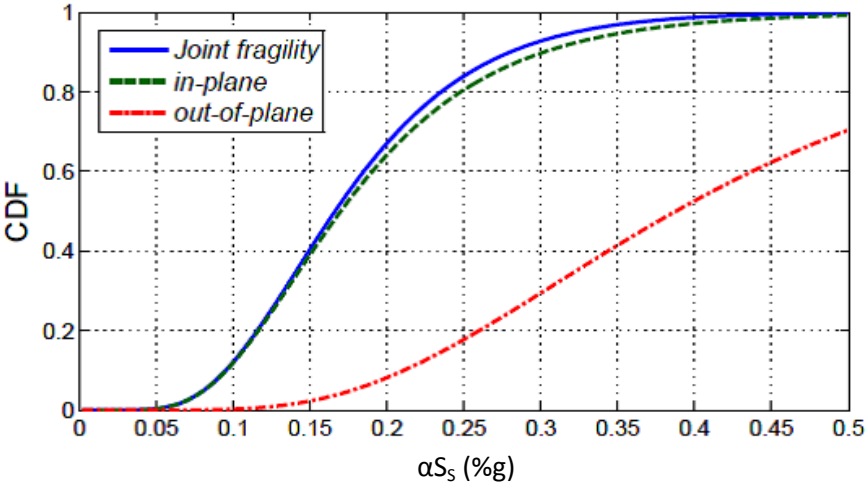

Figure 6.22: The building systems fragility curve P_f(PGA)

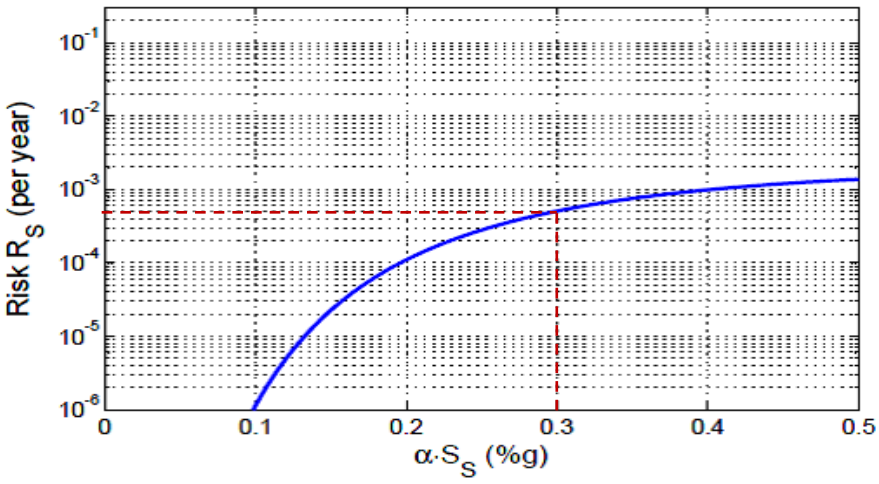

Figure 6.23: Structural risk in function of the reference PGA values (taking local soil conditions S_S)

With the structural fragilities finally defined for a building or a building group, and the hazard curve *H*, as it is obtained in section 3.3.2, the equation 5.13 is finally solved and the structural risk obtained. When plotting the reference seismic action (in terms of %*g* PGA and for local soil condition S_S) and the structural risk R_S, figure 6.23 is obtained.

The reference seismic action to be used to obtain the structural risk is the one corresponding to the return period R_P proposed for the structure according to the local code formulation and the hazard curve. For the hazard curve presented in figure 3.8 and a R_P of 475 years we have a PGA of 0.3. For this action level, the annual structural risk for a hypothetical structure of figure 6.23 example is of $R_S = 5.0 \times 10^{-4}$. The risk value that corresponds to the expected life span of the structure (50 years) can be computed from equation 3.7.

To evaluate results of R_S, following the scheme presented in figure 6.1, the safety and risk evaluation criteria proposed in this study is summarized in figure 6.24. Evaluation aspects are based on the analysis of figure 5.9. A moderate risk qualification is approximately similar to the alarm zone proposed in TEPHRA [Tephra-96]. The risk value obtained from SAUMAC can be used for estimating possible damages for building groups, but only as a description for individual structures.

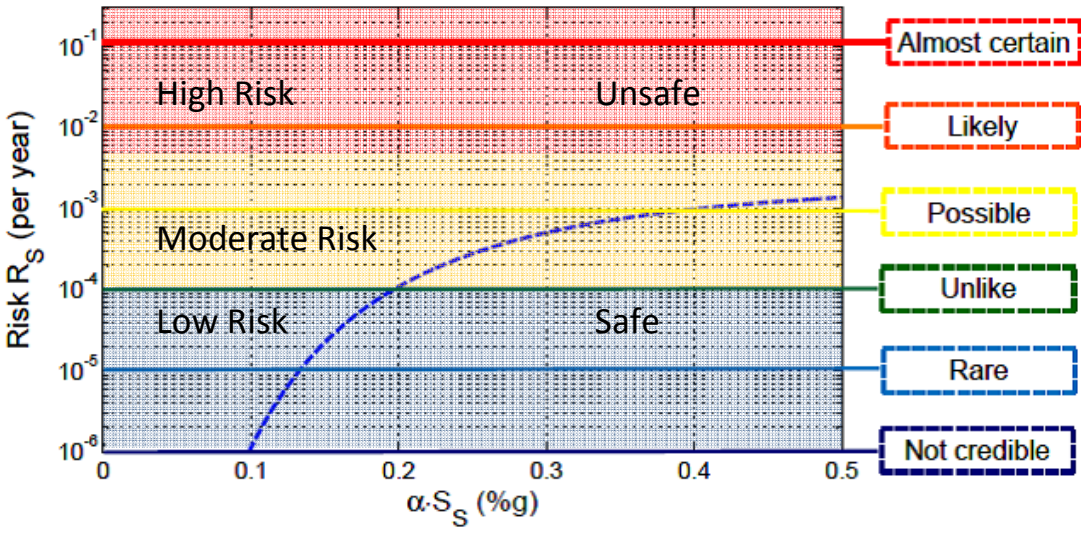

Figure 6.24: Definition of risk levels (building groups) and safety criteria (individual house) for low rise URM. Low risk upper limit = 10^{-4}, high risk lower limit = 5.0×10^{-3}

7 CASE STUDY: SEISMIC DAMAGE ASSESSMENT AT CASTELNUOVO TOWN; ABRUZZO, ITALY

Castelnuovo town is administratively part of the Comune of San Pio delle Camere, province of L'Aquila, Abruzzo region in central Italy. The town was heavily damaged during the L'Aquila earthquake of 2009. Intensities up to 9.5 MM scale were reported presenting, together with Onna, the greatest observed building damage [GC 09]. Five human lives were unfortunately lost[1], a minor consequence considering the extensive damage in the town [ilCentro web]. An aerial view of the town is presented in figure 7.1. The figure presents the state of the village before and after the event.

In Castelnuovo, the construction of the old town (borgo fortificato) dates from the low medieval ages, in the XII century. Initially the town was born as a control point on the road from Foggia to L'Aquila city, very close to the ancient roman town of Peltuinun, in fact, the old roman town was a source of construction materials for Castelnuovo and other surrounding towns [CF 10]. The settlement presents three clear different urban developments, the old medieval town on the top of the hill, an expansion in the XVII century at the gentle slope of the hill, and the recent growth, called the new expansion, located in the surrounding lower areas of the hill [Br 11].

Historically the town had been damage by different events. According to the INGV, six other major events are reported to produce significant damage in the village from 1456, as shown in figure 7.2 [INGV web]. Previous reconstruction traces, as well as common simple earthquake countermeasures (arches, buttress, and iron chains) were widely observed, especially in the Borgo Fortificato, describing a frequent seismic activity in the area.

Figure 7.1: Castelnuovo town, before and after the 2009 L'Aquila earthquake [CF 10]

Event	Year	Moment (M_O)	Intensity (MM)
Molise	1703	7.2	10
Aquilano	1461	6.4	9 to 10
Aquilano	1762	6.7	9 to 10
Aquilano	1456	6.0	8
Avezzano	1915	7.0	8
Gran Sasso	1950	5,7	6

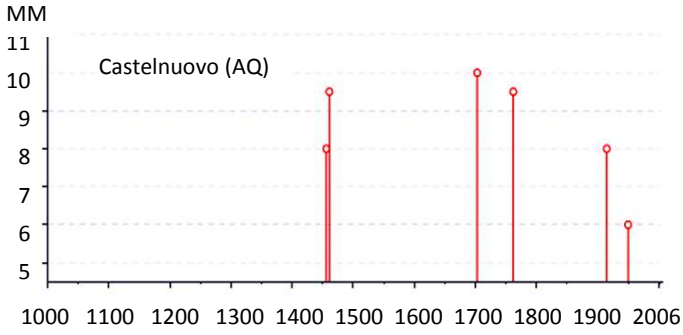

Figure 7.2: Historical seismic activity for Castelnuovo town according to INGV [INGV web]

[1] Fatalities: Demal Hasani (41), Refik Hasani (43), Maria Fina Marrone(85), Emidio Sidoni(87), Emanuele Sidoni(60)

Some weeks after the main earthquake hits Castelnuovo, the University of Florence, through a project presented by the Prof. Andrea Vignoli, started an intensive work focused in two aspects: a detailed description of the earthquake damage at Castelnuovo, and a proposal for the town reconstruction to the Comune of San Pio delle Camere. The project was financed by the Toscana Region local government. Most of the data presented in this chapter is based in damage description performed by the University of Florence team and two short field recognition campaigns executed by the author of this study during May 2009 and October 2011. A further detailed description of the damage at Castelnuovo is presented in section 7.2 and appendix A.

7.1 L'Aquila Earthquake 2009

On April 6, 2009, an intra-plate earthquake with moment magnitude M_O = 6.3 occurred in the region near L'Aquila city in Abruzzo department, Italy. The event was felt throughout central Italy, including the Italian capital, Rome. The earthquake was caused by a normal fault along the Central Apennines [AKTB 09]. Historically, the area had suffered destructive earthquakes in 1315, 1349, 1461, 1703, 1706, and 1915. The 1915 seismic event was the one of greatest energy release with a magnitude of M = 7.0, and the most recent nearby event was the 1996 Umbria (M_O = 6.1) earthquake. A summary of the most important event epicenters, since the Italian unification days in 1861, is presented in figure 7.3.

For L'Aquila earthquake, there were reported at least 294 people killed in L'Aquila city and nearby villages and towns [AKTB 09]. Villages such as Castelnuovo and Onna experienced severe damage and were almost totally destroyed; as well, the historical city center of L'Aquila was heavily hit and is still nowadays partially closed to public. The earthquake major effects were distinctly observed in a 20 km long and 10km wide area around the epicenter as shown in figure 7.4 developed by the Italian National Civil Protection Agency and the National Institute for Geophysics and Vulcanology INGV [GC 09]. It could be inferred from figure 7.4 that there is no evident relationship in between the seismic intensity values and the quake epicentral distance, this, probably related mainly to the topographic/soil amplification and to the conservation state of the buildings, as it will be commented later on for the damage explanation in Castelnuovo town.

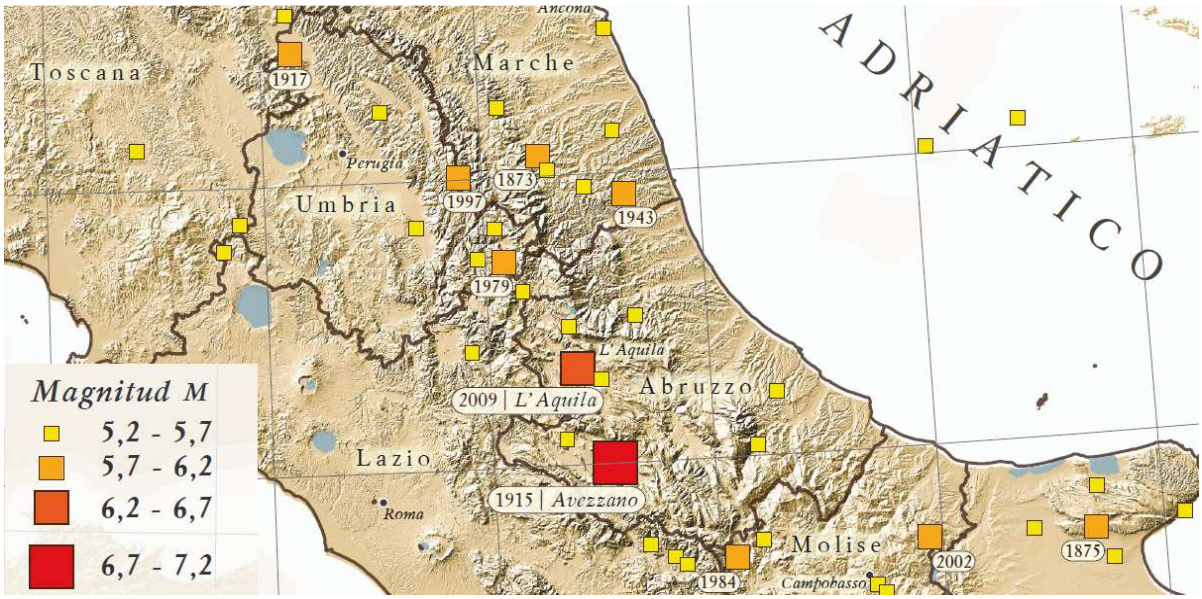

Figure 7.3: Major Earthquakes in Abruzzo area since the Italian Unification (INGV 2011)

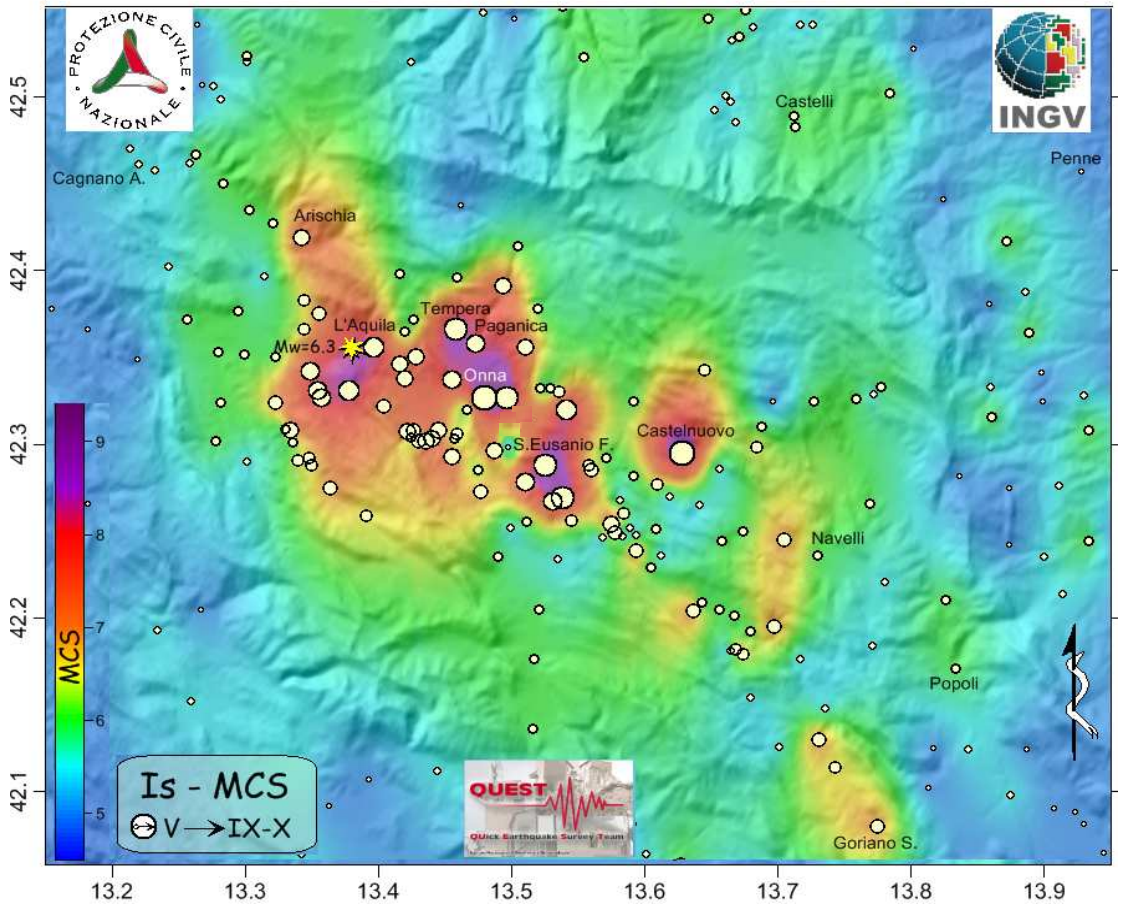

Figure 7.4: Intensity distribution for L'Aquila Earthquake [GC 09]

It is estimated that due to the earthquake, more than 25000 people were displaced, a total of 10000 buildings suffered significant damage, and economical losses exceed US$ 16 billion including financial and reconstruction cost [MY 09].

Most of the deaths occurred when people were buried under collapsed buildings, many of these were residential URM typology houses. The casualty numbers was increased due to the fact that people were caught during the sleeping time (3:32 am), this aspect also made difficult the first efforts to rescue people and to evaluate the emergency magnitude.

According to the INGV seismic risk maps [INGV web], Castelnuovo is located in one of the heaviest seismic risk areas in Italy, as shown in figure 3.12. Peak ground accelerations (PGA) are expected to be up to 2.75 m/s^2 for rigid soil conditions (V_{S30} = 800 m/s). Most of the registered strong motion records during the event are summarized and presented together with the Akkar-Bommer attenuation curves presented by the UK Earthquake Engineering Field Investigation Team in figure 7.5 [EEFIT 09]. Attenuation curves are based in stations data mainly founded on firm ground (V_{S30} = 450-1000 m/s). This attenuation relation correlates well with the recent study presented by Steward [St 12]. No strong motion record station is located near Castelnuovo town, the IX intensity is judged by the INGV by the observed damage (figure 7.4).

From the attenuation curves, it could be inferred that the PGA value in Castelnuovo is between 0.8 and 0.9 m/s^2 for an epicentral distance of approximately 25 km (Castelnuovo distance from the source). Soil amplification or topography aspects are not assessed directly from this attenuation curves. Observing the register data and the attenuation curves, a value of 0.8 m/s^2 is believed to be the one to describe accurately a raw value of PGA to be used later on in this study.

Station	Lat N	Log E	PGA (%g)	Epicentral Dist. (km)
AQV	42.377	13.344	0.675	4.85
AQG	42.373	13.337	0.515	4.34
AGA	42.376	13.339	0.487	4.69
AQK	42.345	13.401	0.373	5.64
GSA	42.421	13.519	0.152	18.01
CLN	42.085	13.521	0.091	31.68
AVZ	42.027	13.426	0.069	34.97
ORC	41.954	13.642	0.066	49.30
MTR	42.524	13.245	0.063	22.35

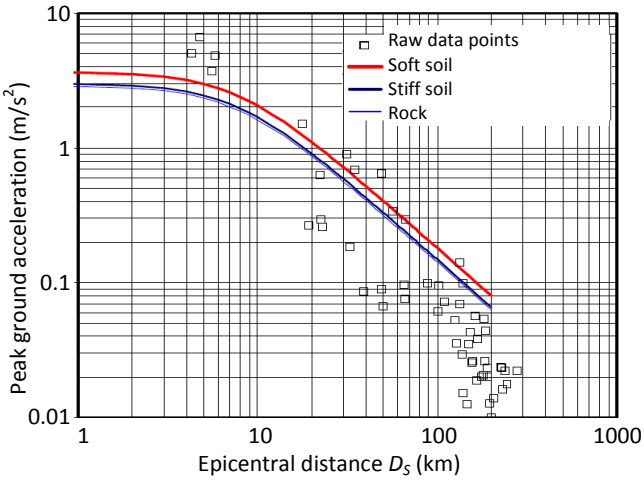

a) b)

Figure 7.5: a) Major ground motion records for L'Aquila earthquake 2009 [GC 09], b) Akkar-Bommer attenuation curves [EEFIT 09][AB 07]

The soil profile consists mainly of white consolidated silts of fluvial/lacustrine origin (figure 7.6). According to the formulated equations developed by University of Napoli [Si 10], the shear velocity for the white silt in the first 30 meters V_{S30} is 350 m/s, and a V_S equal to 200 m/s close to the surface. This shear wave velocity data was obtained by means of a Down Hole test. According to Ciavattone the specific weight γ of the silt is 20 kN/m^3 with a non drained shear resistance c_u of 0,1 MPa at the ground surface [CF 10]. Regarding the soil amplification phenomenon, studies from INGV and the University of Napoli [Si 10], presented that amplification values ranging from 1.6 to 2.5 are founded in the Castelnuovo old town area as shown in figure 7.7. From this amplification studies, it may be assumed that the actual experienced PGA value was around 1.7 m/s^2; this PGA value is also used later to evaluate damage in section 7.5. In figures 7.6 and 7.7, diverse from the amplification factors, some areas are additionally considered unstable (highly vulnerable to subsidence and soil shear failure) due to the existence of underground tunnels, many times with small coverage. During the earthquake one of these cavities collapsed damaging many surrounding structures.

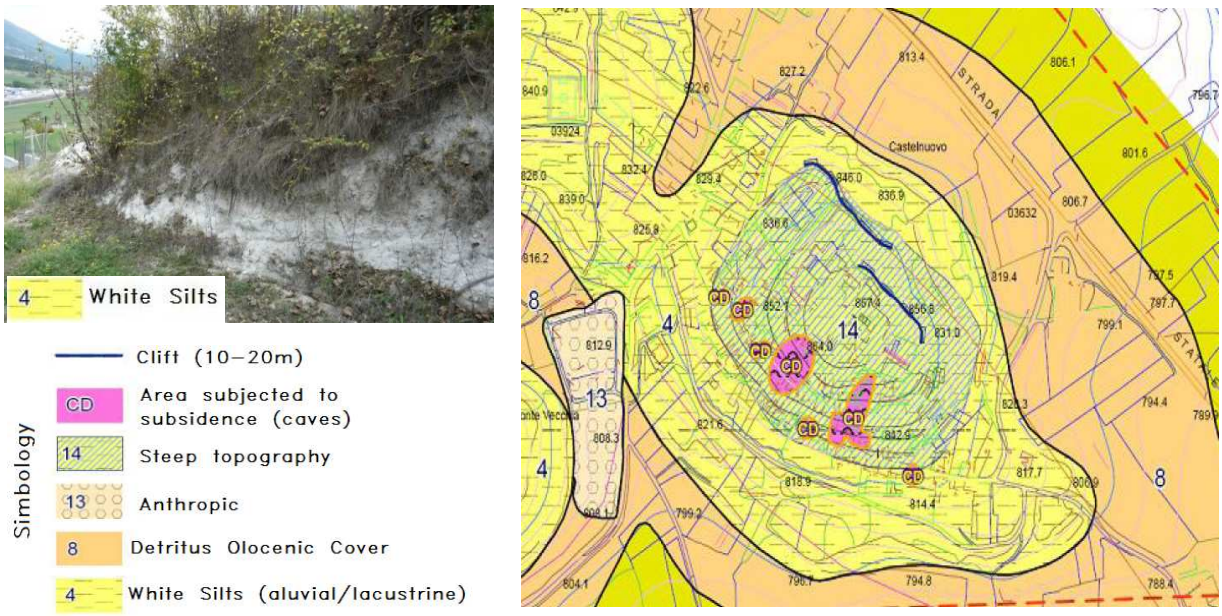

Figure 7.6: Geotechnical information at Castelnuovo and surroundings (adapted from [INGV web])

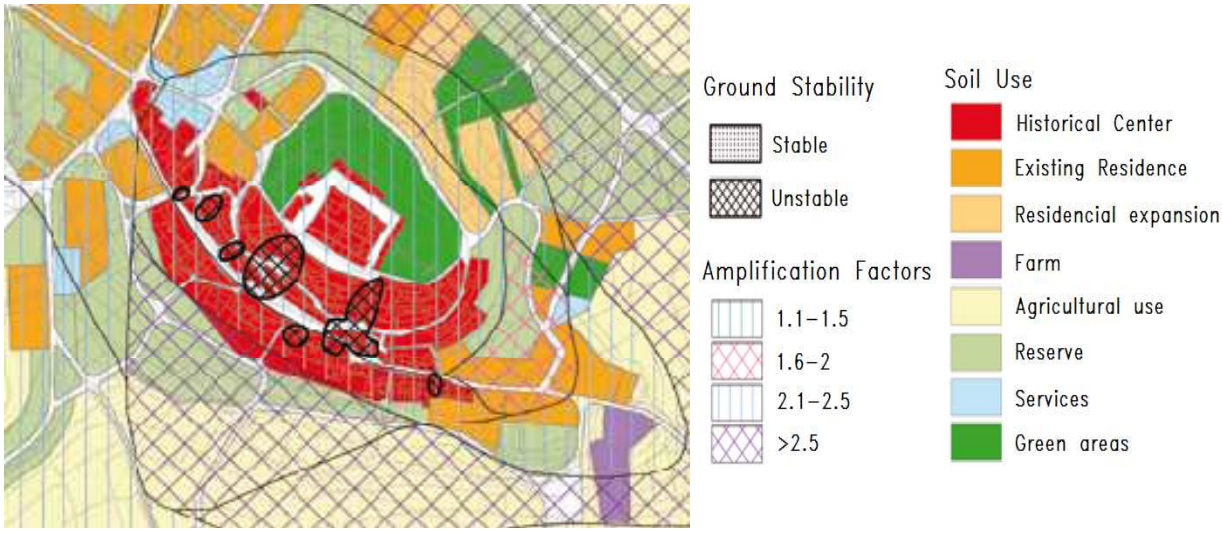

Figure 7.7: Ground Stability, use and Amplification map (adapted from [INGV web])

A high PGA, the terrain amplification, the poor maintenance of buildings and the intrinsic vulnerability of URM (called ordinary masonry in the Italian context) explains the heavy damage experience at this village during the L'Aquila 2009 earthquake. Concerning the URM building conditions in Castelnuovo, section 7.2 explains in detail the particularities of the building typologies founded there. In general, URM are still very common in many countries worldwide, as explained in section 4.2. For the Italian reality, the URM building stock could be up to 62% of the total national population as observed in table 4.2, the second more common building type is reinforced concrete, mainly concentrated to the north of the country and recent housing developments.

7.2 Building Characterization and Damage in Castelnuovo

A building characterization was developed by the research group coordinate by the professor Andrea Vignoli of the University of Florence and corroborated independently by two field surveys by the author of this study in May 2009 and October 2011. This chapter summarizes aspects related with the seismic damage study for Castelnuovo town, developed as base input data for the renovation proposal. The town requires to be reconstructed keeping the old town pre-earthquake building characteristics.

A good summary of the building data characterization from Prof. Vignoli group was presented by Ciavattone [CF 10], here a total of 262 building units were described. The accuracy of the description made was up to three different levels related with the possibility to have internal access to a building. Evaluation of many internal buildings parameters was restricted due to the partial collapse of the structure, the risk of collapse, and legal limitations. According to this, the quality of the building information is described in 3 levels [CF 10]:

- *Poor:* description based on external building inspection only (81 building).
- *Medium:* access to the building is only partial, so structural configuration description is limited (92 buildings).
- *Good:* full access to the structure (89 buildings).

Figure 7.8: Structural unities: 1) regular rectangular group, 2) isolate, 3) articulate [CF 10]

Even thought the limitation on the information resolution, important aspects like the building structural material typology or the structural unity sets are possible to assess easily for most of the cases, even in total collapse. For the characterization into a structural unity, the aerial information previous to the quake is sufficient. This description is useful in order to make a simple judge on the structural irregularities (section 3.3.3). For example, irregular structural configurations are expected for articulate building configurations and corner building in a building group.

The structural unities are described by three types as shown in the figure 7.8 of Ciavattone's study [CF 10]. They are a rectangular group (1), single (2) and articulate (3) structural types. For structural unity one, rectangular building group, edifications present good structural internal regularity, they share intermediate walls and present regularity in height. In opposition to regular rectangular group or single building configurations, there are the articulate buildings. These could be alone or in group. In the articulate group, irregularities are evident for the structural plan and usually also in height. The percentage of each structural unity is presented in figure 7.9b.

Another aspect to be mention is the distribution of the storey number in the village. Here, two and three storeys buildings are dominant as it could be observed in figures 7.9a and 7.10a. It's relevant to mention that in some cases the structural material in between floors is not the same; even the construction period of each level may differ in centuries, for example in the borgo fortificato, it is easy to differ different historical periods market by vertical grown of the structure or reconstruction [Br 11]. Different materials and structural conditions could be assigned to each storey.

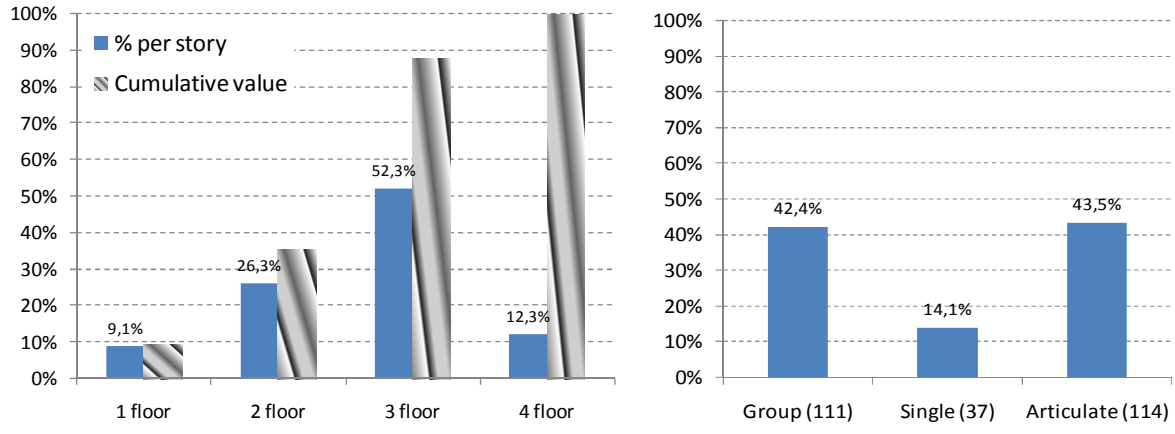

a) b)

Figure 7.9: a) Floor percentage distribution, b) percentage of structural units (based in [CF 10])

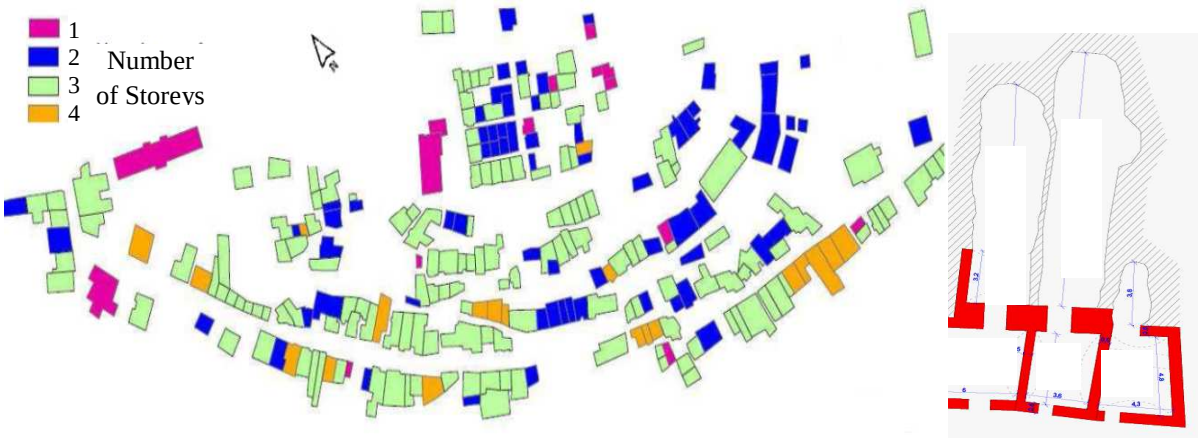

a) b)

Figure 7.10: Town city center. a) location of storey distribution, b) underground caves [CF 10]

The distribution of the storeys in the Castelnuovo Historical town center is presented in figure 7.10a. More than a half of all the building population consist of 3 storeys, were the first storey is usually a semi underground floor following the local topography, sometimes even the first storey is combined with a cave as shown in figure 7.10b.

Caves are common in the area because it's utility as a storage place. Silt soils are founded in the hill; this material is easy to dig and at the same time presents good supporting conditions. According to this good consistency of the material, some of the caves don't even present any sort of additional support like wooden beams or the traditional stone vault covers. In figure 7.11a, it is observed a sinkhole produced due to the collapse of a cave that presented low overlaying soil depth (less than 2 meters in the figure) and no masonry vault support.

The influence of caves may vary significantly the seismic action input on the structures, especially for a low soil depth cover. On the other hand, the soil consolidation process and its consequent subsidence have a negative effect on existent structures due to the differential settlements that may have weaken structures prior the quake. In figure 7.11b, the difference between the unsupported and supported caves is easily observed from the cave roof, were supported roofs made possible wider spaces while the unsupported ones are narrower to maintain stability. Aspects related with the cave influence on the superstructure damage are going to be neglected in this study.

a) b)

Figure 7.11: a) Cave collapse, b) partially unsupported cave

Regarding the horizontal typologies, which refer to floor diaphragms and roof construction techniques, they are diverse possibilities in the town. Diaphragms systems correspond to different improvements along the time of construction and renewal. Traditionally, heavy vaults were used for the lower levels and wooden systems for the upper levels for the medieval period [Br 11]. In more recent constructions, the use of heavy vaults is not common, instead, steel beams with masonry vaults systems or infills are common. Upper levels typologies are very diverse, building renewal and growth of the structure allowed the introduction of new technologies. A summary of the floor/ roof typologies and its frequency in Castelnuovo is presented in figures 7.12 and 7.13.

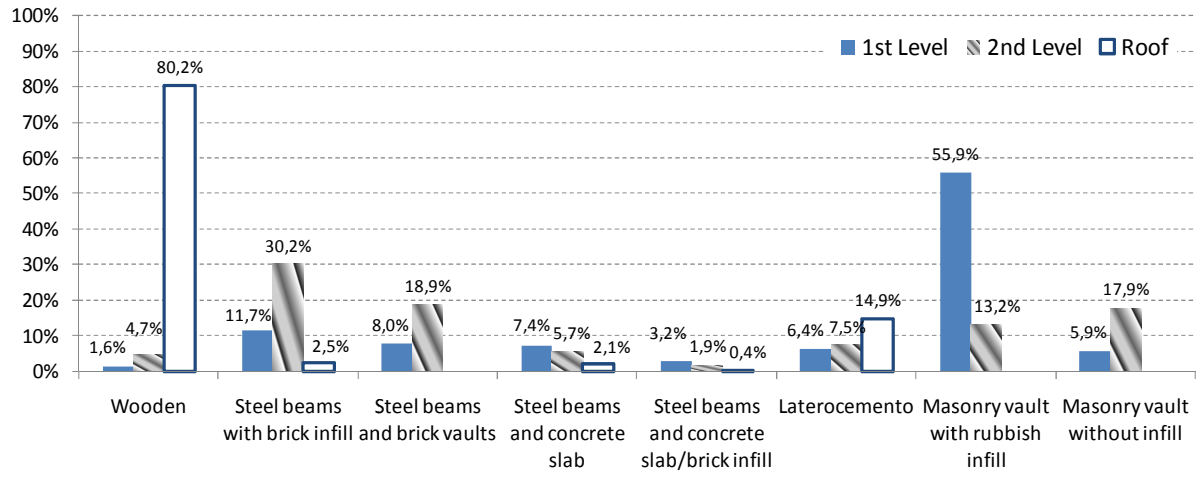

Figure 7.12: Horizontal typologies according to storey level (based in [CF 10])

Figure 7.13: Photographic details for horizontal typologies presented in figure 7.12

Figure 7.14: Buttress and arches as restraining elements for vaults and walls

In figure 7.12, the different slab and roof systems are described in terms of the location. In the case of what its refer as to 2nd level, the data is also representative for the 3rd and 4rd levels.

Regarding the restraining capabilities of these inter-storey systems, laterocement and steel beams with reinforced concrete can be considered to offer a sufficient restraining force to be assigned a rigid slab condition as it is usually formulated in common structural design and normative like the UFC [UFC-07]. In case of heavy masonry vaults, these are also considered as rigid elements that give enough lateral stiffness to the building floor. This is due to the fact that usually in the town heavy vaults are present in combination with neighbor buildings, buttress, arches and chains which provide adequate lateral confinement. This prevented heavy damage on lower storeys in Castelnuovo, especially damage related with out-of-plane failure mechanism. Figure 7.14 presents some of the traditional existing lateral restraining techniques observed in Castelnuovo.

In case of structural vertical construction types, there are founded many variations in the Castelnuovo historical center but, by far, the predominant consist of unreinforced stone masonry buildings. According to the research group of Florence University, which results are summarized by Ciavattone [CF 10], up to 86.7% of the total building stock consists of rubble stone URM, and the total URM is up to 91.3% in the town city center. This is clearly reflected in figures 7.15 and 7.16.

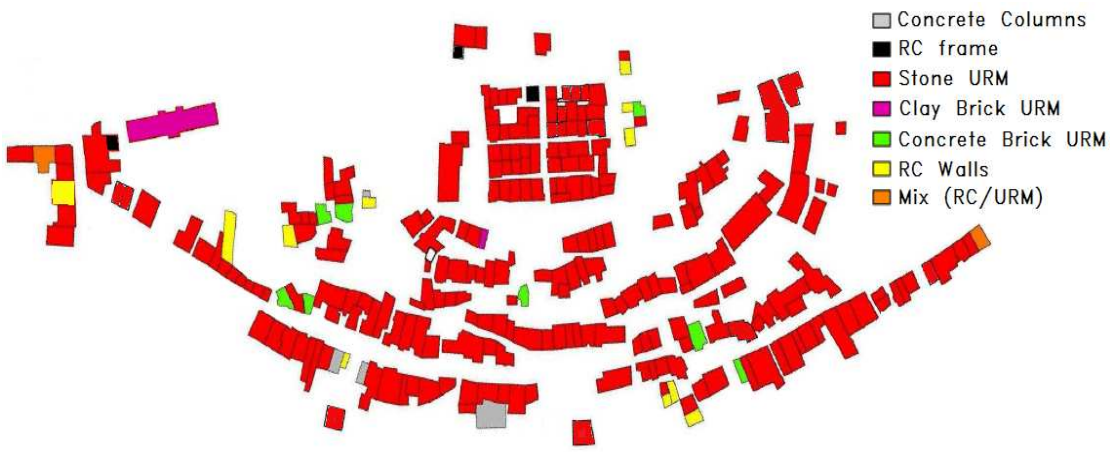

Figure 7.15: Vertical typology distribution at Castelnuovo city center [CF 10]

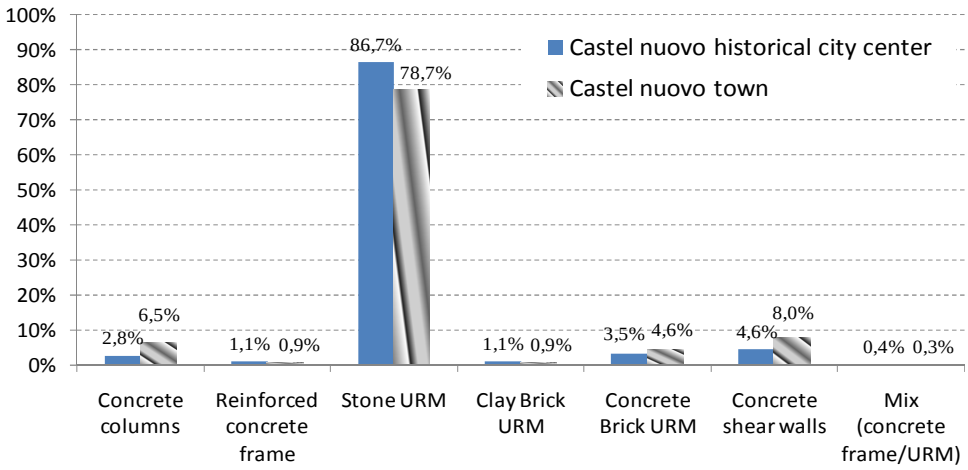

Figure 7.16: Vertical typology frequencies at Castelnuovo city center (based in [CF 10])

As it is evident from figures 17.16 and 17.16, for the case of Castelnuovo town and many other similar towns in Italy, the building seismic evaluation should give special focus on stone URM as it's the dominant construction typology in many Italian towns [Do 06]. Figure 7.17a illustrates a typical rubble stone wall section in Castelnuovo. Other URM are shown in figures 7.17b and 7.17c. It is also evident that the mix of different material is common as the renewals and reconstruction work took place during the life span of the structure.

Another important aspect to be comment here is the state of the occupation and maintenance building condition prior to the L'Aquila 2009 earthquake. The relevant aspects are presented by Ciavattone based on a local engineer inspection of the settlement prepared in 2005 [CF 10].

The migration process to nearby cities like L'Aquila, Rome and Naples leaf many towns like Castelnuovo partially depopulated for most part of the year. During the vacation periods, towns regain part of the population.

One of the reasons for limited human fatalities at Castelnuovo was that the place was almost empty by the time of the earthquake occurrence. This, plus a better maintenance condition of full time occupied houses (if compared with that were abandoned), contributed for only 5 human casualties although the town was largely destroyed [ilCentro web].

a) b) c)

Figure 17: URM material types: a) rubble stone masonry, b) concrete units and c) clay Bricks

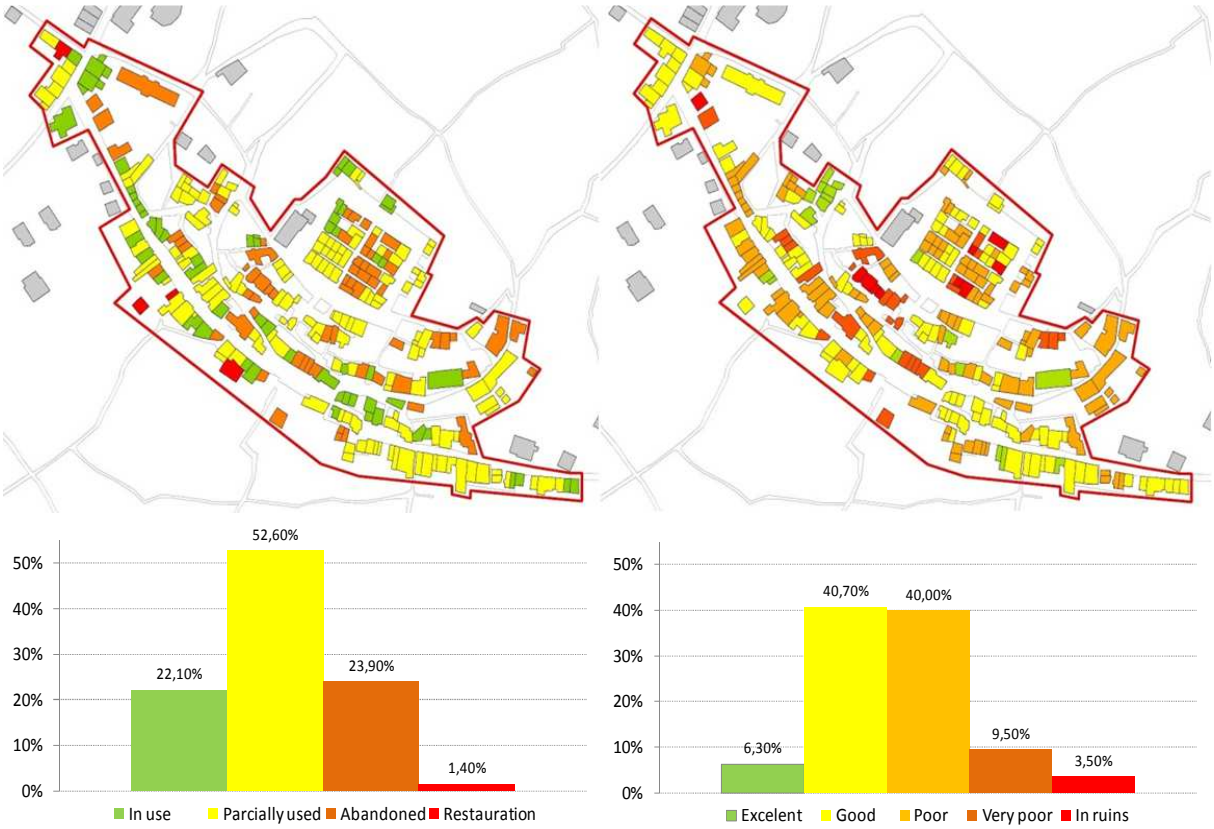

a) b)

Figure 7.18: a) The occupation and b) maintenance building state at Castelnuovo (based in [CF 10])

A complete description of Castelnuovo state before the earthquake is presented in figure 7.18. Here it is observed that less than 25% of the buildings were actually in daily use and another quarter were totally abandoned structures. The pre-earthquake condition reflected that more than 50% of the building stock presented poor, very poor or partially collapse condition. This poor maintenance conditions together with the intrinsic vulnerability of rubble stone URM explains the widespread damage founded at Castelnuovo.

The correlation of the maintenance state to the occupation state is shown in figure 7.19. There, it is evident that people don't actually live any more in those building that are in ruins and in very poor structural condition.

In terms of seismic improvement prioritization, it is observable from figure 7.19 that almost a 40% of the used or partially used houses presented poor maintenance conditions. These will be priority candidates to receive structural improvement since they are the most risky structures given that they present a high vulnerability plus the exposition values to be lost in terms of human life and personal belongings. Around 85% of the building presenting poor, very poor and partially collapse condition are abandoned. Even though these structures presented relatively reduced direct exposed values, their collapse affect neighboring structures, injure people at the street and block exit trails in urban building environment. These structures are recommended to be demolished in case of no historical or urban/architectural value.

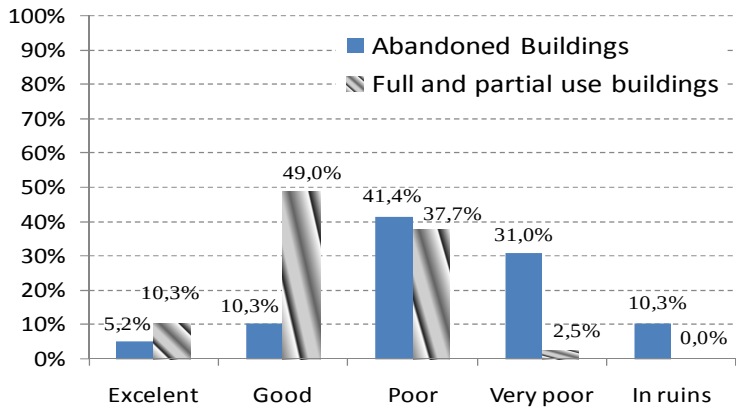

Figure 7.19: Correlation in between occupation and maintenance building state of buildings (based in [CF 10])

In case of the seismic structural vulnerability and damage description for Castelnuovo, the research team of the Florence University followed the procedure establish by the EMS-98 (section 3.1.2). The European Macroseismic Scale presents five levels of damage and a vulnerability description according to building typologies [Gr 98]. The results of the field survey after the earthquake are resumed in figure 7.20, there the level D0 was added for those cases of no damage. The D0 was presented by the RISK-UE group [MT 03]. Since the vulnerability descriptions presented by EMS-98 are quite general, a local description was developed according to the town buildings characteristic to make easier the field work according to Ciavattone, this description is similar to the one recommended by the INGV [Te 09]. This description is presented in table 7.1 and distinguished by two different possibilities for B type vulnerability class.

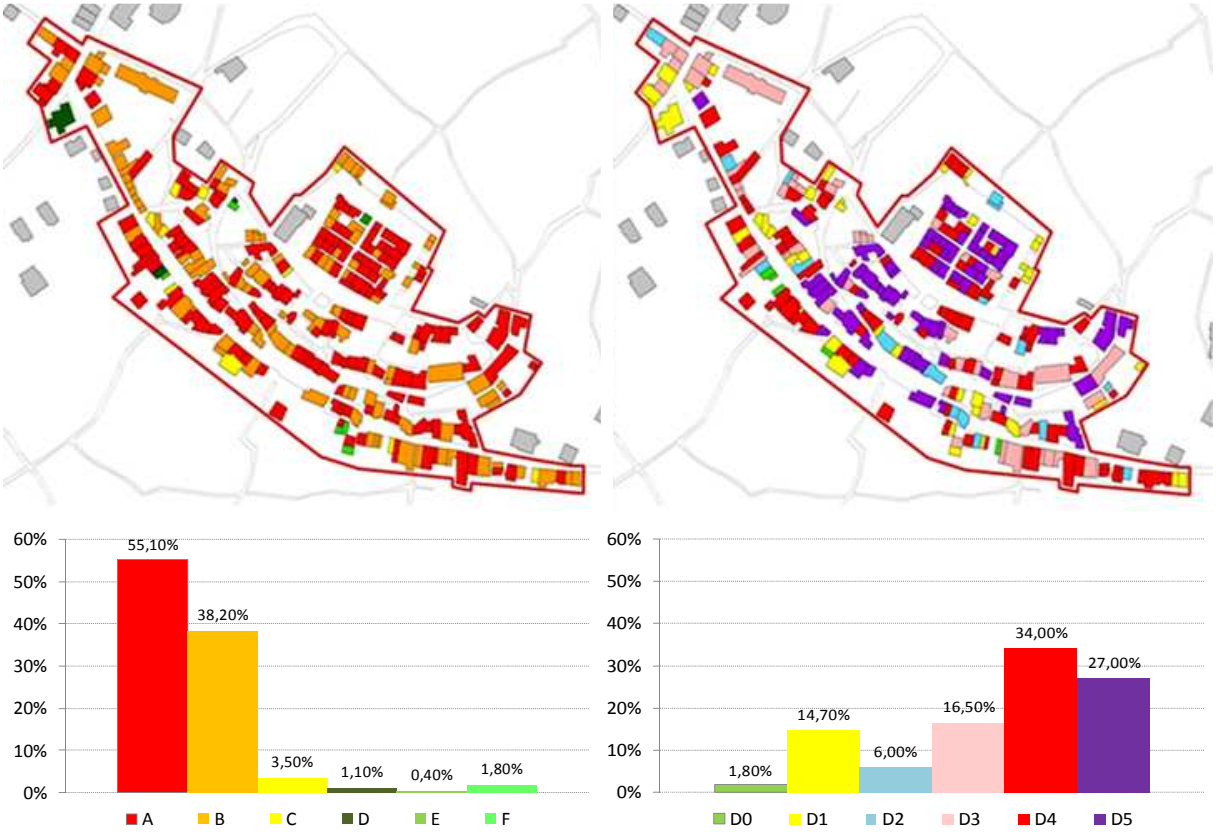

a) b)

Figure 7.20: a) Building vulnerability group and b) damage levels for Castelnuovo (based in [CF 10])

All the stone masonry buildings fall into the A and B vulnerability categories which explains the abundance of A and B building types in figure 7.20. The analyses developed later on in this study focuse mainly on these two vulnerabilities groups. More about the damage description in Castelnuovo town regarding photographic details and description of failure modes is summarized in the Appendix A of this work.

Table 7.1: Vulnerability classes description

Vulnerability Class	Description	
A	URM with irregular units and poor wall connections	
B1	URM with irregular units and good wall connections	
B2	URM with regular units and poor wall connections	
C	Regular URM with good connection and RC frame structures without seismic design	
D	Reinforced masonry, wooden structures and RC frame structures designed with old seismic code requirements	
E	RC frame structures designed with modern seismic codes	
F	Steel structures and other similar ones with very low vulnerability	

As it could be expected, for a high vulnerable A and B concentration of structures, great damage is presented at Castelnuovo as it is evident in figure 7.20. A high number of buildings present also D1 damage; this is explained due to fact that other more robust vulnerability types different from A or B experienced more D1 damage after the event

It is of particular interest of this study to analize individually the damage level experimented to each vulnerability class, this is shown in figure 7.21 for A and B vulnerability classes. The figure was developed based on data presented by Ciavattone [CF 10] and corrected in order to take out the data of those buildings who presents already a very important initial damage state, like the ones that were already collapsed before the earthquake or the ones that were abandoned and present a very poor maintenance condition. In order to carry out this correction, the data presented in figure 7.18 and 7.19 was used. The damage presented for rubble stone (vulnerability type A) in Castelnuovo fits close to the upper limit of 70% proposed by Greene for seismic intensities of IX MSK [GA 09].

It is observed from the figure 7.21 that vulnerability type A presented a damage description which can be fit perfectly into a probability density function and corresponds closely to a solution obtained from fragility curves to some particular seismic action. On the other hand, for the B type there are two observed peaks. This probably due to the fact that B data includes B1 and B2 data together during the field campaign developed by the University of Florence as described in table 7.1. However B1 or B2 are categorized as B, each one may present important differences regarding susceptibilities to out-of-plane failure mode due to the existence or not of anchors. The initial condition of steel anchors is also not easily to be assessed; hence, inefficient tie connection (broken, rusted or fail due to stress) drives to heavy damage, meanwhile a good non failing connection to a smaller damage levels. Other explanation to the double peak could be a subjective description for D2 and D1 damage levels.

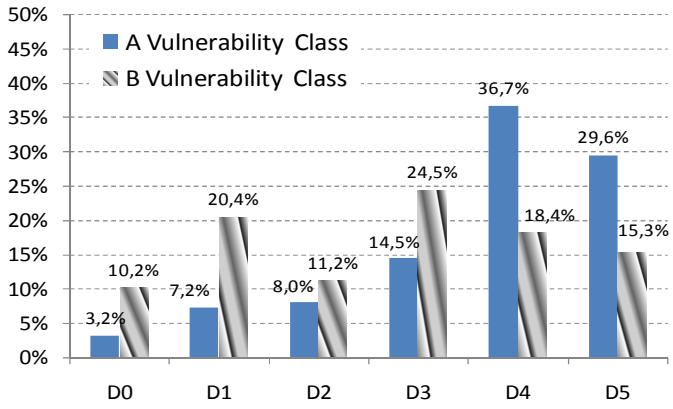

Figure 7.21: Correlation in between vulnerability class and damage levels

7.3 SAUMAC Application

Castelnuovo town was chosen from other earthquake affected towns for the application due to many aspects; the most important was the accessibility of detail information and the possibility of in-situ corroboration of data. Other important aspect was the big concentration of URM buildings, more than 90% of the total in the town and finally, the town housing characteristics are representative for Italy. This town presents characteristics frequent not only for central and south Italy, but also too many other small settlement constructions in other countries bordering the Mediterranean Sea.

After the information presented in sections 7.1 and 7.2, enough data is available for the application of the SAUMAC procedure and, later on, the comparison and corroboration with the actual damage founded at Castelnuovo. It is important to cite that the specific typologies cases were guided according to the ones that can be compared with existing data presented in section 7.2. This is of relevance for the validation of the methodology.

For the definition of the different building typologies in URM, the one mention in the study of Ciavattone, based in EMS-98, is very general. Because of this, more extensive typological formulations are presented in this study. Typologies are evidently related always to the vulnerability levels A and B of interest for rubble stone URM (figure 3.3). The formulation presented in this work is similar to the ones proposed by RISK-UE project and Rota [MT 03][RPM 08]. The typological classification proposed by Rota is actually based on the actual Italian building stock reality, meanwhile the ones of the RISK-UE project are more general.

Buildings at Castelnuovo presented wide rubble stone walls with variable thickness *t*, an estimate mean values of 60-90 cm at the base, and down to 35-70 cm at the upper storeys. The slab floor and roof conditions are described in figure 7.22 by the photo details A, B and C. In general A and B conditions are considered in this study as flexible boundary conditions, meanwhile C is a rigid one. C detail floors are heavy masonry vaults with rubble infill. Not serious damage was reported on these vaults. Their location in the lower level and other structural aspects such as buttress make them good seismic resistant. They are also considered rigid because their thickness provides them with a sufficient stiff condition, and for the good connection with the thick base level walls.

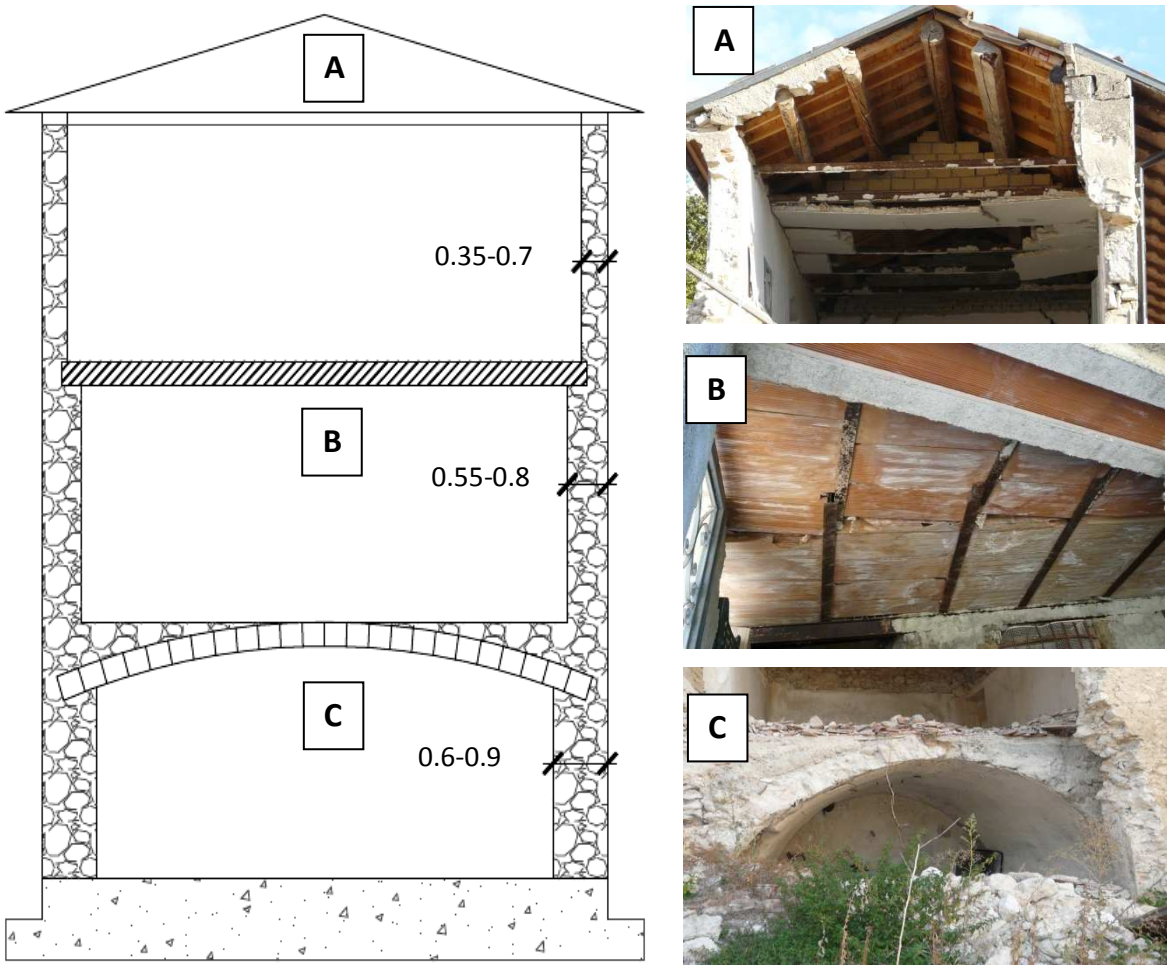

Figure 7.22: Typical 3 storeys building configuration for rubble stone URM

Table 7.2: Weighting factors according to building population and the 12 building types

Vulnerability Class		Irregular Layout		Regular Layout	
		1-2 storeys	3-4 storeys	1-2 storeys	3-4 storeys
Influence Weight (%)	*A*	15.4	28.1	20.0	36.5
	B1 (94%)	14.5	26.4	18.8	34.3
	B2 (6%)	0.9	1.7	1.2	2.2

In figure 7.22 a representative 3 storeys URM house is shown. This is considered the most repetitive construction type in the village and present similar characteristics to more than the 30% of all buildings in Castelnuovo. They are regular 3- 4 storeys building as described in table 7.2. The building schematic of figure 7.22 is used to develop a typological fragility curves, and also to give an example for qualitative use of the proposed methodology for individual buildings.

Based on the building of figure 7.22, 12 different buildings typologies are defined for URM regarding three different aspects: the number of stories, the building layout and finally the vulnerability group as explained in table 7.1. Regarding the building storeys, a separation is developed according to two groups, those with 1- 2 storeys, and those with 3-4 storeys. For the building layout, this is related to the structural irregularities. Since there are already some statistics develop to describe different building structural units, section 7.2, this data was used as a criteria to separate buildings as irregular for the ones described as articulated group, and regular for those described as single and rectangular group structural units.

There is not damage data specifically available for each of the proposed building typologies but just for those ones categorized as A and B types. A weighting table was developed according the expected amount of buildings that felt into each category as shown in table 7.2. The weighting parameters are applied to the obtained fragilities to be compared with available damage field data.

Regarding the failure mechanism, as commented in section 4.5, two different distinctions are made concerning the in-plane and the out-of-plane mechanisms. This is represented schematically in figure 7.23 for the representative 2 and 3 storeys buildings at Castelnuovo, as they will be used later in the application case. Following the formulation of figure 7.22, the first story slab condition is rigid and all the others are assumed as flexible ones.

The deform shape for the failing mode depends on the particular assumed boundary conditions of the structure. Boundary condition formulations are of importance especially for the out-of-plane failure modes. Cantilever failure modes are observed in figure 7.22. According to the figure, in a 3 storeys building, a join multi-storey failure in the out-of-plane is assumed.

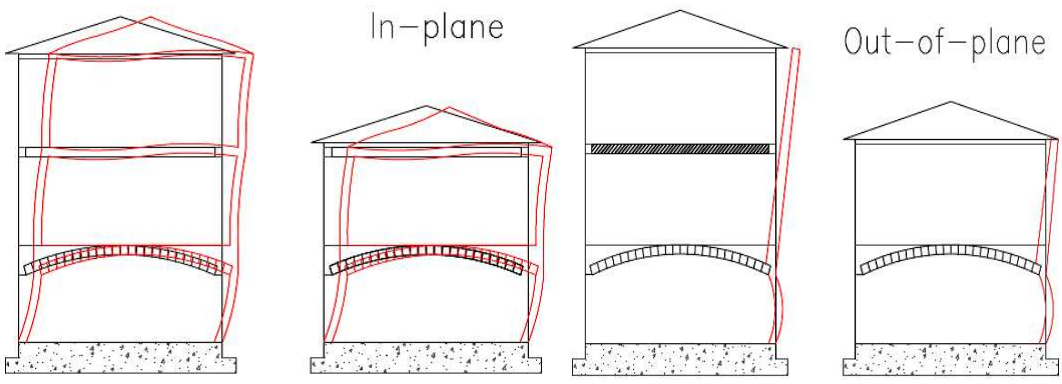

Figure 7.23: Out-of-plane and in-plane failure mechanisms for 3 and 2 storeys buildings similar to figure 7.22

7.3.1 Defined building typologies

The SAUMAC methodology is applied for two building cases: for building typology groups (12 buildings sets), and a particular individual house assessment case. Typological group cases are explained in this section and also will provide in advance the results of the individual house case since one of these 12 cases represents the chosen single case building scenario.

In other to obtain the structural parameters to solve $G(X)$, a MATLAB code is used for determining the constants as it is explained in section 6 in terms of the SHM (Appendix C). The input parameters used for the process of geometrical house generation are resumed in the table 7.3. They are estimated based on visual inspection of the structures in Castelnuovo and the results of the field survey develop by the University of Florence. A heavy slab is considered for the lower level and was calculated taking into account a mean 0.4 m vault thickness and a mean material density of 16 kN/m^3. For the inter-story flexible slab condition, the weight may vary according to the construction type as there are many possibilities present in the town as it is shown in figure 7.13, section 7.2. According to Boscotrecase [BP 09], the values of the weight per square meter may vary from 1.65 kPa in a wooden slab to 3.4 kPa on slabs with steel beans with masonry vaults; a mean value of 2.5 kPa was chosen. For the roof condition, light weight structures are founded to be with similar weight characteristics to a wooden slab but with big variation according to the covering material, a value of 2.0 kPa is used as the mean value for the roof. The average life load coefficients are Q_{kav} = 1.5 kPa and Q_{kt}, = 0.5 (v = 10%).

For data specified in table 7.3, the figures 7.24 and 7.25 are obtained for 3 and 2 storeys edifications, with a total of 2.5x10^4 simulated buildings. The ρ is approximated to 0.12 for X and 0.135 for Y direction for the first storey and considering a house with 7 meters of façade (X direction) and 13 meters of depth computed from equation 6.24. This is an estimate for the common structure in figure 7.22 and corresponds to a conservative mean value since values up to 0.20 are observed.

Table 7.3: Input parameters for the SHM for rubble stone houses

Basic Variables	3 stories building	2 stories building
	min / mid / max	min / mid / max
Height of first story H_{PB} (m)	2.6 / 3.0 / 3.4	2.6 / 3.0 / 3.4
Height of second story H_{P1} (m)	2.4 / 2.6 / 3.0	2.4 / 2.6 / 3.0
Height of third story H_{P2} (m)	2.0 / 2.4 / 2.6	---
Facade length X (m)	4 / 7 / 12	4 / 7 / 12
Deep length Y (m)	4 / 11 / 16	4 / 11 / 16
Thickness of the facade wall e (m)	0.45 / 0.75 / 0.9	0.45 / 0.6 / 0.8
Thickness of internal wall e_I (m)	0.3 / 0.6	0.3 / 0.6
Slab weight 1st Story P_{PB} (kPa)*	3.0 / 5.0 / 7.0	4.0 / 6.0 / 8.0
Slab weight 2nd Story P_{P2} (kPa)*	1.5 / 2.5 / 4.0	1.0 / 1.75 / 2.5
Slab weight 3rd Story P_{P3} (kPa)*	1.0 / 2.0 / 2.5	---
Density range γ (kN/m^3)	16 / 19 / 21	16 / 19 / 21
Void dimension v_O (m)t,v	0.4 / 1.2 / 2.0	0.4 / 1.2 / 2.0
Inside void factor in x f_{ix}	1.1 / 2.0	1.1 / 2.0
External void factor in x f_{ex}	1.05 / 2.5	1.05 / 2.5
Inside void factor in y f_{iy}	1.1 / 2.0	1.1 / 2.0
External void factor in y f_{ey}	1.01 / 1.5	1.05 / 1.5

**slab/ roof load, t window or door (length dimension), v height in between 30 and 75% of total floor height*

For the third and second storeys, ρ values are reduced, this came from a decrease of the wall thickness. The values of ρ chosen were 0.08 for a tree storeys building and 0.1 for a two storey buildings.

The assumed general inputs to be used in the SAUMAC methodology are summarized in table 7.4. In the table, the obtained A_M parameter calculation is already included and is found from figures 7.24 and 7.25 (computed from MATLAB code, Appendix C). Table 7.4 also includes parameters related to the different failure mechanisms that will be used later on for estimating the characteristic resistance of our building. The h_P/l_{Pmax} and h_P/l_{Pmin} ratios are estimated according to local inspection of the houses, the term H_S/t is obtain directly from the mean values of the storey's height and the mean wall thickness, where the 1st storey thickness is decreased according to the top storey reduction factor for rubble stone masonry as explained in the SHM (down to 60% for 3 storeys and for 2 storeys in this case).

Despite the information of figures 7.24 and 7.25, the A_M mean and σ values can be directly approximated from simplified graphs in section 6. At this moment, the information based on the visual characterization of the house typology is finish; the information here is valid for rubble stone buildings related with vulnerability classes A and B1.

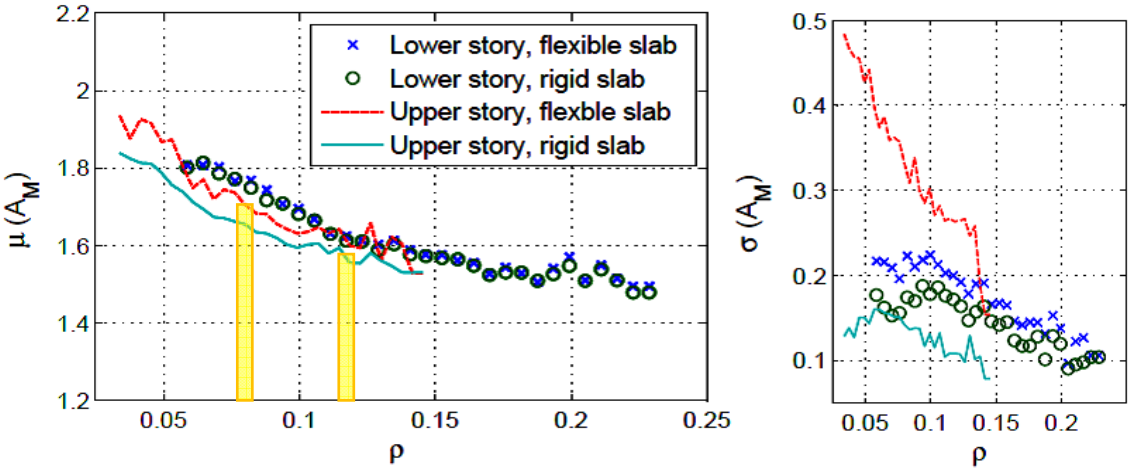

Figure 7.24: A_M (m_T/m_N) values for 3 storeys house (used ρ values are marked)

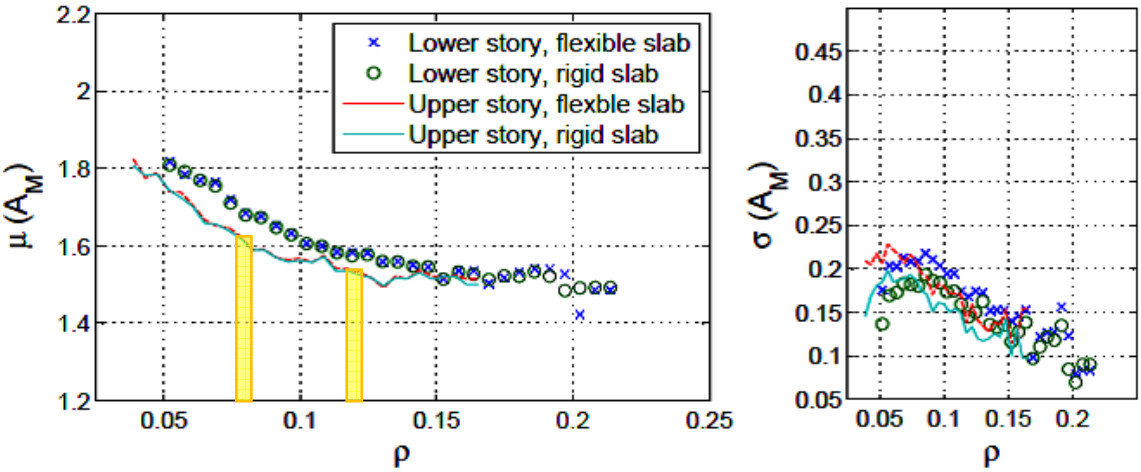

Figure 7.25: A_M (m_T/m_N) values for 2 storeys house (used ρ values are marked)

Table 7.4: Base visual parameters and A_M for A and B1 vulnerability classes

3 Storeys house		Out-of-plane	In-plane			
Floor	Slab	h_P/t	ρ	$h_P/l_{P\max}$	$h_P/l_{P\min}$	Obtained m_T/m_N
1st	Rigid	Not relevant	0.12	0.75	1.0	1.60 ± 0.15
2nd	Flexible	12	Not relevant			
3rd	Flexible		0.08	0.75	1	1.7 ± 0.35

2 Storeys house		Out-of-plane	In-plane			
Floor	Slab	h_P/t	ρ	$h_P/l_{P\max}$	$h_P/l_{P\min}$	Obtained m_T/m_N
1st	Rigid	Not relevant	0.11	0.75	1.0	1.55 ± 0.15
2nd	Flexible	6	0.08	0.75	1	1.6 ± 0.2

Table 7.5: Base visual parameters and A_M for B2 vulnerability class

3 Storeys house		Out-of-plane	In-plane			
Floor	Slab	h_P/t	ρ	$h_P/l_{P\max}$	$h_P/l_{P\min}$	Obtained m_T/m_N
2nd	Flexible	14	Not relevant			
3rd	Flexible		0.08	0.75	1	1.7 ± 0.5

2 Storeys house		Out-of-plane	In-plane			
Floor	Slab	h_P/t	ρ	$h_P/l_{P\max}$	$h_P/l_{P\min}$	Obtained m_T/m_N
2nd	Flexible	9	0.10	0.75	1	1.6 ± 0.4

For B2 the values are obtained directly from graphs in section 6 and are summarized in table 7.5. In this table only the upper levels are presented since the base level remains in rubble stone. In tables 7.4 and 7.5, those aspects considered with no critical failure mechanisms possibilities are labeled as “Not relevant”; hence, there are only 3 computed failing conditions: out-of-plane for the upper levels, in-plane for the ground level and in-plane for the upper level.

In case of the spandrels, it is expected sufficient capacity conditions in the base level to transfer lateral loading on piers, meanwhile for the upper levels they are considered geometrically not sufficient if no additional supporting elements such as iron chains are used (B1 vulnerability class or additional stiffening elements as balconies). Observed damage of spandrels in Castelnuovo supports this assumption (figure 7.26).

Figure 7.26: Limited Damage observed on spandrels in Castelnuovo at the low levels of the houses

After the determination of the visual parameters, the solution process established in section 6 is going to be followed to obtain the structural fragilities. First of all, an initial qualification of the material properties must be done in order to develop the *V/N* curves for rocking, diagonal tension shear and M-C shear wall failing conditions. There are three different URM material classes: rubble stone, hollow brick and hollow concrete masons.

Rubble stone masonry properties are difficult to establish. Probably the most complete available methodology to evaluate its properties is to use the Index of Masonry Quality IQM (Indice di Qualità Muraria) as proposed by Borri [BdD 09]. The masonry quality index is able to take into account many wall physical characteristics and express them in terms of an index value. This index value can be correlated to obtain parameters as the shear resistance τ_o and the masonry compression f_m.

According to the IQM methodology, an index value of 1.4 for rubble stone was obtained; this is correlated to obtain the material properties as presented in table 7.6. Other shear resistance values are founded after Vetturini [VCMB 07] and D'Ayala [DS 02]. In case of the normative values, the actual Italian normative specifies a reference shear value τ_o in between 20 and 32 kPa. In the context of this work, when a range of max-min values is defined in a normative or any other bibliography, it is assumed to be the range in between ±2σ of a Gaussian PDF and minimum/maximum values for triangular PDFs. In table 7.6 it is observed that the IQM produces resistance results very similar to the ones proposed by the NTC (table 4.5).

Table 7.6: Material properties for rubble stone masonry according to different sources

Resistance Parameter		Italy Norm [NTC 09]	Vetturini 2007	D'Ayala 2002	IQM (IQM=1.5)
f_m *MPa*	min/-2σ	1.0			
	med/μ		2.0	4.0	1.8
	max/+2σ	1.8			
τ_o *kPa*	min/-2σ	20	50		26
	med/μ				
	max/+2σ	32	70		41
E *MPa*	min/-2σ	690			710
	med/μ				
	max/+2σ	1050			1050

Table 7.7: Material properties for concrete and clay hollow masons

Resistance Parameter		Italy Norm [NTC 09] concrete blocks	Italy Norm [NTC 09] hollow clay	NZ Norm [NZSEE 06]	IQM (IQM=4.5)
f_m *MPa*	min/-2σ	3.0	3.0	4.1	
	med/μ				3.5
	max/+2σ	4.4	4.0	6.1	
τ_o *kPa*	min/-2σ	180	300	217	500
	med/μ				
	max/+2σ	400	400	434	750
E *MPa*	min/-2σ	2400	3600		1200
	med/μ			7000	
	max/+2σ	35200	5400		1700

**Obtain for stiff brick properties and after table 4.3 for M_4 mortar and equation 4.15 (b=1.5, σ_N=0, α_V=1)*

In a similar way, values are obtained for hollow concrete and clay units as it can be observed in table 7.7. There, the values mention by the New Zealand norm are also shown after some modifications taking into account table 4.3 and equation 4.15 in section 4.

Now that material properties are overviewed, the values obtained from the NTC-2009 are preferred. The SAUMAC methodology requires finding the *V/N* (R_E) relations for our materials to solve the reliability problem. The specific solution is obtained directly by the use of the MATLAB code (Appendix C). Computing input parameters like the ψ' value for the flexural normalized resistance is also required to estimate the flexural capacity. According to figure 6.9 in section 6, a value of $\psi' = 1$ and $\psi' = 0.75$ at the base storeys are founded for 3 and 2 storeys housing. Results for upper level, lower levels and different slab conditions are summarized in figures 7.27 and 7.28.

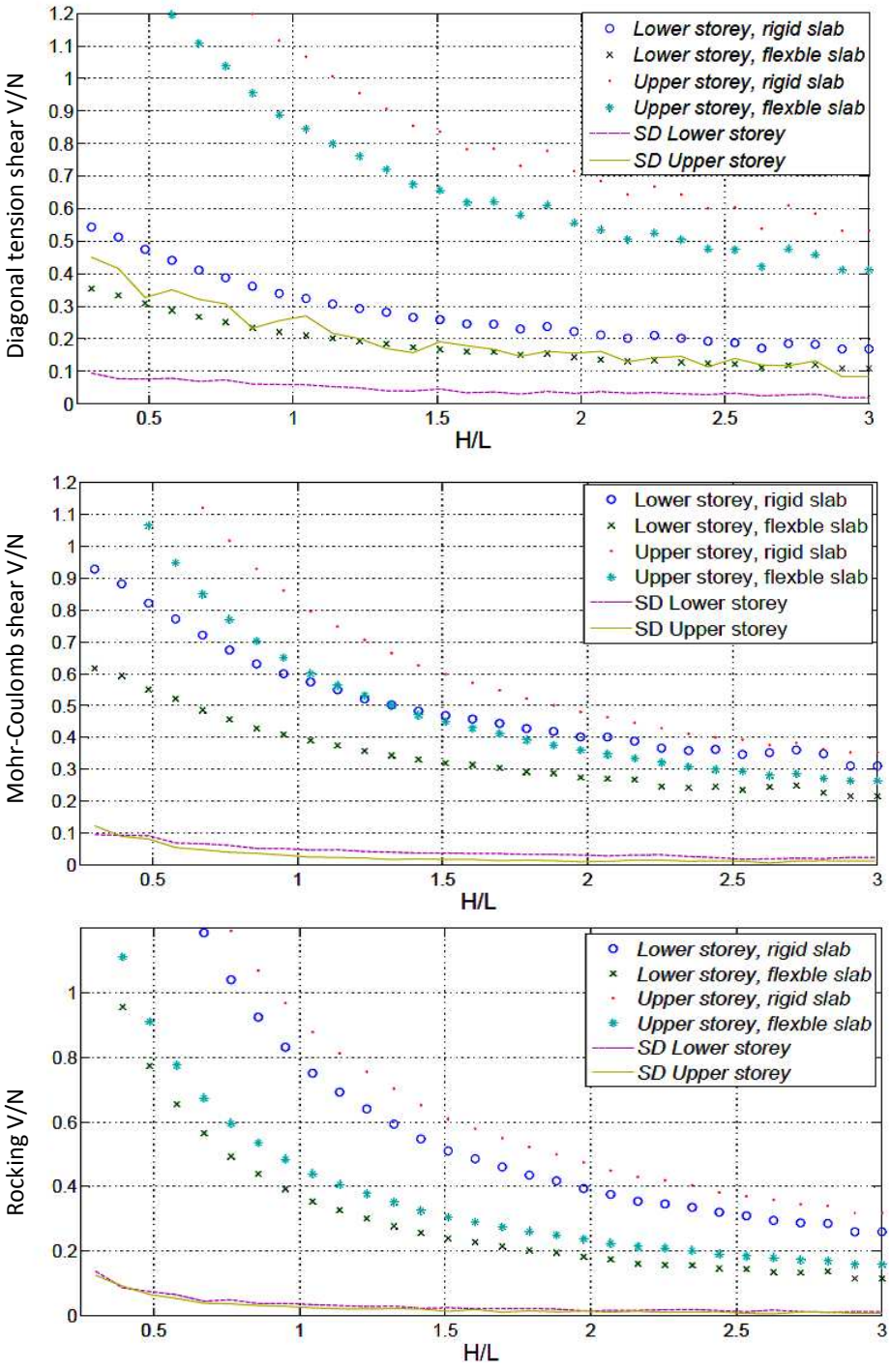

Figure 7.27: Flexural, diagonal and sliding shear for a 3 storeys ($\psi' = 1$ at base level, $\psi' = 1$ at top level)

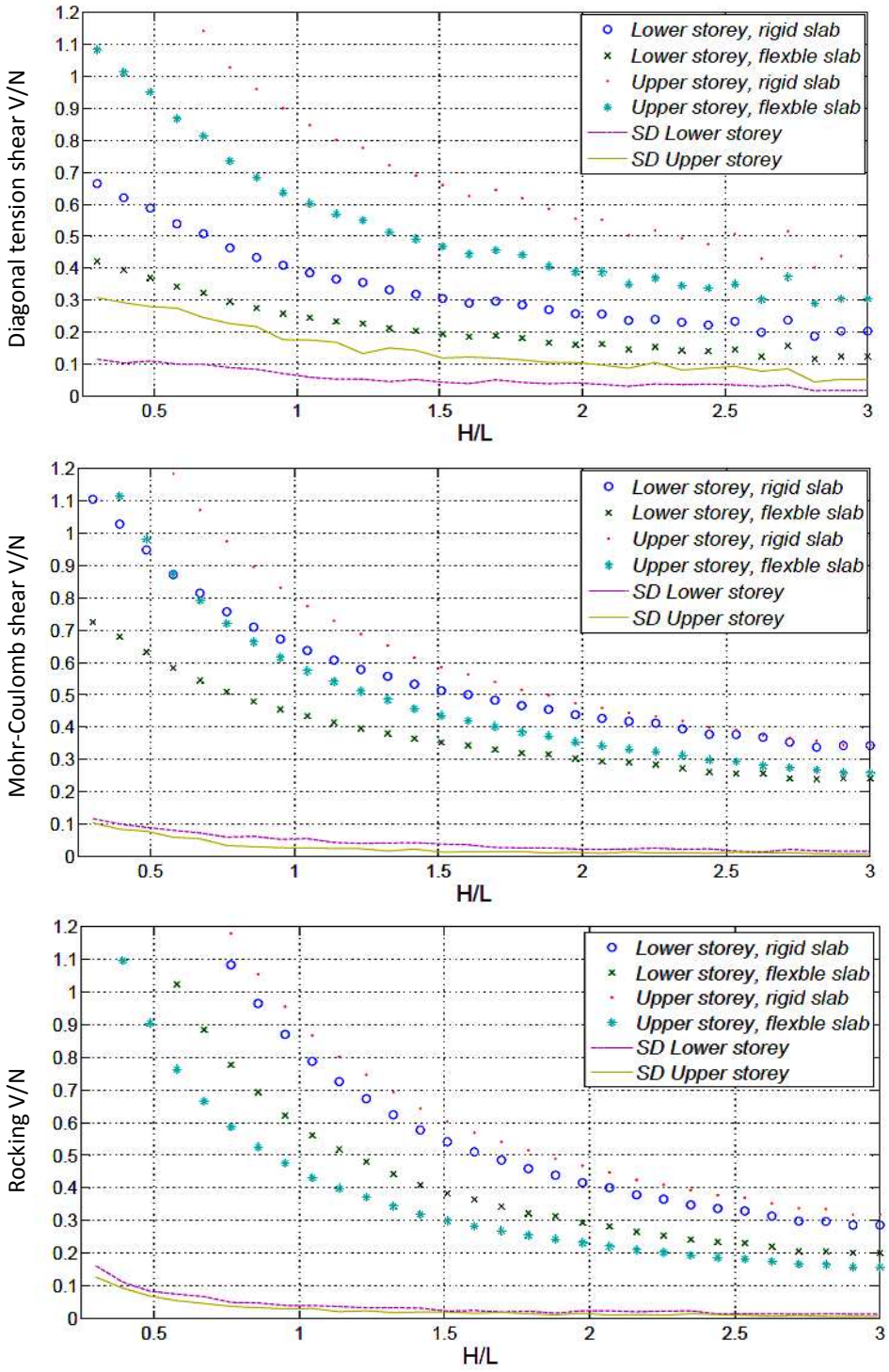

Figure 7.28: Flexural, diagonal and sliding shear for a 2 storeys (ψ' = 0.75 at base level, ψ' = 1 at top level)

For developing the graphs, basically the information relevant to our typology structure is the one regarding the base and top levels since these are the ones presenting the toughest loading or minimum resistance condition if storeys characteristics are continuous for all storeys. Middle story data is not presented in figures 7.27 and 7.28.

The figures 7.29 and 7.30 summarized all the relevant information from the figures 7.27 and 7.28. The data is presented with fitting curves obtained from power/exponential fitting functions. The information of relevance is the one with boundary conditions of flexible diaphragm for top floors and equal to rigid slab for base floor according to table 7.4.

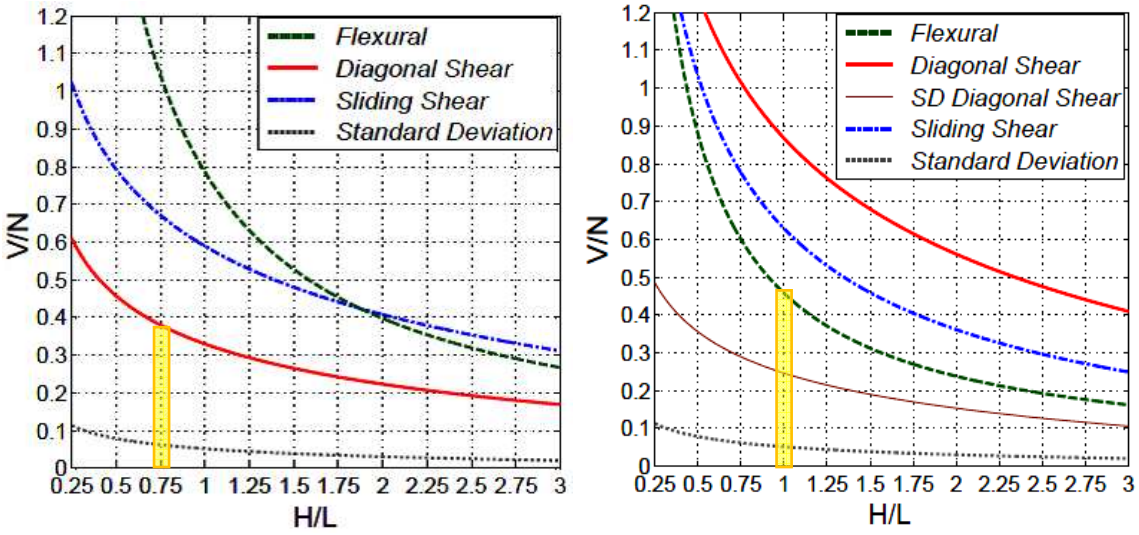

a) b)

Figure 7.29: V/N ratios for the base (a) and upper (b) storeys for 3 storeys building

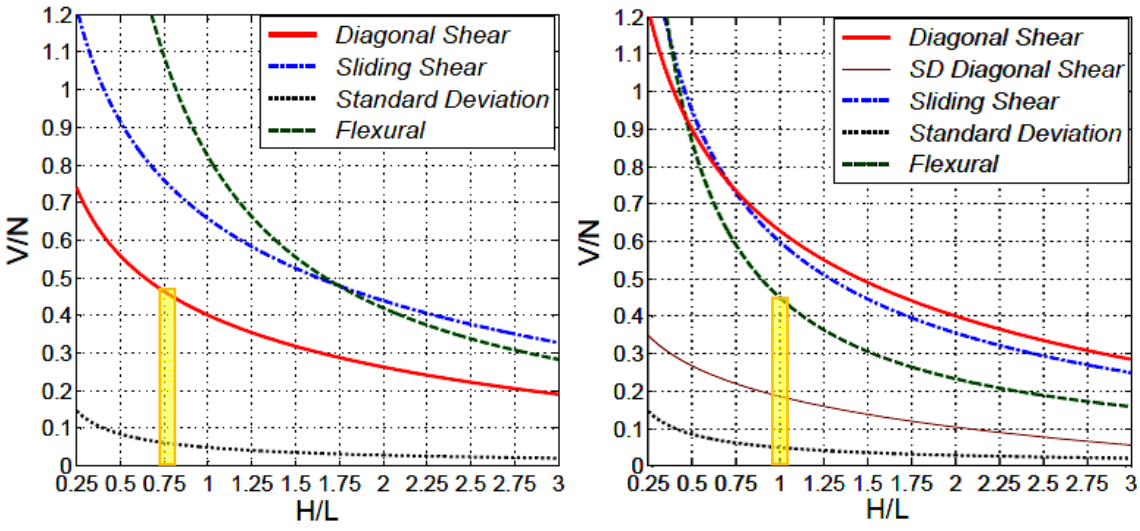

a) b)

Figure 7.30: V/N ratios for the base (a) and upper (b) storeys for 2 storeys building

In figures 7.29 and 7.30 the relevant element geometry values of H/L (h_P/l_P), according to the visual inspection that were reported in tables 7.4 and 7.5, are marked as they represent the base value that will be used for the estimation of R_E in the process to obtain the final I_R value at each storey. It is observed from the figures that the dominant in-plane failing mode for the base storey is clearly the diagonal shear, meanwhile for the upper story the dominant is the rocking one. This is the normal expected situation observed in actual earthquake damage in-situ. Since the importance of the B2 typology has not a strong weight on the final result, the R_E parameters are computed directly from figures 6.16a and 6.16c.

The evidence after the damage survey detailed that much of the damage presented in Castelnuovo is related to the out of plane failure modes as explained by Ciavattone [CF 10]. The out-of-plane triggered modes are consequence of poor connections in between floors and lateral walls. This condition can be founded in many old URM constructions. Also, the out-of-plane fail is usually initiated for other construction architectural aspects such as parapets or heavy fences. Following the SAUMAC procedure, figures 7.31 and 7.32 are showing the normalized shear factor for rubble stone walls ($\gamma \approx 18$ kN/m^3) and lighter hollow clay/concrete units ($\gamma \approx 14$ kN/m^3).

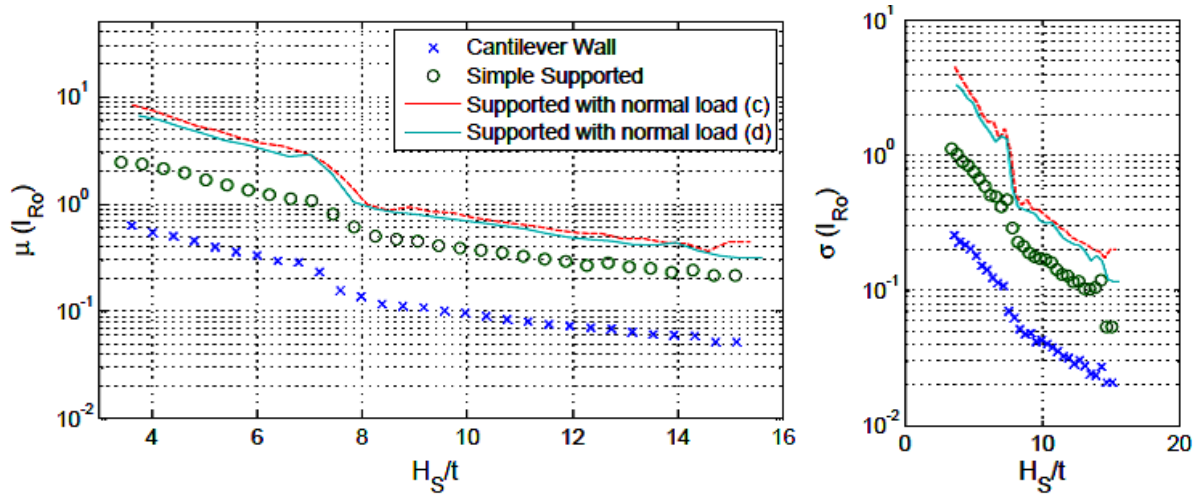

Figure 7.31: Out-of-plain normalized shear capacity for rubble stone ($\gamma \approx 18$ kN/m^3)

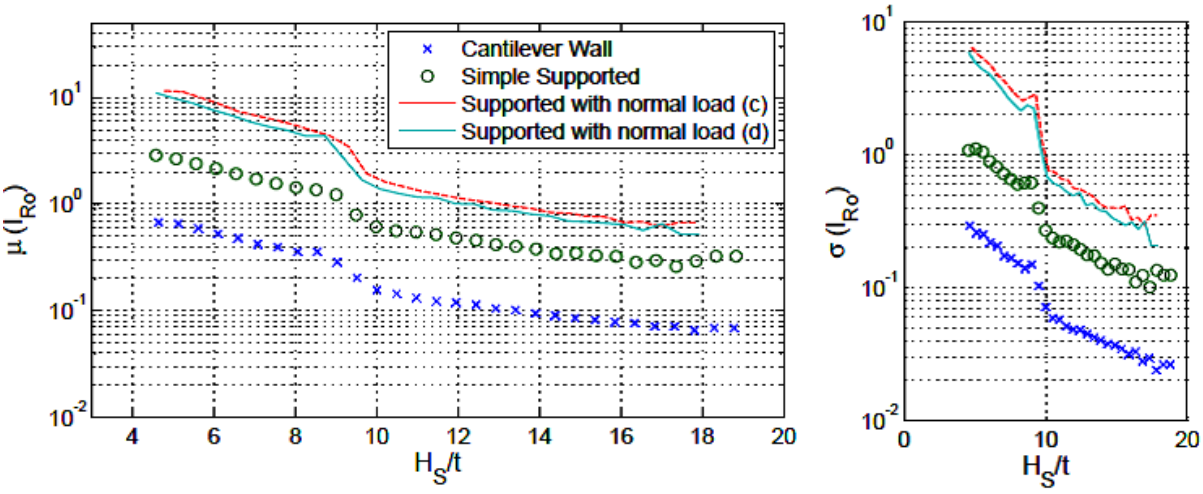

Figure 7.32: Out-of-plain normalized shear capacity for hollow clay/concrete units ($\gamma \approx 14$ kN/m^3)

The results obtained from figures 7.29 to 7.32 are summarized in table 7.8 for the three storey building of figure 7.22, and in table 7.9 for a two storey building similar again to the one in figure 7.22 but following the parameters for two storeys buildings presented in table 7.3. In tables 7.8 and 7.9 a value of $h_P/l_P = 1$ is used for the top storey and similarly $h_P/l_P = 0.75$ for the base storey for all URM studied vulnerability types. With this, practically all the basic information to obtain the building fragilities and the final risk is prepared.

Table 7.8: Structural shear capacities per storey (3 storeys building)

Vulnerability Class		h_P/l_P or h_P/t	V/N	σ
A	Out-of plane	12	0.07	0.02
	In-plane (base Level)	0.75	0.38	0.07
	In-plane (upper Level)	1	0.45	0.04
B1	Out-of plane	7	1	0.3
	In-plane (base Level)	0.75	0.38	0.07
	In-plane (upper Level)	1	0.45	0.04
B2	Out-of plane	14	0.08	0.025
	In-plane (base Level)	0.75	0.65	0.15
	In-plane (upper Level)	1	0.45	0.04

Table 7.9: Structural shear capacities per storey (2 storeys building)

Vulnerability Class		h_P/l_P or h_P/t	V/N	σ
A	Out-of plane	7	0.25	0.07
	In-plane (base Level)	0.75	0.47	0.07
	In-plane (upper Level)	1	0.45	0.04
B1	Out-of plane	7	10	0.4
	In-plane (base Level)	0.75	0.47	0.07
	In-plane (upper Level)	1	0.45	0.04
B2	Out-of plane	9	0.25	0.05
	In-plane (base Level)	0.75	0.75	0.25
	In-plane (upper Level)	1	0.30	0.04

7.3.2 Computing structural vulnerability and risk

Now that the values basic values of R_E and A_M per storey have been found for each storey, the fragility curves for the 12 building types described in table 7.2 can be founded. All the information used for solving $G(X)$ for typology types A, B1 and B2 is summarized in tables 7.10, 7.11 and 7.12. Tables include the information concerning typical values of F_W and the proposed value of F_{EC} (according to figure 3.15) for the calculation of fragility curves corresponding to the life safety LS. The failure mechanism, shadowed in the tables, corresponds to the dominant fragility curve of the system. Fragilities should be inspected easily by using the TFrag.m function developed in MATLAB for finding the dominant one. Results of the TFrag.m function are similar to those observed in figure 6.21.

In tables, the value of the F_S is also presented. The results of F_S are those corresponding to λ=0.85 and q=1.75 for 3 storey building and q=1.75 for 2 storeys. The value of q was obtained from table 4.7.

Once the dominant fragility for each of the 4 types of buildings presenting vulnerability A are founded, results are plotted in figure 7.33. Results in figure 7.33 already include the action of both failure mechanisms (in-plane, out-of-plane) obtained from equation 5.10 and the final weighted value for vulnerability A. The weighting percentages are those presented in table 7.2.

Table 7.10: Summary table for generating fragilities for vulnerability type A and LSLS

			Slab/spandrel	R_E	F_W	F_{EC}	I_R *or* I_{Ro}*	A_M	F_S
Irregular Layout	1-2 floors	Out-of plane	---	0.25 ± 0.07		---	0.25 ± 0.07	---	1
		In-plane (BL)	rigid/good	0.47 ± 0.07	0.9	0.66	0.28 ± 0.04	1.55 ± 0.15	1.4
		In-plane (TL)	flex/poor	0.45 ± 0.04	1	1	0.34 ± 0.03	1.6 ± 0.2	1.4
	3-4 floors	Out-of plane	---	0.07 ± 0.01		---	0.07 ± 0.01	---	1
		In-plane (BL)	rigid/good	0.38 ± 0.07	0.9	0.66	0.23 ± 0.04	1.60 ± 0.15	1.2
		In-plane (TL)	flex/poor	0.45 ± 0.04	1	1	0.3 ± 0.03	1.7 ± 0.35	1.2
Regular Layout	1-2 floors	Out-of plane	---	0.25 ± 0.07		---	0.25 ± 0.07	---	1
		In-plane (BL)	rigid/good	0.47 ± 0.07	0.9	0.8	0.34 ± 0.04	1.55 ± 0.15	1.4
		In-plane (TL)	flex/poor	0.45 ± 0.04	1	1	0.34 ± 0.03	1.6 ± 0.2	1.4
	3-4 floors	Out-of plane	---	0.07 ± 0.01		---	0.07 ± 0.01	---	1
		In-plane (BL)	rigid/good	0.38 ± 0.07	0.9	0.8	0.28 ± 0.04	1.60 ± 0.15	1.2
		In-plane (TL)	flex/poor	0.45 ± 0.04	1	1	0.3 ± 0.03	1.7 ± 0.35	1.2

**Include already reduction by the storey shear factor (equal to 0.75 for 2 storeys and 0.66 for 3 storeys top floor)*

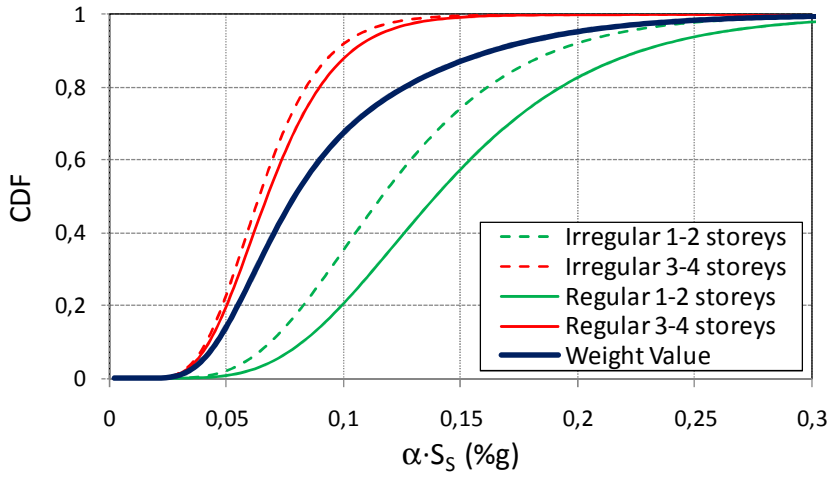

Figure 7.33: Vulnerability A building typologies and weighted value

Figures 7.34 and 7.35 present the results for vulnerabilities B1 and B2, they are obtained similarly to the ones of vulnerability A. Results are based in data from tables 7.11 and 7.12.

Table 7.11: Summary table for generating fragilities for vulnerability type B1 and LSLS

			Slab/spandrel	R_E	F_W	F_{EC}	I_R *or* I_{Ro}*	A_M	F_S
Irregular Layout	1-2 floors	Out-of plane	---	10 ± 0.4		---	10 ± 0.4	---	0.5
		In-plane (BL)	rigid/good	0.47 ± 0.07	0.9	0.66	0.28 ± 0.04	1.55 ± 0.15	1.4
		In-plane (TL)	flex/poor	0.45 ± 0.04	1	1	0.34 ± 0.03	1.6 ± 0.2	1.4
	3-4 floors	Out-of plane	---	1 ± 0.3		---	1 ± 0.3	---	0.5
		In-plane (BL)	rigid/good	0.38 ± 0.07	0.9	0.66	0.23 ± 0.04	1.60 ± 0.15	1.2
		In-plane (TL)	flex/poor	0.45 ± 0.04	1	1	0.3 ± 0.03	1.7 ± 0.35	1.2
Regular Layout	1-2 floors	Out-of plane	---	10 ± 0.4		---	10 ± 0.4	---	0.5
		In-plane (BL)	rigid/good	0.47 ± 0.07	0.9	0.8	0.34 ± 0.04	1.55 ± 0.15	1.4
		In-plane (TL)	flex/poor	0.45 ± 0.04	1	1	0.34 ± 0.03	1.6 ± 0.2	1.4
	3-4 floors	Out-of plane	---	1 ± 0.3		---	1 ± 0.3	---	0.5
		In-plane (BL)	rigid/good	0.38 ± 0.07	0.9	0.8	0.28 ± 0.04	1.60 ± 0.15	1.2
		In-plane (TL)	flex/poor	0.45 ± 0.04	1	1	0.3 ± 0.03	1.7 ± 0.35	1.2

**Include already reduction by the storey shear factor (equal to 0.75 for 2 storeys and 0.66 for 3 storeys top floor.*

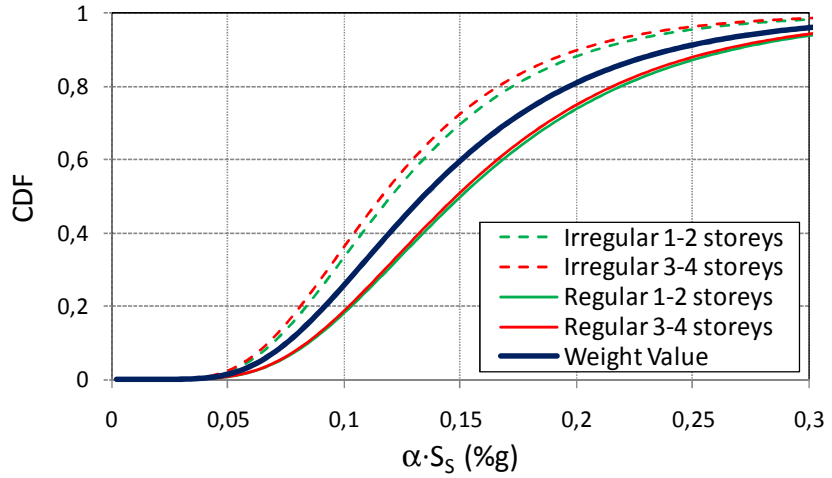

Figure 7.34: Vulnerability B1 building typologies and weighted value

Table 7.12: Summary table for generating fragilities for vulnerability type B2 and LSLS

			Slab/spandrel	R_E	F_W	F_{EC}	I_R or I_{Ro}*	A_M	F_S
Irregular Layout	1-2 floors	Out-of plane	---	0.25 ± 0.07		---	0.25 ± 0.07	---	1
		In-plane (BL)	rigid/good	0.75 ± 0.07	0.9	0.66	0.45 ± 0.04	1.55 ± 0.15	1.4
		In-plane (TL)	flex/poor	0.45 ± 0.04	1	1	0.34 ± 0.03	1.6 ± 0.2	1.4
	3-4 floors	Out-of plane	---	0.08 ± 0.01		---	0.08 ± 0.01	---	1
		In-plane (BL)	rigid/good	0.65 ± 0.07	0.9	0.66	0.39 ± 0.04	1.60 ± 0.15	1.4
		In-plane (TL)	flex/poor	0.45 ± 0.04	1	1	0.3 ± 0.03	1.7 ± 0.35	1.4
Regular Layout	1-2 floors	Out-of plane	---	0.25 ± 0.07		---	0.25 ± 0.07	---	1
		In-plane (BL)	rigid/good	0.75 ± 0.07	0.9	0.8	0.54 ± 0.04	1.55 ± 0.15	1.4
		In-plane (TL)	flex/poor	0.45 ± 0.04	1	1	0.34 ± 0.03	1.6 ± 0.2	1.4
	3-4 floors	Out-of plane	---	0.08 ± 0.01		---	0.08 ± 0.01	---	1
		In-plane (BL)	rigid/good	0.65 ± 0.07	0.9	0.8	0.47 ± 0.04	1.60 ± 0.15	1.4
		In-plane (TL)	flex/poor	0.45 ± 0.04	1	1	0.3 ± 0.03	1.7 ± 0.35	1.4

**Include already reduction by the storey shear factor (equal to 0.75 for 2 storeys and 0.66 for 3 storeys top floor.*

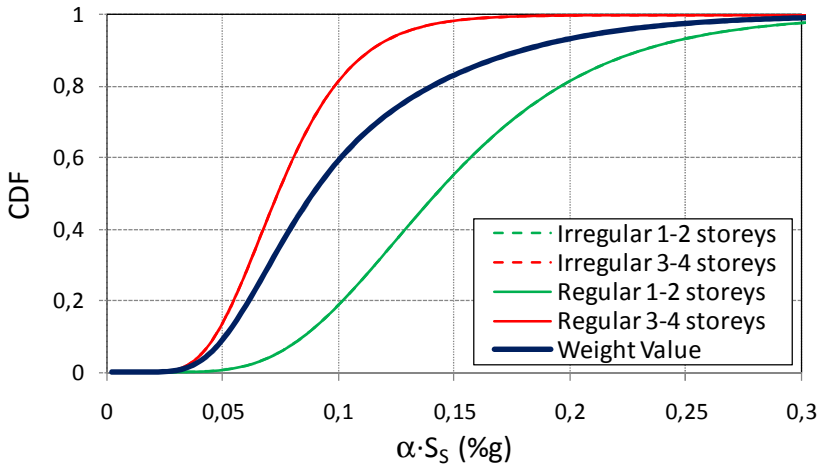

Figure 7.35: Vulnerability B2 building typologies and weighted value

In figure 7.36, finally all the resulting fragilities for the 3 analyzed vulnerabilities are shown.

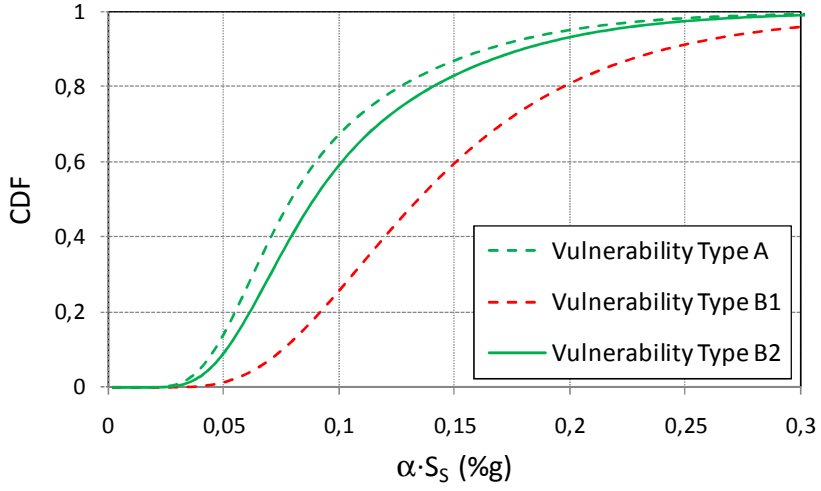

Figure 7.36: Fragility of vulnerability types at Castelnuovo town

From figures 7.33 and 7.35, it is evident a great difference between the obtained results for two storeys and 3 storeys houses groups, where the out of plane failure mode is of importance. In case of the 3 storeys building, a multistory failure in the out of plane was allowed, as explained before in figure 7.23. Big ratios of H_S/t are obtained because of this assumption for 3 storeys and much smaller values for two storey structures (tables 7.4 and 7.5). The difference in case of diverse building storeys results is not relevant when the out-of-plane aspect takes a second roll. This is clearly observed in figure 7.34 for vulnerability B1. In B1, the important aspect is more related with the possible eccentricities effect on buildings, approximated initially by the structure's location and external shape (computed from figure 3.15).

Also it can be clearly observed from the figure 7.36 that the variation of materials is not of the greatest importance when the out of plane mechanism is the relevant aspect. Probably B2 vulnerability group should be included into the vulnerability A set (description from EMS-98 figure 3.3) and not into the B group.

Finally, annual risk values can be computed following equation 5.13, the weighted fragilities of figure 7.36 and the hazard curve of figure 3.8. A plot of the risk variation according to the reference PGA values is observed in figure 7.37 for vulnerabilities A, B1 and B2.

It is evident from the figure that all URM structural groups evaluated presented a high risk condition (falling in the red shadowed area). Vulnerability type B can be described as with a moderate risk just below 0.1 αS_S; meanwhile the local seismic norm for Castelnuovo requests for a much bigger PGA referenc value as it can be determinated from figure 3.12. This high vulnerability is evidently one of the most important reasons for the heavy damage presented at Castelnuovo town.

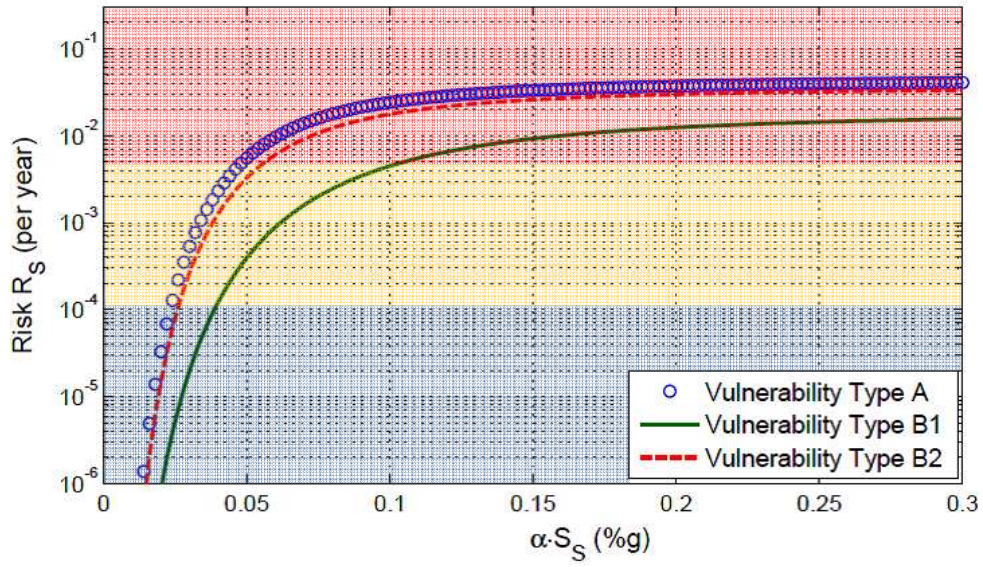

Figure 7.37: Risk calculation for evaluated fragilities

7.4 Reviewing Results

At this point, results were finally obtained from the SAUMAC method for the typical URM typologies described by the research group at the University of Florence (table 7.1). Additionally to this proposal, each vulnerability type had been subdivided into 4 groups according the number of storeys, and irregularity of the structure layout according to the building description in Castelnuovo (section 7.2). This had been made to take into account common different building configurations

possibly founded for the vulnerability types (A, B). A similar typological classification to the proposed ones has been done by other researches for buildings in Italy (Rota 2007).

The main goal of this section if to evaluate the results obtained. This have been made from three different points of view:

- *Evaluation of results from the observed damage at Castelnuovo town.*
- *Evaluation of results from comparison of other investigation results.*
- *Evaluation of results from the target behavior of structures in seismic zones.*

These three aspects are commented in detail from sections 7.4.1 to 7.4.3.

7.4.1 Comparison with survey damage

A detailed review of the damage observed at Castelnuovo town after L'Aquila 2009 earthquake was presented in section 7.2 based on a field work develop by the University of Florence in 2009-2010, resumed in the thesis of Ciavattone [CF 10] and ensured by two field surveys performed by the author of this study. The information provided is sufficient to complete a comparison between the obtained fragilities and the in-situ observed damage.

It is evident that the URM structures under analysis presented extremely poor behavior to seismic actions as it can be observed from the destroyed town picture in figure 7.1. The town was partially destroyed with more than 60% of the total building population in the town center presenting damage levels of D4 and D5 which correspond approximately to the complete damage condition exposed in other methodologies like HAZUS [TR 08].

The developed fragility curves presented in section 7.3.2 where developed for the life safety limit state, to evaluate this limit state is the main goal of this work and is still the focus of most actual normative. The developed curve fits approximate to the D3 curve of the EMS-98 methodology and the extensive damage curves presented by HAZUS or Vision 2000 [SEAOC-95]. Taking into account this, all the building population having damage levels of D3 or more over passed the limit according to the life safety LS criteria. Inspecting figure 7.21, this correspond to 81% of the building presenting vulnerability types A and 58% for those presenting vulnerabilities B. A comparison of these values and the fragilities shown in figure 7.36 is presented in figure 7.38.

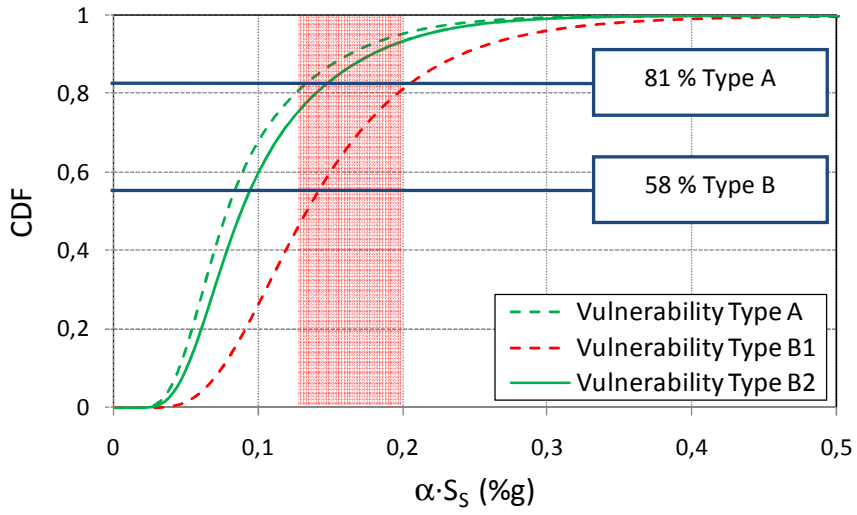

Figure 7.38: Comparison of reported damage at Castelnuovo and the obtained fragilities. The shadowed area corresponds to the possible experienced seismic action (0.8 m/s^2 with amplification factor of 1.6 to 2.5)

According to the intersection of damage and fragilities, the reference PGA values can be approximated to 0.13g for vulnerability type A and to 0.15g for vulnerability type B. From this damage point of view, the experimented PGA values could be expected to be around 0.14g.

According to the results presented in section 7.1, PGA values at the town had been approximated to 0.08g for soft soil (figure 7.5). At the same time studies from the INGV suggest that in the area of the Castelnuovo hill, values of seismic amplification can reach values up to 2.5 (figure 7.7). After this, an uncertain area could be shadowed in figure 7.37 regarding the seismic loading experimented by the structures at the time of 2009 earthquake. Indifferent to this fact, a good correlation in between the expected damage and the experimented damage is observed. Especially for vulnerability type A which at 0.08g already exhibit a very weak behavior.

7.4.2 Comparison with other methodologies

Studies about the seismic fragility of stone URM are not common. It had been just up to recent years that devastating events, such as those observed in table 4.1, and the development of new generation performance base approaches, that relevant reference about URM structural performance is available. Recent works of interest are those developed by Bothara [BDM 09], Rota [RPM 08], Frankie [Fr 10] and Rota [RPS 07].

Of these group, only the study of Rota [RPS 07] and Frankie deal with different URM typologies. The fragilities developed by Rota are based on an extensive study of experienced seismic damage for many types of buildings in Italy. The curves were developed directly from the damage observed and intervals of PGA. In figure 7.39 the curve proposed by Rota for URM with irregular layout, flexible slabs and without tie rods (tie beams) is presented. It could be observed from the figure that correlation of results is poor. Different from this aspect, Rota results shows how a considerate amount of buildings damage is found for low PGA actions as it would be expected for URM failing in the out-of-plane. Then the curve tends to stabilize. Differences in between analytical obtained curves and database obtained curves are evident, especially because the difficulty to relate damage data in databases to a specific PGA value in field.

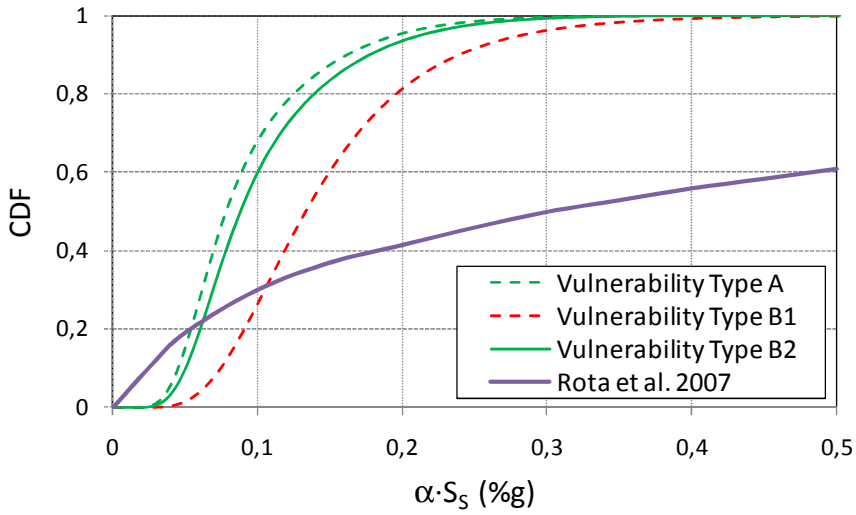

Figure 7.39: Comparison of fragilities for Rubble stone URM

Since there are not enough studies about fragilities for rubble stone URM typologies, the SAUMAC results are compared with the fragility obtained in case of the individual building assessed in the study of Rota [RPM 08]. Frankie had proposed also synthetic generated fragilities that can be comparable with the ones obtained by Rota [Fr 10].

For the case of the Rota building, the structure represents a common URM building in south Italy. It is a three storeys structure with 0.75 thick tuff stone walls. The material properties (with a mean and standard deviation) and construction layouts are presented in the study. Based on this, the wall cross section ratio was calculated for both principal directions of the building having ρ_x = 0.10 and ρ_y = 0.12. It can be deduced from the layout that the critical condition will be found in the *x* direction, as also it is manifest from the ρ value.

Similitude in terms of the building wall thickness and the density of the material, allows the use of figure 7.24 for computing approximately the value of A_M for the building. From the figure, values of 1.7 ±0.2 are founded for the base storey and of 1.6 ±0.2 for the top one.

Regarding the normalized pier resistance R_E *(V/N)*, the values are obtained for the top storey and the base storey according the material properties presented by Rota [RPM 08]. The out-of-plane possibility is neglected due to the thickness of the walls and the good connections; as well the possibility of diagonal tension failure due to the good material properties. Results of the MC to obtain R_E are presented in figure 7.40.

Assuming from the layout that the possible maximum value of h_P/l_P is 1 for external walls, R_E values of 0.77 and 0.9 are obtained for the base and top storeys. The pier elements in the structure presented similar geometry; according to this a value of F_W of 0.9 is obtained. For internal wall, R_E values of 0.85 and 1.05 are observed. Since this values should be multiplied by F_W = 0.75 they don't represent the assumed maximum resistance element. Continuing with the parameters related with the resistance, a F_{EC} of 0.8 is proposed to take into account some effect of eccentricity (section 3.3.3). Finally, only the F_S variable is missing to obtain the fragility curves. The value of F_S is computed for q = 2,5 (table 4.7), after this the F_S value is equal to 1.

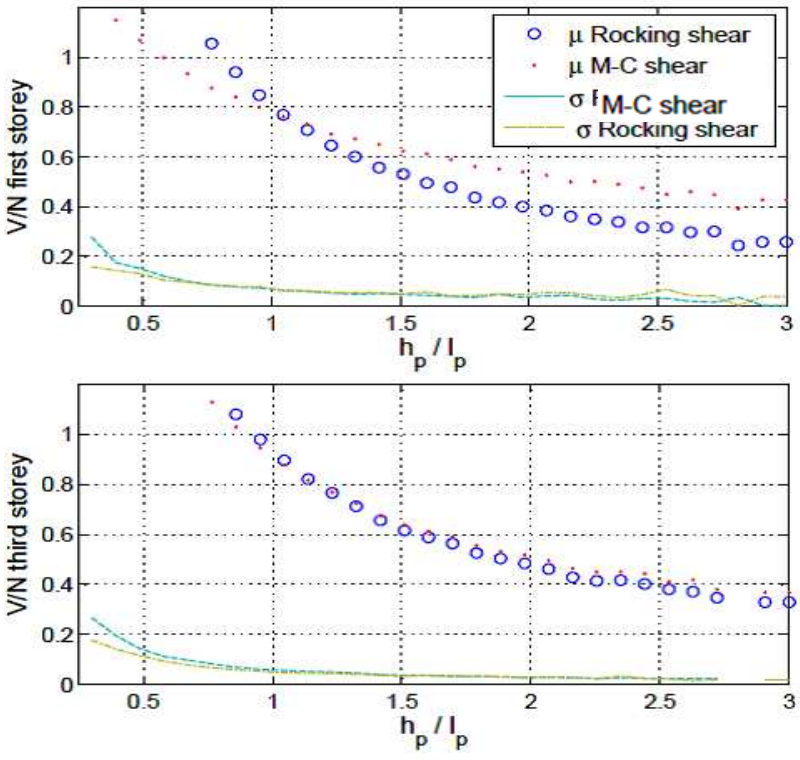

Figure 7.40: R_E values for c = 0.152 ± 0.024 MPa, μ = 0.65 ± 0.07 and f_m = 1.95± 0.37 MPa

For the serviceability LS, the value of R_{SW} must be reduced by 75% (section 6.5.1) and the F_S is equal to 2.1. Results of the fragility curves obtained for the serviceability damage state and the life safety limit state are presented in figure 7.41. In figure 7.41, the results obtained from Rota [RPM 08] and Frankie [Fr 10] are also plotted for comparison. A good correlation among the results is observed for the life safety LS. In case of the LSLS curve obtained from the SAUMAC procedure greater distribution of damage could be observed but with similar mean values of the other authors. The reason of greater dispersion of the curve can be explained to the different amount of building configuration possibilities considered for obtaining A_M and I_R.

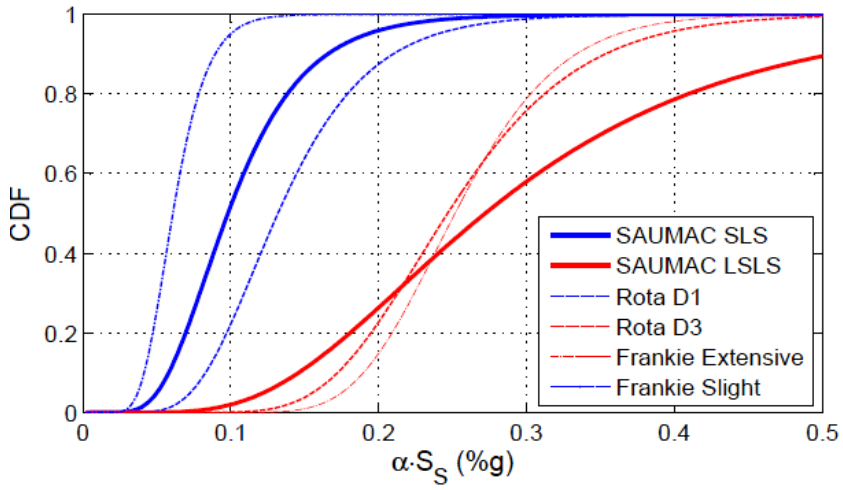

Figure 7.41: Result comparison for life safety and serviceability LS

7.4.3 Evaluation of rubble stone URM

From figure 7.37 it can be observed that the estimated performance of stone rubble URM edifications is poor, expected as highly risky for the investigated A and B building typologies observed at Castelnuovo. From this result, some pertinent questions could be formulated: Is it possible to reach good seismic performance for regular, tied, and rigid floor rubble stone URM? Do we need to upgrade the material properties or we can use the same materials to rebuild? These questions can be answer by means of the SAUMAC methodology.

By the formulation of hypothetical buildings with good spandrels, rigid floors and good structural layout, the maximum capacity of an URM building is achieved. This was done in case of Rubble stone masonry URM for houses of one, two and three floors. The material properties used are the same of the ones used in the Castelnuovo case study. The resulting I_R and A_M are presented in table 7.13.

Table 7.13: I_R, A_M and F_S for developing the maximum expected capacity of rubble stone URM

Number of Floors	Critical floor / failure mode	R_E	I_R	A_M	F_S
3 storeys	Base floor / Diagonal tension	0.47 ± 0.07	0.34 ± 0.04	1.70 ± 0.15	1.1
2 storeys	Top floor / Rocking	0.90 ± 0.1	0.49 ± 0.05	1.60 ± 0.15	1
1 storey	Base floor / M-C shear	0.90 ± 0.1	0.65 ± 0.07	1.80 ± 0.15	1

The values observed in the table correspond already to the critical floors in the building; this is also noted in table 7.13 together with a related failure mode. The R_E values where gotten from figures 6.16a, 6.16b and 6.16c. The F_W and F_{EC} are constant for all the cases and assumed as 0.9 and 0.8. The values of A_M are obtained from figure 7.24. Resulting fragilities are presented in figure 7.42.

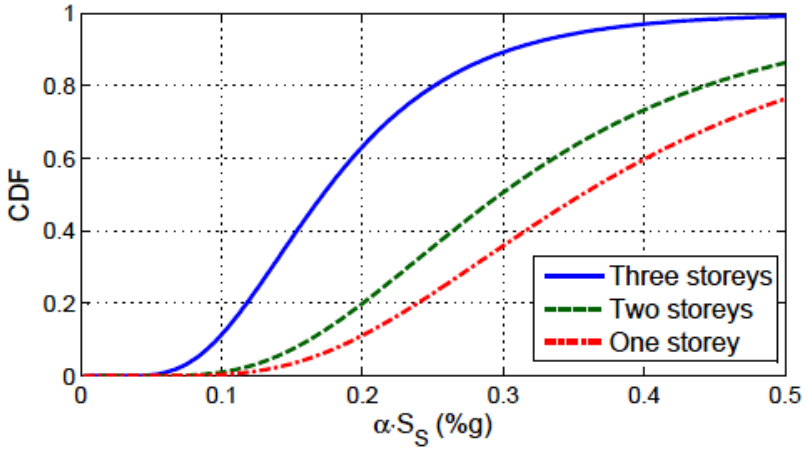

Figure 7.42: Estimated maximum capacity of rubble stone for the life safety for LS

After the fragility is finally obtained, the risk is easily obtained from the hazard curve derived for a specific site. In case of L'Aquila city and surrounding areas, the curve *H* is presented in figure 3.8. For a return period of 475 years, a value of approximately 0.3 %g is founded in figure 3.8e, this value correspond also with the value of 0.27 proposed by the Italian INGV [INGV web].

According to the figure 7.43, for seismic actions expected of αS_S=0.27, well structured systems of one and two floors are located in moderate risk zones. The three storey edification is on the other hand located in the high risk zone, although close to the moderate vulnerability limit. From this figure it can be concluded that in case of rubble stone URM, providing good anchorage and rigid diaphragms is not enough for actual building design for moderate and high seismic areas. The material itself must be upgraded or any other resistant system must be provided for gaining redundancy.

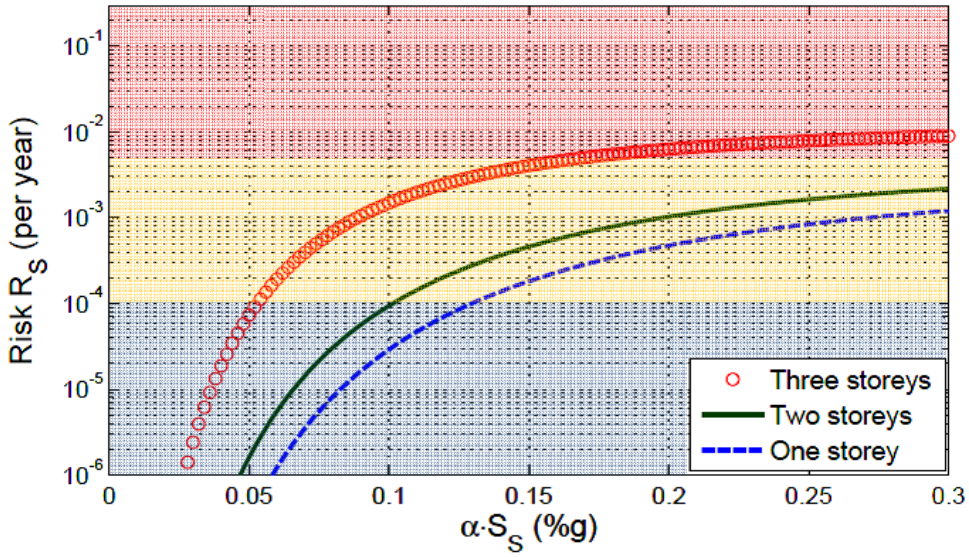

Figure 7.43: Result comparison for life safety and serviceability LS

8 SYNOPSIS

Conventional assessment procedures, based on deterministic variables input, face problems in relation to uncertainties in common unreinforced masonry buildings.

In the case of individual buildings assessment, the problem is solved in seismic provisions in two ways: 1) rising the partial safety factors for seismic actions and structural resistance, or 2) by intensifying in-situ investigations of material properties and use of moderate to high sophisticated structural analysis procedures; simplified procedures are in many occasions not recommended. Regarding URM structures, point number one may be considered a too severe criterion, difficult for many URM constructions to be fulfilled; aspect number two is coherent only for low rise unreinforced masonry structures with a social-cultural-historical value, but, turns to be not economically viable for the vast majority of common URM structures. For the seismic assessment of building groups (typology sets), existent methodologies typically proposed generic or self obtained performance points to build damage fragility curves to an archetype building. The assessed building is assumed to be a typical representative local structure. Problems may arise in the selection of an appropriate representative fragility and the selection of constant material properties for the generation of the fragility meanwhile the reality presents important variations even in one structural unit.

In contrast with classic approaches, the SAUMAC method fits observed behavior of a synthetically generated building population to a specific building typology for developing the damage fragilities. It is creating results to a particular possible condition (theoretical archetype) from the seismic behavior of a building population, of similar conditions, for the generation of useful parameters database. In other words, a deductive process instead of an inductive one has been used. Fragility curves delivered by SAUMAC could describe particular building configurations and variable material conditions of low rise URM buildings in a fast and economical way according to local regulations and probabilistic seismic hazard assessment procedures.

For the damage fragility generation, the method is conceived to compute the two most useful performance levels: life safety and serviceability LS. This was done by assuming seismic load equal to the elastic response spectra and elastic storey resistance for the serviceability limit states, and seismic load equal to design spectra and ultimate floor resistance for the life safety LS. In the case of the life safety limit state, risk limits values were used to categorize a structure as high risk, moderate risk or low risk. This classification is thought to help stakeholders evaluate a seismic risk scenario, and to review the effectiveness of an introduced safety measure in a structure. For building sets, results could be used in a qualitative and quantitative manner.

The problem of individual building assessment in terms of the SAUMAC procedure is still an area for future development and improvement. At this level of research, structures are found to be safe when the structural seismic risk values obtained from the annual risk vs. PGA curves, are in the low risk area when compared to the expected reference peak ground value. Similarly, they are considered unsafe when they are located in the high risk area. When structures are founded unsafe, they are recommended either to be demolished or retrofitted. For structures falling into the moderate risk region, the safety of the building must be judged by other more detailed evaluation procedures to find if the structure is safe or not. Despite this limitation, strategies such as risk transfer (insurance) or risk acceptance could be part of the stakeholder management possibilities in case of moderate risk. Structural risk for evaluation of individual structures should be the one obtained for the life safety limit state.

The proposed methodology had been corroborated with the seismic damage data from Castelnuovo town after the earthquake of L'Aquila in 2009. Additional validation has been done

according to different references founded in bibliography. Corroboration of results is limited to few available existing studies related with URM building fragilities, in particular those regarding rubble stone URM.

8.1 Concluding Remarks

The main goal of assessing URM masonry structures had been fulfilled by the proposed SAUMAC methodology. Here, uncertainties related to seismic actions, resistance and even possible architectural configuration of building were taken into account. Results are presented in terms of structural vulnerability fragility curves and structural risk. The risk in the method can be evaluated quantitatively for applications related with the estimation of loss due to seismic actions, or qualitatively for a safety description of structures. In case individual structures, only the qualitative use of the methodology is recommended.

For the case study, a complete description of the seismic damage is presented. This information is used to corroborate results obtained from the SAUMAC procedure. The damage experienced at the town fits well to the obtained fragility functions; nevertheless there is uncertainty about the possible seismic acceleration experienced at the site. A reference peak ground acceleration of 1.4 m/s^2 is deduced by the developed seismic fragility damage curves estimated for vulnerabilities type A and B (As defined by EMS-98 and Ciabatone).

For rubble stone URM at Castelnuovo, the construction technique is considered as highly risky in concordance with the EMS-98 description for vulnerability classes A and B. This was further corroborated by the application of the SAUMAC procedure, finding for most evaluated structural types a high vulnerability risk value. Three storey building present much higher risk values since for the poor material properties of rubble stone, shear failure mode is likely at the base story. In case of regular outline, rigid slab and tied rubble stone URM constructions, it was found that these structures present a moderate risk in case of 1 or 2 storey houses in high seismicity zones. Also, for low seismicity areas, well conceived 1 or 2 storey houses are found to be in the low risk range, and so, considered safe.

From these results it could be recommended for most rubble stone masonry in Castelnuovo town either to demolished, to upgrade the material constitutive properties, or finally to provide additional resistant structural elements (e.g. reinforcement fibers, reinforced mortar layer, etc). The addition of ties and construction of rigid slabs for rubble stone URM, although working for low seismic hazard levels, is not reaching the life safety limit state performance goal for high seismicity zones.

The proposed methodology results are depending on the definitions of seismic actions and resistant equations of local normative. This is of importance since it takes into account local conditions such as constructions techniques, materials, expected quality of constructions and the economical limitations of the region or country. It is observed in this study that although many seismic provisions followed similar procedures, resulting seismic forces can differ greatly for URM structures. This is particularly true for large countries with presence of low seismicity regions. It is important also to mention that the seismic behavior factor q is the main aspect affecting the performance of structures, the SAUMAC accuracy is evidently conditioned to the use of a correct value. Efforts toward obtaining reliable behavior factors must be made by local authorities to properly characterize URM structures.

A classification into different risk levels is also presented in the study. This was obtained for the life safety limit state based on the likelihood qualification of a possible situation and the target reliability values presented in some norms and other relevant reliability studies. Variability of possible target reliabilities is high and an individual target reliability to assess directly URM structures had not been yet presented in any reference so far.

The variability of the target values may be explained by a non-clear and non-uniform description of the ultimate state condition. This makes the adoption of a limit parameter difficult to be applied directly for the life safety limit state. Target seismic reliability values are normally proposed for middle rise to high rise building (typically RC) after finding the minimum cost level that takes into account the initial construction value, cost of seismic countermeasures and the possible losses related to a damage level (not human or CSH). From this point of view, retrofitting solutions and evaluation techniques for URM must be inexpensive due to low market value of URM, and the proposed target reliabilities turned to be high (on the conservative side) for URM structures.

On the base of keeping the same target reliabilities of other structural typologies for URM (under human life safety rather than economical reasons), it is the opinion of the author of this study that it is time to include other variables for justifying many seismic improvement solutions for URM into an economic viable framework. One good possibility is energy saving due to thermal insulation of houses. Seismic improvement could be thought not only in terms of seismic resistance but also thermal improvement (particularly of walls and roofs) so that seismic retrofitting could not be only justified from the hypothetical saving money situation of damage that may occur, but also from daily saved money due to reduced energy bills.

8.2 Future Developments and Possibilities

There are many open possibilities for the ideas proposed in the SAUMAC procedure, some related with the stochastic house generation, others with extension of the methodology to take into account other variables and finally some to improve the results obtained from the actual procedure. These are summarized in the next points:

- *Automatic generated fragilities from computer software with photo-recognition*: up to now, the procedure is following a visual step by step procedure to estimate the building capacity at each floor to find fragilities. With software that includes visual recognition of external house elements, possible internal house configurations could be developed and the fragility curves derived automatically for a specific building.
- *Life-cycle assessment:* so far the time variable had been neglected from this study. Aspects like maintenance or material degradation affecting the structural capacity of URM could be easily introduced into the reliability problem by additional probability density functions and solved by means of a FORM formulation or a Monte Carlo process.
- *Case studies:* further validation of SAUMAC can be done by analyzing other well documented seismic damage study case; in particular, it would be of great interest the application in a developing country with high seismic hazard and a considerable URM building stock such as Peru or India.

APPENDIX A: Castelnuovo Damage Photographic Description after L'Aquila Earthquake

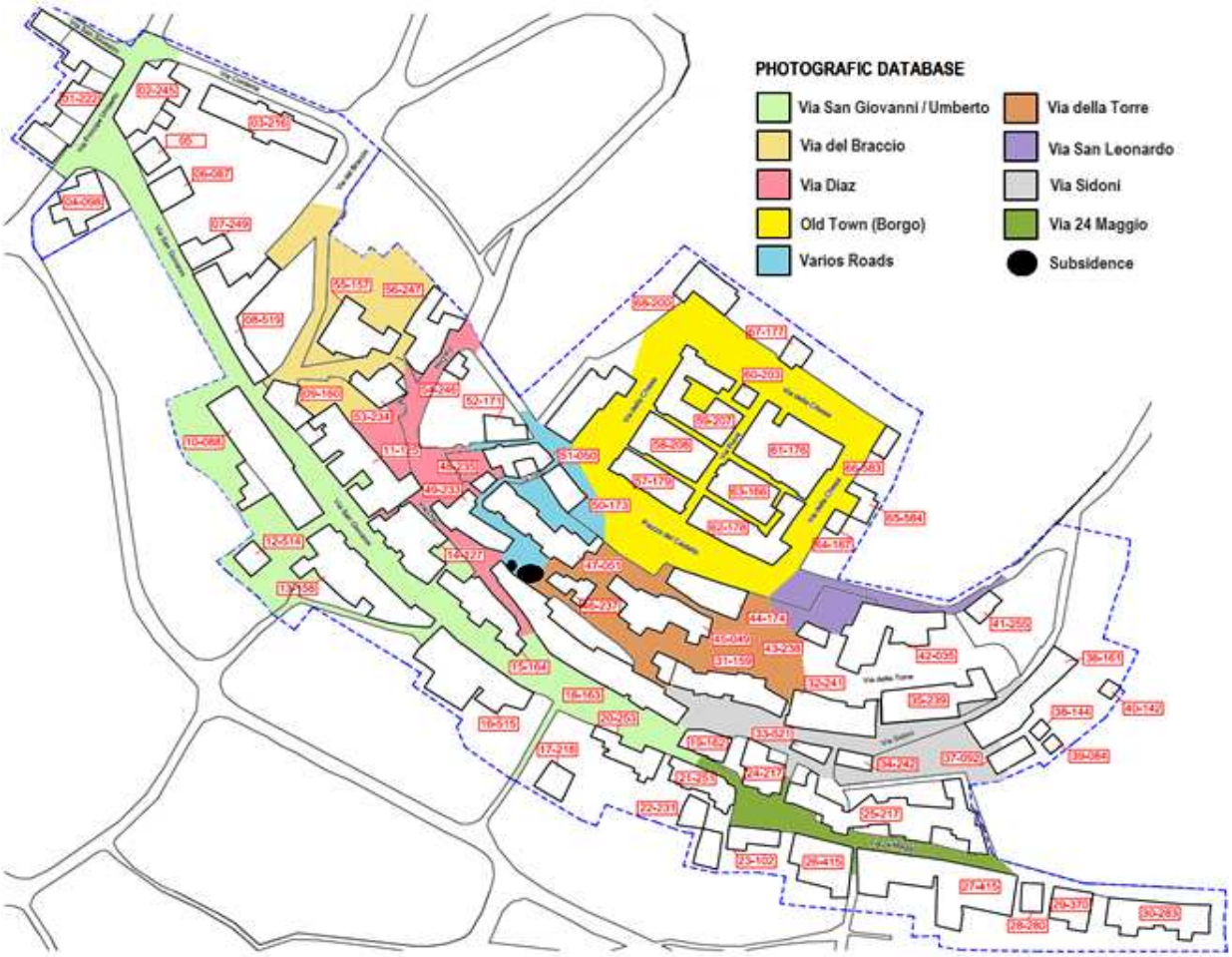

Via San Giovanni/Umberto

Wall material observation and preparation for flatjack testing, temporal wooden support for out-of-plane failing walls


Damage at building spandrels in the base floor and top floor


Damage at building spandrels in the top floor and mix-aggregate structure to the left


Detachment of building walls and failure of rigid masonry vault in the base floor


Damage on internal light weight masonry vaults


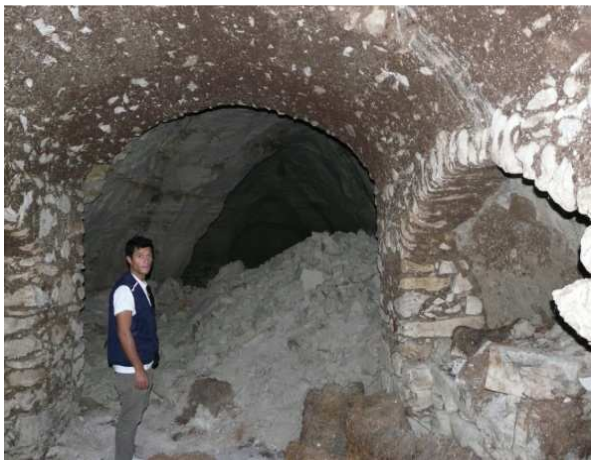

San Giovanni road (two years after main shock) and buildings underground caves (white silt material)


Two directional steel ties in an abandon URM house and out-of-plane failure of the top storey in 3 storeys house

Via del Braccio


Multi-storey out-of-plane failure and generalized damage on spandrels and piers


Typical wooden roof and effective tied wall in the base storey but no ties in the top storey

Via Diaz


Out-of-plane failure, and roof and ceiling details

Various Roads


Buttress and ineffective floor connection (element easily pull out causing floor collapse)


Out-of-plane failure and damage on surrounding structures, and an obstructed path due to collapse

Old Town


Out-of-plane failure and wall elements disaggregation

Wall detachment and layer stone-brick URM (Slight damage)

Out-of-plane failure and road block due to housing collapse

Rigid concrete floor slab in a collapse building and buttress support in the buildings first storey

Via della Torre


Temporal support for out-of-plane failing walls and wall disaggregation


Damage on concrete brick URM and total devastation scenario (D5 building damage scale)


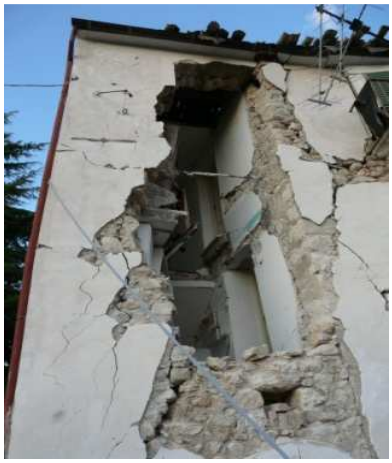

Rigid concrete beam system and out-of-plane wall fail even in presence of steel tie rods


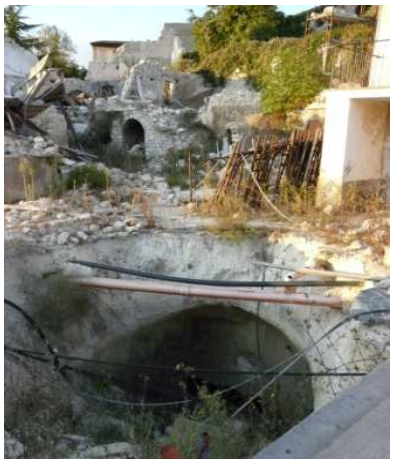

Light weight clay bricks in combination with rubber stones and subsidence fail due to cave collapse

Via San Leonardo and Via 24 di Maggio


Well tied structure presenting slight damage and crack pattern for out-of-plane failing wall


Ineffective steel ties and beams anchorage and old door location appearance due to deformation incompatibility

Via Sidoni


Various out-of-plain collapsing walls in presence of thick vault in the base floor and rigid beam in the top floor


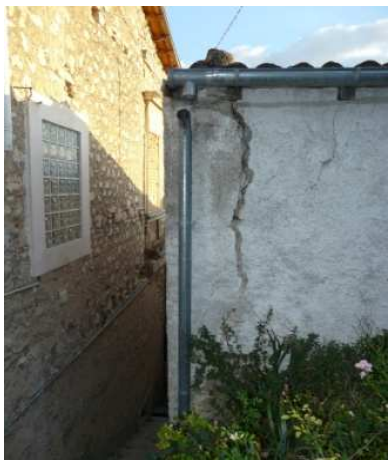

Material variability (façade brick, lateral stone) and wall detachment

APPENDIX B: Standard Normal Distribution (adapted from [Sc 97])

Definition

$$\varphi(u) = \frac{1}{\sqrt{2\pi}} e^{\frac{-1}{2}u^2} \qquad \Phi(u) = \int_{-\infty}^{u} \frac{1}{\sqrt{2\pi}} e^{\frac{-1}{2}u^2}$$

Probability density function PDF

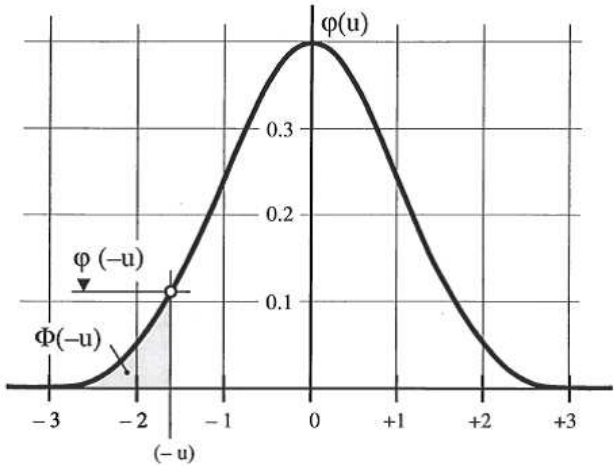

Cumulative distribution function CDF

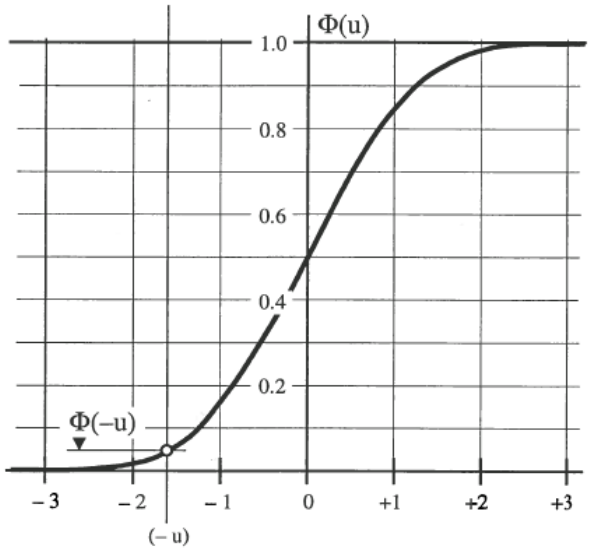

μ or β	$\Phi(-\mu)$	$\varphi(\mu)$
0	0,50000	0,39894
0,1	0,46164	0,39695
0,2	0,42346	0,39104
0,3	0,38586	0,38139
0,4	0,34918	0,36827
0,5	0,31377	0,35207
0,6	0,27991	0,33322
0,7	0,24787	0,31225
0,8	0,21784	0,28969
0,9	0,18998	0,26609
1	0,16440	0,24197
1,1	0,14113	0,21785
1,2	0,12018	0,19419
1,3	0,10151	0,17137
1,4	0,08503	0,14973
1,5	0,07063	0,12952
1,6	0,05817	0,11092
1,7	0,04751	0,09405
1,8	0,03846	0,07895
1,9	0,03087	0,06562
2	0,02456	0,05399
2,1	0,01937	0,04398
2,2	0,01514	0,03547
2,3	0,01173	0,02833
2,4	0,00900	0,02239
2,5	0,00685	0,01753
2,6	0,00516	0,01358
2,7	0,00386	0,01042
2,8	0,00286	0,00792
2,9	0,00209	0,00595
3	0,00152	0,00443
3,1	0,00110	0,00327
3,2	0,00078	0,00238
3,3	0,00055	0,00172
3,4	0,00039	0,00123
3,5	0,00027	0,00087
3,6	0,0001840	0,0006119
3,7	0,0001251	0,0004248
3,8	0,0000843	0,0002919
3,9	0,0000562	0,0001987
4	0,0000371	0,0001338
4,1	0,0000242	0,0000893
4,2	0,0000157	0,0000589
4,3	0,0000100	0,0000385
4,4	0,0000063	0,0000249
4,5	0,0000039	0,0000160
4,6	0,0000023	0,0000101
4,7	0,0000014	0,0000064
4,8	0,0000008	0,0000040
4,9	0,0000004	0,0000024
5	0,0000001	0,0000015

APPENDIX C: MATLAB Functions for SAUMAC and Fragility/Risk calculation

```
%%%%%%%%%%%%%%%%%%%%%%%%%%%%%%%%%%%%%%%%%%%%%%%%%%%
%              MATLAB VERSION 7.7              %
%                                              %
% Program to obtain house characteristics from  %
% scholastic house modeling (SHM) procedure and %
%       normalized pier shear resistance        %
%         Basis of the SAUMAC procedure         %
%                                              %
% Author: Jorge Munoz Barrantes                %
% Technische Universität Braunschweig, 2012     %
% Last modified: 02.02.2012                     %
%%%%%%%%%%%%%%%%%%%%%%%%%%%%%%%%%%%%%%%%%%%%%%%%%%%

clear all;
clc;
T=5000;                % total number of simulations

%%------------------------ BASIC HOUSE IMPUTS ----------------------------

% ------Generation of input text files (Location C:\MATLAB\)------

% House geometry file Pgeo1, Pgeo2 and Pgeo3 for generating triangular (min
% mid and max values) and rectangular PDF (min max values)
% Default for 3 Storeys, for 1 and 2 parameters, blank parameters must be
% input = to 0.00001

% 2.2 2.8 3.5            1. Height first floor, m
% 2 2.6 3.0              2. Height second floor, m
% 1.8 2.4 2.8            3. Height third floor, m
% 2.5 7 16               4. Dimension in X, m
% 4 9 24                 5. Dimension in Y, m
% 0.12 0.25 0.6          6. External wall facade thickness in X, m
% 0.003 0.0045 0.006     7. Diaphragm first floor, MPa
% 0.003 0.004 0.005      8. Diaphragm second floor, MPa
% 0.002 0.003 0.004      9. Diaphragm third floor, MPa
% 0.012 0.014 0.016      10. Material Density MPa/m3
% 0.6 1.2 2              11. Dimension of length of voids (windows), m
% 0.3 0.4                12. Internal wall thickness in  x and y, m
% 1.1 2                  13. Internal wall % factor in "X"
% 1.05 2.5               14. External wall % factor in "X"
% 1.1 2                  15. Internal wall % factor in "Y"
% 1.05 2.5               16. External wall % factor in "Y"

% Material properties file Pmat.dat, normal PDF with mean and standard
% deviation values (recommended coefficient of variation of aprox. 20% if no
% information is available

% 1.4 0.25               1. Masonry compression, MPa
% 0.15 0.03              2. Masonry brick tension resistance, MPa
% 0.1 0.02               3. Cohesion, MPa
% 0.4 0.08               4. Friction coefficient

% ------Generation of the Probability density functions------

NumPi=3;                 % Number of storeys (in between 1 and 3)
Exy=0.2;                 % Variation of wall thickness in y direction compute from
                         % the facade thickness of the first storey
if NumPi == 3
   load C:\MATLAB\Pgeo3.dat;
   Pgeo=Pgeo3;
else
   if NumPi == 2
      load C:\MATLAB\Pgeo2.dat;
      Pgeo=Pgeo2;
   else
      load C:\MATLAB\Pgeo1.dat;
```

```
      Pgeo=Pgeo1;
   end
end

for i=1:5                   % triangular PDF
Med=(Pgeo(i,2)-Pgeo(i,1))/(Pgeo(i,3)-Pgeo(i,1));
  for k=1:T
      r=rand();
      if r<Med
      A(i,k)=Pgeo(i,1)+(Pgeo(i,3)-Pgeo(i,1))*sqrt(Med*r);
      A(i,k)=(round(10*A(i,k)))/10;
      else
      A(i,k)=Pgeo(i,1)+(Pgeo(i,3)-Pgeo(i,1))*(1-sqrt((1-Med)*(1-r)));
      A(i,k)=(round(10*A(i,k)))/10;
      end
  end
end
A(5,1)=6;                   % Initial shape values
A(4,1)=12;
j=0;
  for k=1:T                 % Restriction in geometry X/Y < 3 and X/Y > 1/3
      a=(A(5,k)/A(4,k));
      if a>3 || a<0.3
      A(5,k)=A(5,k-1);
      A(4,k)=A(4,k-1);
      end
  end
for i=6:11                  % triangular PDF
Med=(Pgeo(i,2)-Pgeo(i,1))/(Pgeo(i,3)-Pgeo(i,1));
  for k=1:T
      r=rand();
      if r<Med
      A(i,k)=Pgeo(i,1)+(Pgeo(i,3)-Pgeo(i,1))*sqrt(Med*r);
      else
      A(i,k)=Pgeo(i,1)+(Pgeo(i,3)-Pgeo(i,1))*(1-sqrt((1-Med)*(1-r)));
      end
  end
end
for i=12:16                 % uniform PDF
  for k=1:T
      A(i,k)= Pgeo(i,1)+(Pgeo(i,2)-Pgeo(i,1))*rand();
      A(i,k)=(round(10*A(i,k)))/10;
  end
end
for k=1:T
    u=rand();
    u=(round(10*u));
    if u==1 || u==3 || u==5 || u==7 || u==9
        u=-u/10;
    else
        u=u/10;
    end
    A(6,k);
    A(17,k)=(A(6,k)+A(6,k)*u*Exy);
    A(6,k)=(round(100*A(6,k)))/100;
    A(17,k)=(round(100*A(17,k)))/100;
end

load C:\MATLAB\Pmat.dat;
Com=lognrnd(Pmat(1,1),Pmat(1,2),1,T);  % 1. Masonry compression, MPa
Tra=lognrnd(Pmat(2,1),Pmat(2,2),1,T);  % 2. Masonry brick tension, MPa
Coh=lognrnd(Pmat(3,1),Pmat(3,2),1,T);  % 3. Cohesion, MPa
Fri=lognrnd(Pmat(4,1),Pmat(4,2),1,T);  % 4. Friction coefficient
Em=750*Com;       % Approximate elastic modulus (user defined), MPa
Hpp= A(1,:);                % 1. Height first floor, m
Hsp= A(2,:);                % 2. Height second floor, m
Htp= A(3,:);                % 3. Height third floor, m
X= A(4,:);                  % 4. Dimension in X, m
Y= A(5,:);                  % 5. Dimension in Y, m
Espx= A(6,:);               % 6. External wall facade thickness in X, m
```

```
P1= A(7,:);                 % 7. Diaphragm first floor, MPa
P2= A(8,:);                 % 8. Diaphragm second floor, MPa
Pt= A(9,:);                 % 9. Diaphragm third floor, MPa
Den= A(10,:);               % 10. Material Density MPa/m3
vacio= A(11,:);             % 11. Characteristic length of voids (windows), m
Espintp= A(12,:);           % 12. Internal wall thickness in  x and y, m
Fmi= A(13,:);               % 13. Internal wall % factor in "X"
Fme= A(14,:);               % 14. External wall % factor in "X"
Fmiy= A(15,:);              % 15. Internal wall % factor in "Y"
Fmey= A(16,:);              % 16. External wall % factor in "Y"
Espy= A(17,:);              % 17. External wall thickness in Y, m


% ------ SCHOCASTIC HOUSE MODELLING ------

%------- Parameters ----------------------
Lmin=0.4;                   % minimum length of piers and voids, m
hmin=0.4;                   % minimum height of piers, m
porHmin=0.25;               % minimum height of voids, % of storey height
porHmax=0.75;               % maximum height of voids, % of storey height
CSmin=3;                    % minimum clear span in between walls, m
CSmax=9;                    % maximum clear span in between walls, m
qr2=(0.7+0.35*rand());      % function define by user to take into account
                            % wall thickness reduction ratio in the second floor
                            % (recommended value in between 0.7 to 1.1)
qr3=qr2*(0.8+0.2*rand());   % function define by user to take into account
                            % wall thickness reduction ratio in the third floor
                            % (recommended value in between 0.6 to 1)
Liload=0.001+0.0005*randi([-1,1]);  % Life load function (user defined, code
                                    % formulations recommended)
SlabV=1-0.05+0.05*rand();   % Slab void percentage (user defined, max 0.15)


%-------- Main Code -------------------------
T=T/2;
for k=1:T

%mean value of characteristic void length "v1", for estimating the number
%of piers
    v1(1,k)=vacio(1,k);
    al1=rand()+0.3;
    al2=rand()+0.9;
    if (al1*v1(1,k)>Lmin) && (al1*v1(1,k)<2)    % max. window/door length=2m
        v2(1,k)=al1*vacio(1,k);
    else
        v2(1,k)=1;
    end
    if (al2*v1(1,k)>0.4) && (al2*v1(1,k)<2)
        v3(1,k)=al2*vacio(1,k);
    else
        v3(1,k)=1.6;
    end
    v1(1,k)=(v1(1,k)+v2(1,k)+v3(1,k))/3;

%0.4 is the minimum permitted pier height/length ratio, "Num" is the void
%number computed from the mean void ratio "v1"
    Num(1,k)=round((1-1/Fme(1,k))*X(1,k)/v1(1,k));
    Num1(1,k)=round(0.4*X(1,k)/Hpp(1,k));
    if Num(1,k) < Num1(1,k)
       Num(1,k)=Num1(1,k);
    end

%Generation of external wall in X direction, with an average pier length
%"L" and for a possible amount of doors "puertas" (0 to 3). The average pier
%height "H1" is obtained for the wall, later the characteristic "H1/L" ratio
%for the wall computed as well as the % of voids in the whole wall.
    L(1,k)=round(10*(X(1,k)-(Num(1,k)*v1(1,k)))/(Num(1,k)+1))/10;
    if L(1,k) < Lmin
       L(1,k)=Lmin;
       Num(1,k)=floor((X(1,k)-Lmin)/(v1(1,k)+Lmin));
```

```
    end
    r=porHmin+((porHmax-porHmin)*rand());
    H(1,k)=round(10*Hpp(1,k)*r)/10;
    Fme(1,k)=round(10*1/(1-(Num(1,k)*v1(1,k)/X(1,k))))/10;  % Adjusted Fme
    if (H(1,k)>0.4*Hpp(1,k)) && (X(1,k)<=7)
       puertas(1,k) = randi([0,1]);
       H1(1,k)=(H(1,k)*(puertas(1,k)+(Num(1,k)-puertas(1,k))/2))/Num(1,k);
    else
        if (H(1,k)>0.4*Hpp(1,k)) && (X(1,k)<=12)
        puertas(1,k) = 1+randi([0,1]);
        H1(1,k)=(H(1,k)*(puertas(1,k)+(Num(1,k)-puertas(1,k))/2))/Num(1,k);
        else
            if (H(1,k)>0.4*Hpp(1,k)) && (X(1,k)<=24)
            puertas(1,k) = 1+randi([0,2]);
            H1(1,k)=(H(1,k)*(puertas(1,k)+(Num(1,k)-puertas(1,k))/2))/Num(1,k);
            else
            H1(1,k)=H(1,k);
            end
        end
    end
    Av(1,k)=(1-1/Fme(1,k))*X(1,k)*H1(1,k);
    PorAv(1,k)=Av(1,k)/(X(1,k)*Hpp(1,k));
    HL(1,k)=H1(1,k)/L(1,k);

%Generation of external wall in Y direction
    Num(1,T+k)=round((1-1/Fmey(1,k))*Y(1,k)/v1(1,k));
    Num1(1,T+k)=round(0.4*Y(1,k)/Hpp(1,k));
    if Num(1,T+k) < Num1(1,T+k)
        Num(1,T+k)=Num1(1,T+k);
    end
    L(1,T+k)=round(10*(Y(1,k)-(Num(1,T+k)*v1(1,k)))/(Num(1,T+k)+1))/10;
    if (L(1,T+k) < Lmin)
       L(1,T+k)=Lmin;
       Num(1,T+k)=floor((Y(1,k)-Lmin)/(v1(1,k)+Lmin));
    end
    r=porHmin+((porHmax-porHmin)*rand());
    H(1,T+k)=round(10*Hpp(1,k)*r)/10;
    if (H(1,T+k)>0.4*Hpp(1,k)) && (Y(1,k)<=7)
      puertas(1,T+k) = randi([0,1]);
      H1(1,T+k)=(H(1,T+k)*(puertas(1,T+k)+(Num(1,T+k)-
puertas(1,T+k))/2))/Num(1,T+k);
    else
      if (H(1,T+k)>0.4*Hpp(1,k)) && (Y(1,k)<=12)
      puertas(1,T+k) = 1+randi([0,1]);
      H1(1,T+k)=(H(1,T+k)*(puertas(1,T+k)+(Num(1,T+k)-
puertas(1,T+k))/2))/Num(1,T+k);
      else
      if (H(1,T+k)>0.4*Hpp(1,k)) && (Y(1,k)<=24)
      puertas(1,T+k) = 1+randi([0,1]);  %diference to x direction (1 insteed of 2)
      H1(1,T+k)=(H(1,T+k)*(puertas(1,T+k)+(Num(1,T+k)-
puertas(1,T+k))/2))/Num(1,T+k);
      else
      H1(1,T+k)=H(1,T+k);
      end
      end
    end
    Av(1,T+k)=(1-1/Fme(1,k))*Y(1,k)*H1(1,T+k);
    PorAv(1,T+k)=Av(1,T+k)/(Y(1,k)*Hpp(1,k));
    HL(1,T+k)=H1(1,T+k)/L(1,T+k);
end

for k=1:T

%Defining the number of internal divisions in x and y directions
    Dmix(1,k)=(Y(1,k)-Espx(1,k))/(CSmax-Espx(1,k));
    if Dmix(1,k)>=1
       Dmix(1,k)=floor(Dmix(1,k));
    else
       Dmix(1,k)=0;
    end
```

```
    Dmiy(1,k)=(X(1,k)-Espy(1,k))/(CSmax-Espy(1,k));
    if Dmiy(1,k)>=1
       Dmiy(1,k)=floor(Dmiy(1,k));
    else
       Dmiy(1,k)=0;
    end
    Dmax(1,k)=(Y(1,k)-Espx(1,k))/(CSmin-Espx(1,k));
    if Dmax(1,k)>=1
       Dmax(1,k)=round(Dmax(1,k))-1;
    else
       Dmax(1,k)=0;
    end
    Dmay(1,k)=(X(1,k)-Espy(1,k))/(CSmin-Espy(1,k));
    if Dmay(1,k)>=1
       Dmay(1,k)=round(Dmay(1,k))-1;
    else
       Dmay(1,k)=0;
    end
    if Dmix(1,k) == Dmax(1,k)
        Dx(1,k)=Dmix(1,k);
    else
        Dx(1,k)=randi([Dmix(1,k),Dmax(1,k)]);
    end
    parD(1,k)=Y(1,k)/(Dx(1,k)+1);
    if parD(1,k) >= 5
            Dy(1,k)=Dmay(1,k);
    else
        if Dmiy(1,k) == Dmay(1,k)
            Dy(1,k)=Dmiy(1,k);
        else
            Dy(1,k)=randi([Dmiy(1,k),Dmay(1,k)]);
        end
    end

%determination of the rho ratio (wall cross-section area ratio) for the
%first storeys and approximated for the second and third.
    Rhox(1,k)=((2/Fme(1,k)+Dx(1,k)/Fmi(1,k))*Espx(1,k))/Y(1,k);
    Rhoy(1,k)=((2/Fmey(1,k)+Dy(1,k)/Fmiy(1,k))*Espy(1,k))/X(1,k);
    Rho(1,k)=Rhox(1,k);
    Rho(1,T+k)=Rhoy(1,k);
    Esp(1,k)=(Espx(1,k)+Espintp(1,k))/2;
    Esp(1,T+k)=(Espy(1,k)+Espintp(1,k))/2;
    if Hsp(1,k)>1
    Rho2(1,k)=Rho(1,k)*(qr2);
    Rho2(1,T+k)=Rho(1,T+k)*(qr2);
        if Htp(1,k)>1
        Rho3(1,k)=Rho(1,k)*qr3;
        Rho3(1,T+k)=Rho(1,T+k)*qr3;
        end
    end

%Computing the normal forces for walls and slabs in each floor.  AxialX
%means the total weight of walls in x direction, the total weight of walls
%per floor is (AxialX + AxialY), AxialE is the floor slab weight.  Slabs
%are restricted to less than 20% of their area is perforated
    Hto(1,k)=Hpp(1,k)/2+Hsp(1,k)+Htp(1,k);
    Ht2(1,k)=Hsp(1,k)/2+Htp(1,k);
    Pto(1,k)=P1(1,k)+P2(1,k)+Pt(1,k);
    Pt2(1,k)=P2(1,k)+Pt(1,k);

    AxialX(1,k)=(2*(1-PorAv(1,k))+Dx(1,k)*(1-PorAv(1,k))*(Fme(1,k)/Fmi(1,k)))...
        *((1+qr2+qr3)/3)*Den(1,k)*Hto(1,k)*X(1,k)*Esp(1,k);
    AxialY(1,k)=(2*(1-PorAv(1,T+k))+Dy(1,k)*(1-
PorAv(1,T+k))*(Fmey(1,k)/Fmiy(1,k)))...
        *((1+qr2+qr3)/3)*Den(1,k)*Hto(1,k)*Y(1,k)*Esp(1,T+k);
    AxialE(1,k)=(X(1,k)*Y(1,k)*Pto(1,k)+2.5*Liload)*SlabV;
    if Hsp(1,k)>1
        AxialX2(1,k)=(2*(1-PorAv(1,k))+Dx(1,k)*(1-
PorAv(1,k))*(Fme(1,k)/Fmi(1,k)))...
            *((qr2+qr3)/2)*Den(1,k)*Ht2(1,k)*X(1,k)*Esp(1,k);
```

```
        AxialY2(1,k)=(2*(1-PorAv(1,T+k))+Dy(1,k)*(1-PorAv(1,T+k))*(Fmey(1,k)/...
            Fmiy(1,k)))*((qr2+qr3)/2)*Den(1,k)*Ht2(1,k)*Y(1,k)*Esp(1,T+k);
        AxialE2(1,k)=(X(1,k)*Y(1,k)*Pt2(1,k)+1.5*Liload)*SlabV;
        if Htp(1,k)>1
            AxialX3(1,k)=(2*(1-PorAv(1,k))+Dx(1,k)*(1-PorAv(1,k))*(Fme(1,k)/...
                Fmi(1,k)))*(qr3)*Den(1,k)*Htp(1,k)/2*X(1,k)*Esp(1,k);
            AxialY3(1,k)=(2*(1-PorAv(1,T+k))+Dy(1,k)*(1-
PorAv(1,T+k))*(Fmey(1,k)/...
                Fmiy(1,k)))*(qr3)*Den(1,k)*Htp(1,k)/2*Y(1,k)*Esp(1,T+k);
            AxialE3(1,k)=(X(1,k)*Y(1,k)*Pt(1,k)+0.5*Liload)*SlabV;
        end
    end

%Parameters for the computation of the Architectural mass index "Am" in
%case of flexible and rigid slabs. N refers to the normal stress in
%presence of rigid floors, and NFlex for flexible ones. CI is the value of
%Am for a rigid slab in the first storey
    flex=randi([0,1]);
    if flex == 0
        fley=1;
    else
        fley=0;
    end
    flex2=randi([0,1]);
    if flex2 == 0
        fley2=1;
    else
        fley2=0;
    end
    flex3=randi([0,1]);
    if flex3 == 0
        fley3=1;
    else
        fley3=0;
    end
    Nr(1,k)=AxialX(1,k)+AxialE(1,k)/4;
    N(1,k)=Nr(1,k)/(Rho(1,k)*((1+qr2+qr3)/3)*X(1,k)*Y(1,k));
    Nf(1,k)=AxialX(1,k)+(0.2+0.2*(flex+flex2+flex3))*AxialE(1,k)/2;
    Nflex(1,k)=Nf(1,k)/(Rho(1,k)*((1+qr2+qr3)/3)*X(1,k)*Y(1,k));
    CI(1,k)=(AxialX(1,k)+(AxialY(1,k)+AxialE(1,k))/2)/Nr(1,k);
    CIf(1,k)=(AxialX(1,k)+(AxialY(1,k)+AxialE(1,k))/2)/Nf(1,k);
    Nr(1,T+k)=AxialY(1,k)+AxialE(1,k)/4;
    N(1,T+k)=Nr(1,T+k)/(Rho(1,T+k)*((1+qr2+qr3)/3)*X(1,k)*Y(1,k));
    Nf(1,T+k)=AxialY(1,k)+(0.2+0.2*(fley+fley2+fley3))*AxialE(1,k)/2;
    Nflex(1,T+k)=Nf(1,T+k)/(Rho(1,T+k)*((1+qr2+qr3)/3)*X(1,k)*Y(1,k));
    CI(1,T+k)=(AxialX(1,k)+(AxialY(1,k)+AxialE(1,k))/2)/Nr(1,T+k);
    CIf(1,T+k)=(AxialX(1,k)+(AxialY(1,k)+AxialE(1,k))/2)/Nf(1,T+k);
        Nr2(1,k)=0;       N2(1,k)=0;      Nf2(1,k)=0;      Nflex2(1,k)=0;
        CI2(1,k)=0;       CIf2(1,k)=0;    Nr3(1,k)=0;      N3(1,k)=0;
        Nf3(1,k)=0;       Nflex3(1,k)=0;  CI3(1,k)=0;      CIf3(1,k)=0;
    if Hsp(1,k)>1
        Nr2(1,k)=AxialX2(1,k)+AxialE2(1,k)/4;
        N2(1,k)=Nr2(1,k)/(Rho2(1,k)*X(1,k)*Y(1,k));
        Nf2(1,k)=AxialX2(1,k)+(0.2+0.3*(flex2+flex3))*AxialE2(1,k)/2;
        Nflex2(1,k)=Nf2(1,k)/(Rho2(1,k)*X(1,k)*Y(1,k));
        CI2(1,k)=(AxialX2(1,k)+(AxialY2(1,k)+AxialE2(1,k))/2)/Nr2(1,k);
        CIf2(1,k)=(AxialX2(1,k)+(AxialY2(1,k)+AxialE2(1,k))/2)/Nf2(1,k);
        Nr2(1,T+k)=AxialY2(1,k)+AxialE2(1,k)/4;
        N2(1,T+k)=Nr2(1,T+k)/(Rho2(1,T+k)*X(1,k)*Y(1,k));
        Nf2(1,T+k)=AxialY2(1,k)+(0.2+0.3*(fley2+fley3))*AxialE2(1,k)/2;
        Nflex2(1,T+k)=Nf2(1,T+k)/(Rho2(1,T+k)*X(1,k)*Y(1,k));
        CI2(1,T+k)=(AxialX2(1,k)+(AxialY2(1,k)+AxialE2(1,k))/2)/Nr2(1,T+k);
        CIf2(1,T+k)=(AxialX2(1,k)+(AxialY2(1,k)+AxialE2(1,k))/2)/Nf2(1,T+k);
        if Htp(1,k)>1
            Nr3(1,k)=AxialX3(1,k)+AxialE3(1,k)/4;
            N3(1,k)=Nr3(1,k)/(Rho3(1,k)*X(1,k)*Y(1,k));
            Nf3(1,k)=AxialX3(1,k)+(0.2+0.6*(flex3))*AxialE3(1,k)/2;
            Nflex3(1,k)=Nf3(1,k)/(Rho3(1,k)*X(1,k)*Y(1,k));
            CI3(1,k)=(AxialX3(1,k)+(AxialY3(1,k)+AxialE3(1,k))/2)/Nr3(1,k);
            CIf3(1,k)=(AxialX3(1,k)+(AxialY3(1,k)+AxialE3(1,k))/2)/Nf3(1,k);
```

```
            Nr3(1,T+k)=AxialY3(1,k)+AxialE3(1,k)/4;
            N3(1,T+k)=Nr3(1,T+k)/(Rho3(1,T+k)*X(1,k)*Y(1,k));
            Nf3(1,T+k)=AxialY3(1,k)+(0.2+0.6*(fley3))*AxialE3(1,k)/2;
            Nflex3(1,T+k)=Nf3(1,T+k)/(Rho3(1,T+k)*X(1,k)*Y(1,k));
            CI3(1,T+k)=(AxialX3(1,k)+(AxialY3(1,k)+AxialE3(1,k))/2)/Nr3(1,T+k);
            CIf3(1,T+k)=(AxialX3(1,k)+(AxialY3(1,k)+AxialE3(1,k))/2)/Nf3(1,T+k);
        end
    end
end
MNormal=[N;Nflex;N2;Nflex2;N3;Nflex3];  % Normal stress matrix
MAm=[CI;CIf;CI2;CIf2;CI3;CIf3];         % Arq. mass matrix
MRho=[Rho;Rho;Rho2;Rho2;Rho3;Rho3];     % Building Rho matrix
T=2*T;
A=0;

for z=1:(2*NumPi)
    x = MRho(z,:);
    for j=0:29
        px(1,j+1)=(min(x)*1.3)+j*((max(x)*.7)-(min(x)*1.3))/30;
    end
    y = MAm(z,:);
    j=0;
    for i=1:29
        for k=1:T
            if (x(1,k) <= px(1,i+1)) && (x(1,k)> px(1,i))
            j=j+1;
            A(1,j)=y(1,k);
            Hist(i,j)=A(1,j);
            end
        end
        ax(1,i)=exp(mean(log(A))+0.5*std(log(A))^2);
        sx(1,i)=ax(1,i)*sqrt(exp(std(log(A))^2)-1);
        A=0;
        j=0;
    end
    ax(1,30)=ax(1,29);
    sx(1,30)=sx(1,29);
    MAmm(z,:)=ax;                   % Matrix of Am mean values
    MAmsd(z,:)=sx;                  % Matrix of Am standard deviation values
    MRhor(z,:)=px;                  % Matrix of Rho values
end
save('C:\MATLAB\Out\BasicVandM.mat','MAmm','MAmsd','MRhor')

%%------------------------ NORMALIZED RESISTANCE -------------------------

%%------- OUT OF PLANE ----------------------------

% Basic Input Parameters 3 storeys building

C1=0.050;       % Constant for computing fundamental period
mdegmin=0.4;    % Masonry degradation index, new=.28, moderate=.4, severe=.5
mdegmax=0.5;

Frontera=[0.75,0;3,0;3,1;3,0.8];    % Four possible boundary conditions of the
                                    % wall: cantilever, constrain, and
                                    % constrain with normal loading (3 and 4)
%Obtaining the resistance points according to section 4.5.1
for o=1:4
    fact=Frontera(o,1);
    f2=Frontera(o,2);
for i=1:T
    if i <= T/2
        Dw(1,i)=Dy(1,i);
        APared(1,i)=X(1,i);
    else
        Dw(1,i)=Dx(1,i-T/2);
        Hpp(1,i)=Hpp(1,i-T/2);
        Hsp(1,i)=Hsp(1,i-T/2);
        Htp(1,i)=Htp(1,i-T/2);
        APared(1,i)=Y(1,i-T/2);
```

```
        Den(1,i)=Den(1,i-T/2);
    end

%Defining possible building heights, including up to 2 multi-storey failures
    Ht(1,i)=Hpp(1,i)+Hsp(1,i)+Htp(1,i);
    h33(1,i)=Htp(1,i)*(0.7+0.3*rand());
    h323(1,i)=Hsp(1,i)*(0.5+0.5*rand())+Htp(1,i);
    HT33(1,i)=h33(1,i)/(qr3*Esp(1,i));
    HT323(1,i)=h323(1,i)/(Esp(1,i)*(qr3+qr2)/2);
    T1(1,i)=C1*Ht(1,i);
    LPared(1,i)= APared(1,i)/(Dw(1,i)+1);
    Iner1(1,i)=1*((qr3*Esp(1,i))^3)/12;
    Iner2(1,i)=1*((Esp(1,i)*(qr3+qr2)/2)^3)/12;
    Ncri1(1,i)= (pi^2)*Em(1,i)*Iner1(1,i)/(h33(1,i)^2);
    Ncri2(1,i)= (pi^2)*Em(1,i)*Iner2(1,i)/(h323(1,i)^2);
    omega1(1,i)=((pi^2)/h33(1,i)^2)*sqrt(Em(1,i)*Iner1(1,i)...
        /(1*Den(1,i)*qr3*Esp(1,i)/9.81)*(1-N3(1,i)/Ncri1(1,i)));
    omega2(1,i)=((pi^2)/h323(1,i)^2)*sqrt(Em(1,i)*Iner2(1,i)...
        /(1*Den(1,i)*Esp(1,i)*(qr3+qr2)/2/9.81)*(1-N3(1,i)/Ncri2(1,i)));
    Ta1(1,i)=2*pi/omega1(1,i);
    Ta2(1,i)=2*pi/omega2(1,i);
    if Ta2(1,i) >= T1(1,i)
        Ta2(1,i)=T1(1,i);
    end
    Dzeta1(1,i)=(3*(1+(Ht(1,i)-Htp(1,i)/2)/Ht(1,i)))/(1+(1-Ta1(1,i)/T1(1,i))^2)-
0.5;
    Dzeta2(1,i)=(3*(1+(Ht(1,i)-(Htp(1,i)+Hsp(1,i))/2)/Ht(1,i)))/(1+(1-Ta2(1,i)/...
        T1(1,i))^2)-0.5;
    Etype1(1,i)=2*N3(1,i)/(Den(1,i)*h33(1,i));
    Etype2(1,i)=2*N3(1,i)/(Den(1,i)*h323(1,i));
    FsWc1(1,i)=(1+f2*Etype1(1,i))*fact*(1-(mdegmin+rand()*(mdegmax-mdegmin)))...
    *Esp(1,i)*qr3/(h33(1,i)*Dzeta1(1,i))/(Den(1,i)*h33(1,i)*Esp(1,i)*LPared(1,i));
    FsWc2(1,i)=(1+f2*Etype2(1,i))*fact*(1-(mdegmin+rand()*(mdegmax-mdegmin)))...
    *Esp(1,i)*((qr3+qr2)/2)/(h323(1,i)*Dzeta2(1,i))/(Den(1,i)*h323(1,i)*Esp(1,i)...
    *LPared(1,i));
HTTot(o,i)=HT33(1,i); HTTot(o,T+i)=HT323(1,i);
FsTot(o,i)=FsWc1(1,i); FsTot(o,T+i)=FsWc2(1,i);
end
end
MHTTot=[HTTot(1,:);HTTot(2,:);HTTot(3,:);HTTot(4,:)];
MFsTot=[FsTot(1,:);FsTot(2,:);FsTot(3,:);FsTot(4,:)];
A=0;

for z=1:4
    x = MHTTot(z,:);
    for j=0:29
        px(1,j+1)=(min(x)*1.1)+j*((max(x)*.95)-(min(x)*1.1))/30;
    end
    y = MFsTot(z,:);
    j=0;
    for i=1:29
        for k=1:2*T
            if (x(1,k) <= px(1,i+1)) && (x(1,k)> px(1,i))
            j=j+1;
            A(1,j)=y(1,k);
            Hist(i,j)=A(1,j);
            end
        end
        ax(1,i)=exp(mean(log(A))+0.5*std(log(A))^2);
        sx(1,i)=ax(1,i)*sqrt(exp(std(log(A))^2)-1);
        A=0;
        j=0;
    end
    ax(1,30)=ax(1,29);
    sx(1,30)=sx(1,29);
    MRo(z,:)=ax;                    % Matrix of Iro mean values
    MRosd(z,:)=sx;                  % Matrix of Iro standard deviation values
    Mht(z,:)=px;                    % Matrix of H/t values
end
save('C:\MATLAB\Out\Outplane.mat','MRo','MRosd','Mht')
```

```
%%------- In PLANE ----------------------------

% Basic Input Parameters 3 storeys building

FResidual=0.2;                  % Masonry residual friction angle

% Boundary condition matrix (1 for flexible slab, 0.5 for rigid slab).
% Columns number is equal to failure criteria (1:Rocking, 2:D. tension, 3:M-C
shear)
% lines number related to the number of storeys.  Rocking according to figure 6.16a
MAlfa=[1,0.5,0.5;1.25,1,1;1,1,1];

%Obtaining the resistance in the In-plane

for z=1:(NumPi)

%Rocking
Normal=MNormal((2*z*MAlfa(1,z)),:);
for i=1:T
Alfa(1,i)=MAlfa(1,z);
X(1,i)=0.5*L(1,i)*Normal(1,i)*Esp(1,i)/(HL(1,i)*Alfa(1,i));
V(1,i)=X(1,i)*(1-(Normal(1,i)/(0.85*Com(1,i))));
VNorm(1,i)=V(1,i)/(Normal(1,i)*L(1,i)*Esp(1,i));
end
MFlex(z,:)=VNorm;

%Diagonal Shear
Normal=MNormal((2*z*MAlfa(1,z)),:);
for i=1:T
Alfa(1,i)=MAlfa(1,z);
Xx(1,i)=Tra(1,i)/(2.3*(1+HL(1,i)*Alfa(1,i)));
V(1,i)=Xx(1,i)*sqrt(1+Normal(1,i)/Tra(1,i)); % shear stress
VNorm(1,i)=V(1,i)/(Normal(1,i));
end
MDT(z,:)=VNorm;

%Mohr-Coulomb shear and sliding
Normal=MNormal((2*z*MAlfa(1,z)),:);
for i=1:T
Alfa(1,i)=MAlfa(1,z);
X(1,i)=L(1,i)*Esp(1,i);
V3(1,i)=FResidual*Normal(1,i);
X2(1,i)=(1.5*Coh(1,i)+Fri(1,i)*Normal(1,i));
V2(1,i)=X2(1,i)/(1+3*Coh(1,i)*HL(1,i)*Alfa(1,i)/Normal(1,i));
V1(1,i)=(Coh(1,i)+Fri(1,i)*Normal(1,i))/(1+Alfa(1,i)*HL(1,i));
    if V1(1,i)< V2(1,i) && V1(1,i)> V3(1,i)
        V(1,i)=X(1,i)*V1(1,i);
    else
        if V2(1,i)> V3(1,i)
           V(1,i)=X(1,i)*V2(1,i);
        else
           V(1,i)=X(1,i)*V3(1,i);
        end
    end
VNorm(1,i)=V(1,i)/(Normal(1,i)*L(1,i)*Esp(1,i));
end
MMC(z,:)=VNorm;
end
MTR=[MFlex;MDT;MMC];

    x = HL;
for z=1:(3*NumPi)
    for j=0:29
        px(1,j+1)=(min(x)*1.2)+j*((max(x)*.8)-(min(x)*1.2))/30;
    end
    y = MTR(z,:);
    j=0;
    for i=1:29
        for k=1:T
```

```
            if (x(1,k) <= px(1,i+1)) && (x(1,k)> px(1,i))
            j=j+1;
            A(1,j)=y(1,k);
            Hist(i,j)=A(1,j);
            end
        end
        ax(1,i)=exp(mean(log(A))+0.5*std(log(A))^2);
        sx(1,i)=ax(1,i)*sqrt(exp(std(log(A))^2)-1);
        A=0;
        j=0;
    end
    ax(1,30)=ax(1,29);
    sx(1,30)=sx(1,29);
    MIR(z,:)=ax;                    % Matrix of Ir mean values
    MIRsd(z,:)=sx;                  % Matrix of Ir standard deviation values
    MHL(z,:)=px;                    % Matrix of H/L values
end
save('C:\MATLAB\Out\Inplane.mat','MIR','MIRsd','MHL')
clear all
```

```
%%%%%%%%%%%%%%%%%%%%%%%%%%%%%%%%%%%%%%%%%%%%%%%%%
%                MATLAB VERSION 7.7             %
%                                               %
% Program to solve the limit state equation by  %
%  means of a Monte-Carlo simulation to obtain  %
%  the structural seismic fragility function,   %
%  and to attain the structural seismic risk    %
%          Part of the SAUMAC procedure         %
%                                               %
% Author: Jorge Munoz Barrantes                 %
% Technische Universität Braunschweig, 2012     %
% Last modified: 03.02.2012                     %
%%%%%%%%%%%%%%%%%%%%%%%%%%%%%%%%%%%%%%%%%%%%%%%%%


clear all;
clc;
T=100;                 % total number of simulations
stepacc=0.002;          % acceleration step

%%------------------------ BASIC IMPUTS ----------------------------

NumPi=3;                % Number of storeys (in between 1 and 3)

% Matrix for the obtained in-plane resistance "Ir" values in x direction
% 1st Columns is equal to mean and second to standard deviation
% lines number related to the number of storeys.
MVNX=[0.24,0.04;0.45,0.04;0.4,0.03];

% Matrix for the obtained in-plane resistance "Ir" values in y direction
MVNY=[0.44,0.04;0.5,0.04;0.5,0.03];

% Matrix for the out-of-plane resistance "Iro" values (same for x or y)
MVNO=[0.07,0.02];

% Matrix for the obtained in-plane Am values in x direction
MAMX=[1.6,0.25;1.7,0.25;2,0.4];

% Matrix for the obtained in-plane Am values y direction
MAMY=[1.6,0.25;1.7,0.25;2,0.4];

% Matrix of seismic action FS coefficients.  1st column for in-plane and
% second column for out of plane.  Number of lines according to the number
% of total storeys.  Different mean values of PGA are introduced to develop
% the fragility curve
MSeis=[1,0.5;1.4,0.5;1,1];
SSD=0.5;                % PGA standard deviation value (User defined, recommend
                        % min to 0.37 and max of 0.7)

%%------------------------ Computing Fragility --------------------------

MTR=[MVNX;MVNY;MVNO];
MTA=[MAMX;MAMY;1,0.001];
MTS=[MSeis(:,1);MSeis(:,1);max(MSeis(:,2))];
z=0;
sum=0;
for o=1:(2*(NumPi)+1)   % 2 times for x and y, and +1 for out-of-plane

for j=1:(1/stepacc)     % Computation up to 1 g of reference PGA
    acc(1,j)=j*stepacc; % Mean reference PGA value
    h=0;                % number of fails
    for i=1:T
    logacc(1,i)=log(acc(1,j));
    Rndacc(1,i)=normrnd(logacc(1,i),SSD);
    Rndacc(1,i)=MTS(o,1)*exp(Rndacc(1,i));
    Rndrest(1,i)=normrnd(MTR(o,1),MTR(o,2));
    Rndmasa(1,i)=normrnd(MTA(o,1),MTA(o,2));
    if (Rndacc(1,i)*Rndmasa(1,i))>Rndrest(1,i)
        h=h+1;
    end
```

```
    end
    Pfail(1,j)=h/T;
end
psd=sqrt(std(Pfail)/1.6); %logn std is aprox the varianza value of normal.
z=1-(0.5+(std(Pfail)^2)/2);
for k=1:(1/stepacc)
if Pfail(1,k)>(z-0.025) && Pfail(1,k)<(z+0.025)
    p50=acc(1,k);
end
end
Pcdf=logncdf(acc,log(p50),psd); %lognorm is the best fitting pdf.

if o==(2*(NumPi)+1)
    MFragO(1,:)=Pcdf;
else
    MFragI(o,:)=Pcdf;
end
end

MFragIT=max(MFragI);            % finds the maximum curve values in the in-plane
MIO=1-(1-MFragIT).*(1-MFragO);  % joint, out-of-plane, in-plane fragility

%%------------------------ Computing Fragility -------------------------
% the risk integral is approximated by the midpoint numerical integration
% rule

for j=5:(1/stepacc)
    acc(1,j)=j*stepacc;
    dePcc(1,j)=-0.001*acc(1,j)^(-2.63)+0.000567*acc(1,j)^(-1.63); % derivate of the
                                                                  % risk H function
    Prisk(1,j)=abs(dePcc(1,j))*MIO(1,j)*stepacc;
    sum=sum+Prisk(1,j);
    SPrisk(1,j)=sum;
end

save('C:\MATLAB\Out\Frag&Rrisk.mat','MIO','SPrisk','acc')
clear all
```

APPENDIX D: Seismic Design Base Forces according to various Seismic Codes

COSTA RICA, CSCR 2002 [CFIA-02]

$$V = CW = \left(\frac{a_{ef} IFED}{SR}\right) W \qquad T = 0.05N$$

C= Seismic coefficient
W= Weight (Dead + % of live load combination (100-25%))
a_{ef}= Effective seismic acceleration (for prob. of occurrence= 10% (P_R= 475years) or 2% (P_R=50 years)), varies according to soil type.
I= Importance factor
SR= Over strength factor (2 for reinforced masonry, 1.2 for URM)
V= Seismic Base Shear force (KN)
FED= Response acceleration coefficient (Based T and Damping)
T= Structural natural period (masonry)
N= Total number of storey
μ= Global assigned ductility

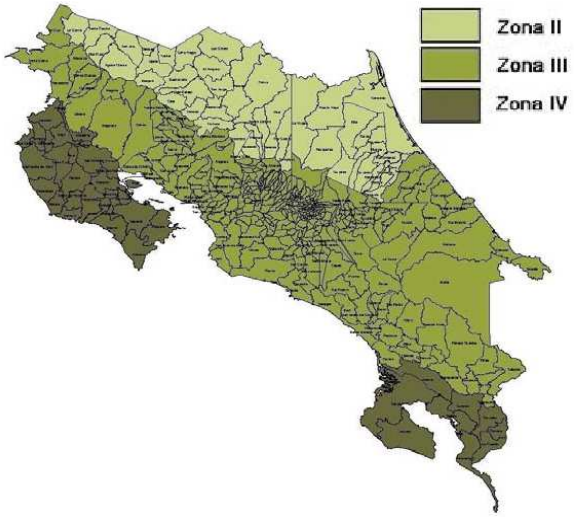

Global Ductility Value

Reinfoced masonry walls (Wall rest. sytem)

Regular	Irregular	Optime ductility	Moderate ductility	Factor "u"
x		x		3
x			x	2
	x	x		1,5
	x		x	1

Unreinfoced masonry walls (Other rest. system)

Regular	Irregular	Optime ductility	Moderate ductility	Factor "u"
x		x		1,5
x			x	1
	x	x		1
	x		x	1

Importance Factors

Group	*Brief Descrition*	*Factor "I"*
A and B	Important community building, hospitals, emergency buildings, large assembly halls, power stations, emergency refuge, risky structures (flamable materials, toxic, explosives)	1,5
C and D	Normal housing, schools, small clinics, offices	1
E	Temporal construction work, fences, agricultoral construction	0.75

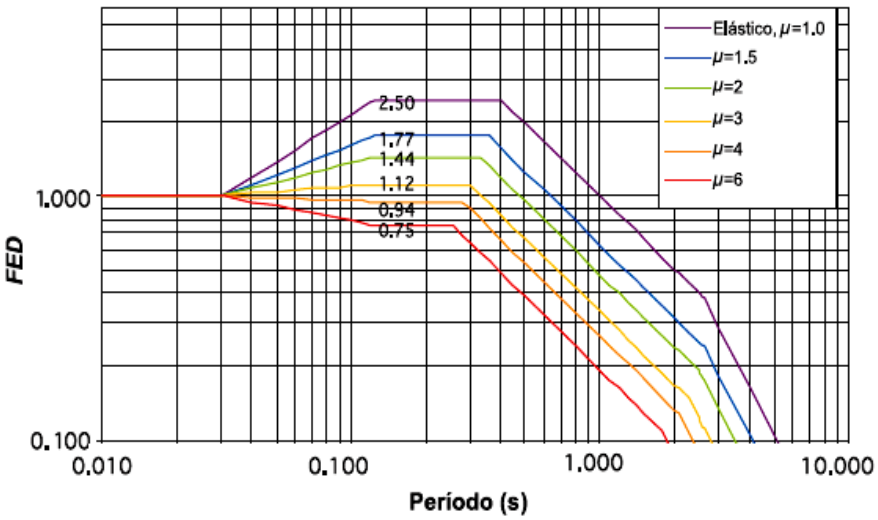

FED Values for a 5% damping and a Stiff soil type

INDIA, IS-1893 [IISEE WEB]

$$V_B = A_h W = \left(ZI \frac{(S_a / g)}{2R} \right) W \qquad T_a = \frac{0.075}{\sqrt{A_w}} h^{0,75}$$

A_h= Design horizontal acceleration spectrum value
W= Weight (Dead + % of live load combination (50-25%))
Z= Zone factor (for prob. of occurrence= 10% (P_R= 475years) or 2% (P_R=50 years)) (g)
I= Importance factor
R= Response reduction factor
V_B= Seismic Base Shear force (KN)
(S_a/g)= Response acceleration coefficient (Based : T_a and Damping)
T_a= Structural natural period (masonry)
A_w= Total effective wall are in the first storey. (in m2)
h= Total building height

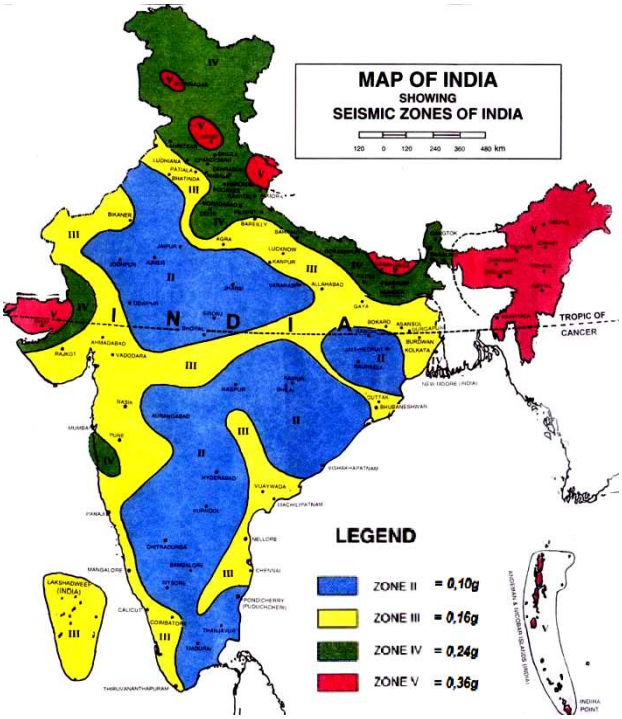

Importance Factors

Group	*Brief Descrition*	*Factor "I"*
I	Important community building, hospitals, school, monuments, emergency buildings, large assembly halls, power stations and subway stations	1,5
II	All Others	1

Responce Reduction Factor

Lateral Load Resistance System	*Factor "R"*
Normal URM	1,5
URM reinforced with horizontal RC bands	2,25
Reinforced Masonry	3
Special Reinforced Shear wall	4

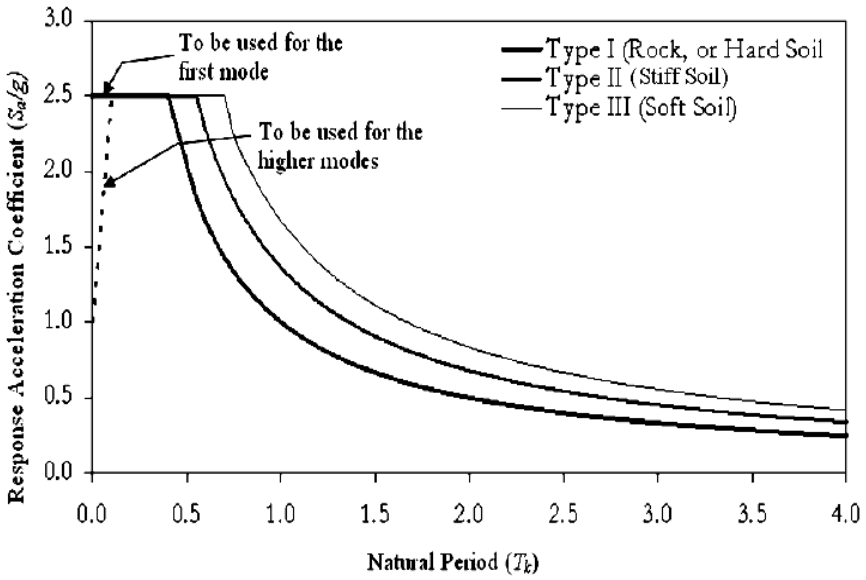

Multiplying factors for obtaining (Sa/g) values for other damping

Damping (%)	Factors
0	3.20
2	1.40
5	1.00
7	0.90
10	0.80
15	0.70
20	0.60
25	0.55
30	0.50

USA, IBC 2003 [IBC-03]

$$V = C_S W$$

$$T_a = 0.055 h_N^{0.75}$$

$$S_{DS} = \frac{2}{3} F_a S_S$$

$$T \le C_u T_a$$

$$C_S \begin{cases} = S_{DS} I / R \\ \ge 0.044 S_{DS} I \end{cases}$$

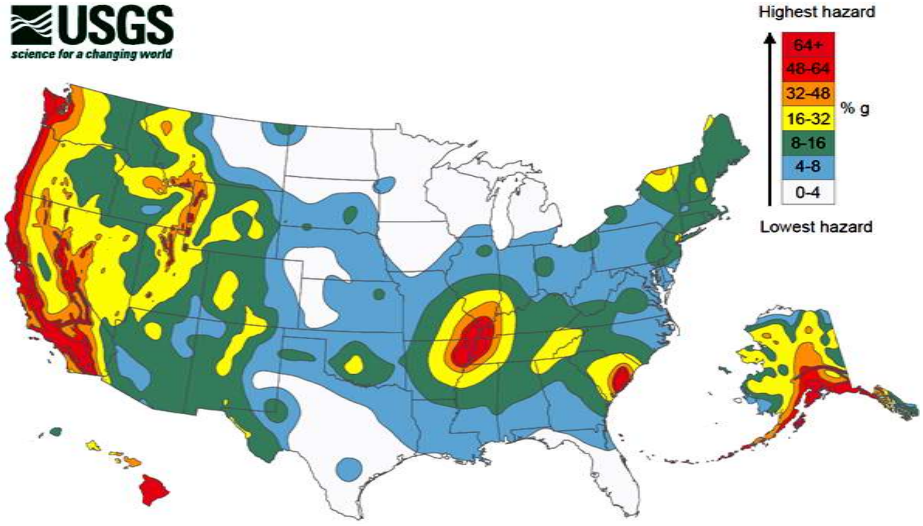

C_S= seismic response coefficient
W= Weight (Dead + % of live load (20-25%))
S_{DS}= design spectral response acceleration in the short period range (units of g) (150% of UBC PGA)
I= Occupancy factor
R= response modification factor
V= Seismic Base Shear force (KN)
S_S= Maximum considered spectral acceleration. (Short periods)
T= Structural natural period (masonry), Ta= Aprox. period
C_u= coefficient for upper limit on calculated period

Response Modification Coefficient

Basic Seismic Force Resisting System	R
Special reinforced masonry shear walls	5
Intermediate reinforced masonry shear walls	3½
Ordinary reinforced masonry shear walls	2½
Detailed plain masonry shear walls	2
Ordinary plain masonry shear walls	1½

Site Class	values of F_a				
	$S_S \le 0.25$	S_S = 0.5	S_S = 0.75	S_S = 1.0	$S_S \ge 1.25$
hard rock	0.8	0.8	0.8	0.8	0.8
rock	1.0	1.0	1.0	1.0	1.0
very dense soil and soft rock	1.2	1.2	1.1	1.0	1.0
stiff soil	1.6	1.4	1.2	1.1	1.0
soil	2.5	1.7	1.2	0.9	0.9
F	*	*	*	*	*

* site specific geotechnical evaluation required

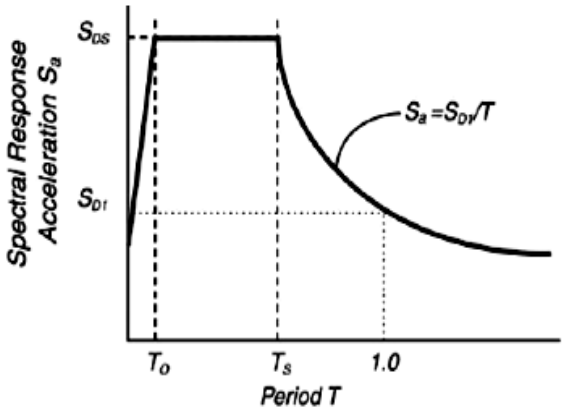

Occupancy Factor, I

Seismic Use Group	Typical Structures	I
I	All buildings not included in II and III (including low hazard buildings (agriculture, temporary structures, etc.))	1.0
II	Substantial hazard to human life (300+ people, day care (150+), schools (250+), college/university (500+), health care (50+), jails, etc.)	1.25
III	Essential facilities (hospital, fire, designated emergency shelters, emergency preparedness facilities, power stations, aviation control, etc.) Structures containing extremely hazardous materials	1.5

Design spectral response acceleration at 1 second	C_u
$S_{D1} \ge 0.4$	1.4
S_{D1} = 0.3	1.4
S_{D1} = 0.2	1.5
S_{D1} = 0.15	1.6
S_{D1} = 0.1	1.7
$S_{D1} \le 0.05$	1.7

NEW ZEALAND, NZS 4203:1992 [IISEE WEB] [NZS-92]

Z= Zone factor, clearly related with the seismic ground acceleration
C_b= Basic seismic acceleration coefficients (related with T and μ from figure)
μ= for URM equal to 1 (when 15% of damping is used) or 1.5 (when an equivalent 5% of damping is used) (from NZS 1170.5)
R= Risk factor for a structure (related to the importance of the structure and the design life)
C= Seismic Base Shear force coefficient. In the ultimate limit state shall not be taken as less than 0.025, and here is for a period less than 0.4
T_1= First structural natural period
L_S= Limit state factor for the serviceability limit state
V= Probable base shear
W= Weight of the structure

$$V = CW = WC_b(0.4, \mu)RZL_S$$

$$T_1 = \leq 0.4s$$

$$L_S \begin{cases} Serviciability = 1/6 \\ Ultimate = 1 \end{cases}$$

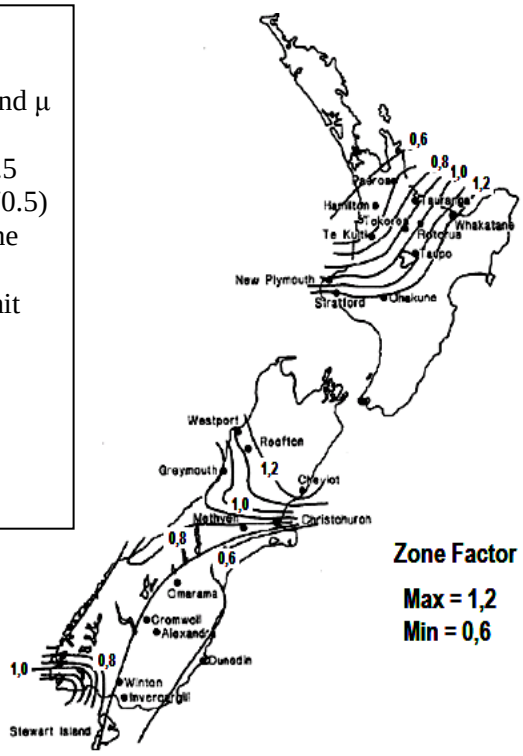

Risk Classification Based on Life Safety Risk

No. of Persons at Risk of Death or Serious Injury from Failure	Hazard level of contents		
	Low	Moderate	High
0	Negligible	Negligible	Slight
0 < No. < 1	Negligible	Slight	Moderate
1 < No. < 10	Slight	Moderate	Serious
10 < No. < 100	Moderate	Serious	Extreme
No. > 100	Serious	Extreme	Extreme

Risk Factors

Consequences of Failure	Recommended Design Return Period (yrs)	Risk Factor
Negligible	50	0.5
Slight	200	0.8
Moderate	450	1.0
Serious	1000	1.3
Extreme	2000	1.6

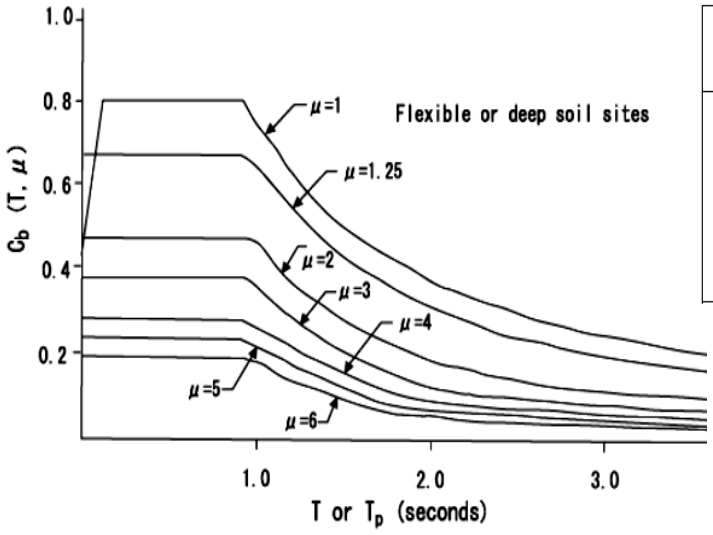

Recommended Risk Factors for Non-standard Design Life

Design Life (yrs)	Risk Category				
	Negligible	Slight	Moderate	Serious	Extreme
< 5	0.2	0.3	0.5	1.3	1.6
10	0.3	0.4	0.6	1.3	1.6
25	0.4	0.6	0.8	1.3	1.6
50	0.5	0.8	1.0	1.3	1.6
100	0.6	1.0	1.2	1.6	2.0

LIST OF ABBREVATIONS AND SYMBOLS

Abbreviations

CDF	Cumulative Density Function
CPLS	Collapse Prevention Limit State
CSH	Cultural, Social and Historical
DLLS	Damage Limitation Limit State
DSHA	Deterministic Seismic Hazard Assessment
EC	European Code
EMS-98	European Macroseismic Scale 1998
ERS	Elastic Response Spectrum
FEMA	Federal Emergency Management Agency
FORM	First Order Reliability Method
GDP	Gross Domestic Product
GRK-802	International Graduate College "Risk Management of Natural and Civilization Hazards on Buildings and Infrastructure"
HAZUS	HAZards United States
IBC	International Building Code
INGV	National Institute of Geophysics and Vulcanology (Istituto Nazionale di Geofisica e Vulcanologia)
IQM	Masonry Quality Index (Indice di Qualità Muraria)
ISO	International Standard Organization
JBDPA	The Japan Building Disaster Prevention Association
JCSS	Joint Commission of Structural Safety
JMA	Japanese Meteorological Agency
LS	Limit State
LSLS	Life Safety Limit State
MC	Monte Carlo simulation
M-C	Mohr-Coulomb failure criteria
MCS	Mercalli-Cancani-Sieberg seismic intensity scale
MM	Modify Mercalli seismic intensity scale
MSK	Medvedev Sponheuer-Karnik seismic intensity scale
NEHRP	National Earthquake Hazards Reduction Program
OLS	Operational Limit State
PDF	Probability Density Function
PGA	Peak Ground Acceleration
PGD	Peak Ground Displacement
PGV	Peak Ground Velocity
PSHA	Probabilistic Seismic Hazard Assessment
RADIUS	Risk Assessment tools for DIagnosis of Urban areas against Seismic disasters
RC	Reinforced Concrete
RISK-UE	European Risk assessment group
SAMCO	Structural Assessment, Monitoring and Control
SAUMAC	Seismic Assessment of Unreinforced Masonry according to local Architectural and Code conditions

SDOF	Single Degree of Freedom
SDS	Seismic Design Spectrum
SEAOC	Structural Engineers Association of California
SHM	Stochastic House Modeling
SLS	Serviceability Limit State
SORM	Second Order Reliability Method
ULS	Ultimate Limit State
UN	United Nations
URM	UnReinforced Masonry buildings

Latin Symbols

A	Amplitude displacement of a seismic record
A_f	Seismic source rupture area
a_g	Peak ground acceleration
a_{gR}	Reference PGA
A_M	Architectural mass index at level i
b	Variable depending in the pier shape ratio
c	Cohesion
C_S	Seismic coefficient
C_{Smix}, C_{Smin}	Minimun and maximum inter-wall clear span
c_u	non-drained shear resistance
D_f	Fault slip distance
D_{LS}	Damage for a limit state
D_S	Distance from seismic source
D_{S95}	Significant damage duration
D_x, D_y	Number of internal walls in the x and y axis directions
E_m	Elastic modulus
e_o	Structural eccentricity
F_a	Horizontal force acting on the mass center
f_{bc}	Compression resistance of bricks
f_{bm}	Mean compression load of bricks from a 30 elements sample
f_{bt}	Traction load resistance of bricks
F_{EC}	Irregularity index
F_{EW}	Wall Elastic Factor
f_{ex}, f_{ix}, f_{ey}, f_{iy}	Parameters for obtaining the wall resistance area in x and y for internal and external walls
$F_G(\cdot)$	Cumulative density function
f_m	Masonry wall compression resistance
F_o	Out-of-plane rigid threshold resistance
f_{tu}	Masonry wall tension resistance
f_v	Masonry wall shear resistance
f_{vo}	Masonry wall shear resistance at zero normal stress
F_W	Wall factor
f_x	Masonry wall flexural bending
g	Gravity acceleration 9.8 m/s2
$G(X)$	Limit state equation

G_c	Fracture energy in compression
G_f	Fracture energy in tension
G_k	Permanent actions weight
G_m	Material shear modulus
H	Annual seismic hazard function
H_o	Effective wall height
h_p	Pier height
H_{PB}, H_{P1},H_{P2}	Floors height at the 1st, 2nd, and 3rd floor
H_S	Total building height
h_s	Spandrel height
I	Seismic intensity or moment of inertia
i	Seismic intensity variable
I_A	Arias intensity
I_R	Normalized storey shear index at level i
I_{Ro}	Resistance in the out-of-plane index
I_S	Seismic design action index
I_{So}	Solicitation in the out-of-plane index
k, k_O	Constants from seismic hazard curves
K_E	Wall elastic stiffness
L_{eff}	Sum of all lp in a wall
L_{max}	Largest lp in a wall
L_O	Loss
l_p	Pier length
l_s	Spandrel length
L_T	Wall length
M	Earthquake Richter magnitude
m	Mass, or seismic magnitude (in equations to refer M)
m_b	Body wave magnitude
M_E	Energy magnitude
M_f	Rocking moment
M_i	Model basic variable for i
m_N	Normal action of mass of storeys over the analyzed i level
M_o	Moment magnitude
M_S	Surface magnitude
m_T	Total mass of storeys over the analyzed i level
n	Total number of storeys, or total number of basic variables
N	Normal force, or total number of samples
N_{crit}	Critical euler force
N_o	Number of fails
P_1	Probability of occurrence in one year
p_f	Element probability of failure
P_f	system probability of failure
$P_f(PGA)$	System fragility curve
p_{fin}	maximum pf in-plane
p_{fout}	maximum pf out-of-plane
$p_{fx,y}$	maximum pf in x and y
P_{PB}, P_{P1}, P_{P2}	Slabs weight at the 1st, 2nd, and 3rd floor

P_V	Probability of occurrence during the life span
q	Behavior factor
q_a	Behavior factor for non-structural elements
q_i	Parameters i to compute FEC
Q_{Kav}	Average live load per storey
Q_{kt}	Live load at the top storey
r	Reliability
R	Resistance
R_E	Shear resistance ratio of single pier elements
R_P	Return period
R_S	Structural risk
R_{SW}	Shear resistance ratio of storey
R_T	Total risk
R_W	Shear resistance ratio of wall
S	Solicitation-Seismic Demand
S_a	Spectral acceleration for non-structural elements
$S_d(T)$	Spectral acceleration
S_{Pa}	Pseudo-acceleration
S_S	Soil factor
T_1	First fundamental vibration period
T_a	Fundamental period of a non-structural element
T_B, T_C, T_D	Design spectrum points
T_d	Total record duration
t_{eq}	Equivalent wall thickness
T_V	Structure life span
V	Shear fore
V_b	Design base shear
V_{DS}	Diagonal tension shear according to Turnsek
V_{DSb}	Diagonal tension shear according to Magenes
V_f	Rocking shear
v_i	Coefficient of variation of any variable i (σi/μi)
$V_i(\delta)$	Wall resistance of individual piers
V_{max}	Minimum shear resistance
v_o	length of void in a wall
V_S	Shear wave velocity
V_{S30}	Shear wave velocity in the terrain first 30 meters
V_{SSC}, V_{SSW}	Mohr-Coulomb shear resistance
$V_W(\delta)$	Total wall shear resistance
w	Angular frequency
W	Weight
W_a	Weight of a wall
X	Façade, front dimension of a house, or random variable
x	Principal axis
y	Principal axis
Y	Depth dimension of a rectangular house
Z	Seismic zone, or safety margin
Z_a	Height of mass center of a wall at storey i from the ground

z_i	height of the concentrated mass from the ground to storey i

Greek Symbols

α	Normalized reference PGA
α_R	Resistance sensibility factor
α_S	Solicitation sensibility factor
α_V	Shear ratio
β	Safety index
β_f	Bound factor of response spectrum
β_o	Target safety index
γ	Material density
γ_I	Structure importance factor
γ_R	Partial safety factor for resistance
γ_S	Partial safety factor for solicitation
Δ	storey drift
δ	Lateral displacement
Δ_1, Δ_2	Displacement parameters for the out-of-plane tri-linear formulation
Δ_{CP}	Collapse prevention drift value
δ_E	Elastic lateral displacement
Δ_{LS}	Life safety drift value
Δ_S	Serviceability drift value
δ_U	Ultimate lateral displacement
Δ_u	Final stable displacement
ζ_i	Standard deviation value of any variable i in a lognormal distribution
η	Damping coefficient
λ	Base shear correction factor
λ_i	Mean value of any variable i in a lognormal distribution
λ_O	Annual rate of earthquakes
μ	Friction
μ_i	Mean value of any variable i
μ_p	Pier ductility factor
ρ	Normalized cross section wall area of resistant walls
σ_i	Standard deviation value of any variable i
σ_N	Normal compressive stress
τ	Shear stress
ϕ_v	Percentage of voids in bricks
ψ	Normal loading factor
ψ'	Boundary condition parameter for computing resistant shear

REFFERENCES

[AB 07] S. Akkar, J.J. Bommer. "Prediction of elastic displacement response spectra in Europe and the Middle East" Earthquake Engineering and Structural Dynamics, 2007

[AdL 97] A.H.S Ang, D. de Leon. "Determination of optimal target reliabilities for design and upgrading of structures" Structural Safety, 1997

[AFPS 10] "Conception et realization d'etablissements de santé en zone sismique" Association Française du génie Parasismique, Cahier Technique n°29, 2010

[AGS 00] "Landslide risk management concepts and guideless" Australian Geomechanics Society, Australian Geomechanics, 2000

[AKTB 09] Ö Aydan, H. Kumsar, S. Toprak and G. Barla. "Characteristics of 2009 L'Aquila earthquake with an emphasis on earthquake prediction and geotechnical damage" Journal of The School of Marine Science and Technology, Tokai University, 2009

[Ao 00] Y. Aoki, Y. Ohashi, H. Fujitani, T. Saito, J. Kanda, T. Emoto, M. Kohno. "Target Seismic Performance Levels in Structural Design for Buildings" 12th World Conference on Earthquake Engineering, Auckland, 2000

[AP 09] N. Augenti, F. Parisi. "Influence of mechanical properties uncertainties on seismic vulnerability of masonry buildings" IF CRASC'09, 2009

[Ba 08] J.W. Baker. "An introduction to probabilistic seismic hazard analysis (PSHA)" ftp INGV, 2008

[BB 11] J. K. Bothara, S. Brzev. "A Tutorial: Improving the seismic performance of stone masonry buildings" Earthquake Engineering Research Institute, California, 2011

[BB 83] R. Bolin, P. Bolton. "Recovery in Nicaragua and the USA" International Journal of Mass Emergencies and Disasters, pp 125-152, 1983

[BBM 01] B. Bhattacharya, R. Basu, K. Ma. "Developing target reliability for novel structures: the case of Mobile Offshore Base" Marine Structures, 2001

[BBŽ 08] V. Bosiljkov, A.W. Page, V. Bokan-Bosiljkov, R. Žarnic. "Evaluation of the seismic performance of brick masonry walls" Journal for Structural Control and Health Monitoring, 2008

[BdD 09] A. Borri, A. de Maria. "IQM, indice di qualita muraria – aplicazioni nell'ambito delle NTC 2008 – L'Edilizia" Centro Studi Sisto Mastrodicasa, 2009

[BDM 09] J. K. Bothara, R. P. Dhakal, J.B. Mander. "Seismic performance of an unreinforced masonry building: An experimental investigation" Earthquake Engineering Structural Dynamics, 2009

[Be 99] A. Bernardini. "Seismic Damage to Masonry Buildings" International Workshop of Seismic Damage to Masonry Buildings, Padua, 1999

[BHAL 98] H.J. Burd, G.T. Houlsby, C.E. Augarde, G. Liu. "Prediction of Tunnel-Induced Settlement Damage to Masonry Structures" Report No. OUEL 2162/98. University of Oxfort, 1998

[BJF 97] D. Boore, W. Joyner, T. Fumal. "Equations for estimating horizontal response spectra and peak acceleration from western North American earthquakes: A summary of recent work" Seismological Research Letters, 1997

[Bl 09] R. Blong. "ADB Consultant Report: Country Natural Hazard and Vulnerability Assessment Procedure" Asian Development Bank, 2009

[Bo 02] J. Bommer, R. Spence, M. Erdik, S. Tabuchi, N. Aydinoglu, Booth, E., Del Re, D., and Peterken, O. "Development of an earthquake loss model for Turkish catastrophe insurance" Journal of Seismology, 2002

[BP 09] L. Boscotrecase, F. Piccarreta. "Edifici in Muratura in Zona Sismica" Dario Flaccovio Editore, 2009

[Br 11] A. Breschi. "Riconstruire dopo il Terremoto "Il Caso Castelnuovo (AQ)": analisi e progetto architettonico" Volume 1, Alinea Editrice srl, Firenze, 2011

[CA 95] A.C. Costly, D.P Abrams. "Dynamic Response of URM Buildings with flexible Diaphragms" Structural Research Series No. 605, University of Illinois at Urbana-Champaign, October 1995

[Ca 99] G.M. Calvi. "A Displacement-Based Approach for vulnerability Evaluation of Classes of Builidng" Journal on Earthquake Engineering, 1999

[CF 10] A. Ciabatone, G. Farina. "Analisi dei Danni e Vulnerabilitá' Sismica della Frazione di Castelnuovo in San Pio delle Camere (AQ) e Progetto Arquitectonico-Strutturale di un Nuovo Edificio Residenziale a Schiera per la Ricostruzione Post-Sisma" Tesi di Laurea. Università di Firenze, 2010

[CFIA-02] "Código sísmico de Costa Rica" Colegio Federado de Ingenieros y Arquitectos (CFIA), Editorial Tecnológica de Costa Rica, Cartago, 2002

[Ch 01] A.K. Chopra. "Dynamics of Structures: Theory and Applications to Earthquake Engineering" Prentice Hall, 2001

[CM 09] J.D. Cummins, O. Mahul. "Catastrophe Risk Financing in Developing Countries: Principles for Public Intervention" The World Bank, Washington D.C, 2009

[CP 93] R.W. Clough, J. Penzien. "Dynamics of Structures" McGraw-Hill, 1993

[Cr 01] G. Croci. "Strengthening of monuments under the effect of static loads, soil settlements and seismic actions – Examples" Historical Constructions, Guimarães, 2001

[CSP 92] A.W. Coburn, R.J.S. Spence, A. Pomonis. "Factors determining human casualty levels in earthquakes: Mortality prediction in building collapse" Proceedings of the 10th World Conference on Earthquake Engineering, Madrid, 1992

[DGL 02] K. Doherty, M.C. Griffith, N. Lam, J. Wilson. "Displacement-based seismic analysis of out-of-plane bending of unreinforced masonry walls" Earthquake Engineering and Structural Dynamics, 2002

[DHB 94] R.G. Drysdale, A.A. Hamid, L.R. Baker. "Masonry Structures—Behavior and Design" Prentice-Hall. Inc., 1994

[Do 00] K. Doherty. "An investigation of weak links in the seismic load path of unreinforced masonry buildings". PhD Thesis, University of Adelaide, 2000

[Do 06] M. Dolce, A. Kappos, A. Masi, G. Penelis, M. Vona. "Vulnerability Assessment and Earthquake Damage Scenarios of the Building Stock of Potenza (Southern Italy) Using Italian and Greek Methodologies" Engineering Structures, 2006

[Do 98] D. Dowrick. "Damage and intensities in the magnitude 7.8 1931 Hawke's bay, New Zealand, earthquake." Bulletin of the New Zealand Society for Earthquake Engineering, 1998

[DRLG 00] K. Doherty, B. Rodolico, N. Lam, M.C. Griffith. "The modeling of earthquake induced collapse of unreinforced masonry walls combining force and displacement principals" 12th World Conference of Earthquake Engineering, 2000

[DS 02] D. D'Ayala, E. Speranza. "Housing Report: Single-family stone masonry house" World Housing Encyclopedia, 2002

[DS 03] D. D'Ayala, E. Speranza. "Definition of collapse mechanisms and seismic vulnerability of history masonry buildings" Earthquake Spectra, 2003

[EC-0] "Eurocode 0, Basis of Structural Design" European Committee for Standardization (CEN), 2002

[EC-6] "Eurocode 6, Design of masonry structures, Part 1: General rules for reinforced and unreinforced masonry structures" European Committee for Standardization (CEN), 2005

[EC-8.1] "Eurocode 8, Design of structures for earthquake resistance, Part 1: General rules, seismic action and rules for buildings" European Committee for Standardization (CEN), 2005

[EC-8.3] "Eurocode 8, Design of structures for earthquake resistance, Part 3: Strengthening and repair of buildings" European Committee for Standardization, 2005

[EEFIT 09] "The L'Aquila, Italy Earthquake of 6 April 2009" A preliminary field report by the UK Earthquake Engineering Field Investigation Team, 2009

[Ei 88] H.H. Einstein. "Landslide Risk Assessment Procedure" Proceedings Fifth International Symposium On Landslides, Lausanne, 1988

[EN 1052-3] "EN 1052-3: Methods of test for masonry-Part 3 Determination of initial shear strength" European Committee for Standardization, 2007

[Er 11] M. Erdik, K.Sesetyan, M.B. Demircioglu, U. Hancılar, C. Zülfikar. "Rapid earthquake loss assessment after damaging earthquakes" Soil Dynamics and Earthquake Engineering, 2011

[FDPS 04] M. Ferrini, L. Decanini, A. Pagliazzi, S. Scarparolo. "Edifici in Muratura in Zona Sismica. Rilevamento delle Carenze Structturali" Regione Toscana. 2004.

[FEMA 97] Federal Emergency Management Agency (FEMA). "Multi-Hazard Identification and Risk Assessement: The Cornerstone of the National Mitigation Strategy" 1997

[FEMA web] HAZUS-MH MR2 http://www.fema. gov/plan/prevent/hazus/hz_manuals.shtm

[FEMA-154] "Rapid Visual Screening of Buildings for Potential Seismic Hazards" Applied Technology Council (ATC), Washington, 2002

[FEMA-273] "NEHRP Guidelines for the Seismic Rehabilitation of Buildings" Federal Emergency Management Agency (FEMA), 1997

[FEMA-306] "Evaluation of earthquake damaged concrete and masonry wall buildings" Applied Technology Council (ATC-43 Project), 1998

[FEMA-310] "Handbook for the Seismic Evaluation of Buildings" Federal Emergency Management Agency (FEMA), 2002

[FEMA-356] "Prestandard and commentary for the seismic rehabilitation of buildings" Report No. 356. Federal Emergency Management Agency (FEMA), Washington, 2000

[FEMA-368] "NEHRP Recommended provisions for seismic regulations for new buildings and other structures" Prepared by the Building Seismic Safety Council for the Federal Emergency Management Agency, 2000

[Fi 10] E.H. Field. "Probabilistic Seismic Hazard Analysis (PSHA)" openSHA.org tutorials, California, 2010

[Fl 07] R. Flesch. "European Manual for in-situ Assessment of Important Existing Structures" LESSLOSS Report No. 2007/02. IUSS Press, Pavia, 2007

[Fo 09] P. Foraboschi. "Coupling effect between masonry spandrels and piers" Materials and Structures, 2009

[Fr 10] T.M. Frankie. "Simulation-based fragility relationships for unreinforced masonry buildings" Master Thesis, University of Illinois at Urbana-Champaign, 2010

[Ga 08] K. A. Ganjouei, L. Ekhlaspour, E. Iranmanesh, P. Poorian, S. Sohbati, N. Ashrah, N. A. Ganjouei, F. Rashid-Farokhi, S. Karamuzuzian. "The Pattern of Injuries among the Victims of the Bam Earthquake" Iran Journal of public health, 2008

[GA 09] M. Greene, D. D'Ayala. "Providing building data in support of PAGER final technical report" Earthquake Engineering Research Institute 2009

[Ga 85] H.R. Ganz. "Mauerwerkscheiben unter Normalkraft und Schub". ETH Zürich, Institut für Baustatik and Konstruktion, Birkhäuser Verlag, Basel, 1985

[GAC 06] T. Glade, M. Anderson, M. Crozier, "Landslide Hazard and Risk" John Wiley and Sons, 2006

[GC 09] P. Galli, R. Camassi. "Rapporto sugli effetti del terremoto aquilano del 6 aprile 2009" Dipartimento della Protezione Civile Nazionale (PCN), Istituto Nazionale di Geofisica e Vulcanologia (INGV), 2009

[Gi 05] S. Giovinazzi. "The Vulnerability Assessment and the Damage Scenario in Seismic Risk Analysis" PhD Thesis, University of Florence, 2005

[GL 97] L. Gambarotta, S. Lagomarsino. "Damage models for the seismic response of brick masonry shear walls. Part II: the continuum model and its applications" Earthquake Engineering and Structural Dynamics, 1997

[GM 05] M. Ghafory-Ashtiany, R. Mousavi. "History, geography, and economy of Bam" Earthquake Spectra, 2005

[GNDT-07] "Manuale per la compilazione della scheda di 1◦ livello di rilevamento danno, pronto intervento e agibilità per edifici ordinari nell'emergenza post-sismica" Gruppo Nazionale per la Difesa dai Terremoti (GNDT), Rome, 2007

[GR 54] B. Gutemberg, C.F. Richter. "Seismicity of the Earth and Associated Phenomena" Princeton University Press, Princeton, 1954

[Gr 98] G. Grünthal. "European Macroseismic Scale" Centre Européen de Géodynamique et de Séismologie, Luxembourg, 1998

[HAZUS 99] "Earthquake loss estimation methodology earthquake HAZUS, technical and users manual" Federal Emergency Management Agency (FEMA), Washington, 1999

[HKB 00] E. Hoek, P.K. Kaiser, W.F. Bawden. "Support of underground excavations in hard rock" Funding by Mining Research Directorate and Universities Research Incentive Fund, 2000

[HL 74] A.M. Hasofer, N.C. Lind. "Exact and invariant second-moment code format" Proc. ASME, Journal of the Engineering Mechanicals Division, 1974

[IBC-03] "The International Building Code: Seismic Design Provisions" International Code Council (ICC), Virginia, 2003

[IISEE web] "Seismic Design Codes" International Institute of Seismology and Earthquake Engineering (IISEE), http://iisee.kenken.go.jp/net/seismic_design_code/index.htm

[ilCentro web] "Abruzzo, 6 Aprile 2009. Le Vittime del Terremoto " GElocal ilCentro, http://http://racconta.kataweb.it/terremotoabruzzo/index.php

[INGV 11] R. Moschillo, M. Pignone, C. Nostro. "150 anni di storia sismica: 150° Aniversario Italia Unita" Istituto Nazionale di Geofisica e Vulcanologia (INGV), 2011

[INGV web] "Mappa di pericolosità sismica del territorio nazionale" Istituto Nazionale di Geofisica e Vulcanologia (INGV), 2006 http://zonesismiche.mi.ingv.it/

[INGV web] Instituto Nazionale di Geofisica e Vulcanologia. http://emidius.mi.ingv.it/DBMI08/

[ISO-2394] "General principles on reliability for structures" International Organization for Standardization (ISO), 1998

[JBDPA-01] "Standard for Seismic Evaluation of Existing Reinforced Concrete Buildings" The Japan Building Disaster Prevention Association, 2001

[JCSS-00] "Probabilistic model code, Part 1: Basis of design" Joint Committee of Structural Safety, 2000

[JW 08] K. Jaiswal, D.J. Wald. "Creating a Global Building Inventory for Earthquake Loss Assessment and Risk Management" Open-File Report 2008–1160, USGS, 2008

[Kr 96] S.L. Kramer. "Geotechnical Earthquake Engineering" Prentice-Hall International Series, New Jersey, 2006

[LB 04] K. Lang, H. Bachmann. "On the seismic vulnerability of existing buildings: a case study of the city of Basel" Earthquake Spectra, 2004

[LIS web] Laboratorio de Ingenieria Sismica. http://www.lis.ucr.ac.cr/index.php?id=Inicio

[Lo96] P.B Lorenço. "Computational strategies for masonry structures" PhD Thesis, Delf University of Tecnology, 1996

[Ma 92] Magenes G. "Seismic behavior of brick masonry: strength and failure mechanism of shear-walls" Ph.D. Thesis, Universita di Pavia, 1992

[MC 97] G. Magenes, G.M. Calvi: "In-plane seismic response of brick masonry walls" Earthquake Engineering and Structural Dynamics, 1997

[Me 99] R.E. Melchers. "Structural Reliability Analysis and Prediction" John Wiley & Sons, 1999

[Me 02] G. Melis. "Displacement-based seismic analysis for out-of-plane bending of unreinforced masonry walls" Master Thesis, University of Pavia, 2002

[Mi 06] M. Mistler. "Verformungsbasiertes seismisches Bemessungskonzept für Mauerwerksbauten" PhD Thesis, University of Aachen, Germany, 2006

[MK 11] M.M. Maniyar, R.K. Khare. "Selection of ground motion for performing incremental dynamic analysis of existing reinforced concrete buildings in India" Current Science, 2011

[MM 08] A. Menon, G. Magenes. "Out-of-plane Response of Unreinforced Masonry. Definitions of Seismic Input" Research Report No. ROSE-2008/04. IUSS Press, 2008

[MM 80] W. Mann, H Müller. „Failure of shear-stressed masonry—an enlarged theory, tests and application to shear walls" Proceedings of the British Ceramic Society 1980

[MMMM 09] L. Milano, A. Mannella, C. Morisi, A. Martinelli: "Schede illustrative dei principali meccanismi di collasso locali negli edifici esistenti in muratura e dei relativi modelli cinematici di analisi. Allegato alle Linee Guida per la Riparazione e il Rafforzamento di elementi strutturali, Tamponature e Partizioni" Proteczione Civile Nazionale, Laboratories University Network of seismic engineering (ReLUIS), 2009

[Mo 04] P. Mouroux, M. Bertrand, M. Bour, B.L. Brun, S. Depinois, P. Masure. "The European Risk-UE Project: an advanced approach to earthquake risk scenarios" Proceedings of the 13th World Conference Earthquake Engineering, Vancouver Canada, 2004

[MOIT 03] M. Midorikawa, I. Okawa, M. Iiba, M. Teshigawara. "Performance-Based Seismic Design Code for Buildings in Japan" Earthquake Engineering and Engineering Seismology, 2003

[MRe web] Munich Re. http://www.munichre.com/en/homepage/default.aspx

[MT 03] Z. Milutinovic, G. Trendafiloski. "An advanced approach to earthquake risk scenarioswith applications to different European towns" RISK-UE ReportWP4: vulnerability of current buildings. European Commission, Brussels 2003

[MY 09] K. Miyamoto, P. Yanev. "L'Aquila Italy M6.3 Earthquake April 6, 2009" Earthquake field investigation report, Global risk Miyamoto, California, 2009

[Ne 82] N.M. Newmark, W.J. Hall. "Earthquake Spectra and Design" Earthquake Engineering Research Institute, Berkeley, 1982

[Ng 06] V.B. Nguyen. "Numerical Modelling of Reinforced Concrete Bridge Pier under Artificially Generated Earthquake Time-Histories" Ph.D. Thesis, University of Birmingham, 2006

[NTC-09] "Nuova circolare delle norme tecniche per le construzioni" Ministerio delle Infrastrutture e dei Trasporti 2009, Circolare 2 febrario 2009 n. 617 C.S.LL.PP, 2009

[NU 08] F. Nemry, A. Uihlein. "Environmental Improvement Potentials of Residential Buildings (IMPRO-Building)" JRC Scientific and Technical Reports, Joint Research Center, 2008

[NZS-92] "Code of Practice for General Structural Design and Design Loading of Buildings" New Zealand Standard NZS 4302:1992

[NZSEE 06] New Zealand Society for Earthquake Engineering (NZSEE). "Assessment and improvement of the structural performance of buildings in Earthquakes" 2006

[Ok 00] K. Okazaki. "RADIUS initiative for IDNDR- How to reduce urban seismic risk" 12th World Conference on Earthquake Engineering, Auckland, New Zealand, 2000

[Ok 01] I. Okawa, T. Kashima, H. Kitamura, M. Tohdo, S Sakai, M. Tanigaki, K. Yamagishi, K. Naraoka. "On the generation of the design earthquake ground motion time history" Power Works Research Institute (PWRI) website. 2001

[PAP 11] F. Parisi, N. Augenti, A. Prota. "The role of spandrels within masonry walls with openings: an experimental investigation" Proceedings of the Ninth Pacific Conference on Earthquake Engineering Building an Earthquake-Resilient Society, Auckland, 2011

[P-C 08] Păuleț-Crăiniceanu, F. "Seismology for Civil Engineers" Lecture notes Technical University from Iasi, update November 2008

[PD 08] J. Padgett, R. DesRoches. "Methodology for the development of analytical fragility curves for retrofitted bridges" Earthquake Engineering and Structural Dynamics, 2008

[Pe 83] Petrovski, J. "Engineering measures for earthquake risk reduction in the Arab countries, in Assessment and Mitigation of Earthquake Risk in the Arab Region (Cidlinsky K., and B. M. Rouhban, eds.)" Prepared by UNESCO for the Arab Fund for Economic and Social Development, 1983

[PGF 04] P.E. Pinto, R. Giannini, P. Franchin. "Methods for seismic reliability analysis of structures" IUSS Press, Pavia, 2004

[Pl 07] T. Pliefke, S.T. Sperbeck, M. Urban, U. Peil, H. Budelmann. "A standardized methodology for managing disaster risk – An attempt to remove ambiguity" Proceedings of the 5th International Probabilistic Workshop, Ghent, 2007

[PTCG 09] J. Park, P. Towashiraporn, J.I. Craig, B.J. Goodno. "Seismic fragility analysis of low-rise unreinforced masonry structures" Engineering Structures, 2009

[RdLV 10] P. Ricci, F. De Luca, G.M Verderame. "6th April 2009 L'Aquila earthquake, Italy: Reinforced concrete building performance" Bulletin Earthquake Engineering, Springer, 2010

[RI 10] A.P. Russell, J.M. Ingham. Prevalence of New Zealand's unreinforced masonry buildings" Bulletin of the New Zealand Society for Earthquake Engineering, 2010

[RMI 07] A.P. Russell, H. Mahmood, J.M. Ingham. "Assessment of the material properties of New Zealand's unreinforced masonry building stock" Millpress. Proceedings of the

Third International Conference on Structural Engineering, Mechanics and Computation, Cape Town, 2007

[RPM 08] M. Rota, A. Penna, G. Magenes. "A procedure for deriving analytical fragility curves for masonry buildings" 14th World Conference on Earthquake Engineering, Beijing, 2008

[RPS 07] M. Rota, A. Penna, C.L. Strobbia. "Processing Italian damage data to derive typological fragility curves" Soil Dynamics and Earthquake Engineering, 2007

[SA 02] C.C. Simsir, M.A. Ascheim, D.P. Abrams. "Response of unreinforced masonry bearing walls situated normal to the direction of seismic input motion" Proceedings of the 7th US National Conference on Earthquake Engineering, Boston, 2002

[SAMCO-06] "Guideline for Assessment of Existing Structures", W. Rücker, F. Hille, R. Rohrmann. Federal Institute of Materials Research and Testing (BAM), Berlin, 2006

[Sc 97] J. Schneider. "Introduction to Safety and Reliability of Structures" International Association for Bridge and Structural Engineering, 1997

[SEAOC-95] "Vision 2000 Committee. Performance Based Seismic Engineering" Report prepared by Structural Engineers Association of California, 1995

[Si 10] F. Silvestri. "La lezione del terremoto de l'Aquila: Aspetti geotecnici nell'interpretazione del danneggiamento, nella gestione dell'emergenza e nella ricostruzione" Università di Napoli and INGV, 2010

[Sp 08] S. Sperbeck. "Seismic Risk of Assessment of Masonry Walls and Risk Reduction by Means of Prestressing" PhD Thesis, TU Braunschweig, 2008

[Sp 09] R. Spence. "Estimating shaking-induced casualties and building damage for global earthquake events" Final Technical Report, Cambridge Architectural Research Ltd, 2009

[Sr 10] T. Srikanth, R.P. Kumar, A.P. Singh, B.K. Rastogi, S. Kumar. "Earthquake vulnerability assessment of existing buildings in Gandhidham and Adipur Cities Kachchh, Gujarat (India)" European Journal of Scientific Research, 2010

[St 04] S. Steimen. "Uncertainties in Earthquake Scenarios" PhD Thesis, Swiss Federal Institute of Tecnology, 2004

[St 12] J.P. Steward, G. Lanzo, A. Pagliaroli, G. Scasserra, G. Di Capua, S. Peppoloni, R. Darragh, N. Gragor. "Ground Motion Recordings from the M_W 6.3 L'Aquila Earthquake in Italy and their Engineering Implications" Earthquake Spectra, 2012

[SW 03] K. Sang-Cheol, D.W. White. "MDOF Response of Low-Rise Buildings. Final Report" Project ST-5, Mid-America Earthquake Research Center. Georgia Institute of Tecnology, 2003

[T&T 06] Tonkin & Taylor Ltd. "Natural Hazard Management" Research Report, for Quality Planning, New Zealand government, 2006

[TČ 71] V. Turnšek, F. Čačovič. „Some experimental results on the strength of brick masonry walls" Proceedings of the 2nd International Brick Masonry Conference, Stoke-on-Trent, West HWH, British Ceramic Res. Assoc., London, 1971

[TDAES-00] "Guidelines for Seismic Assessment of Stone-Masonry Structures" Technology Directorate Architectural & Engineering Services, Public Works and Government Services Canada, 2000

[Te 09] A. Tertulliani, L. Arcoraci, M. Berardi, F. Bernardini, R. Camassi, C.Castellano, S. Del Mese, E. Ercolani, L. Graziani, I. Leschiutta, A. Rossi, M. Vecchi. "An application of EMS-98 in a medium-sized city: The case of L'Aquila (central Italy)

after the april 6, 2009 Mw 6.3 earthquake" Istituto Nazionale di Geofisica e Vulcanologia (INGV), 2009

[Tephra-96] "Integrated Risk Management for Natural and Technological Disasters" P. Helm, Department of the Prime Minister & Cabinet, Wellington, 1996

[TheEc web] The economist. http://www.economist.com/blogs/dailychart/2011/03/natural_disasters

[To 99] M. Tomaževič. "Earthquake-Resistant Design of Masonry Buildings" Imperial College Press, London, 1999

[TR 08] M. Till, T. Rossetto. "Comparison of building damage scales and damage descriptions for use in earthquake loss modeling in Europe" Bulletin of Earthquake Engineering, 2008

[UFC-07] "Seismic design for buildings" Unified Facilities Criteria (UFC), 2007

[UN 04] United Nations Development Programme (UNDP) "Reduced Disaster Risk: A Challenge for Development. A Global Report" Bureau for Crisis Prevention and Recovery, 2004

[VCMB 07] R. Vetturini, A. Cleri, F. Mollailoli, P. Bazzurro. "Housing Report: Unreinforced stone wall rural housing (upper income)" World Housing Encyclopedia, 2007

[WCHE 96] Y.K. Wen, K.R. Collins, S.W. Han, K.J. Elwood. "Dual-level designs of buildings under seismic loads" Structural Safety, 1996